Fire risk analysis framework at the wildland-urban interface

Pascale Vacca

Ph.D. Thesis

Fire Risk Analysis Framework at the Wildland-Urban Interface

Pascale Vacca

Advisors:

Prof. Elsa Pastor Ferrer

Prof. Eulàlia Planas Cuchi

Submitted to the Universitat Politècnica de Catalunya for the degree of

Doctor of Philosophy

2023

Abstract

Wildfires that reach the border between the wildland and urban areas, defined as the Wildland-Urban Interface (WUI), have rapidly expanded in frequency and severity over the past few decades, and the number of structures lost each year has increased significantly. As WUI fires pose great management challenges in terms of civil protection and fire mitigation, self-protection has become a growing necessity and focus must be placed in creating fire-adapted communities that can safely co-exist with wildfires.

At the WUI microscale (i.e., homeowner level), susceptibility of a home to wildfire depends on the management of its surroundings and the hardening of the structure itself. The goal of this thesis is to develop a risk analysis framework based on the analysis of the fire hazard posed by the fuels located in the surroundings of a building and on the identification of building vulnerabilities for Mediterranean WUI scenarios.

To meet this goal, an analysis of the different types of fuels present on a property and of the vulnerable elements of a building is performed and three scenarios are selected for further analysis with performance-based strategies. Performance criteria are identified for each of the selected scenarios and an analysis of the available information on the fire characteristics of the different types of fuels located at the microscale is presented, which highlights a lack of quantitative knowledge on WUI fire hazards. Real-scale tests of four fuel packs that contain artificial fuels that could be present in WUI environments have therefore been performed, and the obtained results can be used for the analysis of WUI fire scenarios.

A methodology for the quantitative analysis of the vulnerability of building and property sub-systems based on a Performance-Based Design (PBD) approach is presented and applied to the three selected WUI scenarios. The methodology includes the modelling of the scenarios with the Computational Fluid Dynamics tool FDS (Fire Dynamics Simulator). Results obtained from this modelling can be compared to the previously set performance criteria.

When it comes to building vulnerability, a Vulnerability Assessment Tool (VAT) for Mediterranean WUI structures is developed, based on the results obtained from the sub-system scenario analysis and an extensive literature review. The tool is presented in form of a checklist and is intended to be used by homeowners, with the goal of identifying home vulnerability in a quantitative way by highlighting the main issues of a property by analysing the building and its surroundings. The application of the VAT is presented for three different case studies located in Mediterranean landscapes.

Finally, a WUI specific PBD guideline is presented for the quantitative risk analysis of WUI scenarios. Within the guideline, performance criteria are presented for both life safety and property protection and suggestions on the choice of design fire scenarios for WUI environments are given, together with the different variables that should be included, such as fire, environmental and property characteristics. The methodology presented in the guideline is applied to a case study, which is modelled in FDS, based on the strategies identified for the analysis of the sub-system scenarios. The application of the methodology to the case study shows how fire safety at the WUI can be quantified and gives an example of strategies that can be implemented to reach the desired fire safety level.

Acknowledgments

First of all, I’d like to express my deepest gratitude to my thesis advisors Elsa and Eulàlia, who gave me this great opportunity. Your guidance, support and encouragement are greatly appreciated. I’m also very grateful to the CERTEC team, especially Alba for her encouragements, and fellow PhD students Juanan and Vahid, with whom I’ve shared most of this journey.

I gratefully acknowledge the funding sources that provided financial support for this work, which include the European Commission’s Directorate-General for European Civil Protection and Humanitarian Aid Operations (DG ECHO), the Spanish Ministry of Economic Affairs and Digital Transformation (MINECO), and the COST action FIRElinks, which financed my three-month stay in Portugal. I would also like to thank the ADAI team at the University of Coimbra, who kindly hosted me for three months.

A big thank you goes to Balsa, former roommate, fellow PhD student, cat lover and friend, who helped me out a lot and was very patient in answering all my questions and, most importantly, psychologically supported me throughout the PhD. Another big thank you goes to the pizzendres crew, for supporting me and feeding me especially during the final months of my PhD. I’ll forever be grateful for your friendship.

And, last but not least, I’d like to thank my family, who always has my back and supports me in everything I do.

Contents

List of Figures

List of Tables

Nomenclature and Acronyms

A	Area (m^2)
c_p	Specific heat capacity ($kJ \cdot kg^{-1} \cdot K^{-1}$)
D	Horizontal flame depth (m)
D^*	Characteristic fire diameter (m)
g	Gravitational constant (m/s^2)
H	Low heat of combustion (kJ/kg)
h_{conv}	Convective heat transfer coefficient ($W \cdot m^{-2} \cdot K^{-1}$)
I_B	Fireline intensity (kW/m)
k	Thermal conductivity ($W \cdot m^{-1} \cdot K^{-1}$)
L	Thickness (m)
M	Bending moment (N·m)
N	Axial force (N)
N_{amb}	Axial force at ambient temperature (N)
N^t	Maximum axial force for a point in time (N)
p_{max}	Maximum pressure (bar)
p_{PRV}	PRV set point pressure (bar)
$\dot{Q}$	Heat Release Rate (kW)
Q_{peak}	Peak Heat Release Rate (kW)
$\dot{q}''_{inc}$	Incident heat flux (kW/m^2)
$\dot{q}''_{loss}$	Heat flux lost on the non-exposed side of a wall (W/m^2)
$\dot{q}''_{rad}$	Radiant heat flux (kW/m^2)
$\dot{q}''_{tot}$	Total net heat flux (W/m^2)
r	Linear rate of fire spread (m/s)
$S_{a,max}$	Maximum surface area where the temperature is higher than 400°C (m^2)
S_c	Critical surface area (m^2)
t	Time (s)
T	Temperature (°C)
T_{AST}	Adiabatic surface temperature (K)
T_S	Ambient surface temperature (K)
T_{surf}	Surface temperature (°C)
T_∞	Ambient temperature (K)
u	Wind speed (m/s)
w	Fuel consumption (kg/m^2)
y	Coordinate (m)

Greek letters

α	Fire growth rate (kW/s^2)
ΔT_{cr}	Critical temperature difference (°C)
δx	Nominal mesh cell size (m)
ε	Emissivity (-)
ε_0	Average strain (-)
ε_{mech}	Mechanical strain (-)
ε_{therm}	Thermal elongation (-)
ε_{tot}	Total strain (-)

η_{fi}	Reduction factor (%)
ρ	Density (kg/m^3)
ρ_∞	Ambient air density (kg/m^3)
σ	Stress (Pa)
σ	Stefan-Boltzmann constant (W·m^{-2}·K^{-4})
χ	Curvature (m^{-1})

Acronyms	
AST	Adiabatic Surface Temperature
CFD	Computational Fluid Dynamics
FDS	Fire Dynamics Simulator
FED	Fractional Effective Dose
HL	Heat load (kJ/m^2)
HRR	Heat Release Rate
HRRPUA	Heat Release Rate Per Unit Area (kW/m^2)
LPG	Liquefied Petroleum Gas
MLR	Mass Loss Rate (kg/s)
PBD	Performance-Based Design
POF	Probability Of Failure
PRV	Pressure Relief Valve
PRVI	Pressure Relief Valve Index
PVC	Polyvinyl Chloride
VAT	Vulnerability Assessment Tool
WSI	Weakened Surface Index
WUI	Wildland-Urban Interface

Chapter 1

Introduction

1.1. The Wildland-Urban Interface problem

Wildfires are an integral part of forest dynamics in many ecosystems, where they are an essential element of forest renewal (European Environment Agency, 2017). In wildfire dependent ecosystems, disturbance is manifested by disruptions in the natural fire regime, often when fires are eliminated or the frequency of burning increases (Keeley and Pausas, 2019). Extreme weather conditions severely affect forests as well: as fuels are transitioning to drier complexes, which are more prone to wildfires (Costa et al., 2020), burnt area is increasing and, in the European Union (EU), the burnt area in 2022 was the second highest ever, only behind the year 2017 (San-Miguel-Ayanz et al., 2023). Climate change is expected to influence wildfire regimes and risk in Europe and elsewhere: an increase in frequency and intensity of droughts and heat waves has been observed as a consequence of global warming, which causes the expansion of fire-prone areas as well as longer fire seasons in areas that are already fire-prone, such as southern Europe (European Environment Agency, 2017; Jones et al., 2022). Wildfire risk depends not only on climatic conditions, but also on vegetation, forest management practices and other socio-economic factors (European Environment Agency, 2017).

Extreme wildfire events are affecting not only biodiversity and ecological services, but also human well-being, livelihoods, and national economies (International Union of Forest Research Organizations, 2018). Wildfires that reach the border between the wildland and urban areas, defined as the Wildland-Urban Interface (WUI), have rapidly expanded in frequency and severity over the past few decades. The number of structures lost per year has increased significantly also due to the increased development in rural areas, which is projected to grow in the future (Caton et al., 2017; Mitsopoulos et al., 2020). The consequences of these fires, may they be economic, social or environmental, are therefore also predicted to escalate.

WUI fires are also posing great management challenges in terms of civil protection and fire mitigation, as firefighters' capacities are often exceeded due to the need of a simultaneous response to wildfire suppression, community evacuation, and structure protection (Vacca et al., 2020a)[1]. If the number of burning and vulnerable homes overwhelms the local fire protection capability, fire protection effectiveness is reduced and many homes are left unprotected (Caton et al., 2017). Self-protection has thus become a growing necessity, and therefore, in the years to come, the focus must be placed on the creation of fire-adapted communities, which can safely co-exist with wildfires (Vacca et al., 2020a), because, although wildfires are inevitable, the destruction of homes and lives is not (Calkin et al., 2014).

[1] Part of the content included in this chapter has been published as two journal paper (Vacca et al.2020a, Àgueda et al. 2023).

1.1.1. Past events

In recent years, large forest fires have repeatedly affected Europe, in particular the five Mediterranean countries Portugal, Spain, Italy, Greece and France, which on average account for around 85% of the total burnt area in Europe per year (De Rigo et al., 2017).

The most recent catastrophic WUI fires recorded in Southern Europe include the fire in Mati (Greece) on July 23rd 2018 (Figure 1.1), which killed 102 people, and the one in Pedrógão Grande (Portugal) on June 17th 2017 (Figure 1.2), with 66 fatalities (Molina-Terrén et al., 2019). These fires also respectively destroyed 998 and 457 structures and severely damaged another 794 and 427 (Vacca et al., 2020a).

Figure 1.1: Mati, Greece. Adapted from The Guardian (2018).

Figure 1.2: Pedrógão Grande, Portugal. Adapted from De Melo Moreira (2017).

Wildfires are systematically affecting northern European countries as well. On January 19th 2014 the Laerdal fire (Norway) devastated the historic town of Lærdalsøyri (UNESCO World Heritage), destroying 30 timber structures. In July of the same year, a fire spread over the county of Västmanland (Sweden), affecting 14,000 hectares of forested land and destroying 32 structures. A summary of the most recent catastrophic fires in Europe is given in Table 1.1. Estimated losses due to catastrophic fires in the European Union during the period 2000-2017 accounted for 63.3B EUR (International Union of Forest Research Organizations, 2018).

These extreme events are not only occurring in Europe, but all over the world. The states of California, Oregon, Washington and Colorado experienced record breaking wildfires in the year 2020, with losses that amounted to 16B US$ (approximately 13B EUR) (Munich RE, 2021). Over 3000 houses were destroyed and 33 people were killed during the 2019/2020 Australian bushfire season, also known as Black Summer, and its total impact is estimated to be as much as 40B A$ (approximately 25.3B EUR) (Filkov et al., 2020).

Table 1.1: Summary of recent WUI fires in Europe. Adapted from Vacca et al. (2020a) and updated with more recent information.

Fire	**Date**	**Structure damage**	**Effects on humans**
Västmanland, Sweden	July 31st 2014	35 structures with light or no damage 32 structures destroyed or severely damaged	1 fatality 1 civilian seriously injured 9 firefighters injured
Funchal, Portugal	August 9th 2016	37 structures completely destroyed 117 structures severely damaged	3 fatalities 200 injured
Rognac, France	August 10th 2016	24 houses completely destroyed 15 structures moderately damaged 117 structures lightly damaged	No fatalities 6 injured
Benitatxell, Spain	September 4th 2016	3 structures severely damaged 197 houses lightly damaged	No fatalities
Pedrógão Grande, Portugal	June 17th 2017	153 structures with light or moderate damage 427 with remarkable damage 457 structures completely destroyed	65 fatalities 200 injured
Mati, Greece	July 23rd 2018	1713 structures with light or no damage 794 structures with remarkable or severe damage 998 structures completely destroyed	102 fatalities 200 injured
Llutxent, Spain	August 7th 2018	30 structures with remarkable damage 13 structures completely destroyed	No fatalities
Chernobyl Exclusion zone, Ukraine	April 6th 2020	Several uninhabited villages and touristic attractions burned down completely	Resuspension of ^{137}Cs and other radionuclides into the atmosphere, unknown effects
Manaygat, Turkey	July 28th 2021	1000 structures completely destroyed Kemerkoy power plant affected	9 fatalities 560 injured
London, UK	July 20th 2022	60 structures completely destroyed	16 firefighters injured
Pont de Vilomara, Spain	July 17th 2022	42 structures with remarkable damage 126 structures with light damage	No fatalities

These multiple-fatality events show that there is still a noticeable gap between the observed fire behaviour and the applied firefighting and self-protection capacity. At the moment, civilians are mostly relying on their personal instincts for self-protection and on the available resources to survive (Molina-Terrén et al., 2019).

Numerous studies also document the tendency for people to ‘wait and see’ what a fire is like, or wait until they are threatened, before deciding to stay or leave (Whittaker et al., 2013; McNeill et al., 2016). Additionally, people will wait for instructions mandated by the civil protection or by the firefighters.

In the 2009 Black Saturday fire a large proportion of people died inside while sheltering, marking a significant shift in bushfire fatality trends, which previously saw the majority of deaths occurring outside while residents attempted to protect assets or evacuate. There was a limited degree of preparedness for sheltering.

A better fire preparedness of homes in WUI areas is therefore needed, so that not only fire-practitioners, but also homeowners can be prepared in the event of a wildfire, and its consequences can be diminished.

1.1.2. WUI observation scales

A WUI fire involves the presence of both wildland and structural (artificial) fuels. The WUI fire problem is therefore inherently complex, as it is characterized by the interaction of multiple phenomena of diverse nature occurring at different observation scales (Vacca et al., 2020a), shown in Figure 1.3:

- The macroscale or landscape scale, associated with large forestry and operational management strategies such as landscape design, fuel reduction planning, management of strategic points for suppression, etc.
- The mesoscale, at a settlement level, where preventive and protective measures to keep settlements safe must be planned and implemented (e.g. fuel reduced strips around communities, water supply points, etc.).
- The microscale or homeowner scale, as the extended concept of the well-known *home ignition zone* (Mell et al. 2010; Cohen, 2010), where the specific phenomena threatening people and dwellings take place. It is associated with preventive actions at the immediate surroundings of houses to guarantee structural integrity, create self-defensible spaces and increase safety in eventual shelter-in-place operations.

Figure 1.3: Example of the three observation scales in the municipality of Capoterra, Italy.

Many communities have developed within or adjacent to fire-prone ecosystems; these communities vary widely in their levels of wildfire exposure and susceptibility (Calkin et al., 2014). The Federal Register of the United States (Thompson, 2001) divided the WUI in three categories of communities: *(i)* the *interface* community, where structures directly abut wildland fuels and there is a clear line of demarcation between the two; *(ii)* the *intermix* community, where structures are scattered throughout a wildland area; *(iii)* the *occluded* community, where structures abut an island of wildland fuels. Buildings located at the perimeter of interface communities are potentially more exposed to flame fronts of approaching fires, compared to those sited in the centre of the settlement. In intermix communities the inner properties are also threatened by very near wildfire fronts due to the combustion of surrounding wildland vegetation.

The spatial scale determining home ignitions corresponds more to specific home and community sites than to the landscape scales of wildland fire management. Thus, the WUI fire loss problem primarily depends on the home and its immediate site (Hakes et al., 2017). This work will focus on the events that happen at the microscale level, where the presence of vegetation, structures and other fuels affect human vulnerability, structure survivability and overall fire danger for a property.

1.1.3. Ignition pathways at the WUI microscale

To appropriately analyse and mitigate WUI fire destruction risk, we must first understand how wildfires cause home ignitions, and how home destruction occurs during wildfires (Calkin et al., 2014). Ignition pathways for the fuels located at the WUI microscale must therefore be investigated, in order to identify potential vulnerabilities of a property. Wildland fire and home ignition research indicates that a home's exterior along with site characteristics significantly influence its ignitability and thus its chances for survival. Three fundamental pathways have been identified for the spread of fire into and within WUI communities (Caton et al., 2017):

- Firebrands generated either by the main fire front, nearby flammable material or nearby burning structures can directly ignite components of vulnerable structures or nearby vegetation and other combustibles. They are thought to be one of the primary sources of ignition in the WUI (Maranghides and Mell, 2011; Ribeiro et al., 2020).
- Radiant exposure may occur where large flames are close to exposed structural elements or other fuels.
- Direct flame contact occurs when flames are in contact with adjacent fuels.

Each of these mechanisms (firebrands, radiant heat exposure, direct flame contact) can be the direct cause of ignition by themselves, but they often appear simultaneously or in sequence, one after the other, producing a domino effect involving different elements present on the parcel.

These ignition pathways occur during one or more of the fire exposure phases that affect a property during a wildfire (Vacca et al., 2020a), as shown in Figure 1.4. The first phase is the *pre-impact*, when the wildfire front has not yet reached the property in the settlement. Firebrands can be driven by the wind onto the property, where they are able to ignite vegetation or other combustible materials, and even buildings (Hakes et al. 2017; Maranghides and Mell 2011). The phase in which a flame front reaches a property is named *impact*, where both radiant exposure and direct flame contact can occur, along with the arrival of firebrands. Fire propagation through the elements on a property will occur during the *fire transfer* phase. The fire spreads commonly through vegetation (e.g., hedges, unbuilt parcels) into the neighbouring parcels along the settlement, as well as through the new production of firebrands from the elements that are burning on a property into remote parts of the settlement. The final fire exposure phase is the *post-frontal* *combustion*, in which all the items that ignited in any of the previous phases continue burning and can eventually cause further damage or chained events due to direct flame contact or radiant exposure. In this phase, quite an amount of energy and combustion gases can still be released.

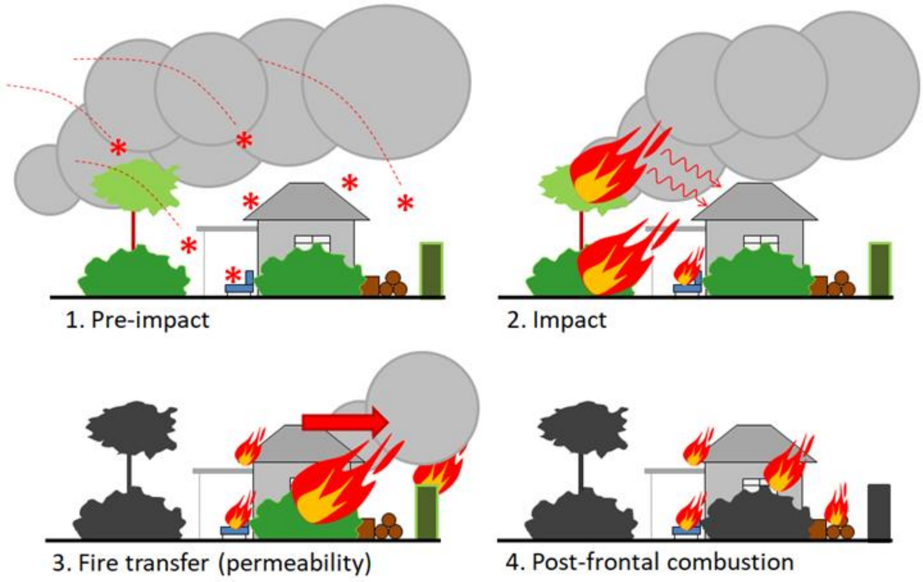

Figure 1.4: Fire exposure phases at the WUI microscale. Adapted from Caballero and Sjöström (2019).

The location of a property within the landscape plays a key role in its exposure to a flame front and the arrival of firebrands and smoke. Buildings located on mid-slopes, ridges or hilltops are potentially more exposed compared to those located in valleys or flat terrain (Figure 1.5). Houses located in saddles or box canyons are more likely to receive smoke, firebrand showers and more intense fire run, due to the phenomenon of wind channelling (Caballero and Sjöström, 2019).

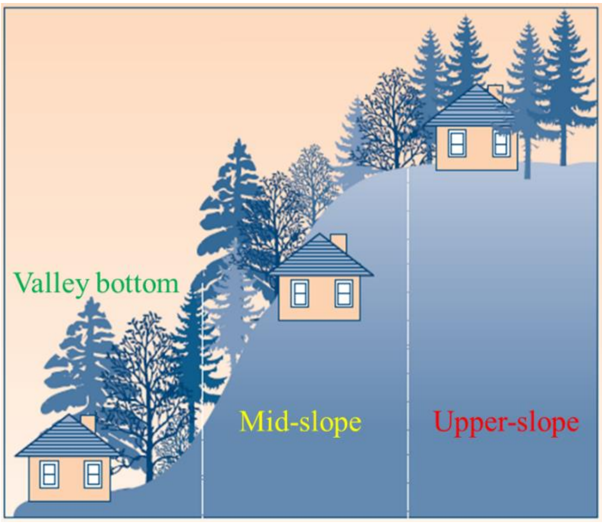

Figure 1.5: How the location of the structure on the slope affects its fire hazard: buildings at the valley are less exposed (green), while exposure gradually increases at the mid-slope (yellow) and at the upper slope (red). Adapted from Partners in Protection (2003).

On a community level, the layout of structures and the space between them has been shown to be extremely important in mitigating wildfire risk. Blanchi and Leonard (2005) performed a study on the buildings affected by the 2003 Canberra bushfires, and observed that window breakage had occurred due to their exposure to radiant heat from an ignited neighbouring house. Structure-to-structure fire spread was also observed in the Waldo Canyon Fire in Colorado, USA (Maranghides et al., 2015).

More locally, creating a defensible space around homes has been effective in mitigating exposure from both radiation and direct flame contact (Hakes et al., 2017). This is a space around a structure clear of combustible materials that can either directly ignite components of vulnerable structures or nearby vegetation and other combustibles, which can subsequently ignite the structure via radiant heating or direct flame contact (Caton et al., 2017). Reducing WUI fire losses in the context of home ignitability also involves mitigating the fuel and heat components sufficiently to prevent ignitions (Hakes et al., 2017).

Whether a home survives depends initially on whether it ignites; if ignitions with sustained burning occur, survival then depends on effective fire suppression. The lower the home ignitability the lower the chance of incurring an effective ignition (Hakes et al., 2017). Most homes ignite as a result of firebrands igniting lower-intensity surface fires adjacent to and/or spreading to contact the home (causing indirect fire exposure), as well as firebrand ignitions directly on the home (Calkin et al., 2014). The indirect exposure of a building to fire, which occurs when a secondary fuel is ignited, is therefore related to the fuels located in the surroundings of the building.

1.2. Need for risk reduction

Risk reduction strategies are needed in order to create fire-adapted communities, and local community involvement in planning, mitigating and reducing the hazard is a key factor (International Union of Forest Research Organizations, 2018). These strategies must include actions that can effectively reduce human and asset vulnerability along with fire danger (Costa et al., 2020). The evaluation of risk mitigation options begins with the questions of what are appropriate wildfire management objectives, and how risk mitigation options realistically vary in terms of cost, likely effectiveness, and the appropriate identification of who bears the responsibility (Calkin et al., 2014). A change needs to take place in the relationship between homeowners and the fire services. Instead of home-related pre-suppression and fire protection responsibilities residing solely with fire agencies, homeowners must take the principal responsibility for ensuring adequately low home ignitability (Hakes et al., 2017), given that this is the main issue when it comes to WUI fire disasters. Home survival is especially critical when sheltering in place becomes an option. This could happen when early evacuation is not possible, and factors such as late awareness, traffic jams, etc., avert people from evacuating safely (Whittaker et al., 2017).

The WUI fire sequence described in Figure 1.6 shows that WUI fire disasters depend on the exposure of ignitable homes to the flames and firebrands of uncontrollable, extreme wildfires. Many burning and highly ignitable homes overwhelm firefighters, resulting in many homes without protection (Cohen, 2010). This progression can only be broken, and disaster avoided, by substantially increasing the proportion of homes that are resistant to ignition (Westhaver, 2017), along with creating a defensible space around a home. Considering home and site characteristics when designing, building, siting, and maintaining a home can reduce WUI fire losses (Cohen, 2000).

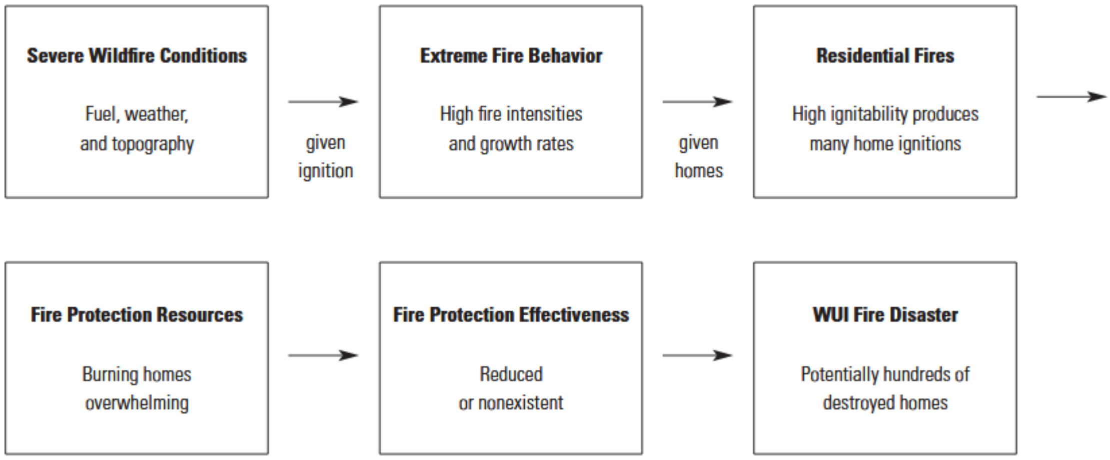

Figure 1.6: WUI fire sequence. Adapted from Cohen (2010).

Case studies indicate that a home's structural characteristics and its immediate surroundings determine a home's ignition potential in a WUI fire and thus influence its chances of survival (Cohen, 2000; Maranghides et al., 2022). If the pathways to ignition are fundamentally prevented via hardening structures, communities, and surrounding wildland, then the WUI problem can be greatly reduced. A coupled approach of managing landscapes to reduce fire, ember, and radiation exposure conditions, while at the same reducing vulnerabilities at the community level and engineering structures to resist to these fire exposures has perhaps the best chance of success (Caton et al., 2017).

Calkin et al. (2014) presented a conceptual model for the reduction of the risk of home loss in WUI fires (Figure 1.7). The risk of home loss is jointly determined by the probability of home exposure to wildfire and the susceptibility of a home to wildfire, which in turn depend on other factors, such as those presented in level 3 of Figure 1.7. Actions and responsibilities for strategically managing risk factors vary across land management agencies, local governments, and private homeowners. As previously stated, this work focuses on the events that happen at the WUI microscale level, where the primary responsibility lays with the homeowners.

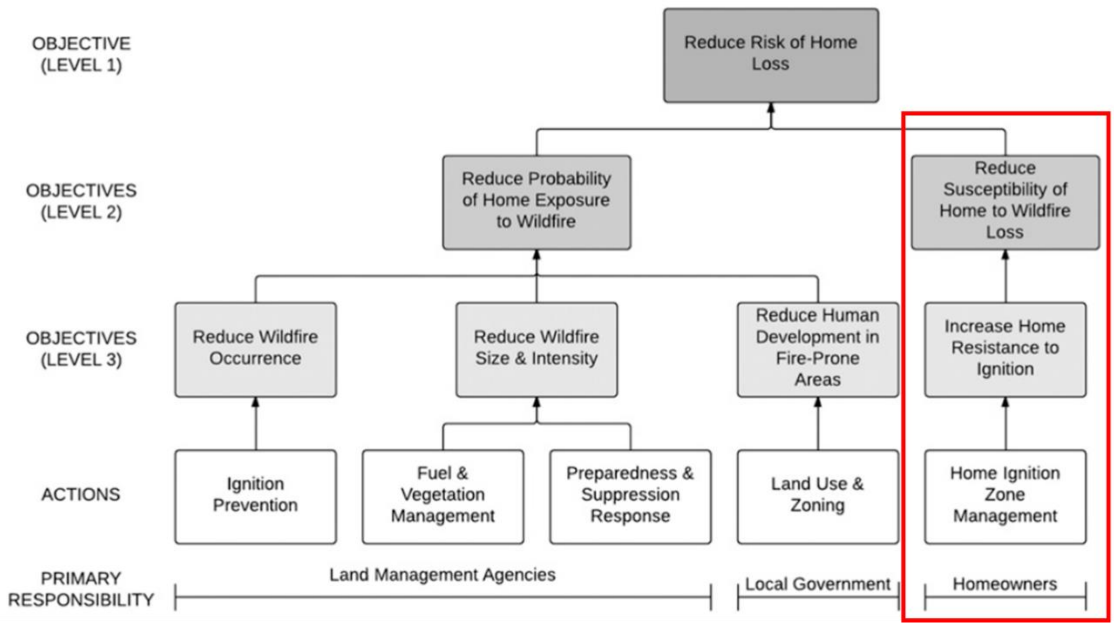

Figure 1.7: Conceptual model highlighting the major fundamental objectives (level 1), means-based objectives (levels 2 and 3), and actions for reducing the risk of home loss as a result of wildfire. Adapted from Calkin et al. (2014). This work focuses on the steps contained in the red rectangle.

The primary risk factors are the probability of home exposure to flames and firebrands, and a home's susceptibility to loss, which vary geographically according to environmental and socioeconomic variables (Calkin et al., 2014). The environmental variables include for example the type of vegetation, topography, weather, while the socioeconomic ones can include building materials, settlement configuration within the landscape, property configuration within a settlement, and fuel management within a property. As previously stated, fire, ember and radiation exposure is to be managed at landscape level and also at community level, so that settlement and therefore property exposure can be reduced. Additionally, communities must be managed so to reduce fire spread within the settlement, while, at the property level, a home's susceptibility to loss is to be reduced.

1.2.1. Residential fuels

Direct home ignitions by radiation or flame contact from a burning forest are not expected in urban interface areas where vegetation has been appropriately treated and adequate clearance between homes and wildland vegetation exists. However, due to the extraordinary ability of wildland fires to generate and transport firebrands, fuel management is far less effective in countering the primary threat to interface structures (Westhaver, 2017). This is why fuel management and ignition of buildings must be addressed at the microscale, where firebrands arrive and ignite structures or fuels located on a property.

The WUI microscale is characterized by the presence of all sorts of combustible elements that may jeopardize the main structure: ornamental vegetation, ground fuels, fences, stored material, outbuildings (e.g., garages, garden or storage sheds) or even adjacent structures and LPG tanks (Scarponi et al., 2020). These fuels very often lack any type of management (Molina-Terrén et al., 2019). In case of ignition of these fuels, and provided flames duration and intensity are significant enough, consequences might have a severe impact (Pastor, 2019).

Residential fuels can be divided into two categories: natural (e.g., ornamental vegetation) and non-natural, or artificial (e.g., outdoor furniture).

While many studies have been performed on the fire behaviour of wildland fuels (e.g. Cheney 1990; Alexander 1982), when it comes to residential natural fuels, little is known about their quantitative fire behaviour (Meerpoel-Pietri et al., 2022). Among the key features that favours the spreading of fires toward dwellings, ornamental plants, whether in the form of trees, shrubs or hedges, constitute important vectors of propagation (Vacca et al., 2020a). The intensity at which this vegetation burns as well as the duration of the flaming phase depend on the species and its level of maintenance (i.e. trimming, pruning, watering), which conditions the fuel load, the density and the moisture content of the vegetation (Vacca et al., 2020b).

Westhaver (2017) analysed the behaviour of residential fuels, along with their impact onto structures, during the Fort McMurray fire disaster in 2016. His study showed that more than half of the hazard accruing from vegetation/fuel at the microscale resulted from landscaping materials chosen and planted by the residents or landscape contractors and not from residual native (i.e., forest) vegetation. In addition, bulky and highly flammable ornamental shrubs placed within 1-3 m of windows, walls or eaves were revealed to be a fatal flaw. Untended grass areas (i.e., taller or matted grass) often augmented with leaves or needles appeared to be effective in spreading fire and igniting heavier fuels, thus extending fire pathways towards nearby structures. Ornamental evergreen shrubs that formed dense, linear hedges were also observed to play a role in the fire spread throughout the settlement. Hedgerows are commonly used in gardening because of their aesthetic value and their capacity to give privacy by acting as green walls around properties. They do however combine all the characteristics of extremely flammable vegetation (i.e., high fuel volume, easily ignited, and high-intensity long duration burning). They can generate enough heat to break windows, melt gutters, and ignite nearby fuels, and they provide a pathway for fire spread not only through a property, but through the settlement as well, since they can connect multiple properties (Ganteaume et al., 2021; Vacca et al., 2020b; Westhaver, 2017). Examples of the consequences of the presence of hedgerows are shown in Figure 1.8 and Figure 1.9.

Proper selection and treatment of vegetation emerges thus as being crucial to home survival.

Figure 1.8: Fire spread through a hedgerow in La Nucia, Spain. Adapted from Caballero and Sjöström (2019).

Figure 1.9: Fire impact on a home from a hedge in Montesión, Spain. Adapted from Caballero and Sjöström (2019).

When it comes to artificial fuels, the burning behaviour of those that can be commonly found indoors (e.g., furniture and small appliances) has been extensively analysed in small- and real-scale tests (Hurley et al. 2016; National Fire Research Laboratory 2020). There is, however, a lack of quantitative data on the burning behaviour of artificial fuels and fuel packs that are frequently located in the surroundings of WUI structures (Vacca et al., 2022). These artificial fuels have the potential to burn for long periods of time, and they are those that can create the most damage during the post-frontal combustion fire phase. Examples of artificial fuels present on WUI properties are given in Figure 1.10. The hazard associated with these fuel packs is given for example by the large heat accumulation due to their ignition in semi-confined spaces (e.g., porch, space under decks, garage, shed), which can lead to fire spread through a property due to the ignition of other surrounding elements (Vacca et al., 2020a).

Figure 1.10: Examples of residential fuels at the WUI. On the left, a covered patio with outdoor furniture adjacent to wildland vegetation; on the right, a furnished porch along with a fence and outdoor pet houses.

In the Fort McMurray fire of 2016, it was observed that there was a positive correlation between home survival and properties that had minimum amounts of materials, machinery, and general “clutter” stored in open areas and accessible to wind-driven embers. The most common and significant sources of combustibles were general yard ‘clutter’, firewood, construction materials, recycling and compost storage, machinery and recreational vehicles, petroleum products, and patio furniture or amenities (Westhaver, 2017).

Another issue related to the fire spread on a property is caused by the presence of aboveground domestic LPG (liquefied petroleum gas) tanks, which are used as an energy source for heating, hot water, or cooking in WUI developments. When these tanks are exposed to flames coming from fuels located very near, they heat up and the pressure will increase. If the tank pressure reaches the Pressure Relief Valve (PRV) set point, this will open, releasing LPG that will immediately ignite forming a jet fire. The jet fire will hence worsen the heat load to the tank and its surroundings. If no measure is taken in order to cool down the tank and/or extinguish the fire, the tank may fail, leading to a loss of containment (Scarponi et al., 2020). Fourteen WUI accidents in which LPG reservoirs are involved are described by Barbosa et al. (2023), reporting two fatalities and the partial destruction of three buildings related to the burst of LPG cylinders.

The need for quantitative information of the burning behaviour of WUI microscale fuels has been identified as extremely important in order to define and characterize the role of these fuels in a home's ignition process (Vacca et al., 2022).

1.2.2. Structural vulnerabilities

Existing structures and their ignition vulnerabilities must be investigated in order to reduce the risk of home loss. This way it is possible to suggest scientific-based retrofitting methods (Manzello et al., 2018) for the protection of buildings.

Effective fire protection depends on ignition resistant homes during extreme wildfires (Calkin et al., 2014). Regardless of building designs and practices, houses at the WUI always present elements that are weak to fire exposure. These building sub-systems are responsible for houses' vulnerability, either because they are combustible or made out of materials sensitive to fire, or because their geometry enhances heat transfer (Vacca et al., 2020b).

One of the structural components that is the most exposed to an incoming flame front, its radiation and the landing of firebrands is the roof of a building. Roofs located under overhanging tree branches tend to accumulate fine fuels such as pine needles, particularly in the valleys and other convex shapes or on flat roofing (Figure 1.11). These points also accumulate firebrands that can provide local combustion, which may entail the involvement of the roof structure. Clay tiles are very frequent in Southern Europe, and although they are fire-resistant, they may break or displace, creating little to medium size gaps through which firebrands can easily enter and cause the ignition of the roof structure (Figure 1.12). Located beneath the hedge of a roof, also gutters accumulate vegetal debris, which may burn and slowly but steadily involve external parts of the eave and eventually the structure of the roof. Half round and other PVC gutters generally melt, deform and eventually fall in case of a nearby source of heat, or due to the combustion of the debris they hold. This may separate flame contact from eaves and other elements thus preventing their involvement. Metal gutters have a better resistance to the effect of radiation or flame contact, thus keeping the burning debris close to the eave's fringe and easing the involvement of external elements (Vacca et al., 2020a).

Figure 1.11: Accumulation of pine needles on a roof in San Martín de Valdeiglesias, Spain. Adapted from Caballero and Sjöström (2019).

Figure 1.12: Clay tile roofing severely affected by spot fires in the 2016 Funchal wildfire, Portugal. Adapted from Vacca et al. (2020a).

Along with the roof, glazing systems are frequently the most exposed elements of a structure. Cracking or collapsing of window panes are observed as a consequence of flame impingement or heat exposure coming from the wildfire front or from close objects or vegetation previously ignited mainly by flying embers (Figure 1.13). Once the window has failed, flying embers can also enter the structure and cause the ignition of the inside elements (Vacca et al., 2020a).

Figure 1.13: Glazing collapse in Neos Voutzas-Mati (Greece, 2018) due to the combustion of a pine tree. Adapted from Vacca et al. (2020a).

Other openings through which firebrands, smoke and eventually flames can enter buildings are vents, which are used to facilitate air circulation. Most common vents are located on the roof, while others are found as part of the wall siding, frequently protected with screens and grilles. Baseboard vents are mandatory for rooms with gas installations, such as kitchens, and they must be covered with a grille (Vacca et al., 2020a).

At the WUI, secondary structures such as sheds, garages, or other types of storage areas are common. These can be attached to the main building or located several meters from it, and are populated with many different non-natural fuels. Generally, these spaces are semi-confined, and thus open on at least one side. The objects stored in these structures can therefore be exposed to flying embers and to flames, which could cause the ignition of these items, which will subsequently burn for long periods of time. If one of these secondary structures is connected to the main buildings and the elements present in these areas are ignited, the great heat build-up created by the fire could cause great damage to the main structure's envelope (Vacca et al., 2020a). Examples of the damage caused by the ignition of fuels in semi-confined spaces are given in Figure 1.14 and Figure 1.15.

Figure 1.14: Shed containing tools and other materials destroyed during the Monchique fire in Portugal, 2018. Adapted from Caballero and Sjöström (2019).

Figure 1.15: Garage containing artificial fuels destroyed during the Mati fire in Greece, 2018. Adapted from Caballero and Sjöström (2019).

External elements of a house such as terraces, balconies, decks or porches also create opportunities for embers to accumulate and foster ignitions, as shown in Figure 1.16. These are areas where residential fuels such as outdoor furniture are commonly placed, and where vegetal debris can accumulate, enhancing the fire danger on a property.

Figure 1.16: Ember burn on a wooden deck in Fort McMurray. Adapted from Westhaver (2017).

1.3. Existing WUI guidelines and standards

The development (and continuous revision) of standards and guidelines can be crucial in reducing the negative impacts of WUI fires on communities involved through appropriate dedicated measures and design guidance (Intini et al., 2019). Countries that have historically been affected by wildfires at the WUI have created standards and guidelines for new and/or existing buildings that include WUI home-owner scale (i.e., WUI microscale) risk reduction strategies related to both building and property characteristics (Àgueda et al., 2023). While an International Code for WUI fires is currently available (International Code Council, 2021), some countries (e.g., Australia, Canada, USA) provide standards and codes concerning measures for response planning, prevention, protection, fighting, etc. of WUI fires, whereas others, especially in Europe, delegate the management of these issues to regional and municipality levels, or rely on provisions that cover the issue of WUI fires, but are included in other general codes (e.g., Building Codes, Environmental Codes, Fire Codes, etc.) (Intini et al., 2019). In France, Italy and Spain, regions are co-responsible of forest fire prevention and have to articulate national laws by issuing local regulations and guidelines and ensuring compliance of provisions at municipal levels (Pastor et al., 2019). A selection of standards and guidelines that specifically address the WUI microscale, along with the building and property elements for which strategies are suggested, is given in Table 1.2.

Some of the standards and guidelines that address WUI fires start with the assessment of the hazard level of the exposed structure. The key aspects assessed to define a wildfire hazard level on a property are climate and weather, wildfire history, topography (slope, sun exposure), surrounding vegetation, and construction materials and design of the structure. Some countries have developed an assessment methodology that measures the severity of a building’s potential exposure, such as the Bushfire Attack Level (BAL) in Australia (Australian Standards, 2018) or the Structure and Site Hazard Assessment in Canada (Partners in Protection, 2003).

All of the analysed guidelines and standards address the management of the defensible space around a building, with different degrees of detail. This entails the removal of most or all vegetation within a radius of 10 to 100 m (depending on the country) around the structure. Specific rules on the spacing of fuels within this radius are analysed in Chapter 2 and Chapter 4.

Requirements on construction materials and design are also given, although not for all countries. In Table 1.2 it can be noted that Portugal and Italy only provide regulations for the defensible space, but do not provide any guidelines on building construction or maintenance. France guidelines mention some building elements; however, they are not analysed with the appropriate detail (Àgueda et al., 2023). These requirements focus on the following key points:

- Construction materials should be non-combustible as much as possible, the definition of which may vary depending on the country (i.e., it might depend on the testing methodologies).
- Regular cleaning of combustible litter falling on roofs, decks, balconies, alongside periodic maintenance of the roof.
- Protection of vents, eaves, chimneys with non-combustible meshes to prevent flying embers from entering the structure.
- Glazing systems resistant to heat (double-pane, tempered glass, small windows, etc.) and protected by shutters.

Some of the guidelines mentioned in Table 1.2 (Firewise, Guidelines from the regions of Valencia and Catalunya in Spain, and FireSmart) also provide checklists for WUI homeowners/residents that focus on fuel management around a house and hardening vulnerable construction elements. While Firewise (USA) provides a guidance document, the other analysed checklists also provide a scoring system that results in the hazard level of the building and property (FireSmart - Canada) or in the vulnerability of the building to the incoming fire (Spanish regional checklists). FireSmart provides a more in-depth scoring system, dividing the defensible space into 3 different zones and assigning different weights to different categories: for example, the characteristics of the home and its attachments account for approximately 34% of the total score, while the different zones (0-1.5m,1.5- m, 10-30 m and 30-100 m) account respectively for 7%, 29%, 15% and 15% of the total score - based on the latest version of the Home Ignition Zone assessment score card (FireSmart Canada, 2020). The scoring in the checklists of the region of Valencia (Spain) is based more on whether the answer to the questions is affirmative or not (i.e., the more affirmative answers, the more the house is vulnerable), while the scoring of the region of Catalunya is divided in 3 different levels (high, medium or low vulnerability). The degree of detail of these two checklists designed for the Mediterranean landscape and building characteristics is however scarce and none of them really enforce any instruction (Pastor et al., 2019).

Many of these existing standards and guidelines are based on test results from laboratory experiments in which different wall, window, or deck materials are exposed to heat fluxes. Standards that specify the methodology for the evaluation of the performance of building sub-systems are available at national or regional levels, although many do not include wildfire exposure characterises, but rather use standard fire curves typical for fires inside buildings. Recently, some standard test methods that specifically consider wildfire exposure have been developed (e.g., AS 1530.8, Australia, 2018, ASTM E2632/E2632M-20 and ASTM E2886/E2886M-20, USA, 2020).

Additionally, there has been little empirical research examining the role of structural attributes in home survival during actual wildfires, where a wide range of conditions are present (Syphard et al., 2017). The current WUI hazard assessment tools have also generally not been developed using the results from a systematic and standardized field data collection methodology. This uncoupled approach limits the reliability of these tools as there has been no framework for coupling field exposure data to structure survivability (Maranghides and Mell, 2013). Thus, the systematic study using empirical pre- and post-fire data has been identified as critical research needed for better understanding structure loss at the WUI, particularly in terms of the relative effectiveness of building design materials, relative to other factors such as defensible space and housing density (Mell et al., 2010). The knowledge base on WUI fire behaviour and risk at community scale must therefore be improved (Pastor et al., 2019), and a shift should be made towards a quantitative analysis of the risks at the WUI, rather than a qualitative one. Additionally, the summary presented in Table1.2 highlights the lack of specific WUI microscale legislation, guidelines and quantitative tools in the most wildfire-prone European countries (Àgueda et al., 2023).

Table 1.2: Building and property elements for which risk reduction strategies/suggestions are mentioned in code, standards and guidelines that address WUI microscale risks. Adapted from (Àgueda et al., 2023).

Standards and Guidelines	**Defensible space**	**Roof**		**Gutters**	**Vents**	**Semi-confined spaces**	**Façade materials**	**Glazing systems**	**Shutters**
		Materials	**Maintenance**						
International WUI Code (International Code Council, 2021)	X	X		X	X[A]	X	X	X	X
AS 3959 – Australia (Australian Standards, 2018)	X	X		X	X	X	X	X	X
FireSmart – Canada (Government of Alberta, 2013)	X	X	X	X	X	X	X	X	X
Firewise - USA (NFPA, 2022)[B]	X	X	X	X	X	X	X	X	X
France (Ministère de l'Écologie et du Développement durable, 2002)	X	X	X		X		X		X
Portugal (Autoridade Florestal National, 2008)	X								
Italian regional guidelines: Piemonte (Regione Piemonte, 2021), Sardegna (Regione Autonoma della Sardegna, 2022)	X								
Spanish regional guidelines: Generalitat Valenciana (Manca and López, 2014), Catalunya (Generalitat de Catalunya, 2019)	X	X	X	X	X	X	X	X	X

[A] Requirements for vents refer to ignition-resistant classes 1 and 2.
[B] Guideline for homeowners based on NFPA Standards such as NFPA 1140 (National Fire Protection Association, 2022).

1.4. Quantitative approach

Two issues must be dealt with to make the scale quantitative: the critical lack of quantitative information on the exposure of properties and structures to embers and fire; and the lack of a well-characterized, systematic effort that combines pre- and post-fire observations, laboratory and field experiments, and fire modelling. An exposure and structure response database is also required to successfully develop the WUI-scale approach (Maranghides and Mell, 2013).

Modelling frameworks are already available to the scientific community, which are capable of handling the complexity of WUI microscale scenarios with a high degree of reliability, and therefore assist fire risk analysis and inform policy-making processes. They are physically-based CFD (Computational Fluid Dynamics) tools, which, relying on a proper characterization of fire energy released and building features, can provide information on key variables for WUI risk management (e.g. temperatures and heat exposure on people and assets, evolution of the smoke layer and toxic doses, etc.). These CFD tools can be used for Performance-Based Design (PBD) evaluations of complex fire scenarios (Vacca et al., 2020a).

Performance-Based Design is an *engineering approach to fire protection design based on agreed upon fire safety goals and objectives, deterministic and/or probabilistic analysis of fire scenarios, and quantitative assessment of design alternatives against the fire safety goals and objectives using accepted engineering tools, methodologies, and performance criteria* (Society of Fire Protection Engineers, 2007). It is established on three key aspects (Hurley and Rosenbaum, 2016):

- The definition of the desired level of fire safety, meaning the type of performance the proposed design must guarantee to meet the fire safety goals and objectives related to life, assets and environment protection.
- The definition of design scenarios, which include the potential type of fires and the occupants and building characteristics for which protection must be provided.
- The analysis of the proposed design strategies to determine whether or not they provide the intended level of safety.

PBD is being significantly applied to face particular fire safety challenges related to prescriptive codes compliance when applied to singular constructions or new materials (e.g., high-rise buildings, atria, long tunnels, green buildings (Chow 2015; Chu et al. 2007)); to update old prescriptions of existing code (Meacham, 2010); and to design according to advanced goal-oriented building acts - e.g., (Machado Tavares, Lopes Tavares, and Parry-jones 2008; Borg 2015). PBD has taken root in several regions with a settled fire engineering culture (e.g., Northern Europe, Southeast Asia, New Zealand, and Australia) and is being implemented in many others (e.g., Southern Europe, North America). Moreover, PBD gives valuable insights on how a building performs in case of fire, it is a suitable methodology to address unique design characteristics and its outcomes are clearer and more targeted (Hurley and Rosenbaum, 2016).

When it comes to the WUI, regulatory bodies, research institutions and practitioners are starting to address its fire safety challenges with the aid of PBD methods. In the USA, the

National Fire Protection Agency (NFPA) has recommended considering a design fire scenario of an outside fire exposure for PBD projects involving WUI structures (National Fire Protection Association, 2018).

Empirical observations from past fires can give valuable information on factors, processes and consequences responsible of fire damage at home-owner scale (Blanchi et al., 2006). Analysis of past fires allows for the identification of complex interactions between fuels, fire and assets from which initial assumptions regarding structure damage can be drawn. These lessons learnt from WUI fires can be used as a baseline for the design of scenarios that can be analysed by CFD tools through performance-based criteria (Vacca et al., 2020a). This way, the degree of safety that meets the objectives of life and property protection can be assessed in a quantitative way.

FDS (Fire Dynamic Simulator, NIST, 2020) has been validated in multiple fire engineering applications and it is nowadays the most popular CFD modelling tool for PBD evaluations of complex fire scenarios. It allows to model the many variables and thus scenarios these problems present with great flexibility in the definition of different configurations, materials and fire loads present at the WUI microscale, which is otherwise very difficult to achieve in experimental tests. With the proper characterization of the fire source and of the building features, FDS can provide information on key variables for WUI risk management. This tool allows for the analysis of a large number of scenarios and can cover the diverse fire safety needs of the WUI microscale, such as the quantification of the hazards associated to combustible materials placed close to structures, the assessment of the vulnerability of these structures, or the testing of current regulations. Results from these simulations can then be compared to previously set performance criteria, in order to obtain relevant and solid conclusions. By following a PBD methodology, fire scenarios which involve the following issues can be analysed (Vacca et al., 2020a):

- Houses vulnerability assessment: building performance analysis for structure triage (i.e. defensible/indefensible houses).
- Sub-systems hazard testing: hazard assessment of individual fuels (e.g. stored materials, ornamental and wildland vegetation, etc.) and performance evaluation of specific building components (e.g. openings, glazing systems, etc.).
- Post-fire investigation: quantitative analysis of past incidents to identify main causes of fire losses, illustrate lessons learnt and provide evidences to insurance covering assessment.
- Fire safety regulations improvements: design of PBD WUI-specific standards/codes and revision of prescriptive ones.

1.5. Thesis scope and Objectives

The goal of this work is to analyse fire hazards and building vulnerabilities present at the WUI microscale, and to develop a risk analysis framework that will help creating fire-adapted communities. The scope includes buildings and properties located within the Mediterranean landscape.

Specific objectives are set in order to meet the goal of the thesis:

- To assess structural survivability of Southern-European WUI structures by analysing the different paths of ignition at the microscale.
- To develop a methodology to quantitatively assess vulnerability in Mediterranean WUI microscale environments.
- To develop a quantitative risk analysis guideline applicable to new and existing buildings at the WUI, with the aim of providing Performance-Based Design strategies for the WUI microscale. This will be useful to fire practitioners for the analysis of complex scenarios, in order to create safer designs.

1.6. References

Àgueda, A., Vacca, P., Planas, E., Pastor, E., 2023. Evaluating wildfire vulnerability of Mediterranean dwellings using fuzzy logic applied to expert judgement. Int. J. Wildl. Fire. https://doi.org/10.1071/WF22134

Alexander, M.E., 1982. Calculating and interpreting forest fire intensities.Can. J. Bot. 60:349-357. https://doi.org/10.1139/b82-048

Australian Standards, 2018. AS 3959: Construction of buildings in bushfire-prone areas.

Autoridade Florestal National, 2008. Gestão de Combustíveis Para Protecção de Edificações - Manual. OPAL. https://fogos.icnf.pt/sgif2010/InformacaoPublicaDados/gestao_comb_final.pdf

Barbosa, T.F., Reis, L., Raposo, J., Rodrigues, T., Viegas, D.X., 2023. LPG stored at the wildland–urban interface: recent events and the effects of jet fires and BLEVE. Int. J. Wildl. Fire 1–15. https://doi.org/10.1071/wf22084

Blanchi, R., Leonard, J., 2005. Investigation of bushfire attack mechanisms resulting in house loss in the ACT bushfire 2003. Bushfire CRC Report, 61. https://www.bushfirecrc.com/sites/default/files/downloads/act_bushfire_crc_report.pdf

Blanchi, R., Leonard, J.E., Leicester, R.H., 2006. Lessons learnt from post-bushfire surveys at the urban interface in Australia. For. Ecol. Manage. 234, S139. https://doi.org/10.1016/j.foreco.2006.08.184

Borg, A., 2015. A Framework for Selecting Design Fires 995–1017. https://doi.org/10.1007/s10694-014-0454-x

Caballero, D., Sjöström, J., 2019. WUIVIEW Deliverable D5.1 - Inventory of pattern scenarios.

Calkin, D.E., Cohen, J.D., Finney, M.A., Thompson, M.P., 2014. How risk management can prevent future wildfire disasters in the wildland-urban interface. Proc. Natl. Acad. Sci. U. S. A. 111, 746–751. https://doi.org/10.1073/pnas.1315088111

Caton, S.E., Hakes, R.S.P., Gorham, D.J., Zhou, A., Gollner, M.J., 2017. Review of Pathways for Building Fire Spread in the Wildland Urban Interface Part I: Exposure Conditions. Fire Technol. 53, 429–473. https://doi.org/10.1007/s10694-016-0589-z

Cheney, N.P., 1990. Quantifying bushfires. Math. Comput. Model. 13, 9–15. https://doi.org/10.1016/0895-7177(90)90094-4

Chow, W.K., 2015. Performance-based approach to determining fi re safety provisions for buildings in the Asia-Oceania regions. Build. Environ. 91, 127–137. https://doi.org/10.1016/j.buildenv.2015.04.007

Chu, G.Q., Chen, T., Sun, Z.H., Sun, J.H., 2007. Probabilistic risk assessment for evacuees in building fires 42, 1283–1290. https://doi.org/10.1016/j.buildenv.2005.12.002

Cohen, J., 2010. The wildland-urban interface fire problem. Fremontia 38:2. https://www.fs.usda.gov/rm/pubs_other/rmrs_2010_cohen_j002.pdf

Cohen, J.D., 2000. Preventing Disaster: Home Ignitability in the Wildland-Urban Interface. J. For. 98, 15–21.

Costa, H., De Rigo, D., Libertà, G., Houston Durrant, T., San-Miguel-Ayanz, J., 2020. European wildfire danger and vulnerability in a changing climate: towards integrating risk dimensions. https://doi.org/10.2760/46951

De Melo Moreira, P., 2017. Portugal-Fire. Getty Images. https://www.gettyimages.es/detail/fotografía-de-noticias/picture-shows-a-burnt-house-whose-owner-died-fotografía-de-noticias/697642522?adppopup=true (accessed 6.12.23).

De Rigo, D., Libertà, G., Houston Durrant, T., Artes Vivancos, T., San-Miguel-Ayanz, J., 2017. Forest fire danger extremes in Europe under climate change: variability and uncertainty. https://doi.org/10.2760/13180

European Environment Agency, 2017. Climate change adaptation and disaster risk reduction in Europe. Enhancing coherence of the knowledge base, policies and practices, EEA Report. https://doi.org/10.1007/s13398-014-0173-7.2

Filkov, A.I., Ngo, T., Matthews, S., Telfer, S., Penman, T.D., 2020. Impact of Australia's catastrophic 2019/20 bushfire season on communities and environment. Retrospective analysis and current trends. J. Saf. Sci. Resil. 1, 44–56. https://doi.org/10.1016/j.jnlssr.2020.06.009

FireSmart Canada, 2020. FireSmart Home Ignition Zone Assessment Score Card. https://firesmartbc.ca/wp-content/uploads/2021/04/FSC-CRI-Home-Ignition-Zone-Assessment-Score-Card-Fillable.pdf

Ganteaume, A., Barbero, R., Jappiot, M., Maillé, E., 2021. Understanding future changes to fires in southern Europe and their impacts on the wildland-urban interface. J. Saf. Sci. Resil. 2, 20–29. https://doi.org/10.1016/j.jnlssr.2021.01.001

Generalitat de Catalunya, 2019. Protegeos de los incendios forestales. Pla INFOCAT. https://interior.gencat.cat/web/.content/home/030_arees_dactuacio/proteccio_civil/consells_autoproteccio_emergencies/incendi_del_bosc/documents/llibret_incendis_forestals_cast.pdf

Government of Alberta, 2013. FireSmart Guidebook for Community Protection: A Guidebook for Wildland/Urban Interface Communities. https://open.alberta.ca/dataset/7d246651-b1c2-4689-bc18-4e23f5a6e4fd/resource/8c5d6f82-ec68-4466-85ae-4b28878ae21d/download/7032001-2013-11-firesmart-guidebook-community-protection-guidebook-wildland-urban.pdf

Hakes, R.S.P., Caton, S.E., Gorham, D.J., Gollner, M.J., 2017. A Review of Pathways for Building Fire Spread in the Wildland Urban Interface Part II: Response of Components and Systems and Mitigation Strategies in the United States. Fire Technol. 53, 475–515. https://doi.org/10.1007/s10694-016-0601-7

Hurley, M.J., Gottuk, D.T., Hall, J.J.R., Harada, K., Kuligowski, E.D., Puchovsky, M., Torero, J.L., Watts, J.J.M., CJ, W., 2016. SFPE Handbook of Fire Protection Engineering, 5th ed. Springer. https://doi.org/10.1007/978-1-4939-2565-0

Hurley, M.J., Rosenbaum, E.R., 2016. Performance-Based Design, in: Hurley, M.J., Gottuk, D.T., Hall, J.J.R., Harada, K., Kuligowski, E., Puchovsky, M., Torero, J.L., Watts, J.J.M., Wieczorek, C.J. (Eds.), SFPE Handbook of Fire Protection Engineering. Springer, pp. 1233–1261.

International Code Council, 2021. International Wildland-Urban Interface Code (IWUIC). https://codes.iccsafe.org/content/IWUIC2021P1

International Union of Forest Research Organizations, 2018. Global Fire Challenges in a Warming World. https://pure.iiasa.ac.at/id/eprint/15707/1/op32.pdf

Intini, P., Ronchi, E., Gwynne, S., Bénichou, N., 2019. Guidance on Design and Construction of the Built Environment Against Wildland Urban Interface Fire Hazard: A Review. Fire Technol. 56, 1853–1883. https://doi.org/10.1007/s10694-019-00902-z

Jones, M.W., Abatzoglou, J.T., Veraverbeke, S., Andela, N., Lasslop, G., Forkel, M., Smith, A.J.P., Burton, C., Betts, R.A., van der Werf, G.R., Sitch, S., Canadell, J.G., Santín, C., Kolden, C., Doerr, S.H., Le Quéré, C., 2022. Global and Regional Trends and Drivers of Fire Under Climate Change. Rev. Geophys. 60, 1–76. https://doi.org/10.1029/2020RG000726

Keeley, J.E., Pausas, J.G., 2019. Distinguishing disturbance from perturbations in fire-prone ecosystems. Int. J. Wildl. Fire 28, 282–287. https://doi.org/10.1071/WF18203

Machado Tavares, R., Lopes Tavares, J.M., Parry-jones, S.L., 2008. The use of a mathematical multicriteria decision-making model for selecting the fire origin room 43, 2090–2100. https://doi.org/10.1016/j.buildenv.2007.12.010

Manca, T., López, M., 2014. Guía Metodológica de Actuaciones de Prevención, Defensa y Autoprotección en la Interfaz Urbano-Forestal, Generalitat Valenciana. https://agroambient.gva.es/documents/162905929/162908876/Gu%C3%ADa+metodol%C3%B3gica+de+Actuaciones+de+Prevenci%C3%B3n%2C%20Defensa+y+Autoprotecci%C3%B3n+en+la+Interfaz+Urbana-Forestal+%286%2C8Mb%29/d24a0daf-d777-405b-8938-b4a54394831f

Manzello, S.L., Blanchi, R., Gollner, M.J., Gorham, D., McAllister, S., Pastor, E., Planas, E., Reszka, P., Suzuki, S., 2018. Summary of workshop large outdoor fires and the built environment. Fire Saf. J. 100, 76–92. https://doi.org/10.1016/j.firesaf.2018.07.002

Maranghides, A., Link, E.D., Quarles, S.L., Gorham, D.J., 2022. NIST Technical Note 2205 WUI Structure / Parcel / Community Fire Hazard Mitigation Methodology. https://doi.org/10.6028/NIST.TN.2205

Maranghides, A., Mcnamara, D., Vihnanek, R., Restiano, J., Leland, C., 2015. A Case Study of a Community Affected by the Waldo Fire – Event Timeline and Defensive Actions. http://dx.doi.org/10.6028/NIST.TN.1910

Maranghides, A., Mell, W., 2013. Framework for Addressing the National Wildland Urban Interface Fire Problem--Determining Fire and Ember Exposure Zones Using a WUI Hazard Scale. NIST Tech. Note 1748 Framew. 1–33. https://doi.org/http://dx.doi.org/10.6028/NIST.TN.1748

Maranghides, A., Mell, W., 2011. A Case Study of a Community Affected by the Witch and Guejito Wildland Fires. Fire Technol. 47, 379–420. https://doi.org/10.1007/s10694-010-0164-y

McNeill, I.M., Dunlop, P.D., Skinner, T.C., Morrison, D.L., 2016. A value- and expectancy-based approach to understanding residents' intended response to a wildfire threat. Int. J. Wildl. Fire 25, 378–389. https://doi.org/10.1071/WF15051

Meacham, B.J., 2010. Performance-Based Building Regulatory Systems-Principles and Experiences. Inter-jurisdictionalRegulatory Collab. Comm. 174. https://doi.org/ISBN 978 0 7559 9238 6

Meerpoel-Pietri, K., Tihay-Felicelli, V., Graziani, A., Santoni, P.A., Morandini, F., Perez-Ramirez, Y., Bosseur, F., Barboni, T., Sánchez-Monroy, X., Mell, W., 2022. Modeling with WFDS Combustion Dynamics of Ornamental Vegetation Structures at WUI: Focus on the Burning of a Hedge at Laboratory Scale. Combust. Sci. Technol. 00, 1–31. https://doi.org/10.1080/00102202.2021.2019235

Mell, W., Manzello, S.L., Butry, D., Rehm, R.G., 2010. The wildland-urban interface fire problem - Current approaches and research needs. Int. J. Wildl. Fire 19, 238–251. https://doi.org/10.1071/WF07131

Ministère de l'Écologie et du Développement durable, 2002. Plans de prévention des risques naturels (PPR): Risques d'incendies de forêt. https://www.ecologie.gouv.fr/sites/default/files/PPR_feux_de_foret_complet_0.pdf

Mitsopoulos, I., Mallinis, G., Dimitrakopoulos, A., Xanthopoulos, G., Eftychidis, G., Goldammer, J.G., 2020. Vulnerability of peri-urban and residential areas to landscape fires in Greece: Evidence by wildland-urban interface data. Data Br. 31, 106025. https://doi.org/10.1016/j.dib.2020.106025

Molina-Terrén, D.M., Xanthopoulos, G., Diakakis, M., Ribeiro, L., Caballero, D., Delogu, G.M., Viegas, D.X., Silva, C.A., Cardil, A., 2019. Analysis of forest fire fatalities in Southern Europe: Spain, Portugal, Greece and Sardinia (Italy). Int. J. Wildl. Fire 28, 85–98. https://doi.org/10.1071/WF18004

Munich RE, 2021. Record hurricane season and major wildfires – The natural disaster figures for 2020. https://www.munichre.com/en/company/media-relations/media-information-and-corporate-news/media-information/2021/2020-natural-disasters-balance.html (accessed 6.12.23).

National Fire Protection Association, 2022. NFPA 1140, Standard for Wildland Fire Protection.

National Fire Protection Association, 2018. NFPA 101 - Life Safety Code.

National Fire Research Laboratory, 2020. Fire Calorimetry Database (FCD).

https://doi.org/https://doi.org/10.18434/mds2-2314

NFPA, 2022. Prepare Your Home Wildfire Risk Reduction Steps That Can Make Your Home Safer During a Wildfire. https://www.nfpa.org//-/media/Files/Firewise/Fact-sheets/FirewiseHowToPrepareYourHomeForWildfires.pdf

NIST, 2022. Fire Dynamics Simulator.

Partners in Protection, 2003. Firesmart: Protecting Your Community from Wildfire, Partners in Protection. https://firesmartcanada.ca/wp-content/uploads/2022/01/FireSmart-Protecting-Your-Community.pdf

Pastor, E., 2019. Direct Flame Contact. Encycl. Wildfires Wildland-Urban Interface Fires 1–7. https://doi.org/10.1007/978-3-319-51727-8_64-1

Pastor, E., Muñoz, J.A., Caballero, D., Àgueda, A., Dalmau, F., Planas, E., 2019. Wildland-Urban Interface Fires in Spain: Summary of the Policy Framework and Recommendations for Improvement. Fire Technol. https://doi.org/https://doi.org/10.1007/s10694-019-00883-z

Regione Autonoma della Sardegna, 2022. Prescrizioni regionali antincendio. https://www.sardegnaambiente.it/documenti/19_173_20220505140518.pdf

Regione Piemonte, 2021. Piano regionale per la programmazione delle attività di previsione, prevenzione, e lotta attiva contro gli incendi boschivi. https://www.regione.piemonte.it/web/sites/default/files/media/documenti/2021-03/piano_aib_2021_2025.pdf

Ribeiro, L.M., Rodrigues, A., Lucas, D., Viegas, D.X., 2020. The impact on structures of the pedrógão grande fire complex in June 2017 (Portugal). Fire 3, 1–22. https://doi.org/10.3390/fire3040057

San-Miguel-Ayanz, J., Durrant, T., Boca, R., Maianti, P., Libertà, G., Oom, D., Branco, A., De Rigo, D., Ferrari, D., Roglia, E., Scionti, N., 2023. Advance report on Forest Fires in Europe, Middle East and North Africa 2022. https://doi.org/10.2760/091540

Scarponi, G.E., Pastor, E., Planas, E., Cozzani, V., 2020. Analysis of the impact of wildland-urban-interface fires on LPG domestic tanks. Saf. Sci. 124, 104588. https://doi.org/10.1016/j.ssci.2019.104588

Society of Fire Protection Engineers, 2007. SFPE Engineering Guide to Performance-Based Fire Protection. Society of Fire Protection Engineers (SFPE).

Syphard, A.D., Brennan, T.J., Keeley, J.E., 2017. The importance of building construction materials relative to other factors affecting structure survival during wildfire. Int. J. Disaster Risk Reduct. 21, 140–147. https://doi.org/10.1016/j.ijdrr.2016.11.011

The Guardian, 2018. Greece fires: state of emergency declared as deadly blazes rage. https://www.theguardian.com/world/2018/jul/23/greeks-urged-to-leave-homes-as-wildfires-spread-near-athens (accessed 5.21.21).

Thompson, C., 2001. USA Federal Register. 66, 3. https://www.govinfo.gov/content/pkg/FR-2001-01-04/pdf/01-52.pdf

Vacca, P., Caballero, D., Pastor, E., Planas, E., 2020a. WUI fire risk mitigation in

Europe: A performance-based design approach at home-owner level. J. Saf. Sci. Resil. 1, 97–105. https://doi.org/10.1016/j.jnlssr.2020.08.001

Vacca, P., Àgueda, A., Muñoz, J.A., Planas, E., Pastor, E., Heymes, F., Ismael, E., Eyssette, R., Cozzani, V., Scarponi, G.E., 2020b. WUIVIEW Deliverable 6.1 - Recommendations on structure survivability and sheltering capacity. https://wuiview.webs.upc.edu/download/D6.1_F_Recommendations%20on%20structure%20survivability%20and%20sheltering%20capacity.pdf

Vacca, P., Planas, E., Mata, C., Muñoz, J.A., Heymes, F., Pastor, E., 2022. Experimental analysis of real-scale burning tests of artificial fuel packs at the Wildland-Urban Interface. Saf. Sci. 146. https://doi.org/10.1016/j.ssci.2021.105568

Westhaver, A., 2017. Why some homes survived: Learning from the Fort McMurray wildland/urban interface fire disaster, ICLR research paper series. https://retooling.ca/wp-content/uploads/2020/10/ICLR_Why_Some_Homes_Survived.pdf

Whittaker, J., Blanchi, R., Haynes, K., Leonard, J., Opie, K., 2017. Experiences of sheltering during the Black Saturday bushfires: Implications for policy and research. Int. J. Disaster Risk Reduct. 23, 119–127. https://doi.org/10.1016/j.ijdrr.2017.05.002

Whittaker, J., Haynes, K., Handmer, J., McLennan, J., 2013. Community safety during the 2009 Australian “Black Saturday” bushfires: An analysis of household preparedness and response. Int. J. Wildl. Fire 22, 841–849. https://doi.org/10.1071/WF12010

Chapter 2

Identification and characterisation of pattern scenarios at the WUI microscale

2.1 Introduction

As presented in Chapter 1, susceptibility of a home to wildfire depends on the management of its surroundings and the hardening of the structure itself. Three types of fuels have been identified within the surroundings of a building located at the WUI: these are natural fuels such as wildland or ornamental vegetation, and artificial fuels such as other buildings or adjacent structures, outdoor furniture, stored materials, etc. As for the structure, vulnerable elements have been identified based on the analysis of ignition pathways of buildings during past WUI fire events. Building elements that are weak to fire exposure are the roof, glazing systems and vents. Additionally, structural damage can be caused by the presence of secondary structures adjacent to the building that are populated with all sorts of fuels, which, if ignited, will release enormous amounts of heat that can possibly damage the envelope of the building.

In this chapter, the pathways at the WUI microscale that lead to fire entrance in a building are analysed with the aid of a fault tree. Scenarios that lead to this top event involving both structural vulnerabilities and surrounding fuels are presented, which include the presence of vegetation and artificial fuels in front of a glazing system, the presence of combustible materials in a semi-confined space, and the proximity of fuels to LPG tanks. Given the lack of scientific data on these scenarios, they are further analysed with CFD tools in Chapter 3. For this purpose, performance criteria are identified for each of the selected scenarios. Moreover, an analysis is performed on the characteristics of potential fire exposure for these scenarios. Fire characteristics that can be used as inputs for FDS simulations are presented for wildland and ornamental vegetation as well as for artificial fuels. Given the lack of quantitative information on the combustion of artificial fuels located at the WUI microscale, and especially on fuel packs, four tests have been performed on four different fuel packs. Results on the burning behaviour of these fuel packs are also presented in this chapter[1].

2.2 Scenarios based on microscale vulnerabilities

The different ways that can lead to a fire entering a building at the WUI, focusing on Mediterranean-type structures, can be synthetized within a fault tree. Fault tree analysis is a deductive failure analysis that focuses on an undesired event (named top event) and provides a method for determining causes of this event. A fault tree is a complex of entities known as gates, which serve to permit or inhibit the passage of fault logic up the

[1] The content included in this chapter was published as two journal papers (Vacca et al., 2020; Vacca et al., 2022) and one conference paper (Heymes et al., 2021).

tree (U.S. Nuclear Regulatory, 1981). The gates show the relationships of events (inputs) needed for the occurrence of a higher event, which is the output of the gate. Events that do not require further development are called basic events (symbolized by circles), while intermediate events (symbolized by rectangles) occur because of one or more antecedent causes acting through logic gates. There are two basic types of fault tree gates: the OR-gate and the AND-gate. The OR-gate is used to show that the output event occurs only if one or more of the input events occur, while the AND-gate is used to show that the output fault occurs only if all the input faults occur.

Following this top-down logical method, a fault tree has been created for the undesired top event of fire entering a building, as shown in Figure 2.1. This fault tree reports the different observed patterns that can lead to the fire entering a structure during all of the fire exposure phases presented in Chapter 1 (pre-impact, impact, fire transfer and post-frontal combustion), therefore identifying the weaknesses of Mediterranean-type WUI structures. Currently, buildings in the Mediterranean area are constructed with industrial materials such as concrete or bricks and aluminium or PVC (e.g., for window frames, gutters, etc.), while the roof covering is usually made out of terracotta (clay) tiles (OERCO2, 2017a, 2017b). Identified patterns of fire entrance consider therefore this building typology.

One of the observed ways a fire can enter a building is through windows or doors that are left open due to sudden and unprepared evacuation, or through poorly designed or maintained vent ducts, which directly connect the interior of the building with the exterior. Flames or firebrands can enter the building through these openings and can start indoor ignition of curtains, furniture, or any light fuels. This may progress into full involvement of a room and the eventual burning of the entire building, if left unattended. In a wildfire, roofing is directly exposed to firebrands, radiation and even flames. The degree of maintenance and the accumulation of debris on the roof valleys and gutters are two of the suspected factors behind the entrance of fire through the attic, the involvement of the roofing structure and its eventual collapse. Another pathway through which a fire can enter a building is through broken window panes. The combustion of fuels commonly present on a property, if placed close to unprotected glazing elements (i.e., fuels are poorly managed), can cause cracking or collapsing of the glass, hence giving way to the entrance of smoke, firebrands and flames. Direct flame impingement or high radiative heat loads onto window panes or other weak points within the house envelope can greatly affect structures' integrity. Confined or semi-confined spaces such as garages, sheds, or storage areas, which contain non-natural fuels, are also vulnerable to firebrands, radiation exposure and flame impingement. As previously stated, these secondary structures are often placed close to the main structure or are extensions of it. A large accumulation of heat in those areas due to the ignition of their contents could lead to fire spread to the main structure through internal doors, passageways, or windows, as well as to structural damage to the house envelope (Vacca et al., 2020).

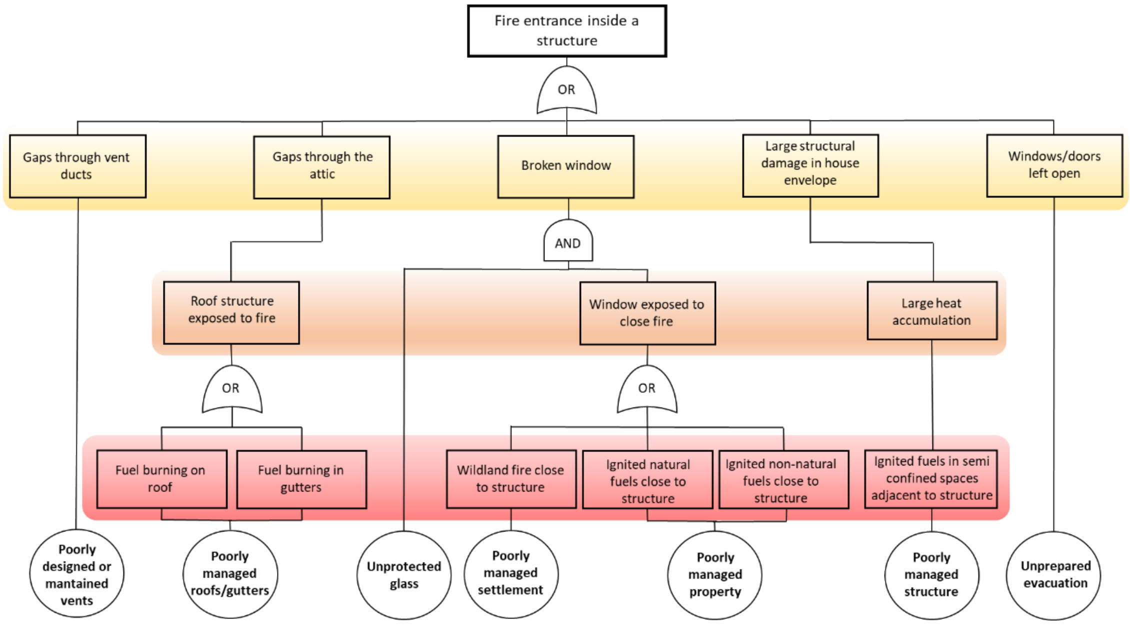

Figure 2.1: Fault tree describing observed patterns that lead to fire entrance inside a structure. The red area identifies the fire source, the orange one the impact of the fire onto the structure, and the yellow one pinpoints the ways through which the fire can enter the structure. Adapted from Vacca et al. (2020).

The WUI microscale standards and guidelines presented in Chapter 1 address some of the identified issues. When it comes to vents, all guidelines or standards state that they should be protected by a non-combustible mesh, therefore vents are deemed to be poorly designed when they are unprotected, protected by a combustible mesh or when the non-combustible mesh is damaged. As for the roof, all guidelines or standards require a non-combustible roof covering (typical of Mediterranean buildings), and some also require adequate maintenance of the roof and gutters by clearing the accumulation of leaves and branches (Generalitat de Catalunya, 2019; Government of Alberta, 2013; International Code Council, 2021; Manca and López, 2014) and non-combustible gutters (Australian Standards, 2018; International Code Council, 2021). As the roof covering of Mediterranean buildings is typically made of non-combustible materials, the roof and gutters are deemed to be poorly maintained when no cleaning is performed or the roof covering presents missing, displaced or broken tiles.

A poorly managed settlement is identified when properties located at the border of a settlement located at the WUI are directly facing the forested land where no fuel reduction strip is present or, when present, it is not well maintained. Additionally, abandoned plots within a settlement, where no fuel management is performed, can intensify the impact of the wildfire onto the neighbouring properties.

A poorly managed property is identified when fuels are located too close to the building, and specifically to windows, which are very vulnerable to radiant heat exposure or direct flame impingement. Existing guidelines and standards that specifically address the Mediterranean-type WUI microscale include some rules on the distancing between vegetation and buildings: some regions in France (Préfet de Bouches-du-Rhône, 2014; Préfet de la Haute-Corse, 2022; Préfet des Alpes-de-Haute-Provence, 2013; Prefet des Alpes-Maritimes, 2014; Préfet du Var, 2015) as well as in Spain (Manca and López, 2014) set the minimum distance between trees or shrubs and a building at 3 m; in Portugal, this distance is set at 5 m (Autoridade Florestal National, 2008). Other guidelines and standards do not provide a distance, but simply state to trim overhanging trees and shrubs (Cal Fire, 2022; South Australia County Fire Service, 2022; Victoria County Fire Authority, 2022), remove or prune flammable plants and shrubs near windows (Cal Fire, 2022) or to not place plants greater than 10 cm in height at maturity directly in front of a window or other glass feature (Victoria County Fire Authority, 2022).

Properties can also be poorly managed when fuels are not spaced correctly. During a wildfire, firebrands will land on a property, possibly being the first source of ignition of fuels located in the area. Should these fuels be ignited, and distancing from other fuels or the building is appropriate, this will not cause further fire spread to other elements nor impact the building’s vulnerable elements (Àgueda et al., 2023). Rules for the distancing between fuels within these standards and guidelines are examined in Chapter 4, although one specific scenario is here analysed further: the placing of fuels (natural and artificial) close to LPG tanks. As described in Chapter 1, when a tank is exposed to flames or radiation from a fire, its pressure will increase possibly causing the opening of the PRV (Pressure Relief Valve), which will create a jet fire. The jet fire will worsen the heat load to the tank and the surroundings. If no measure is taken in order to cool down the tank and/or extinguish the fire, the tank may fail, leading to a loss of containment. Depending on the type of failure, intense jet fires from shell cracks, BLEVEs (Boiling liquid Expanding Vapor Explosions) and fireballs may follow. Rules for safety distances are not harmonized worldwide, and in Europe they are different in each country and depend on the volume of the tank, as given in Figure 2.2. Italy has the most restrictive requirements, while Spain has the less restrictive ones (Scarponi et al., 2020).

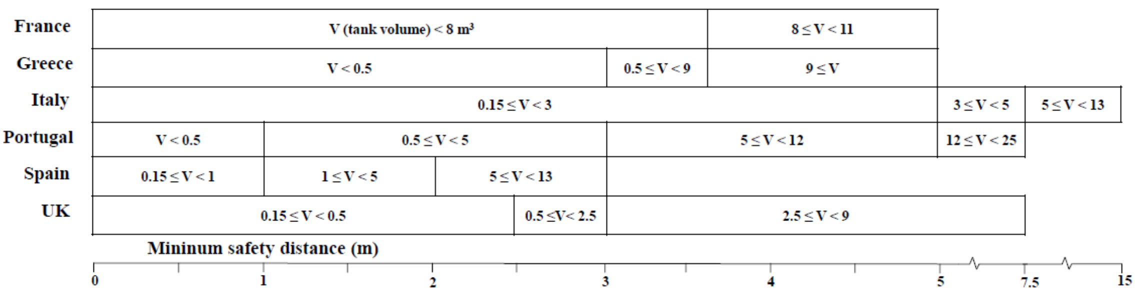

Figure 2.2: Minimum safety distances as a function of tank volume V (in m^3) for different European countries. Adapted from Scarponi et al. (2020).

When it comes to semi-confined spaces, most standards and guidelines only mention that decks and porches should be built out of non-combustible or fire-resistant materials. Few rules exist on the presence of fuels in these spaces, and they mostly only include firewood as the type of fuel. Only in the USA rules state to never store flammable materials underneath decks or porches (Cal Fire, 2022; NFPA, 2022). More information is thus needed on how to identify a poorly managed structure.

Given the identified discrepancies within standards and guidelines and the fact the rules they enforce are frequently poorly supported by scientific evidence and studies that consider the appropriate parameters and processes that explain fire behaviour and effects on assets at the relevant scale (Pastor et al., 2019), the following scenarios are further analysed in this thesis:

- The placing of fuels (natural and artificial) in front of glazing systems (including the effect of frame and shutters) in order to scientifically identify safe distances at which different fuel types can be located;
- The placing of fuels (natural and artificial) close to LPG tanks for the identification of safe distances at which the pressure inside the tank will not rise to reach the value that will cause the opening of the PRV;
- The combustion of fuels inside concrete semi-confined spaces, in order to identify the heat load at which failure of the envelope can occur.

These are scenarios that include especially vulnerable elements, and have been highlighted as critical, as described in Chapter 1, especially within the Mediterranean landscape. Additionally, for these cases, an optimal degree of maintenance does not influence the vulnerability of the selected building or property sub-system, as it might for other scenarios identified in the fault tree in Figure 2.1.

The selected scenarios are analysed in depth in Chapter 3 following a Performance Based Design (PBD) approach. To do this, performance criteria and fire source inputs need to be selected, which is done in the following sections.

2.3 Definition of performance criteria

The vulnerability to fire of a building’s sub-system can be quantified by analysing the response of the material to the radiation coming from a fire. Threshold values, defined as performance criteria, can be set to indicate when unacceptable damage will occur (Hurley and Rosenbaum, 2016). These threshold values are here identified for each of the previously mentioned scenarios.

2.3.1 Glazing systems

No standard or guideline gives a performance criterion for glazing systems exposed to a fire located at the exterior of a building. PBD guidelines such as the Verification Method from New Zealand (Ministry of Business Innovation and Employment, 2013) suggest as criterion for the breaking of windows with non-fire resisting glazing either the moment when the average upper smoke layer temperature reaches 500°C or when the fire becomes limited by ventilation. These are criteria that cannot be used in outdoor scenarios, therefore a literature review of the performance of glazing systems exposed to fire is carried out to identify the best criterion for these types of scenarios. This review focuses on findings for framed glazing systems with float glass, which is the type of glass commonly used in residential windows (Feldmann and Kasper, 2014).

The breaking mechanism for framed glass panes exposed to a fire environment has been identified as the temperature difference between the heated part of the pane and the shielded edge located below the frame (Keski-Rahkonen, 1988; Pagni, 1988). Thermal stress is built up at the edge, causing cracking to occur usually at a small defect of the pane. Given the uncertainty in the values of the tensile stress at breakage for float glass due to its variation in composition, treatment and flaws, the measured variable mostly found in the literature when analysing framed windows is the critical temperature difference for cracking, ΔT_{cr}. Keski-Rahkonen suggests a value of 100°C as a criterion for cracking and immediate breakage (i.e., creation of a vent), while Pagni identified a much lower value of 58°C (both values are independent form the thickness of the pane). Skelly et al. (1991) confirmed this methodology for the prediction of the time of window breakage by performing full-scale experiments in a compartment setting, where aluminium framed window panes (2.4 mm thick with 25 mm frame width) were immersed in a hot smoke layer. In this case, the authors suggest a ΔT_{cr} value of 70°C as a performance criterion for window breakage and they observed that breakage happened in less than 1 s after the first crack occurred.

Mowrer (1998) performed both small- and large-scale tests on framed windows (wooden and vinyl frames) exposed to a uniform radiative heat flux (float glass, unknown thickness). He identified another performance criterion as the product of the imposed heat flux by the time required for the cracking of the pane: the heat load. For both types of tests, the imposed heat load at cracking was an average value of 900 kJ/m^2 (data for vinyl framed windows is not included because breakage occurred at low heat fluxes due to the melting of the frame). In the large-scale tests with single pane wooden-framed windows, he also identified the average ΔT_{cr} at cracking as 68°C for the lower light of the window and 96°C for the upper light. These values remain in the same range as those identified by the previously mentioned authors. Average measured glass temperature at failure was 123°C for the lower light and 157°C for the upper light. Other tests on 3 mm framed float glass (with a frame width of 15 mm) exposed to a uniform radiant heat flux were performed by Harada et al. (2000), which identified an average ΔT_{cr} of 52°C and an average temperature at the centre of the pane of 89°C at cracking. The information given in this paper allows to calculate the heat load at cracking, which had an average value of 971 kJ/m^2. Tests on glazing systems exposed to laboratory simulated wildfires were performed in Australia by Bowditch et al. (2006). Most tests were performed on unframed float glass or on laminated or toughened glazing systems. Some data is however available on timber framed 4 mm thick float glass. An average heat load at failure could be calculated, obtaining a value of 800 kJ/m^2. The average glass temperature at failure was recorded as approximately 100°C (average based on the peak measurements recorded for each test). The temperature of the glass below the frame was not provided; therefore, the ΔT_{cr} could not be calculated. Wang et al. (2017) exposed single and double pane (6 mm thickness) framed systems (with 10 mm shading) to a heptane pool fire, where the primary heat transfer mode was thermal radiation. The authors identified a ΔT_{cr} of 60-90°C, which includes also coated and laminated glass types. For float glass, the average critical ΔT is 74°C, and the average critical temperature at the centre of the glass is 155°C. The heat load at failure could only be calculated for one of the tests, and resulted in a value of 1679 kJ/m^2. It was also identified that the breakage of the second pane in double pane assemblies required significantly higher heat fluxes compared to the first one, but that the breakage occurred at approximately the same ΔT_{cr}. In all performed experiments, it was observed that cracking initiated at the edges. Chen et al. (2017) exposed 6 mm thick glass panes with a stainless-steel frame to a radiant heating source. They analysed different shading widths of the frame, with values from 10 mm to 50 mm. For comparison with other tests, only results for the 10 mm and 20 mm are analysed. As expected, the temperature of the glass below the frame at cracking decreases with the increasing of the width of the frame; therefore, the difference between the temperature at the centre of the pane and the one below the frame increases with the increase of the width of the frame.

For a width of 10 mm and 20 mm, the average value of ΔT_{cr} was found to be respectively 108°C and 123°C. The average temperature of the centre of the pane at cracking, which does not depend on the width of the frame, was 174°C.

As can be noted from these results, summarized in Table 2.1 critical values for float glass cracking in framed assemblies vary significantly: average ΔT_{cr} values vary in the range 52-123°C, average surface temperature values vary between 89°C and 174°C while calculated heat load values vary in the range 800-1679 kJ/m^2. According to the reviewed literature, there seems to be a trend when it comes to the thickness of the pane only for the surface temperature of the glass (the thicker the pane, the higher the surface temperature at cracking). This trend is not reflected in the other two criteria.

Given the significant variation of the identified critical values, a decision on the selection of the performance criteria needs to be made. As the thickness of the glass does not seem to influence the criteria, average values obtained from the analysed literature data are chosen as performance criteria for the analysis of the scenarios that include glazing systems. Failure will occur for whichever value is reached first.

Table 2.1: Summary of tests performed on framed float glass. Average values obtained from each set of experiments are presented for each criterion. ΔT_{cr} is the critical temperature difference between the heated part of the pane and the shielded edge located below the frame, T_{surf} is the glass temperature at failure and HL is the heat load at failure.

Reference	**Pane thickness [mm]**	**ΔT_{cr} [°C]**	**T_{surf} [°C]**	**HL [kJ/m^2]**
Keski-Rahkonen, 1988	All thicknesses	100	-	-
Pagni, 1988	All thicknesses	58	-	-
Skelly et al., 1991	2.4	70	-	-
Mowrer, 1998	-	82	140	900
Harada et al., 2000	3	52	89	971
Bowditch et al., 2006	4	-	100	800
Wang et al., 2017	6	74	155	1679
Chen et al., 2017	6	108 and 123	174	-
Average values	-	**83**	**132**	**1087**

Performance criteria are also selected for the frame of glazing systems, due to the fact that its deformation could cause the glass pane to break, or the ignition of a combustible frame can contribute to the heat load onto the glass. Frame materials include aluminium, PVC and wood. For aluminium and PVC frames, the melting point is chosen as a performance criterion. For aluminium this is reached when the temperature of the material is 660°C, while this temperature is 220°C for PVC (Chen et al., 2011). As for wood, it is a charring material, therefore, during combustion, it will build up a layer of char on its surface that will tend to shield the unaffected fuel lying beneath; when wood is burnt, 15-25% normally remains as char (Drysdale, 2011). Although this char layer protects the underlying materials, the heat produced by the combustion of wood can impact the glass pane that is supported by the frame. Therefore, the performance criteria for wood are the critical radiant heat flux ($\dot{q}''_{rad}$) and the critical surface temperature for ignition (T_{surf}), given in Table 2.2. To be conservative, the values for piloted ignition are those considered as performance criteria. Failure is considered when one of these criteria is reached. The same criteria will be used for aluminium, PVC and wooden shutters.

Table 2.2: Criteria for ignition of wood (Drysdale, 2011).

Critical radiant heat flux [kW/m^2]		**Critical surface temperature [°C]**	
Piloted ignition	Spontaneous ignition	Piloted ignition	Spontaneous ignition
12	28	350	600

2.3.2 LPG tanks

According to the API 2510 (American Petroleum Institute, 2001), the integrity of an LPG tank exposed to fire is not compromised as long as: (i) the tank is equipped with a properly designed PRV (Pressure Relief Valve), i.e., the PRV prevents the vessel pressure from rising more than 21% above the design pressure, and (ii) the incident radiation is below 22 kW/m^2. The first considered performance criterion is therefore the value of 22 kW/m^2 for the incident radiation onto the tank. If the value of the incident radiation stays below this threshold, the scenario will be deemed safe. If this value is however larger than the threshold, further investigation on the integrity of the tank will be needed.

A methodology for the analysis of the impact of WUI fires on LPG domestic tanks has been developed by Scarponi et al. (2020), which identified performance criteria based on two different indicators: the WSI (Weakened Surface Index) and the PRVI (Pressure Relief Valve Index). The WSI is the ratio between the maximum surface area $S_{a,max}$ where the temperature is higher than 400°C (value above which the yield strength of plain carbon steel is decreased by 70% with respect to ambient temperature conditions) and the critical surface area S_c (with a value of 0.48 m^2), as given in Equation 2.1 (Scarponi et al., 2020):

$$WSI = \frac{S_{a,max}}{S_c} \tag{2.1}$$

The value of S_c has been derived from findings that suggest a rectangular defect larger than 1.2 m x 0.4 m (resulting in a surface area of 0.48 m^2) may cause a tank rupture in case of fire exposure. Here, this concept is extended considering that, if a fire generates a hot zone on the tank wall larger than S_c, the tank integrity is no longer guaranteed. Values of WSI higher than 1 indicate that the fire scenario under analysis represents a threat for the tank integrity, meaning that if a fire generates a hot zone on the tank wall larger than S_c, the tank integrity is no longer ensured.

The second performance criterion considers the additional critical point represented by the opening of the PRV. The PRVI is the ratio between the maximum pressure p_{max} reached during the tank response simulation and the PRV set point pressure p_{PRV}, as given in Equation 2.2 (Scarponi et al., 2020):

$$PRVI = \frac{p_{max}}{p_{PRV}} \tag{2.2}$$

Scenarios presenting a PRVI higher than 1 have the potential to result in an escalation of consequences, since the PRV will open releasing the content of the tank, which, if ignited, creates a jet fire.

A safety factor is applied to both criteria, setting thus the threshold at a value 0.9 (Scarponi et al., 2020).

2.3.3 Semi-confined spaces

As the majority of homes located in the Mediterranean region are built with non-combustible materials such as concrete, scenarios that include semi-confined spaces will be analysed with this material. Within EU member states, the Eurocode 2 is recognized as a reference document for the design of concrete structures (European Committee for Standardization, 2004a, 2004b). In scenarios that include semi-confined spaces attached to the main structure of a building, structural integrity is required during the entire time of fire exposure, meaning that the load bearing function (R) of the structure must be maintained. The reduction of the load bearing capacity of a concrete wall exposed to fire can be calculated according to Part 1-2 of Eurocode 2 (European Committee for Standardization, 2004b). The effects of actions on the structural member in case of fire can be obtained by multiplying the design value of actions for normal temperature by a reduction factor η_{fi}. This reduction factor ranges between 74% and 33% for all combinations of live/dead load ratio ($Q_{k,1}/G_k$, this is the ratio between the variable loads and the permanent loads the wall is subjected to) with a combination factor $\psi_{1,1}$= 0.5 (for domestic and residential buildings; this is a factor that takes into account the frequent variable actions imposed on the structure). This correlation is given in Figure 2.3, although the value of 33% is not pictured. Under the assumption that the member was designed with 100% utilization, it can be concluded that if the reduction factor η_{fi} (and therefore the load bearing capacity) is higher than 74% the wall will not fail, and that if it falls below 33%, then collapse of the structure is guaranteed.

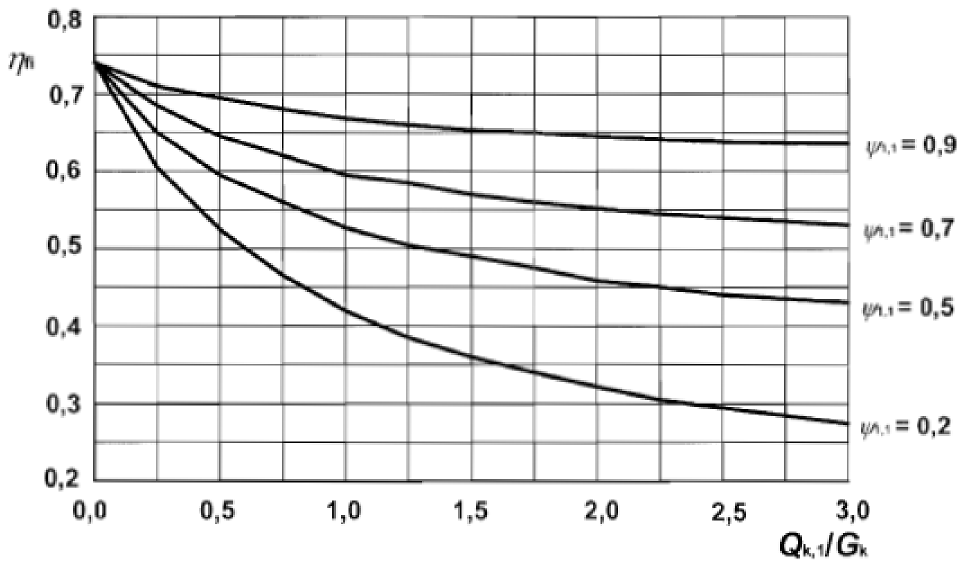

Figure 2.3: Variation of the reduction factor η_{fi} with the load ratio $Q_{k,1}/G_k$. Adapted from European Committee for Standardization (2004b).

2.4 Fire source characterisation

Four main fire sources that can approach a WUI microscale property have been identified: the wildfire front, the arrival of firebrands on the property and building, and the burning of natural and artificial fuels present at the microscale. As pointed out by observations from past fires (Blanchi et al., 2006; Leonard et al., 2009; Maranghides and Mell, 2011), the likelihood of house loss is mostly related to the interaction of firebrands attack with surrounding combustible elements, which results in flames too close to the structure, excepting those cases of houses adjoining the wildland which might then be exposed to shrubland or forest fire.

The threat posed by the burning of vegetation depends on the residence time of the fire (i.e. the length of time for the flame front to pass a given point (Alexander, 1982)) and on the flames' geometry. For wildfires, these characteristics vary greatly depending on the type of fuels (e.g. grassland, shrubland, forest stand, logging slash) (Alexander et al., 2007). Natural fuels placed around the house consist mostly of ornamental vegetation. As mentioned in Chapter 1, the intensity at which this vegetation burns as well as the duration of the flaming phase depend on the species and its level of maintenance (i.e. trimming, pruning, watering), which conditions the fuel load, the density and the moisture content of the vegetation (Vacca et al., 2020). As for artificial fuels, they vary significantly and are composed mostly out of plastic and wooden materials. Their Heat Release Rates (HRR) and burning times are also substantially variable, and they have the potential to burn with significant intensity and duration (Vacca et al., 2020).

When simulating fire exposure of a building or a building sub-system with CFD tools such as FDS, a simple pyrolysis model can be used, which needs as input either the Heat Release Rate Per Unit Area (HRRPUA, in kW/m^2) or the Mass Loss Rate Per Unit Area (MLRPUA, in kg/m^{2}s) of the ignited fuel or fuel pack. Complex pyrolysis models on the other hand need information on the products of the combustion of the material, as well as its physical and chemical properties. A complex pyrolysis model can also be used to simulate the combustion of vegetation (McGrattan et al., 2022). Fire sources for the simulations of the abovementioned scenarios are specified in the following sub-sections.

2.4.1 Wildland and ornamental vegetation

When it comes to wildland vegetation, the fireline intensity I_B (kW/m) represents the heat release rate of a linear segment of the fire perimeter, and it is a function of the fuel low heat of combustion H (kJ/kg), the amount of fuel consumed in the active flaming front w (kg/m^2), and the linear rate of fire spread r (m/s), as shown in Equation 2.3 (Byram, 1959):

$$I_B = H \cdot w \cdot r \tag{2.3}$$

Assuming a fuel low heat of combustion of 18000 kJ/kg, the fireline intensity can be obtained from the graph in Figure 2.4 for four different fuel complexes (Alexander and Cruz, 2019). If needed, the rate of fire spread r can be estimated to be 10% of the wind speed (Cruz and Alexander, 2019). The HRRPUA can then be calculated depending on the size of the fuel bed or, for an approaching wildfire front, on the horizontal flame depth

D. The flame depth (m) can be correlated with information on fuel consumption and wind speed, as shown in Equation 2.4 (Nelson and Adkins, 1988), where w is the fuel consumption (kg/m^2) and u is the ambient wind speed (m/s).

$$D = 0.39 \cdot w^{0.25} \cdot u^{1.51} \tag{2.4}$$

Once the flame depth and the fireline intensity are known, the HRRPUA (kW/m^2) can be calculated with Equation 2.5.

$$HRRPUA = \frac{I_B}{D} \tag{2.5}$$

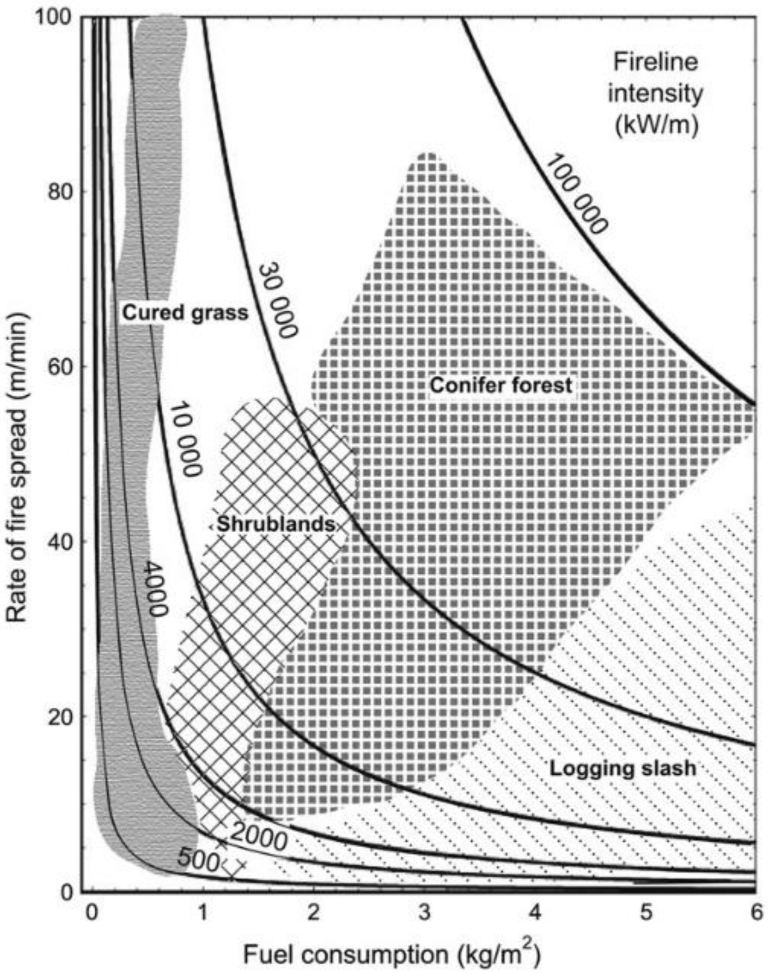

Figure 2.4: Fireline intensity as a function of rate of fire spread and fuel consumption, assuming a fuel low heat of combustion of 18000 kJ/kg, for four fuel complexes (Alexander and Cruz, 2019).

As for ornamental vegetation, many studies that focus on the burning of ornamental vegetation have been carried out at particle scale, although studies on the burning of whole vegetation elements are necessary for the validation of physics-based fire models (Meerpoel-Pietri et al., 2022) as well as for the selection of fire scenarios for Performance Based Design at the WUI. Currently, little data is available and it mostly consists of the burning of some tree species and shrubs, not all characteristic of the Mediterranean vegetation. Data from tests on ornamental vegetation is given in Table 2.3. The tests performed by Tramoni et al. (2018) and Meerpoel-Pietri et al. (2022) were however performed on vegetation with a very low moisture content, within the range of 3-20%, which do not necessarily correspond to a real situation. Tests performed by Etlinger and Beall (2004) included vegetation placed in pots and drip-watered every 2-3 days.

Table 2.3: Data on experimental burning of ornamental vegetation. MC: Moisture Content.

Species	**Dimensions width x length x height**	**Peak HRR [kW]**	**Burning time [s]**	**Reference**
Rockrose (*Cistus monspeliensis*)	0.68 m (diameter) x 1.23 m	228 ± 15	44 ± 9	Tramoni et al. (2018)
Rockrose	0.5 m x 0.5 m x 1 m	624.4± 61	400 ± 37	Meerpoel-Pietri et al. (2022)
Juniper (*Juniperus chinensis*)	-	150 (114% MC) 800 (31% MC)	-	Etlinger and Beall (2004)
Oleander (*Nerium oleander*)	-	150	-	Etlinger and Beall (2004)

Experiments were also performed during the WUIVEW project (Ribeiro et al., 2020), and preliminary results show that small shrubs of *Cupressus Arizonica* have a Mass Loss Rate (MLR) of 0.04 kg/s for an area of about 0.16 m^2, resulting in an HRRPUA of 4500 kW/m^2 when assuming a fuel low heat of combustion of 18000 kJ/kg (Alexander and Cruz, 2019).

Currently, FDS allows to model vegetation in form of Lagrangian particles, which undergo a solid-phase thermal decomposition process. The pyrolysis is modelled based on inputs which include the moisture content and bulk density of the vegetation and its physical properties (density, conductivity, specific heat capacity). The study performed by Meerpoel-Pietri et al. (2022) also included FDS modelling of their experiment, which provided a satisfactory prediction of the HRR curve and mass loss, although it has not yet been validated, while the simulation in FDS of the combustion of Douglas Fir trees (Mell et al., 2009) has been validated (McGrattan et al., 2022). When modelling vegetation as particles, the HRR curve is an output of the simulation. The HRR curve of a Douglas Fir tree of a height of 1.9 m and a moisture content of 14%, simulated in FDS 6.7.9, is shown in Figure 2.5.

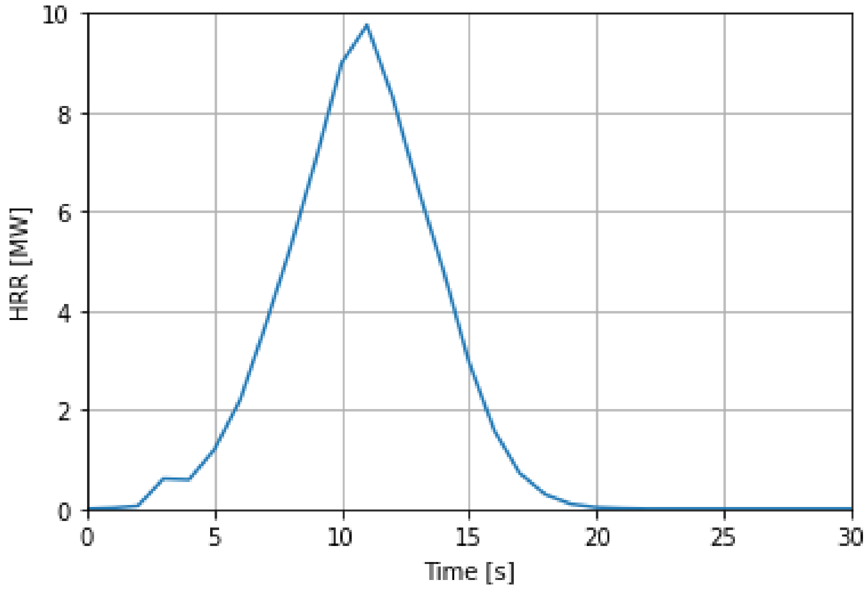

Figure 2.5: HRR curve for a Douglas Fir tree with a height of 1.9 m and 14% moisture content.

2.4.2 Artificial fuels

The burning behaviour of common artificial fuels that can be found indoors (e.g. pieces of furniture and small appliances) has been extensively analysed in small- and real-scale tests (Hurley et al., 2016; National Fire Research Laboratory, 2020). Some of these analysed fuels can also be found on a property, for example a stack of wooden pallets with a height of 0.9 m, with an HRR curve given in Figure 2.6. Additionally, studies of fires in indoor parking lots have identified the HRR curve for the combustion of two cars, as shown in Figure 2.7. This curve is used for the Performance-Based Design of ventilation systems in car parks.

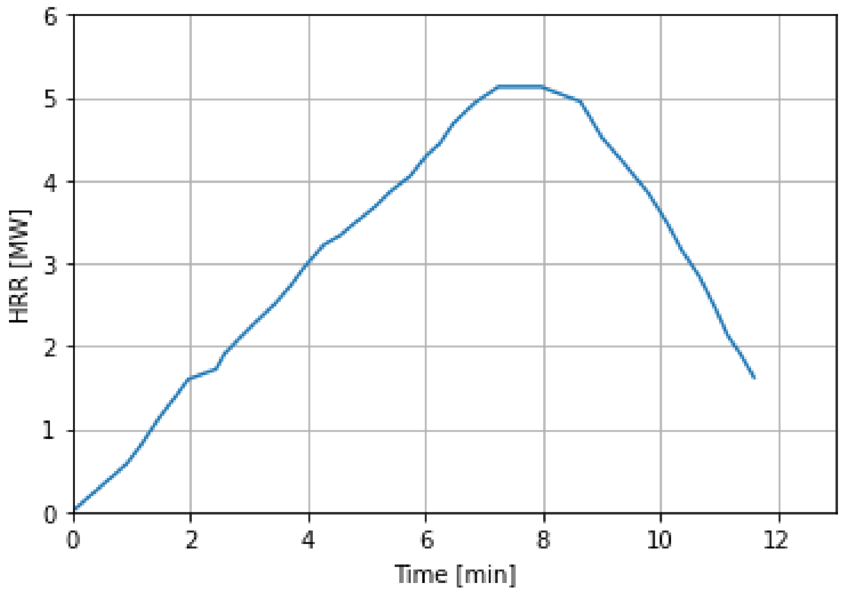

Figure 2.6: HRR curve of a stack of a stack of wooden pallets (Karlsson and Quintiere, 2000).

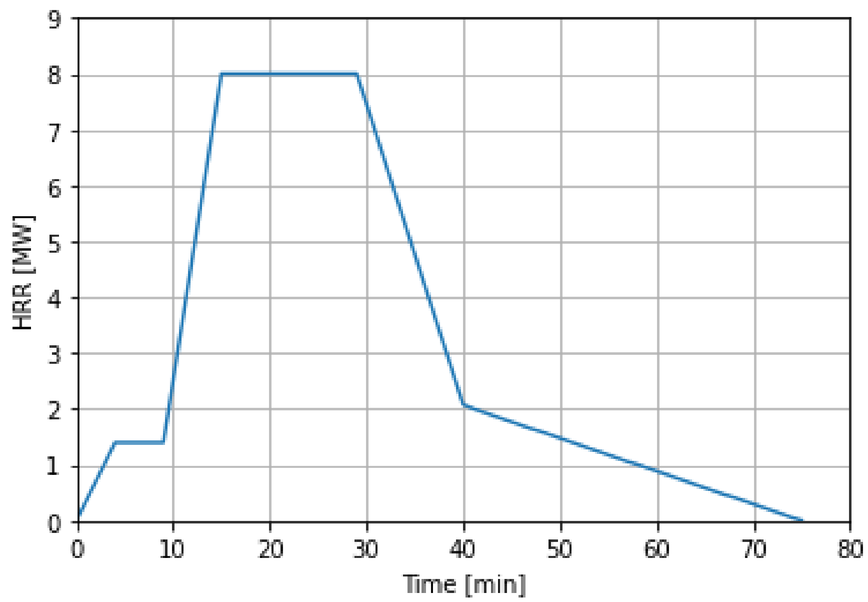

Figure 2.7: HRR curve of the combustion of two cars. Adapted from Belgische normcommissie (2014).

However, there is a lack of quantitative data on the burning behaviour of fuels and fuel packs (i.e., accumulation of various fuels that consist of different types of materials) that are frequently located in the surroundings of WUI structures. Subsequently, the hazard posed by these fuels is poorly understood (Mell et al., 2010).

2.5 Real-scale tests on artificial fuel packs

Given the lack of quantitative information on fuel packs located at the WUI microscale, real-scale tests of four different fuel packs have been performed on items that are commonly present at WUI properties. All four fuel packs contain items commonly found on WUI properties, and they correspond to residential fuel scenarios identified from past fires. The tests were performed in the large-scale testing platform of The French National Institute for Industrial Environment and Risks (INERIS), equipped with a Tewarson calorimeter with a capacity up to 10 MW. The facility consisted of a 10 m x 10 m room with a 5 m x 5 m scale, covered by sand, on which the items were placed. The hood was located directly above the scale at a height of approximately 10 m, and air could flow in the room through two openings located on its northern and southern sides. Ambient temperature was around 7°C for the first two tests, 6°C for the third and 9°C for the final test.

The instrumentation used in the tests is given in Figure 2.8. Medtherm Gardon heat flux sensors were located in the same position for each test. Meters F1, F2, F5 and F6 measured the total heat flux at a height of 1 m, meters F3 and F7 at a height of 2 m, and meter F4 at 2.5 m. Five visual cameras recorded the tests for the identification of their timeline, while an infrared camera (Optris PI-640) recorded flame temperatures. Flame heights and width could also be extracted from the recordings of the IR camera located on the north side of the facility. This was performed with the aid of a software that allows to segment video sequences, extracting a mask of the flame contour from several IR-images (Mata et al., 2018).

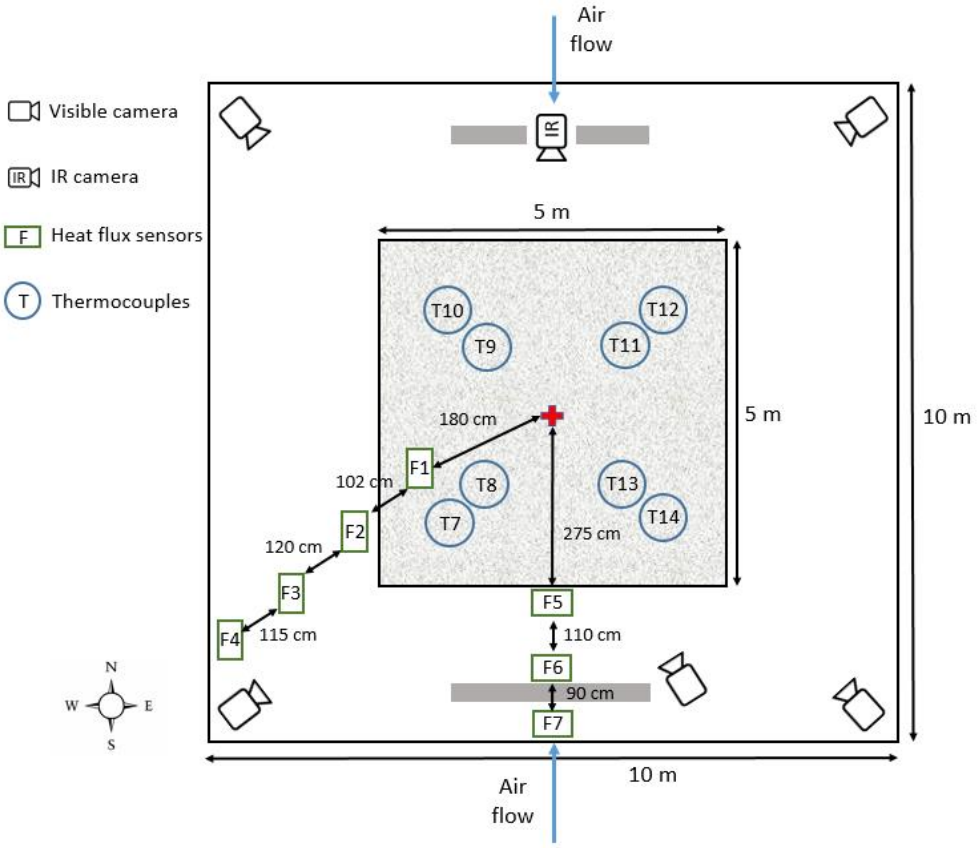

Figure 2.8: Experimental setup.

Six type K 1.5 mm thermocouples (T1-T6) were located on the fuel pack items to record flame temperatures. The recording system however malfunctioned during tests 2 and 4, so data from these thermocouples was only obtained for tests 1 and 3. Eight 1 mm thermocouples (T7-T14) were placed at certain distances from the burning fuel pack to record air temperatures at a height of 60 cm. The distance between these eight thermocouples and the fuel packs was different for each test, as can be seen from Table 2.4, due to the different sizes of the packs. Thermocouple T13 did not record any data for test 2 due to malfunction.

Table 2.4: Location of thermocouples measuring air temperatures.

Thermocouple	Distance from the fuel pack [m]			
	Test 1	Test 2	Test 3	Test 4
T7	1.10	1.21	1.11	1.10
T8	0.60	0.71	0.61	0.60
T9	1.02	1.55	0.74	0.72
T10	1.52	2.05	1.24	1.22
T11	0.52	0.74	0.60	0.55
T12	1.02	1.24	1.10	1.05
T13	0.57	-	0.36	0.60
T14	1.07	0.98	0.86	1.10

Heat Release Rate (HRR), mass loss, smoke’s species concentration, heat flux and temperature data was recorded every two seconds. Two gas burners were used for the ignition of the items, which provided a HRR up to 140 kW and were turned off once the items showed self-sustained flaming, given that the goal of the tests was to determine their burning behaviour once ignited, and not their critical values for ignition. The tests were performed in well-ventilated conditions. Smoke species concentrations were measured from the exhaust flow. CO_2 and CO concentrations were given by a Non-Dispersive Infrared (NDIR) analyser, the total unburned hydrocarbons (THC) concentrations were measured by a Flame Ionization Detector (FID), and O_2 concentrations by a paramagnetic oxygen analyser.

The first fuel pack consisted of outdoor children's toys, bags with clothes and boxes with paper and books, the second one of pallets, cardboard sheets, paint buckets and foam mats. The fuels in the third test were an outdoor table with six chairs, six cushions and a parasol, and those in the final test consisted of three oil-based paint buckets (the same as those in test 2). Items' dimensions, weight and material composition for each test are given in Table 2.5.

Table 2.5: Item characteristics for each test. Test 4 contains the same paint buckets as those in test 2.

Item	Length [m]	Width [m]	Height [m]	Mass [kg]	Material
Test 1					
Toy house	1.08	1.40	1.15	13.9	Polypropylene
Slide	1.35	0.46	0.67	3.32	Polyethylene
Cotton clothes bag	0.60	0.60	0.80	10.7	Cotton, polyethylene
Wool clothes bag	0.60	0.60	0.80	3.4	Wool, polyethylene
Synthetic clothes bag	0.60	0.60	0.80	3.8	Polyamide, polyester, polyethylene
Toy lawn mower	0.60	0.23	0.25	0.36	Polypropylene
Tricycle	0.52	0.68	0.52	3.4[a]	Polypropylene, steel
Painting	0.90	0.60	0.03	1.4	Wood, paper, paint
Box with books	0.30	0.40	0.30	13.48	Paper, cardboard
Box with paper	0.30	0.40	0.30	14.76	Paper, cardboard
Box of tricycle	0.47	0.22	0.46	0.2	Cardboard
Test 2					
Pallet 1 Pallet 2 Pallet 3	1.2	0.8	0.13	11.4 13.2 15.7	Wood
Foam mat	1.2	0.6	0.12	2.15	Polyester
Cardboard	1.6	0.004	0.65	0.55	Cardboard
Paint bucket	0.28	0.28	0.22	12.27	Oil-based paint Polypropylene bucket
Test 3					
Table	2.20	1.00	0.72	23.00	Polypropylene
Chair	0.58	0.59	0.91	2.72	Polypropylene
Cushion	0.38	0.38	0.02	0.07	Cotton, polyester
Parasol	3.00	3.00	2.50	11.50[b]	Polyester, steel

[a] including 1.4 kg of steel
[b] including 8.25 kg of steel

2.5.1 Test 1

The fuel pack in test 1 consisted of fuels that could be found together in backyards or stored in secondary structures at the WUI. These comprised plastic toys, 3 bags of clothes (one containing cotton, one wool and one synthetic fabrics) and 2 boxes containing books and paper (Figure 2.9). The total mass of the fuel pack amounted to about 69 kg. The two burners pointed towards opposite sides of the fuel pack, one towards the slide and the other towards the back of the toy house, and were active for 70 seconds. By this time, the toy house had partially melted and its roof had collapsed on top of the items placed in the house. After 3 minutes all plastic items had completely melted, creating a pool fire scenario.

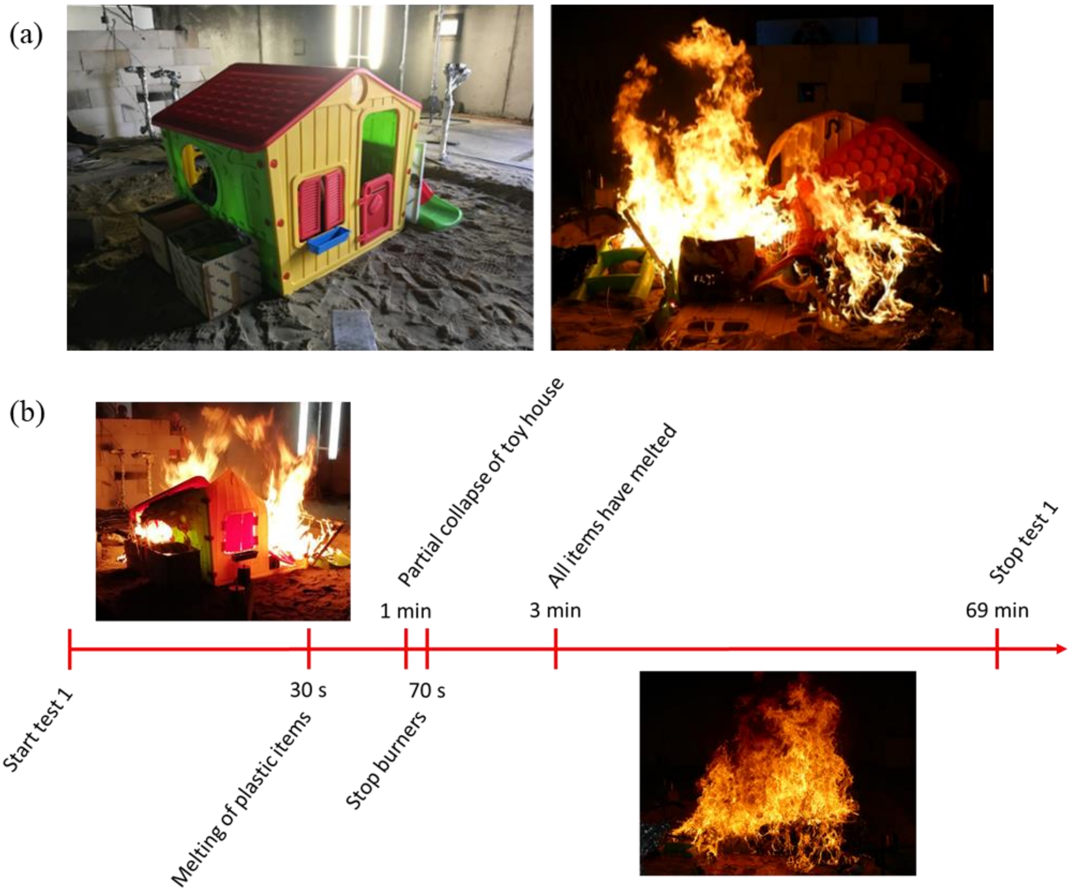

Figure 2.9: Test 1; (a) on the left: fuel pack just before ignition, on the right: fuel pack burning 90 seconds after ignition; (b) timeline of the test.

Thermocouple T1 was placed on top of the toy house, T2 inside the bag containing cotton clothes, T3 inside the bag of synthetic clothes, T4 inside one of the boxes, T5 inside the bag containing wool clothes and T6 at the bottom of the house. The other thermocouples were placed according to the distances given in Table 2.4.

2.5.2 Test 2

Test 2 consisted of a fuel pack containing typical fuels that are stored in semi-confined spaces located on WUI properties. These are 3 pallets, 4 small mattresses, 11 cardboard sheets, and 7 plastic buckets containing each 12 l of oil-based paint (Figure 2.10). The items' characteristics are given in Table 2.5 and the total weight of the fuel pack amounted to 140.8 kg. The two burners were placed on opposite sides of the fuel pack, pointing towards the stack of pallets, and were active for about 30 seconds, during which nearly all items ignited, with the exception of the cardboard sheets shielded from the flames. The paint started spilling from the buckets after about 40 seconds, creating a pool underneath the pallets and the cardboard. The foam mats melted on top of the pallets after 70 seconds. By this time all items of the fuel pack had ignited. In test 2 thermocouples registering air temperature were placed around the fuel pack as given in Table 2.4.

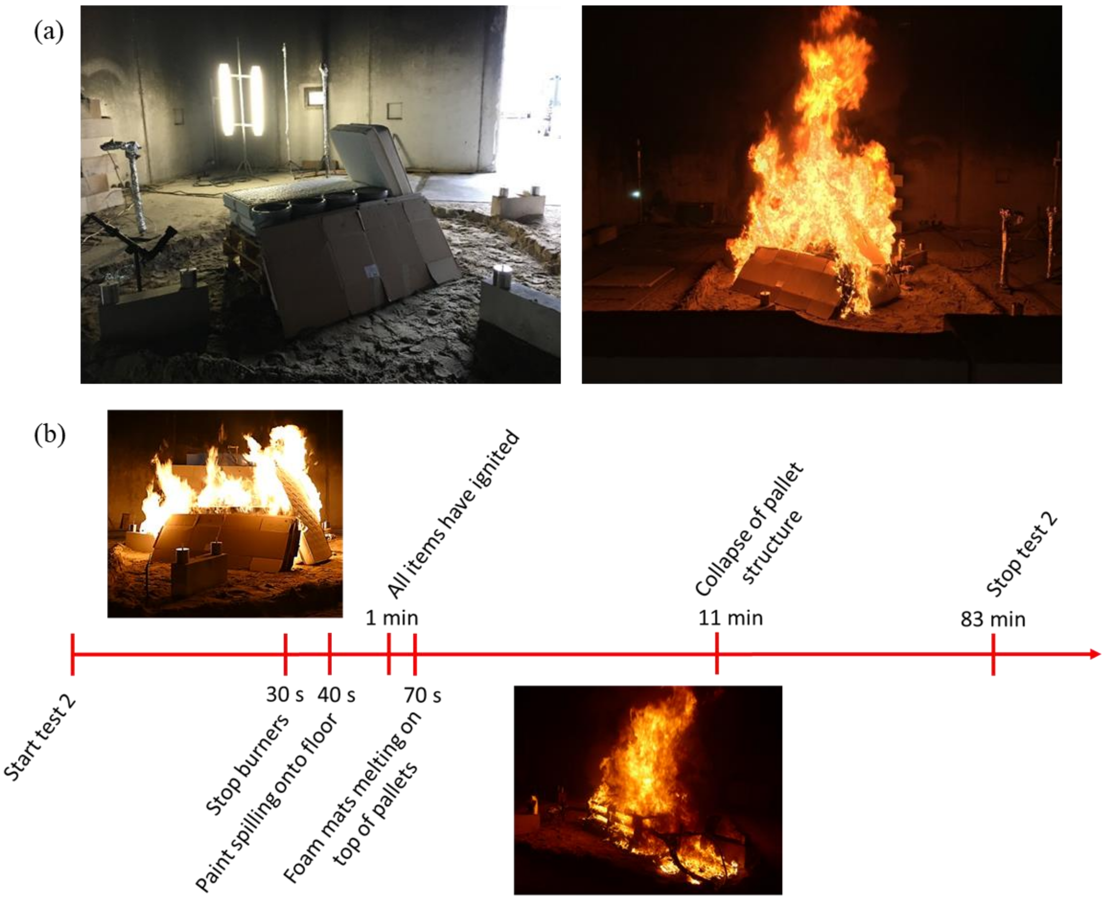

Figure 2.10: Test 2; (a) on the left: fuel pack just before ignition, on the right: fuel pack burning 90 seconds after ignition; (b) timeline of the test.

2.5.3 Test 3

The third fuel pack represents a typical outdoor furniture set, present in gardens or porches, usually located in the vicinity of a WUI dwelling. It consisted of an outdoor table with 6 chairs, 6 cushions and 1 parasol, as can be seen in Figure 2.11. The dimensions, weight and material composition of the items are given in Table 2.5. The total weight of the fuel pack amounted to 51.3 kg. The two burners were directed towards each end of the table, pointing underneath the table towards the back of the chairs. The table and chairs started melting within 20 seconds from the activation of the burners, and within 1 minute, four chairs had collapsed to the ground. During this test the two burners malfunctioned and did not flare in a continuous way, providing effective ignition for a total of about 1.5 minutes. They were then stopped after 130 seconds from the start of the test. Within 4 minutes all the items had melted creating a pool fire scenario, which burned until the stop of the test, after 49 minutes. In this test, five thermocouples (T1, T2, T3, T5, T6) were placed on five chairs, T4 was placed on the table underneath a cushion, while the other eight were placed further from the fuel pack, at the distances given in Table 2.4.

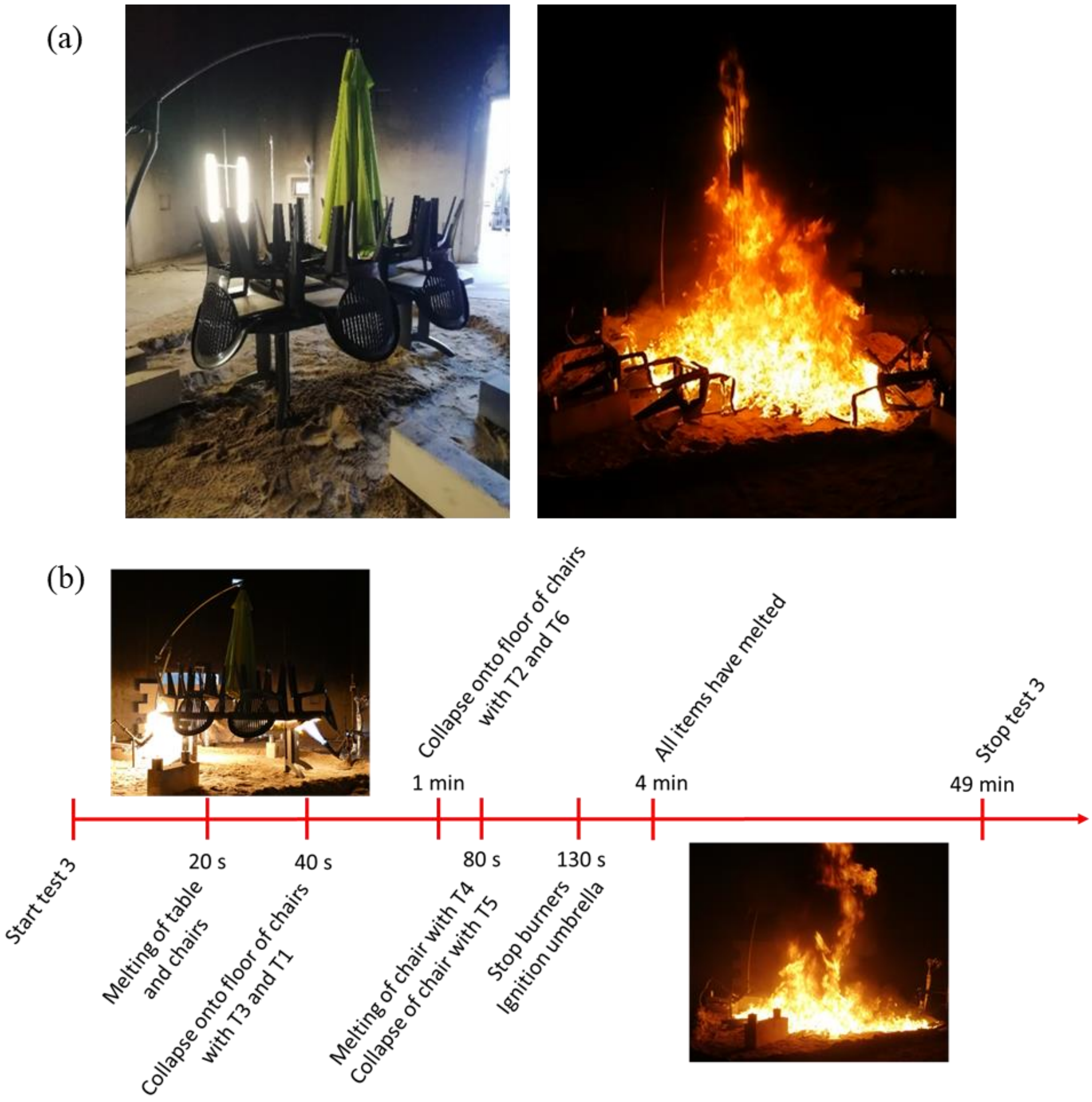

Figure 2.11: Test 3; (a) On the left: fuel pack just before ignition, on the right: fuel pack burning 150 seconds after ignition; (b) timeline for the test.

2.5.4 Test 4

Test 4 consisted of 3 plastic buckets containing each 12 l of oil-based paint (Figure 2.12), which are typical fuels that are stored on properties at the WUI. These buckets had the same characteristics as those present in test 2. The total weight of this fuel pack amounted to 36.8 kg. Only one burner, pointing towards the middle bucket, was used to ignite the items for 35 seconds. Within 45 seconds from the start of the test all three buckets had partially melted and released the paint onto the floor, creating a pool fire scenario. After 85 seconds all the buckets had completely melted. In this test, the thermocouples were located at different distances from the fuel pack, as given in Table 2.4.

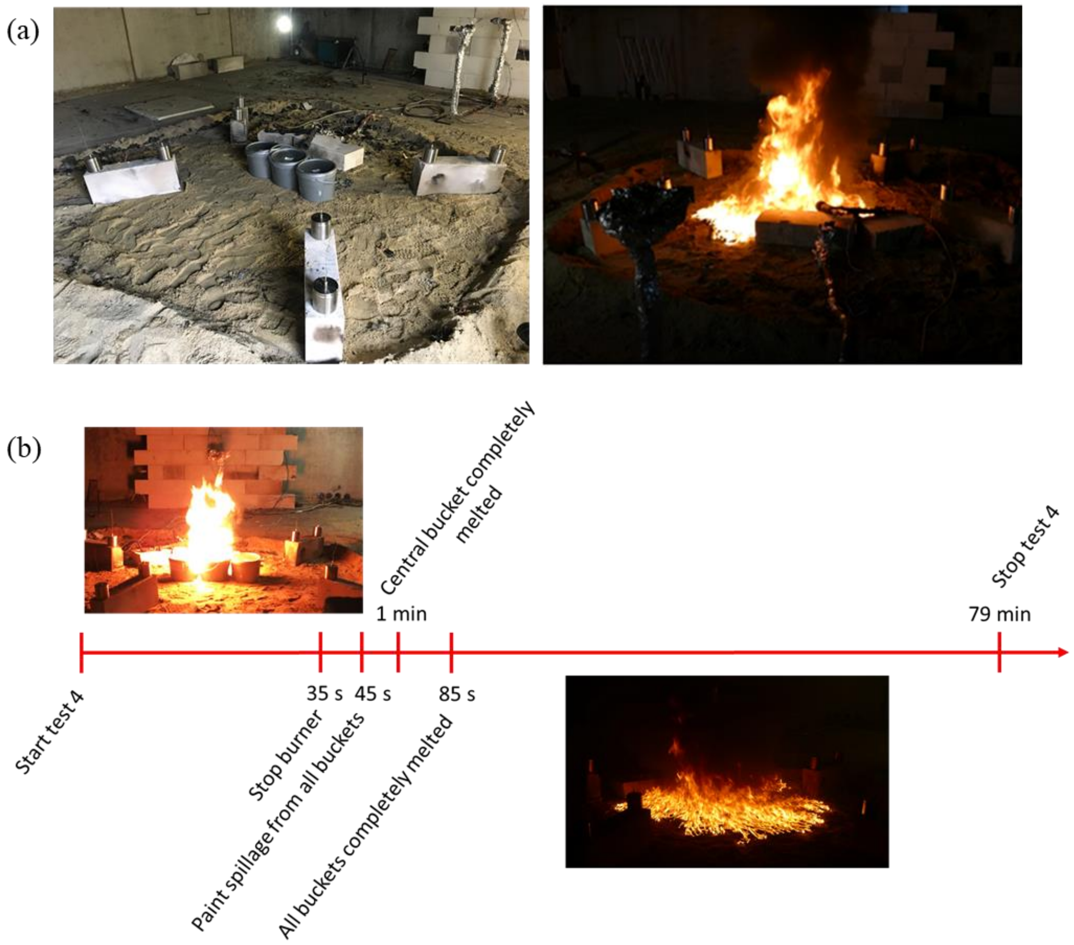

Figure 2.12: Test 4; (a) On the left: fuel pack just before ignition, on the right: fuel pack burning 70 seconds after ignition; (b) timeline for the test.

2.5.5 Results

As previously mentioned, the combustion of the fuel packs in test 1, test 3 and test 4 created pool fire scenarios, due to the presence of a high amount of plastic materials. This did not happen in test 2, which mostly consisted of cellulosic materials. HRR, MLR, fire load, smoke species concentrations, heat fluxes, temperatures and flame heights have been obtained for each test. Peak values are given in Table 2.6, while details are discussed in the following sub-sections.

Table 2.6: Values recorded for each test.

	Test 1	**Test 2**	**Test 3**	**Test 4**
Initial mass [kg]	69.0	140.8	51.3	36.8
Peak HRR [kW]	1472	2551	2178	383
Peak MLR [kg/s]	0.20	0.30	0.25	0.15
Peak CO concentration [ppm]	73.2	192.8	160.9	62.8
Peak flame height [m]	2.65	3.23	3.60	2.64
Peak air temperature [°C]	76	104	148	115
Peak heat flux [kW/m^2]	11.4	19.9	21.1	4.3
Fire duration [min]	69	82	49	72
Effective fire load [MJ]	1121	1743	1008	313

Heat Release Rate, growth rate, Mass Loss Rate and fire load

Heat Release Rates were recorded for each test as given in Figure 2.13. The HRR measured for each fuel pack also includes the one of the burners, which is considered as negligible given the fact that the maximum operational time of the burners is 1.5 minutes, corresponding to a HRR of 140 kW, and that for test 3, in which the operational time was discontinuous. Tests 3 and 4 were stopped once the fire had extinguished, while tests 1 and 2 ran until the HRR values dropped below 45 kW. All test reached the peak HRR values within the first 5 minutes. The fuel pack of test 2 presented the highest HRR values, reaching a peak of 2.55 MW, while the one of test 4 resulted in much lower HRR values, not even reaching 400 kW.

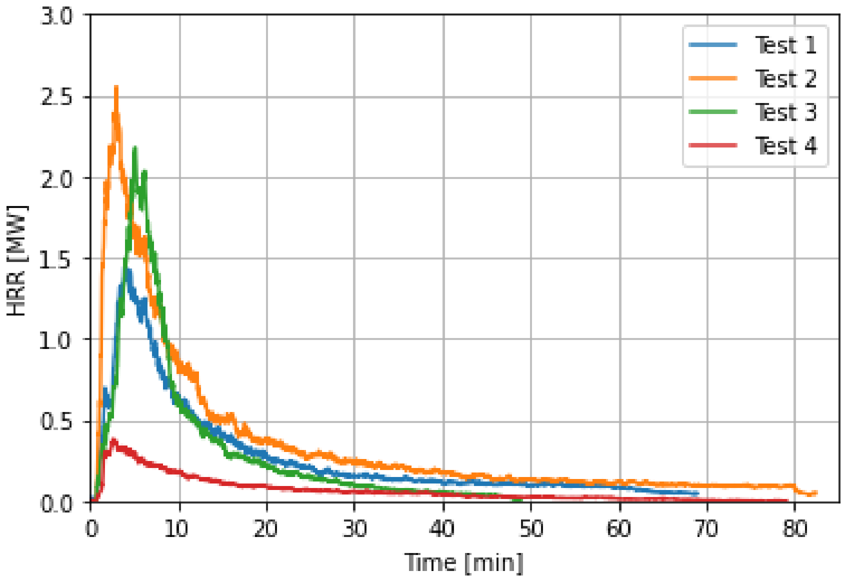

Figure 2.13: Heat Release Rates.

The fire growth rate of the different fuel packs indicates how fast a fire will reach its peak HRR and can be calculated with Equation 2.6 (Heskestad, 1982).

$$\alpha = \frac{Q_{peak}}{t^2} \tag{2.6}$$

The fuel pack of test 2, which is the one that contained the most cellulosic materials, had a fire growth of 0.077 kW/s^2, which is between a fast and ultra-fast growth (National Fire Protection Association, 1985). Tests 1 and 3 showed a similar fire growth, of respectively 0.026 kW/s^2 and 0.023 kW/s^2, between medium and fast. These are the fuel packs with the most plastic materials. The paint in test 4 had the lowest fire growth, of 0.015 kW/s^2, closer to a medium one.

The mass loss and the Mass Loss Rates (MLR) averaged over time were recorded as given in Figure 2.14 and Figure 2.15 respectively. The most significant mass loss happened for all tests during the first 500 seconds, and the third fuel pack showed the most substantial mass loss during this time. When the tests were stopped, the fuel packs lost 63%, 52%, 65% and 21% in tests 1, 2, 3 and 4 respectively (excluding the non-combustible materials present in fuel packs 1 and 3).

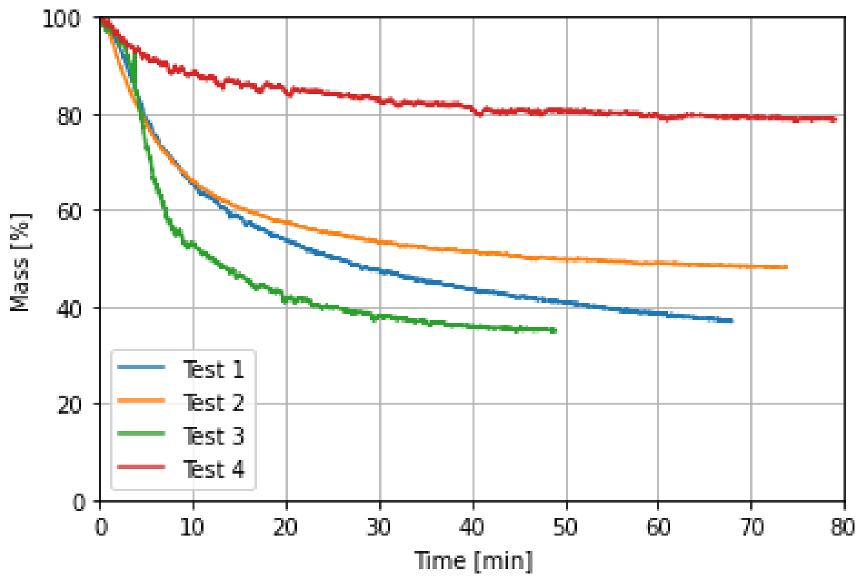

Figure 2.14: Mass loss progression over time for each test.

As for the MLR, the fuel pack in test 2 showed higher MLR peak values (Figure 2.15b). The fuel pack in test 4 showed much lower values (Figure 2.15d), which are reflected in the much lower HRR curve.

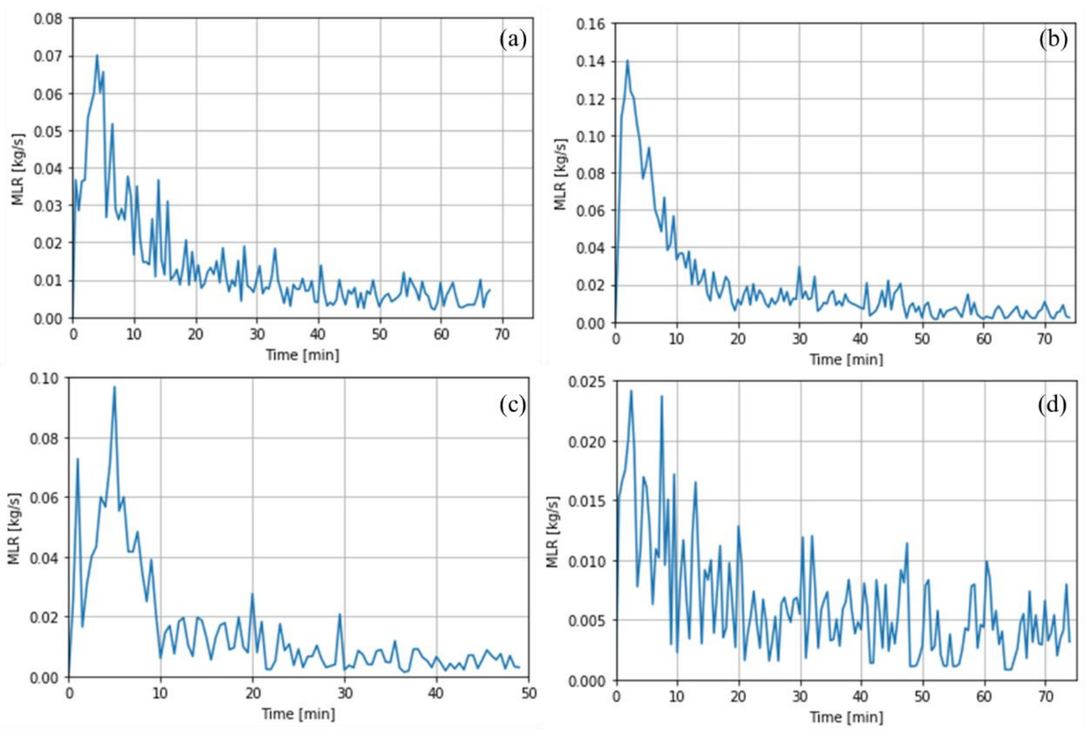

Figure 2.15: Mass Loss Rate averaged every 30 second for: (a) test 1, (b) test 2, (c) test 3 and (d) test 4.

Because the combustion under natural fire conditions is usually incomplete, the effective contribution of the fire load to the energy released during a fire is smaller than the total fire load (Fontana et al., 2016). The effective fire load for each test, calculated by integrating the HRR curves, is given in Table 2.6. The fuel pack reaching the highest HRR value is also the one with the highest effective fire load. The fire load of test 1 is higher than the one of test 3, which presented a higher HRR peak value but a shorter fire duration.

Species concentrations

Oxygen (O_2), carbon dioxide (CO_2), carbon monoxide (CO) and the total unburned hydrocarbons (THC) concentrations were measured in the exhaust duct (Figure 2.16). For all fuel packs, the concentration of CO_2 remained well below 5%, and the one of O_2 always above 19%. The fuel pack that produced the highest CO_2 concentration is that of test 2, reaching 1.3%. Test 2 also reached the highest CO and THC concentrations, at 193 ppm and 89 ppm respectively. Average CO_2 and CO yields (amount generated per unit mass of burned fuel) calculated for each test are given in Table 2.7. The fuel pack in test 3 provided the highest average CO_2 yield, while the highest average CO yield was found for the fuel pack of test 1. The fuel packs containing a bigger variety of materials (tests 1 and 2) are those which present higher average CO yields. CO_2/CO ratios are between 118/1 and 67/1, indicating an efficient combustion (Hurley et al., 2016). When looking at the smoke concentrations, the combustion of none of the fuel packs leads to incapacitation or death, given that the concentration of CO_2 remained well below 5%, and the one of CO never reached 30,000 ppm/min (Hurley et al., 2016), corresponding to a well-ventilated scenario, which is expected at the WUI. Other toxic combustion products such as HCN and HCl were not measured, although these can also pose a hazard to people located near the burning fuels.

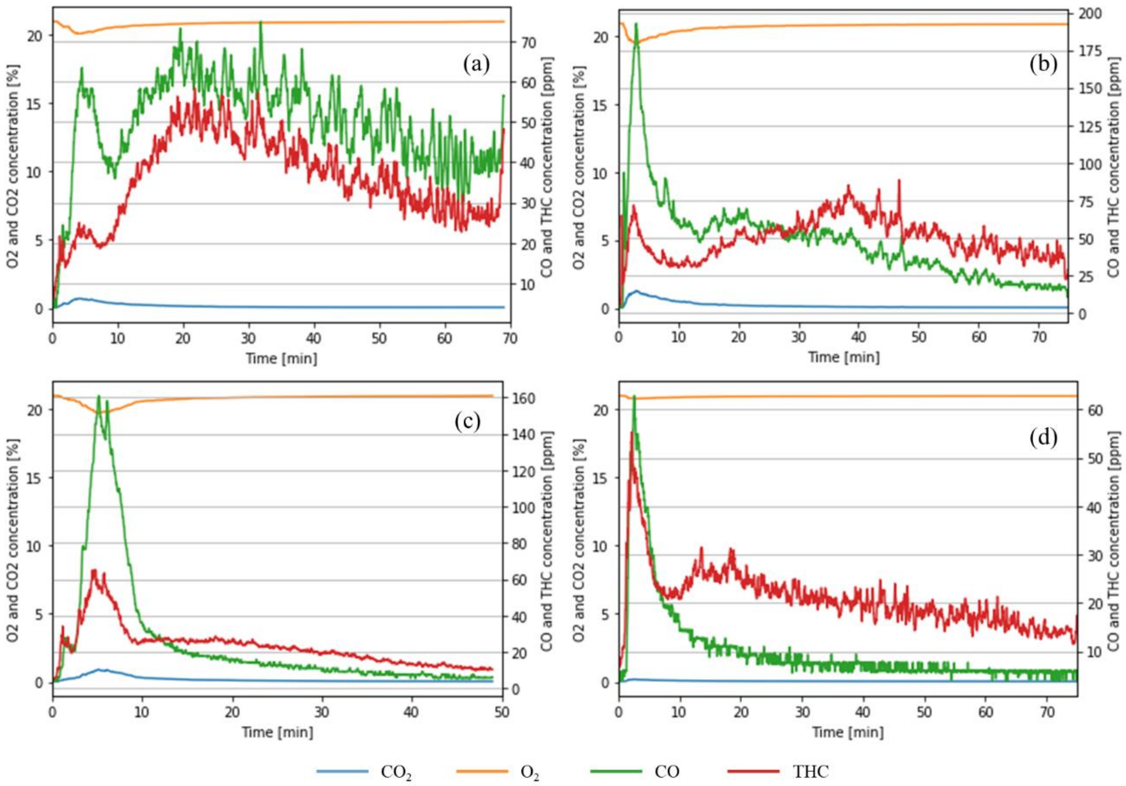

Figure 2.16: Species concentrations for: (a) test 1, (b) test 2, (c) test 3 and (d) test 4.

Table 2.7: Average CO2 and CO yields.

Yield [kg/kg]	Test 1	Test 2	Test 3	Test 4
Y_{CO2}	2.10	2.63	2.73	2.56
Y_{CO}	0.07	0.06	0.02	0.02

Heat fluxes

The recorded total heat fluxes for each test are given in Figure 2.17. The peak heat fluxes were recorded by meters F1 and F5, which were located the closest to the fire at a distance of approximately 1.5 m for tests 1 and 4, 2 m for test 2 and 1.3 m for test 3, at the lowest measuring height. For all tests, peak heat fluxes were registered before the fire reached its peak HRR, but at instants when the burners had already been switched off. This depends on the fact that the items located the closest to the heat flux sensors were reaching their peak HRR when other items had not yet done so. The highest heat fluxes were recorded for test 2 and test 3 as respectively 19.9 kW/m^2 by F5 (located approximately 2 m from the fuel pack) and 21.1 kW/m^2 by F1 (located approximately 1.3 m from the fuel pack). The peak heat flux value for test 1 was recorded as 11.4 kW/m^2, and the one for test 4 as 4.3 kW/m^2.

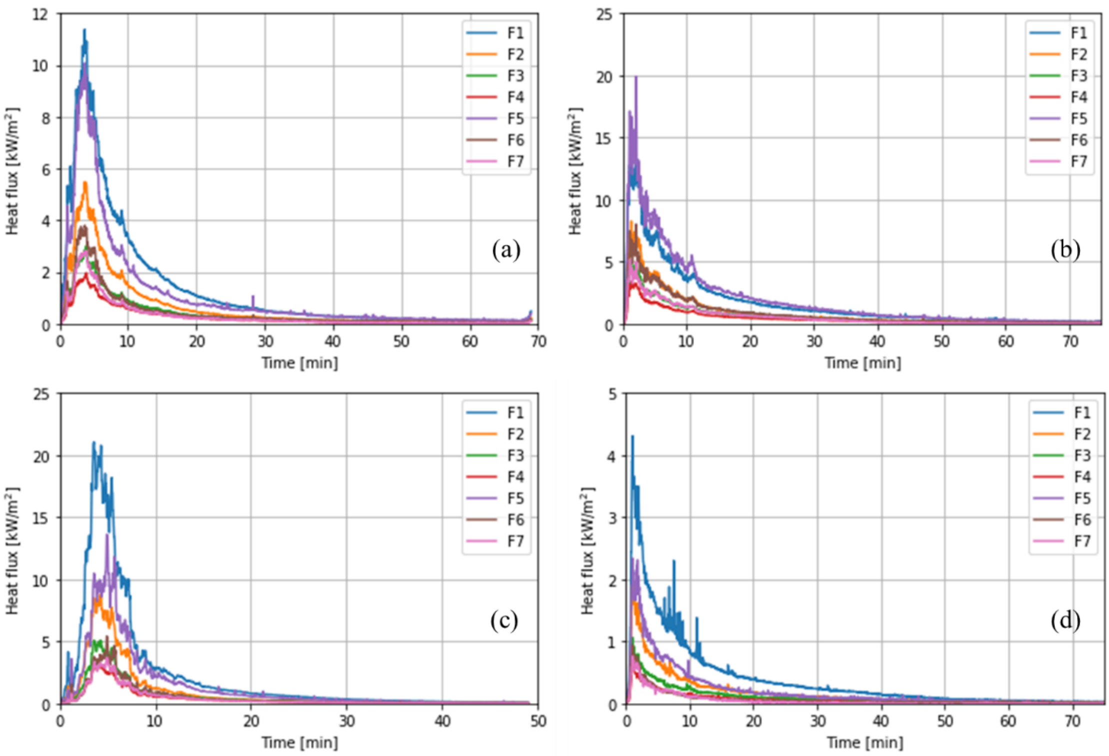

Figure 2.17: Recorded heat fluxes for: (a) test 1, (b) test 2, (c) test 3 and (d) test 4.

Temperatures

The temperature profiles registered by the thermocouples in test 1 are given in Figure 2.18. A peak fire temperature of 931°C was recorded by T2, located inside the bag containing cotton clothes (Figure 2.18a). T5, located in the bag of clothes under the slide, registered temperatures above 500°C for the majority of the duration of the fire. The highest air temperatures were registered by T8 and T11, located on the opposite sides of the fuel pack, at respectively 76°C at 232 s and 67°C at 120 s (Figure 2.18b).

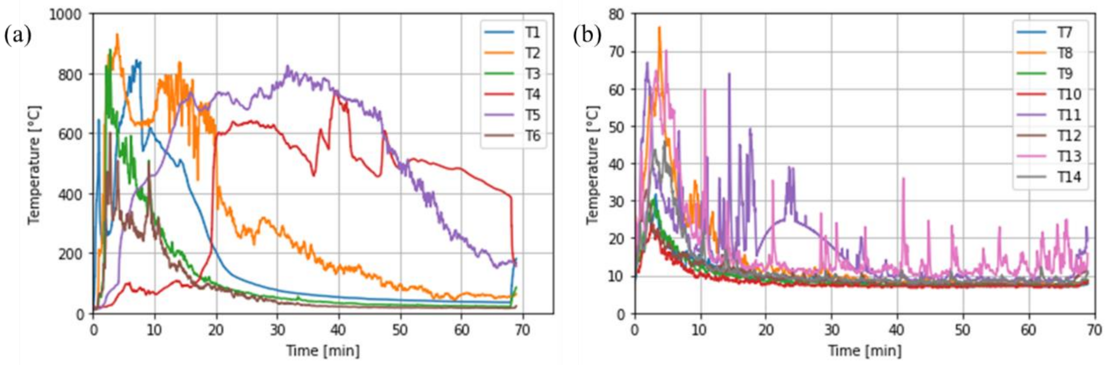

Figure 2.18: Temperatures for test 1: (a) flame and (b) air.

For test 2, only air temperatures were recorded by the thermocouples, as given in Figure 2.19. The highest temperatures were recorded by T8 and T14, with peaks of respectively 104°C at 74 s and 103°C at 122 s. These peaks were registered before the HRR reached its peak value. The IR camera recorded flame temperatures greater than 900°C, with an emissivity of 1 (Figure 2.20).

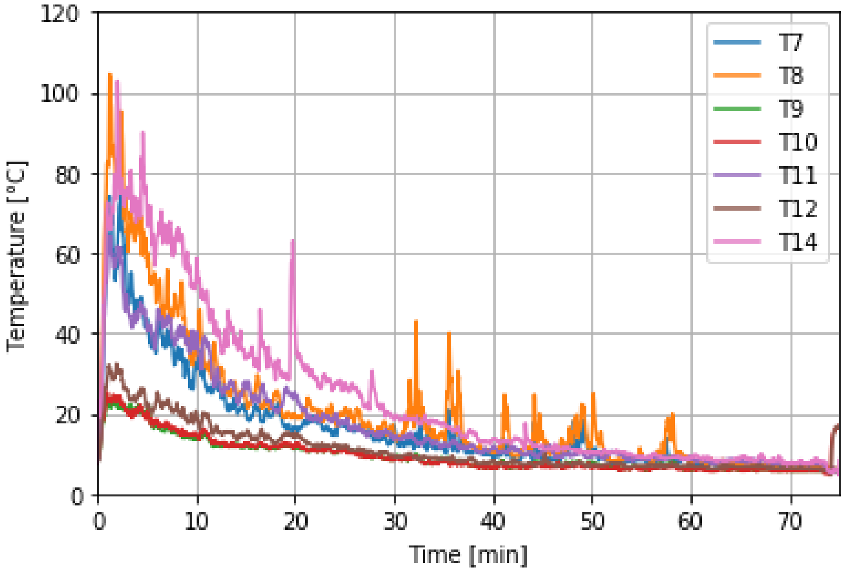

Figure 2.19: Air temperatures for test 2.

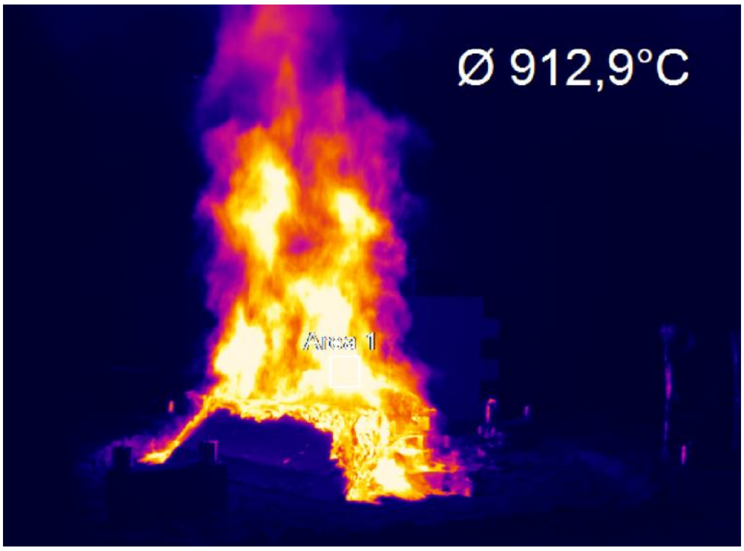

Figure 2.20: Flame temperatures for test 2 1min 40s after the start of the test.

The temperature profiles registered by the thermocouples in test 3 are given in Figure 2.21. A peak temperature of 964°C is recorded by T2, initially located on the back of one of the chairs, at 162 s. At this time both the chair and the table had collapsed and were melting. The highest air temperature values were recorded by T8, with a peak of 148°C at 262 s. Temperature peaks are registered around the time the fire reaches its peak HRR values, with the exception of those registered by T1, which reaches a peak temperature of 743°C at 666 s. This delay is caused by the fact that the chair to which the thermocouple was attached to, collapsed further from the table and thus melted at a later stage.

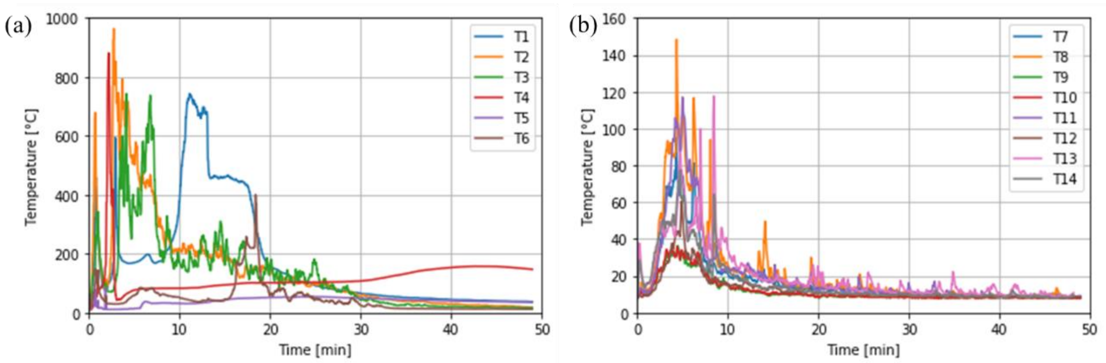

Figure 2.21: Temperatures for test 3: (a) flame and (b) air.

In the final test, only air temperatures were recorded by thermocouples (Figure 2.22). Peak temperatures were given by T8 as 115°C at 394 s and by T13 as 99°C at 162 s (when the peak HRR is recorded). The thermocouples were placed on the side of the burner, thus on the side where the buckets melted first, releasing most of their content towards them. The IR camera recorded flame temperatures greater than 900°C (Figure 2.23).

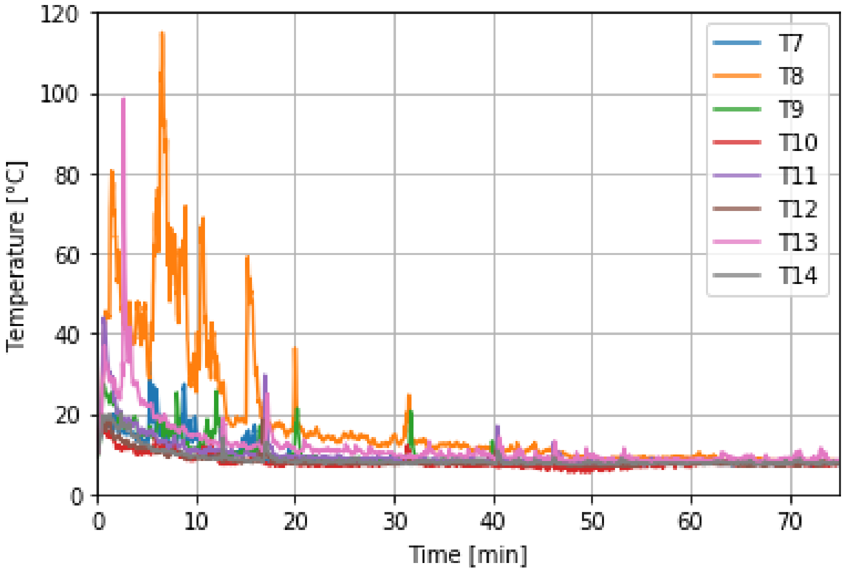

Figure 2.22: Air temperatures for test 4.

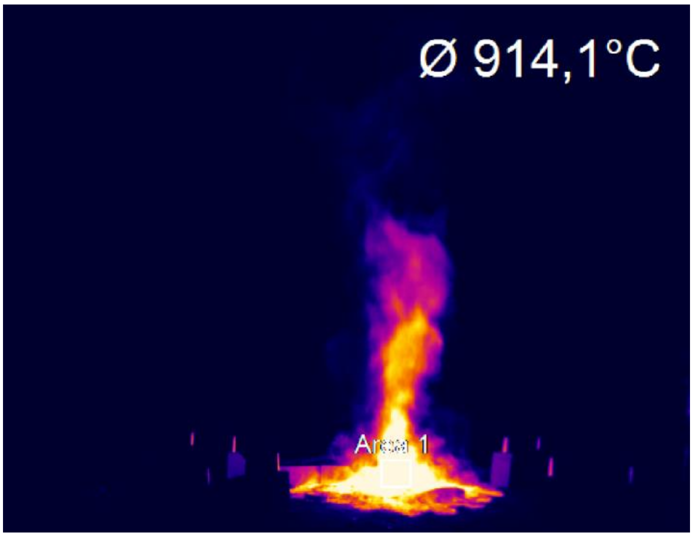

Figure 2.23: Flame temperatures for test 4 1min 21s after the start of the test

For all tests, thermocouple T8 registered the highest air temperature values at distances between 0.6 and 0.71 m from the fuel packs. The distance between the flaming source and the thermocouples was however reduced during tests 1, 3 and 4, since they resulted in pool fire scenarios and the fuel reached the base of the stand of the thermocouple. For test 2 this distance remained unchanged.

Flame height and fire width analysis

Flame heights and width could be extracted from the recordings of the IR camera located on the north side of the facility. Figure 2.24 shows an example for each test of an IR frame corresponding to an original image on the left (a); the segmented image is shown in the middle (b), and finally an example of the measurement of the flame height is depicted in the last image (c).

A description of the obtained results for each test is depicted in Table 2.8. The average flame height was recorded for the first 32 minutes for test 1, 20 minutes for tests 2 and 3, and 29 minutes for test 4. After these times, flame height had significantly reduced.

Table 2.8: Average and maximum flame heights for each test.

Test	Number of frames (images)	Average flame height [m]	Maximum flame height [m]	Time at which maximum flame height is reached [s]
Test 1	516	1.22	2.65	170
Test 2	645	1.47	3.23	134
Test 3	1564	1.61	3.60	271
Test 4	509	1.05	2.64	67

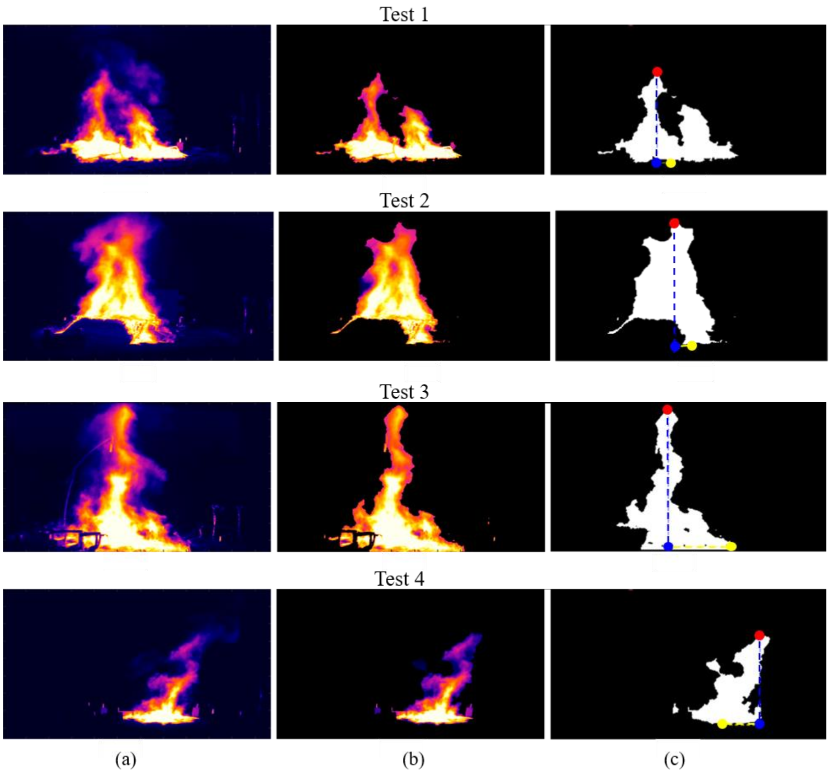

Figure 2.24: Example of the results obtained from: (a) an original IR frame, (b) the segmented image and (c) the calculation of the corresponding flame height for test 1 at 219 s, test 2 at 90 s, test 3 at 194 s and test 4 at 88 s. The yellow and red dots indicate the lowest and highest pixels, while the blue dot is the horizontal projection of the lowest pixel. The dashed line between the red and blue dot gives the flame height.

Flame heights averaged every 10 seconds are given in Figure 2.25. Peak flame heights were recorded before the fire reached its peak HRR for all tests. Tests 1, 2 and 3 showed a sudden drop in flame height of approximately 0.8 m at 505 s, 600 s and 400 s respectively. Before these instants, the average flame height is 1.8 m for test 1, 2.1 m for test 2 and 2.7 m for test 3. Afterwards the average dropped down to 0.7 m, 0.9 m and 0.8 m. Tests 4 showed a more gradual flame height decrease over the course of time.

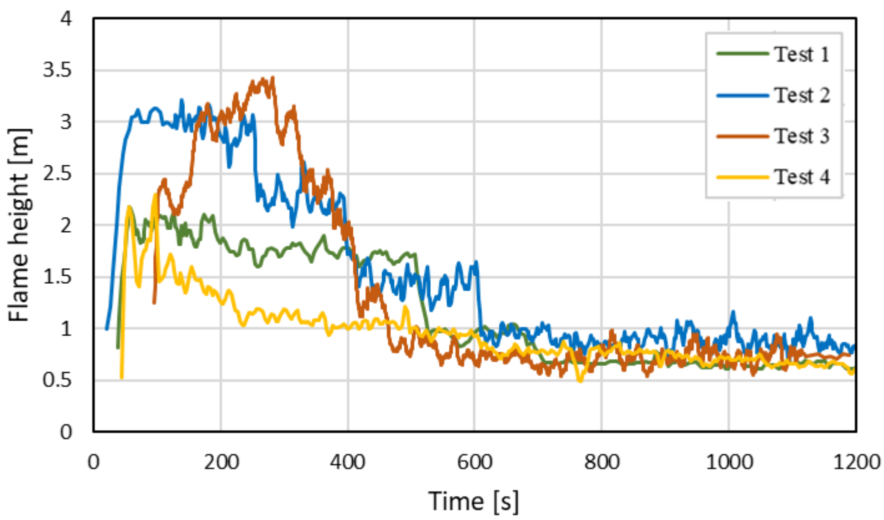

Figure 2.25: Flame height for the first 20 minutes of each test, averaged every 10 seconds.

The same methodology was applied to obtain the maximum width of the fire, which is 4.3 m for test 1, 4.0 m for test 2, 4.4 m for test 3 (Figure 2.26), and 1.6 m for test 4. Considering a circular fire, an approximate peak Heat Release Rate Per Unit Area (HRRPUA) can be calculated for each fuel pack based on these values, which results in 100 kW/m^2 for test 1, 202 kW/m^2 for test 2, 143 kW/m^2 for test 3 and 198 kW/m^2 for test 4.

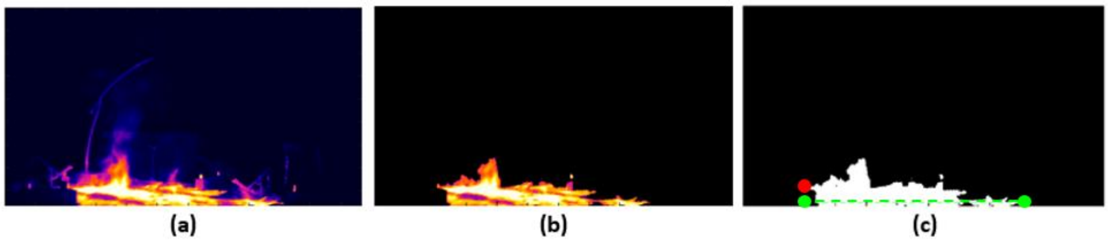

Figure 2.26: Example of the results obtained from: (a) an original IR frame, (b) the segmented image and (c) the calculation of the corresponding fire width for test 3 at 621 s.

Discussion of the results

The fuel packs that gave the highest values, and are therefore considered the most hazardous out of the four, are the one in test 2 (pallets, cardboard, paint buckets and foam mats) and the one in test 3 (table, chairs, pillows and parasol). The fuel pack of test 2, with the highest HRR and HRRPUA, is also the one with the highest mass. However, those of tests 1 and 3 do not follow this trend: test 3 has a lower mass than test 1, but a higher HRR and HRRPUA. This suggests that the total mass of fuel packs cannot be used as an indicator of the risk they pose in case of combustion, but a calculation of their approximate gross heat content can be useful. This can be calculated for each fuel pack considering the mass of each item and the gross heat of combustion of the materials composing the item. The items made out of polypropylene (e.g. table, chairs, toy house) and the oil-based paint result to be those with the highest gross heat of content, since these are some of the items with the highest mass and highest material gross heat of combustion, with 46.4 MJ/kg and 39.3 MJ/kg respectively (Babrauskas, 1991). These are the items that drive the combustion, and are therefore the most hazardous ones, in the fuel packs in tests 1 and 2, which contain a bigger variety of materials compared to the other two packs. The toy house in the first test and the oil-based paint in the second one account for respectively 36% and 76% of the total gross heat content of the fuel packs. The total approximate gross heat content for each fuel pack was calculated as 1807 MJ for test 1, 4505 MJ for test 2, 1916 MJ for test 3 and 1460 MJ for test 4. Also in this case, the fuel pack of test 2 is the most hazardous one, with a much higher gross heat content compared to the others. The fuel packs of the other three tests present close values when it comes to their gross heat content, still showing however the one in test 3 as the second hazardous one, and the one of test 4 as the least hazardous. The absorption of the paint by the sand placed to protect the scale and the subsequent fact that a big portion of the paint was not exposed to the air might explain why test 4 showed the lowest HRR and mass loss, especially since its calculated gross heat content is much higher than the effective fire load. Part of the paint in test 2 was also absorbed by the sand, while part of it spilled on top of the other items, remaining therefore exposed to the air.

Also the obtained fire growth rate reiterates that the fuel pack of test 2 is the most hazardous one, given that it will reach its peak HRR very rapidly (within about 3 minutes). All fuel packs however reach their peak HRR within 5 minutes from ignition, giving very little time for firefighting intervention to avoid the fires from reaching their peak values. Potential fire spread through a property could also be a consequence of late intervention, since the obtained peak flame heights for each test are high enough to potentially provide ignition due to direct flame impingement of fuels located above the fuel packs (e.g. trees, fuels located on higher floors of a structure, etc.). This can allow fire spread through other elements on a property even when the wildfire has already passed through, especially taking the long period of time for the combustion of these fuels into account. The melting of the plastic items and the spill of the paint from the buckets could also cause fire spread through other elements located on a property, since it increased the surface of the fire by almost doubling its width for all fuel packs. This creates a risk for the ignition of other items located at further distances from the fuel packs. The spacing between these types of fuels and others present on the property should consider this flaming surface expansion in order to avoid fire spread through a property. In addition, the paint in fuel packs 2 and 4 was partly absorbed by the sand placed to protect the scale. On other types of surfaces, the paint would expand even more, creating an even bigger flaming surface.

The data gathered in these tests are very useful as inputs for CFD simulations that include these WUI microscale scenarios, so that results can be compared to performance criteria for the evaluation of the hazard caused by the combustion of these fuel packs. When comparing the obtained HRR curves to the one of the stack of pallets (Figure 2.6), peak HRR values are lower for the tested fuel packs, although burning time is longer. The combustion of two cars has approximately the same burning time as the one of tests 1, 2 and 4, although peak HRR values are more than three times higher than those registered in the 4 tests, making this scenario a worst-case one.

2.6 Conclusions

Based on the different vulnerabilities and hazards identified at the WUI microscale, a fault tree has been created to establish the various events that can lead to a fire entering a building. These events depend on the maintenance level of the community, building, and property as well as on the materials and characteristics of the structure. From this fault tree, three scenarios are chosen to be analysed with more detail. The first scenario involves the presence of fuels in front of glazing systems, the second one includes the placing of fuels close to LPG tanks, and the third one consists of analysing the effects of the combustion of fuels and fuel packs to the concrete envelope of semi-confined spaces. Performance criteria for the analysis of these three scenarios are then identified. While studies on concrete walls and failure of LPG tanks have identified these criteria, failure of glazing systems such as windows in an outdoor environment is currently understudied. Therefore, a literature review is presented and average values are proposed. Additionally, quantitative information for the characterization of fire scenarios is provided for the three types of fuels present at the WUI microscale. While information is available for the combustion of wildland vegetation, the behaviour of ornamental vegetation is a field that is currently being studied, and not much information is available at this time. Therefore, a validated model for the pyrolysis of Douglas Fir trees will be used as representative of this type of vegetation, indicating a worst-case scenario. The burning behaviour of WUI artificial fuels is also analysed. While studies have been performed on characterizing HRR curves for fuels that can be found indoors (in buildings and in parking lots or tunnels), there is little information available on the burning behaviour of fuels and fuel packs located in WUI environments. Therefore, the burning behaviour of four different fuel packs has been analysed in real-scale tests. The first fuel pack consists of outdoor children's toys, bags with clothes and boxes with paper and books, the second one of pallets, cardboard sheets, paint buckets and foam mats. The fuels in the third test are an outdoor table with six chairs, six cushions and a parasol, and those in the final test consist of three oil-based paint buckets (the same as those in test 2). The obtained data can be used as input for PBD methodologies for the quantification of hazards and vulnerabilities of WUI microscale scenarios, in order to expand the current knowledge of the defensible space in these environments.

2.7 References

Àgueda, A., Vacca, P., Planas, E., Pastor, E., 2023. Evaluating wildfire vulnerability of Mediterranean dwellings using fuzzy logic applied to expert judgement. Int. J. Wildl. Fire. https://doi.org/10.1071/WF22134

Alexander, M.E., 1982. Calculating and interpreting forest fire intensities. Can. J. Bot. 60:349-357. https://doi.org/10.1139/b82-048

Alexander, M.E., Cruz, M.G., 2019. Fireline Intensity. Encycl. Wildfires Wildland-Urban Interface Fires 1–8. https://doi.org/10.1007/978-3-319-51727-8_52-1

Alexander, M.E., Mutch, R.W., Davis, K.M., 2007. Wildland Fires: Dangers and Survival, in: Wilderness Medicine. pp. 286–335. https://doi.org/10.1016/b978-0-323-03228-5.50017-3

American Petroleum Institute, 2001. Design and Construction of LPG Installations, API STANDARD 2510 eight edition.

Australian Standards, 2018. AS 3959: Construction of buildings in bushfire-prone areas.

Autoridade Florestal National, 2008. Gestão de Combustíveis Para Protecção de Edificações - Manual. OPAL. https://fogos.icnf.pt/sgif2010/InformacaoPublicaDados/gestao_comb_final.pdf

Babrauskas, V., 1991. Tables and Charts, in: Cote, A.E., Linville, J. (Eds.), Fire Protection Handbook. National Fire Protection Association.

Belgische normcommissie, 2014. NBN S 21-208-2: Fire protection in buildings - Design of smoke and heat exhaust ventilation systems (SHEV) for enclosed car park.

Blanchi, R., Leonard, J.E., Leicester, R.H., 2006. Lessons learnt from post-bushfire surveys at the urban interface in Australia. For. Ecol. Manage. 234, S139. https://doi.org/10.1016/j.foreco.2006.08.184

Bowditch, P., Sargeant, A., Leonard, J., Macindoe, L., 2006. Window and glazing exposure to laboratory-simulated bushfires, Bushfire CRC. https://www.bushfirecrc.com/sites/default/files/managed/resource/__66d_window_and_glazing_2006-205.pdf

Byram, G.M., 1959. Combustion of forest fuels, in: McGraw-Hill (Ed.), Forest Fire: Control and Use. pp. 61–89.

Cal Fire, 2022. Defensible Space. https://www.fire.ca.gov/programs/communications/defensible-space-prc-4291/ (accessed 12.9.22).

Chen, H., Wang, Q., Wang, Y., Zhao, H., Sun, J., He, L., 2017. Experimental and Numerical Study of Window Glass Breakage with Varying Shaded Widths under Thermal Loading. Fire Technol. 53, 43–64. https://doi.org/10.1007/s10694-016-0596-0

Chen, Z., Li, Q., Zhang, L., Meng, Q., 2011. Thermal properties of Aluminum&PVC co-extrusion sliding window, in: 2011 International Conference on Multimedia Technology. Hangzhou, pp. 5660–5663. https://doi.org/10.1109/ICMT.2011.6002899

Cruz, M.G., Alexander, M.E., 2019. The 10% wind speed rule of thumb for estimating a wildfire's forward rate of spread in forests and shrublands. Ann. For. Sci. 76. https://doi.org/10.1007/s13595-019-0829-8

Drysdale, D., 2011. An Introduction to Fire Dynamics, Third Edit., Wiley.

Etlinger, M.G., Beall, F.C., 2004. Development of a laboratory protocol for fire performance of landscape plants. Int. J. Wildl. Fire 13, 479–488. https://doi.org/10.1071/WF04039

European Committee for Standardization, 2004a. EN 1992-1-1: Eurocode 2: Design of concrete structures - Part 1-1: General rules and rules for buildings.

European Committee for Standardization, 2004b. EN 1992-1-2: Eurocode 2: Design of concrete structures - Part 1-2: General rules - Structural fire design.

Feldmann, M., Kasper, R., 2014. Guidance for European Structural Design of Glass Components. https://doi.org/10.2788/5523

Fontana, M., Kohler, J., Fischer, K., De Sanctis, G., 2016. Fire Load Density, in:

Hurley, M.J., Gottuk, D.T., Hall, J.J.R., Harada, K., Kuligowski, E., Puchovsky, M., Torero, J.L., Watts, J.J.M., Wieczorek, C. (Eds.), SFPE Handbook of Fire Protection Engineering. Springer US, pp. 1131–1142.

Generalitat de Catalunya, 2019. Protegeos de los incendios forestales. Pla INFOCAT. https://interior.gencat.cat/web/.content/home/030_arees_dactuacio/proteccio_civil/consells_autoproteccio_emergencies/incendi_del_bosc/documents/llibret_incendis_forestals_cast.pdf

Government of Alberta, 2013. FireSmart Guidebook for Community Protection: A Guidebook for Wildland/Urban Interface Communities. https://open.alberta.ca/dataset/7d246651-b1c2-4689-bc18-4e23f5a6e4fd/resource/8c5d6f82-ec68-4466-85ae-4b28878ae21d/download/7032001-2013-11-firesmart-guidebook-community-protection-guidebook-wildland-urban.pdf

Harada, K., Enomoto, A., Uede, K., Wakamatsu, T., 2000. An experimental study on glass cracking and fallout by radiant heat exposure. Fire Saf. Sci. 1063–1074. https://doi.org/10.3801/IAFSS.FSS.6-1063

Heskestad, G., 1982. Engineering Relations for Fire Plumes, in: SFPE TR 82-8. Boston, MA, USA.

Heymes, F., Ismael, E., Vacca, P., Chanut, C., Planas, E., Pastor, E., 2021. Experimental analysis of glazing breakage at the Wildland-Urban Interface microscale, in: 12th Asia-Oceania Symposium on Fire Science and Technology. https://doi.org/10.14264/91bc3d4

Hurley, M.J., Gottuk, D.T., Hall, J.J.R., Harada, K., Kuligowski, E.D., Puchovsky, M., Torero, J.L., Watts, J.J.M., CJ, W., 2016. SFPE Handbook of Fire Protection Engineering, 5th ed. Springer. https://doi.org/10.1007/978-1-4939-2565-0

Hurley, M.J., Rosenbaum, E.R., 2016. Performance-Based Design, in: Hurley, M.J., Gottuk, D.T., Hall, J.J.R., Harada, K., Kuligowski, E., Puchovsky, M., Torero, J.L., Watts, J.J.M., Wieczorek, C.J. (Eds.), SFPE Handbook of Fire Protection Engineering. Springer, pp. 1233–1261.

International Code Council, 2021. International Wildland-Urban Interface Code (IWUIC). https://codes.iccsafe.org/content/IWUIC2021P1

Karlsson, B., Quintiere, J.G., 2000. Energy Release Rates, in: Enclosure Fire Dynamics. CRC Press. ISBN 0-8493-1300-7.

Keski-Rahkonen, O., 1988. Breaking of Window Glass Close to Fire. Fire Mater. 12, 61–69. https://doi.org/https://doi.org/10.1002/fam.810120204

Leonard, J., Blanchi, R., Lipkin, F., Newnham, G., Siggins, A., Opie, K., Culvenor, D., Cechet, B., Corby, N., Thomas, C., Habili, N., Jakab, M., Coghlan, R., Lorenzin, G., Campbell, D., Barwick, M., 2009. Building and land-use planning research after the 7th February 2009 Victorian bushfires – Preliminary findings. https://www.bushfirecrc.com/sites/default/files/managed/resource/chapter-3-building-and-land-web.pdf

Manca, T., López, M., 2014. Guía Metodológica de Actuaciones de Prevención, Defensa y Autoprotección en la Interfaz Urbano-Forestal, Generalitat Valenciana.

https://agroambient.gva.es/documents/162905929/162908876/Gu%C3%ADa+metodol%C3%B3gica+de+Actuaciones+de+Prevenci%C3%B3n%2C%20Defensa+y+Autoprotecci%C3%B3n+en+la+Interfaz+Urbana-Forestal+%286%2C8Mb%29/d24a0daf-d777-405b-8938-b4a54394831f

Maranghides, A., Mell, W., 2011. A Case Study of a Community Affected by the Witch and Guejito Wildland Fires. Fire Technol. 47, 379–420. https://doi.org/10.1007/s10694-010-0164-y

Mata, C., Pastor, E., Rengel, B., Valero, M., Planas, E., Palacios, A., Casal, J., 2018. Infrared Imaging Software for Jet Fire Analysis. Chem. Eng. Trans. 2283–9216. https://doi.org/https://doi.org/10.3303/CET1867147

McGrattan, K., Hostikka, S., McDermott, R., Floyd, J., Weinschenk, C., Overhold, K., 2022. Sixth Edition Fire Dynamics Simulator User's Guide (FDS). NIST Spec. Publ. 1019.

McGrattan, K., McDermott, R., Vanella, M., Hostikka, S., Floyd, J., 2022. Fire Dynamics Simulator Technical Reference Guide Volume 3: Validation 3. https://doi.org/http://dx.doi.org/10.6028/NIST.SP.1018

Meerpoel-Pietri, K., Tihay-Felicelli, V., Graziani, A., Santoni, P.A., Morandini, F., Perez-Ramirez, Y., Bosseur, F., Barboni, T., Sánchez-Monroy, X., Mell, W., 2022. Modeling with WFDS Combustion Dynamics of Ornamental Vegetation Structures at WUI: Focus on the Burning of a Hedge at Laboratory Scale. Combust. Sci. Technol. 00, 1–31. https://doi.org/10.1080/00102202.2021.2019235

Mell, W., Manzello, S.L., Butry, D., Rehm, R.G., 2010. The wildland-urban interface fire problem - Current approaches and research needs. Int. J. Wildl. Fire 19, 238–251. https://doi.org/10.1071/WF07131

Mell, W., Maranghides, A., McDermott, R., Manzello, S.L., 2009. Numerical simulation and experiments of burning douglas fir trees. Combust. Flame 156, 2023–2041. https://doi.org/10.1016/j.combustflame.2009.06.015

Ministry of Business Innovation and Employment, 2013. C/VM2 Verification Method: Framework for Fire Safety Design For New Zealand Building Code Clauses C1-C6 Protection from Fire.

Mowrer, F.W., 1998. Window breakage induced by exterior fires, in: Second International Conference on Fire.

National Fire Protection Association, 1985. Guide for Smoke and Heat Venting, NFPA 204M.

National Fire Research Laboratory, 2020. Fire Calorimetry Database (FCD). https://doi.org/https://doi.org/10.18434/mds2-2314

Nelson, R.M., Adkins, C.W., 1988. A dimensionless correlation for the spread of wind-driven fires. Can. J. For. Res. 18, 391–397. https://doi.org/https://doi.org/10.1139/x88-058

NFPA, 2022. Prepare Your Home Wildfire Risk Reduction Steps That Can Make Your Home Safer During a Wildfire. https://www.nfpa.org//-/media/Files/Firewise/Fact-sheets/FirewiseHowToPrepareYourHomeForWildfires.pdf

OERCO2, 2017a. Study of most used materials in construction sector in Spain. https://oerco2.eu/wp-content/uploads/2013/02/1.2.1.-Report-Construction-materials-in-Spain_EN.pdf

OERCO2, 2017b. Study of most used materials in italian construction sector. https://oerco2.eu/wp-content/uploads/2013/02/1.2.1.-Report-Construction-materials-in-Italy_EN.pdf

Pagni, P.J., 1988. Fire Physics - Promises, Problems, and Progress, in: Fire Safety Science Proceedings of the Second International Symposium. pp. 49–66.

Pastor, E., Muñoz, J.A., Caballero, D., Àgueda, A., Dalmau, F., Planas, E., 2019. Wildland-Urban Interface Fires in Spain: Summary of the Policy Framework and Recommendations for Improvement. Fire Technol. https://doi.org/https://doi.org/10.1007/s10694-019-00883-z

Préfet de Bouches-du-Rhône, 2014. Arrête nº 2014316-0054 relatif au débroussaillement et au meintien en état débroussaillé dans les espaces exposés aux risques d'incendies de forêt. Direction départementale des Territoires et de la Mer, Saervice de l'Agriculture et de la Forêt. https://fransylva-paca.fr/wp/wp-content/uploads/2015/08/2014-11-12-Arr%C3%AAt%C3%A9-OLD-13.pdf

Préfet de la Haute-Corse, 2022. Arrête DDT2B/SEBF/FORET/Nº 2B-2022-04-05-00006. Direction départementale des territoires, Service Eau-Biodiversité-Forêt, Unité Forêt. https://www.haute-corse.gouv.fr/IMG/pdf/arrete_2b-2022-04-05-00006_du_5_avril_2022.pdf

Préfet des Alpes-de-Haute-Provence, 2013. AP 2013-1473 relatif à la prévention des incendies de forêts et des espaces naturels dans le département des Alpes-de-Haute-Provence et concernant le débroussaillement. Direction Departementale des Territoires, Service de l'Environnement et des Risques. http://fransylva-paca.fr/wp/wp-content/uploads/2015/08/2013-07-04-Arr%C3%AAt%C3%A9-OLD-04.pdf

Prefet des Alpes-Maritimes, 2014. Arrêté nº 2014-452 portant règlement permanent du débroussaillement obligatoire et du maintien en état débroussaillé dans le département des Alpes-Maritimes. Direction départementale des Territoires et de la Mer des Alpes-Maritimes, Service Économie Agricole, Ruralité, Espaces naturels. http://fransylva-paca.fr/wp/wp-content/uploads/2015/08/2014-06-10-Arr%C3%AAt%C3%A9-OLD-06.pdf

Préfet du Var, 2015. AP portant règlement permanent du débroussaillement obligatoire et du maintien en état débroussaillé dans le sépartement du Var. Direction départementale des territoires et de la mer du Var. http://fransylva-paca.fr/wp/wp-content/uploads/2015/08/2015-03-30-Arr%C3%AAt%C3%A9-OLD-83.pdf

Ribeiro, L.M., Almeida, M., Muñoz, J.A., 2020. Deliverable D2.1 - Report on real scale experiments. https://wuiview.webs.upc.edu/download/WUIVIEW_D2.1_F.pdf

Scarponi, G.E., Pastor, E., Planas, E., Cozzani, V., 2020. Analysis of the impact of wildland-urban-interface fires on LPG domestic tanks. Saf. Sci. 124, 104588. https://doi.org/10.1016/j.ssci.2019.104588

Skelly, M.J., Roby, R.J., Beyler, C.L., 1991. Experimental investigation of glass breakage in compartment fires. J. Fire Prot. Eng. 3, 25–34.

https://doi.org/10.1177/104239159100300103

South Australia County Fire Service, 2022. Your guide to Bushfire Safety. Government of South Australia. https://www.cfs.sa.gov.au/about/publications/publications/your-guide-to-bushfire-safety/

Tramoni, J.B., Santoni, P.A., Morandini, F., 2018. Experimental and numerical investigation of shrub combustion. J. Phys. Conf. Ser. 1107. https://doi.org/10.1088/1742-6596/1107/5/052002

U.S. Nuclear Regulatory, 1981. Fault Tree Handbook (NUREG-0492). U.S. Nucl. Regul. Com. 209.

Vacca, P., Caballero, D., Pastor, E., Planas, E., 2020. WUI fire risk mitigation in Europe: A performance-based design approach at home-owner level. J. Saf. Sci. Resil. 1, 97–105. https://doi.org/10.1016/j.jnlssr.2020.08.001

Victoria County Fire Authority, 2022. Landscaping for Bushfire: Garden Design and Plant Selection.

Wang, Y., Wang, Q., Wen, J.X., Sun, J., Liew, K.M., 2017. Investigation of thermal breakage and heat transfer in single, insulated and laminated glazing under fire conditions. Appl. Therm. Eng. 125, 662–672. https://doi.org/10.1016/j.applthermaleng.2017.07.019

Chapter 3

Analysis of WUI microscale scenarios

3.1 Introduction

The scenarios selected in Chapter 2 are analysed in detail in this chapter[1] with the aid of the CFD modelling tool FDS (Fire Dynamics Simulator). FDS has been validated in multiple fire engineering applications and it is nowadays the most popular CFD modelling tool for PBD evaluations of complex building fire scenarios. This tool can also be used for WUI microscale scenarios, because it allows to model with great flexibility the many variables and thus scenarios that WUI fire problems present, including the definition of different configurations, materials and fire loads, which is otherwise very difficult to achieve in experimental tests. With the proper characterization of the fire source and of the building features, FDS can provide information on key variables for WUI risk management. This tool allows for the analysis of a large number of scenarios and can cover the diverse fire safety needs of the WUI microscale. Results from simulations can then be compared to previously set performance criteria, in order to obtain relevant and solid conclusions (Vacca et al., 2020a). This way the same tool can be used to analyse simultaneously all the different sub-systems of a building, making the analysis time and cost effective.

A methodology for the in-depth analysis of scenarios involving the combustion of natural and artificial fuels close to glazing systems, LPG tanks and inside semi-confined spaces is presented and results are analysed to identify criteria that create safe conditions in case of fire. These criteria are safe distances for fuels located close to glazing systems and LPG tanks, and wall thicknesses when it comes to the envelope of semi-confined spaces. Additionally, different types of frame and shutter materials are analysed for the glazing system scenarios (PVC, aluminium, wood), in order to identify weaknesses or strengths of each material.

3.2 Glazing systems scenarios

The analysis of the combustion of fuels in the vicinity of glazing systems (unprotected as well as protected by shutters) aims at identifying safe distances at which the integrity of the glazing is not compromised. The analysis is performed with FDS and looks at different criteria for cracking of the glass pane as well as the melting of the frame that supports the pane (identified in Chapter 2). Three criteria are chosen for the failure of the glass pane: (i) the temperature difference between the exposed part of the glass pane and the part hidden below the frame, with a critical value of 83°C, (ii) the surface temperature of the glass pane, with a critical value of 132°C, and (iii) the heat load received by the pane over time, with a critical value of 1087 kJ/m^2. Failure (i.e., glass breakage) is assumed to occur at the time when one of these criteria is met. Since breakage of glazing systems can also be caused due to the failure of the frame that supports the glass panes, two different frame

[1] Part of the content included in this chapter has been published as a conference paper (Vacca et al., 2022)

materials are also analysed. These are aluminium, which melts at a temperature of 660°C, and PVC, which melts at 220°C.

Analysed scenarios include the exposure to the combustion of both artificial and natural fuels without wind as well as in windy conditions. Double pane windows are analysed in all scenarios and breakage of single pane windows is assumed to happen when the first pane of the double pane glazing fails. Panes of a thickness of 3 mm, used in older glazing systems and still present in many European homes, and 6 mm, which is the most common larger thickness for window glazing. Two different window sizes are analysed: 0.5 m x 0.5 m, which is a representation of a small window (as the one used in the tests performed by Harada et al. (2000)), and 1.2 m x 1.2 m, which is an average size for a glazing system.

The analysed scenarios are simulated with an ambient temperature of 25°C and both in calm (i.e., no wind) and windy conditions. First, safe distances are identified for calm conditions, then these distances are analysed in windy conditions, with a wind profile that peaks at 30 km/h at a height of 10 m (situation for extreme fire behaviour potential (Steffens, 2016)). Fire scenarios include both natural and artificial fuels. The first fire scenario for artificial fuels consists of the combustion of a stack of wooden pallets of a 0.9 m height. The HRR curve for this scenario is given in Figure 2.6. The safe distances identified for this scenario are then tested against the fire scenario of the fuel pack of test 2 that is presented in Chapter 2 (HRR curve is given in Figure 2.13). In this scenario the peak HRR value is approximately half of the one of the wood pallets, but fire duration is much longer (specifically 1 hour and 8 minutes longer), therefore the glazing might be exposed to a higher heat dose. The fire scenario with natural fuels consists of the combustion of 3 Douglas fir trees (Mell et al., 2009), which are simulated as particles. An ignitor is placed at the bottom of each tree. The HRR curve of this scenario is not prescribed, as the combustion process of the particles that compose the trees is simulated in FDS, therefore the HRR curve is one of the outputs of the simulation. The chosen fire scenarios are representative of very high fire loads, according to the analysis performed in Chapter 2.

Three scenarios involving shutters placed in front of a window are also analysed. These scenarios consist of the stack of wooden pallets burning 3.5 m from a 1.2 x 1.2 m^2 window with a pane thickness of 3 mm. Shutters made out of aluminium, PVC and wood (yellow pine) and a thickness of 5 cm (typical thickness for shutters made out of the three analysed materials, not of roller shutters, which are thinner) are placed in front of the glass, at a distance of 10 cm.

3.2.1 FDS scenario build-up

All scenarios simulate fuels in front of a small building with one window, with either a PVC or an aluminium frame. All glazing system scenarios are run on the FDS version 6.7.9 (NIST, 2022). The representation of the scenario with the wood pallets located 3.5 m from the window of 1.2 m x 1.2 m is shown in Figure 3.1a. Material properties used for the simulations are given in Table *3.* 3.1. FDS allows to define an obstacle that contains different layers of materials, therefore the obstacle used to simulate the frame is assigned two layers: the frame, with a thickness of 15 mm, and the glass pane, which lies directly below the frame and has a thickness of either 3 mm or 6 mm. Double pane windows are analysed in all scenarios, with an air gap between the two panes. The second pane is bigger than the first pane, as it lies underneath the frame (i.e., on the frame side, the simulated obstacles include the following layers: frame, first glass pane, air gap, second glass pane), as shown in Figure 3.1b.

Table 3.1: Material properties for the glazing systems scenarios.

Material	Specific heat capacity [$kJ \cdot kg^{-1} \cdot K^{-1}$]	Conductivity [$W \cdot m^{-1} \cdot K^{-1}$]	Density [kg/m^3]	Emissivity [-]
Float glass (Wang and Hu, 2019)	0.82	0.94	2500	0.85
PVC (Thunderhead Engineering, 2022)	1.29 –1.59[A]	0.134 – 0.192[A]	1380	0.95
Aluminium (Hurley et al., 2016)	0.89	175 – 204[A]	2707	0.05
Yellow pine (Thunderhead Engineering, 2022)	2.85	0.14	640	0.9

[A] The property varies with the temperature of the material.

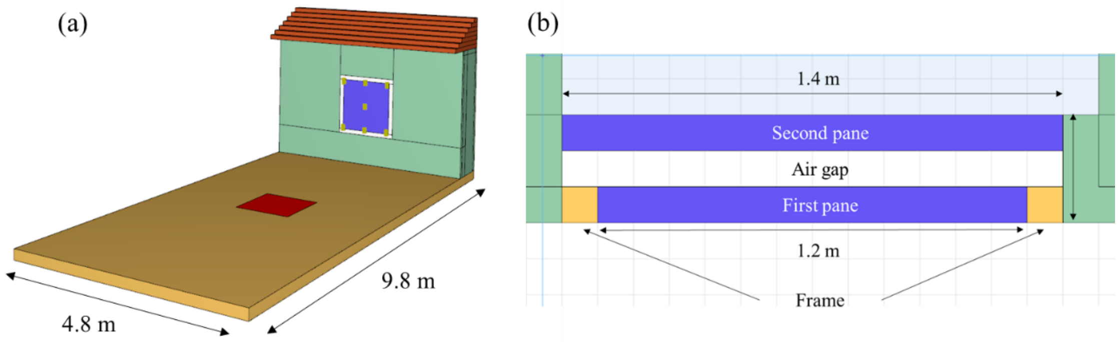

Figure 3.1: (a) Geometry of the scenario of the stack of wooden pallets located 3.5 m from the window of 1.2 m x 1.2 m and (b) geometry of the simulated double pane glazing system (top view, the upper part of the frame is hidden to show the glass pane).

The fire source in the scenarios that include artificial fuels is represented as a vent (i.e., a flat surface), whose dimensions vary according to the different fuels. Simulations time, peak HRRPUA and fire size are given for the two scenarios in Table 3.2.

Table 3.2: Simulation parameters for the glazing systems scenarios

Scenario	Simulation time [s]	HRRPUA [kW/m^2]	Fire size [m^2]
Wood Pallets	770	3563	1.44
Fuel pack test 2	5000	202	12.48

In the scenarios that include shutters, the shutter is located 10 cm from the first pane, therefore there is an air gap of one cell between the shutter and the first pane (Figure 3.2b). The shutter covers the entire glazing system (frame and glass pane), as shown in Figure 3.2a.

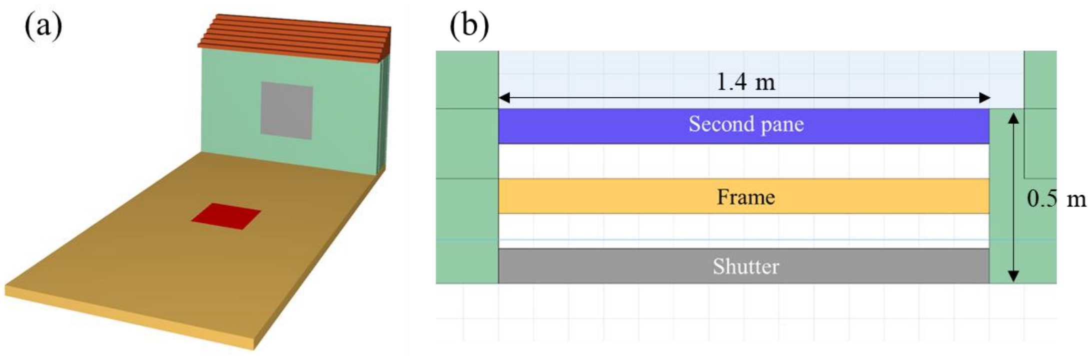

Figure 3.2: (a) Geometry of the scenario of the stack of wooden pallets located 3.5 m from the window of 1.2 m x 1.2 m, including the shutter, and (b) geometry of the simulated double pane glazing system that includes the shutter (top view).

For fire scenarios with the 3 Douglas fir trees, the vegetation is represented with particles, divided into four categories: foliage, small roundwood, medium roundwood and large roundwood. The trees are in the shape of a cone, with a height of 1.9 m and a lower diameter of 1.7 m, as shown in Figure 3.3. Ignitors are placed underneath the particles and are activated for 10 s. The simulation time is set at 50 s.

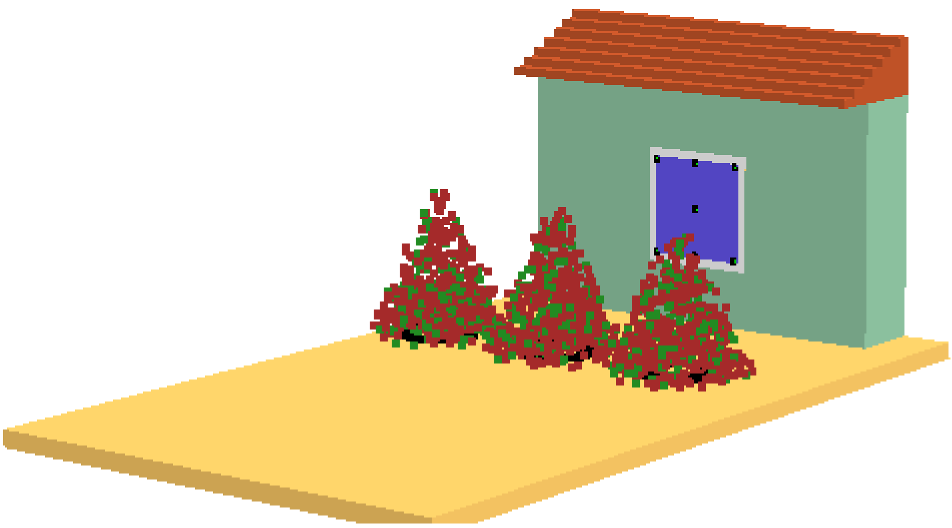

Figure 3.3: Geometry of the scenario of the three Douglas fir trees located 2 m from the window of 1.2 m x 1.2 m.

The fire curve for the three trees scenario is simulated in FDS, it is not prescribed. In calm environmental conditions the computed HRR curve of the three trees is approximately the same for each of the scenarios, as shown in Figure 3.4a, reaching peaks between 26 MW and 28 MW. In windy scenarios, the HRR curve varies depending on the distance between the trees and the window, as shown in Figure 3.4b, reaching peaks between 19.5 MW for a distance of 0.5 m between trees and window and 22.9 MW for a distance of 2.5 m. This difference is most likely due to the different air entrainment inside the particle cluster in each scenario due to the modification of the wind profile because of the presence of the trees and the wall where the window is located.

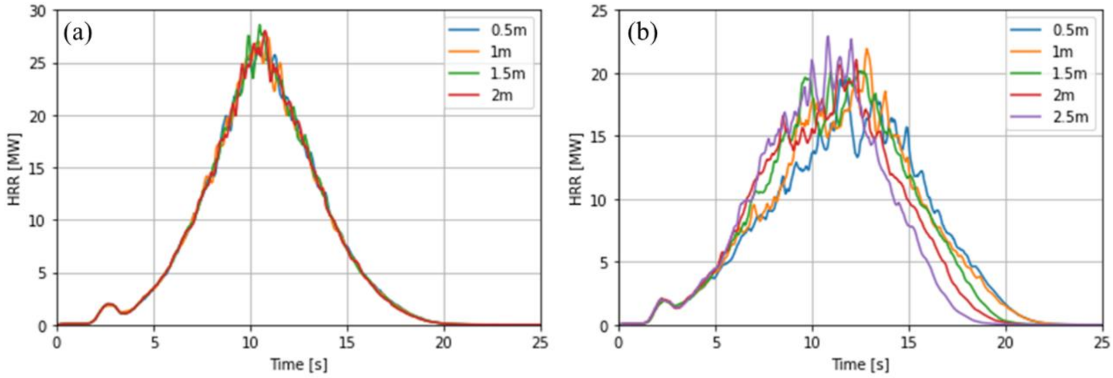

Figure 3.4: HRR curves for scenarios with three trees in calm environmental conditions (a) and in windy conditions (b) for a 1.2x1.2 m^2 window, 6 mm pane, aluminium frame at different distances from the window.

The domain size is 5.8 x 9.8 x 9.6 m^3 for all scenarios, with the exception of a few of the simulations that included wind, for which the domain on the x axis was made slightly bigger (6.2 m) to avoid numerical instabilities caused by the flames impinging on the sides of the domain. The mesh size for each scenario is calculated according to the characteristic fire diameter D^*, which depends on the HRR of the fire $\dot{Q}$ (kW), ρ_∞ the density of air (kg/m^3), the specific heat capacity of air c_p (kJ·kg^{-1}·K^{-1}), the ambient temperature T_∞ (K) and the gravitational constant g (m/s^2), as shown in Equation 3.1:

$$D^* = \left(\frac{\dot{Q}}{\rho_\infty c_p T_\infty \sqrt{g}}\right)^{\frac{2}{5}} \tag{3.1}$$

For a coarse mesh, the quantity $D^*/\delta x$, where δx is the nominal size of a mesh cell, has a value of 4 while for a fine mesh this value is 16. In this type of simulations, a fine mesh is chosen for the area where the fire as well as where the devices (and the glazing system) are located, therefore δx is 0.1 m. Areas that are not of particular interest will have a cell size which is double the value of δx. Given the complexity of the geometry of double pane windows, a further mesh sensitivity analysis is performed to see if the size of the gap between the two panes within the simulation will influence the results. At least one row of mesh cells needs to be placed between the two panes in order for FDS to recognize the gap. Four different mesh sizes are analysed: the smallest mesh size is 0.015 m, which represents the real size of the gap, followed by 0.03 m, 0.06 m and 0.1 m, which is the mesh size obtained by using Equation 3.1. Results of this analysis show that the difference in the results of the simulations with the different mesh sizes is not significant, therefore it is possible to simulate these types of scenarios with a mesh of 0.1 m, which will save a lot of computational time and space. The complete mesh sensitivity analysis is given in Appendix A.

The wind profile is modelled by using the Monin-Obukhov similarity theory, where the wind speed profile varies vertically with height (McGrattan et al., 2022). In all simulations, wind is characterized by neutral conditions and a very rough aerodynamic roughness length (assigned to a WUI landscape with scattered buildings and mixed farm fields and forest clumps). As previously mentioned, a wind speed of 30 km/h at 10 m height blowing in the direction of the window is simulated.

The needed outputs for these scenarios are the temperature of the surface of the glass pane and of the frame, the temperature behind the frame at the depth of 15 mm (thickness of the frame), and the heat flux received by the glass pane. Surface temperatures are obtained by placing *wall temperature* devices at the centre and at the corners of the two glass panes. The temperature of the frame as well as of the glass laying underneath are obtained through *PROF* devices that can compute the temperature through the thickness of the analysed obstacle. *Gauge heat flux* devices are placed on the surface of the glass pane to calculate the received heat flux, which is used to calculate the received heat load (this type of output has been chosen because it is compared with experimental values, obtained with heat flux gauges). The location of these devices is given in Figure 3.5. Devices are named according to their location, where M stands for middle, L for left or low, U for up and R for right, as shown in Figure 3.5a. In the scenarios that include shutters, *PROF* devices are placed in the same location as those of the frame and an additional one is placed in the centre of the shutter.

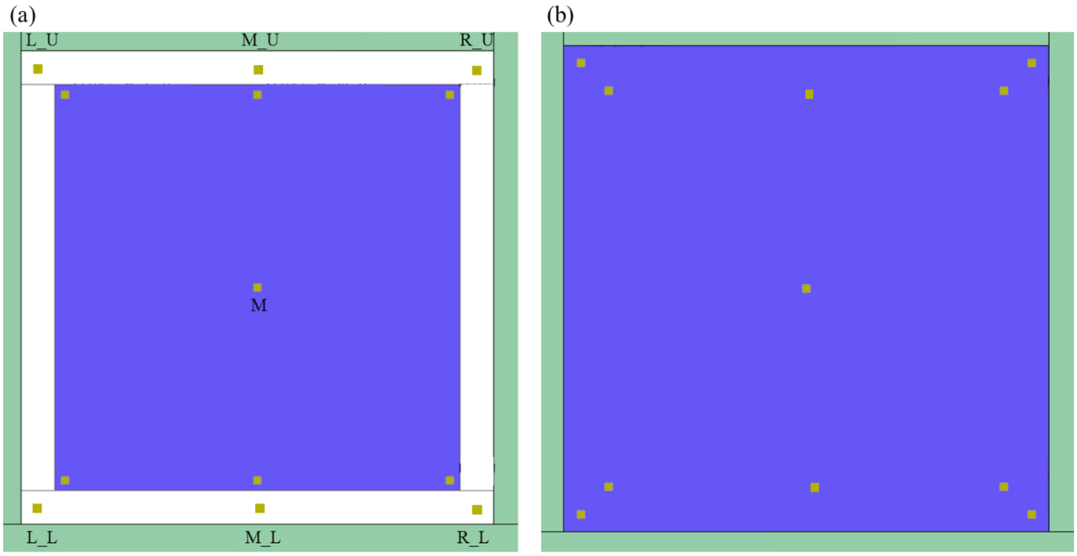

Figure 3.5: Location of the devices (a) on the frame and first glass pane and (b) on the second glass pane.

3.2.2 FDS results

Artificial fuels scenarios

Safe distances which result from the analysis of the wooden pallet fire scenarios are given in Table 3.3. A distance of 5 m from the fire source is needed to avoid failure of a single pane window of 0.5 m x 0.5 m with a pane thickness of either 3 mm or 6 mm and a frame made out of PVC or aluminium in calm environmental conditions (i.e., no wind). The safe distance for a double pane window with the same characteristics is found to be 3.5 m, because the second pane is protected by the first pane for at least half of the burning time of the analysed fuel. When windy conditions are analysed, these distances increase by 1.5 m for both single pane and double pane glazing. In calm environmental conditions, these distances increase for a bigger window size (1.2 m x 1.2 m): no failure will occur at a distance of 6 m for single pane and 4 m for double pane windows. In windy conditions, safe distances for the bigger window size are the same as for the smaller one: 6.5 m for single pane windows and 5 m for double pane windows.

Both analysed pane thicknesses (3 mm and 6 mm) and frame materials (PVC and aluminium) gave the same results when it came to safety distances in the analysed fire scenario.

Table 3.3: Safe distances for glazing systems exposed to the wooden pallets fire scenario.

Pane thickness [mm]	Frame material	Window size [m^2]	Atmospheric conditions	Safety distance [m]	
				Single pane	Double pane
3 and 6	PVC and Al	0.5 x 0.5	No wind	5	3.5
			Windy	6.5	5
		1.2 x 1.2	No wind	6	4
			Windy	6.5	5

The time at which each of the performance criteria is met is shown in Table 3.4 for a few selected scenarios. The complete results for each of the analysed scenarios is given in Appendix A. As can be noticed in Table 3.4, the thickness of the pane does influence the time at which the criteria are met. For the ΔT_{cr} and T_{surf} criteria, the difference is very clear: the thicker the pane, the longer it will resist. This is highlighted by the fact that the surface temperature of the exposed side of the pane is higher when the thickness is lower, as shown in Figure 3.6. As for the heat load, this pattern is not as clear. In some simulations the thicker pane resisted longer, and in others the time of failure was approximately the same for both thicknesses.

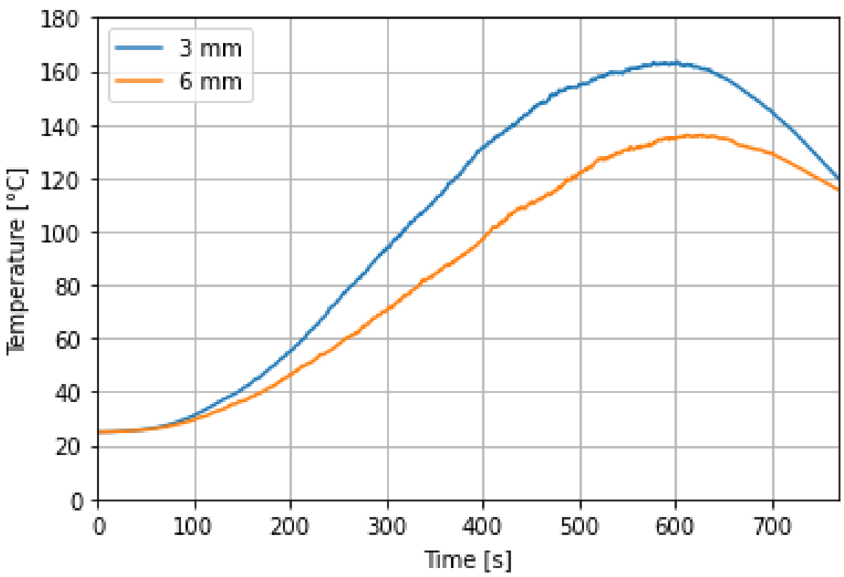

Figure 3.6: Surface temperature of a 3 mm and 6 mm glass pane recorded by the device placed in the middle of the pane for a distance of 3 m from the wood pallet fire scenario in calm environmental conditions.

Table 3.4: Results for selected scenarios of the combustion of the wooden pallet stack.

Window size [m²]	Atmospheric conditions	Distance [m]	Pane thickness [mm]	Frame material	Glass pane	Time of reaching performance criteria [s]			
						ΔT_{cr}	T_{surf}	HL	T_{surf} frame
0.5 x 0.5	No wind	3	3	PVC	1	310	370	356	-
					2	517	-	545	
				Al	1	312	377	361	-
					2	506	-	550	
			6	PVC	1	420	502	354	-
					2	-	-	585	
				Al	1	413	510	358	-
					2	-	-	599	
		4	3	PVC	1	-	-	519	-
					2	-	-	-	
				Al	1	553	-	521	-
					2	-	-	-	
			6	PVC	1	-	-	527	-
					2	-	-	-	
				Al	1	-	-	543	-
					2	-	-	-	

Overall, results show that at closer distances, the first criterion that is reached is the ΔT_{cr}, followed by the heat load and finally by T_{surf} for the 3 mm pane. For a thickness of 6 mm, the heat load is the first criterion to be met, followed by the ΔT_{cr} and finally by T_{surf}. This is caused by the difference in the temperature of the surface of the pane, which will cause bigger ΔT values for the 3 mm pane. The value of ΔT is also influenced by the frame material. PVC is more insulating than aluminium, as its thermal inertia is lower, therefore the temperature at the surface of the frame is higher, and it quickly lowers through the depth of the frame, insulating the glass pane at the back, which will not experience very high temperatures. On the other hand, aluminium has a very low emissivity, and reflects therefore more radiant energy compared to PVC. Due to its high thermal inertia, however, aluminium does not insulate the glass pane as well as PVC does. This can be seen in Figure 3.7, where the temperature profile through a PVC and aluminium frame and a 3 mm glass pane lying underneath is shown. For the same fire exposure, the surface temperature of the PVC frame is much higher compared to the one of aluminium, however, at 15 mm (at the glass surface), the temperatures are very similar. In some cases, such as the scenario at a distance of 4 m shown in Table 3.4, the temperature of the glass pane is higher when lying below a PVC frame, and therefore the ΔT criterion is not met, while it is met for panes with aluminium frames, which will have a lower pane temperature underneath the frame.

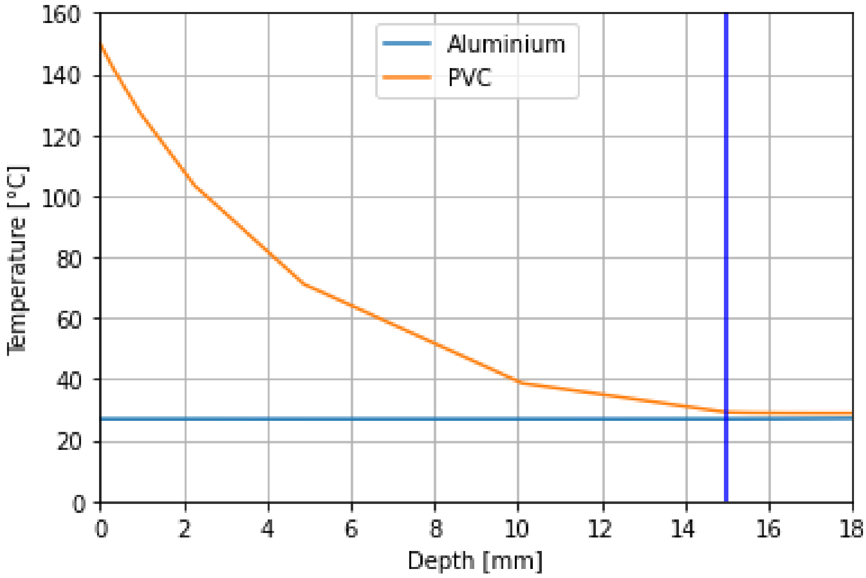

Figure 3.7: Temperature profile through the frame and glass pane recorded in the lower right corner of the window of 0.5 x 0.5 m^2 at 400 s (wood pallet scenario placed 3 m from the window in calm environmental conditions). The vertical line indicates the interface between the frame and the glass.

The fuel pack analysed in Test 2 (see Chapter 2) was simulated at a distance of 5 m from the glazing system with a pane size of 0.5 m x 0.5 m, a thickness of 3 mm and a PVC frame (this is the identified safe distance for the previous scenario in calm environmental conditions). While the temperature difference and surface temperature criteria are never met, along with the surface temperature of the frame, glass cracking and therefore failure of the glazing will occur due to the heat load the pane is exposed to. Results show that the pane will receive a total heat load of 1087 kJ/m^2 after approximately 70 min of exposure to the combustion of a fuel pack containing wooden pallets, cardboards, mattresses and paint buckets. The safe distance between this fuel pack and the analysed window is 5.5 m in both calm and windy environmental conditions.

Natural fuels scenarios

Safe distances which result from the analysis of the three Douglas fir trees scenarios are given in Table 3.5. In these scenarios the safe distances vary between glazing systems with aluminium frame and those with PVC frame. PVC framed windows need larger distances for the frame not to melt: in these scenarios it is the performance criterion of the frame that dictates what is the safe distance. These distances are 2 m for both window sizes in calm environmental conditions, while in windy conditions the distance increases to 3.5 m for the smaller window and 3 m for the bigger one. This difference between small and big window with PVC frames is caused by the way the temperature of the hot gases and flames that are pushed by the wind towards the windows. As can be seen in Figure 3.8, peak gas temperatures by the 0.5 x 0.5 m^2 are higher compared to the 1.2 x 1.2 m^2 window, while in Figure 3.9 it can be seen how the distance between the flames and the window is different between the two analysed simulations.

A distance of 2 m from the fire source is needed to avoid failure of a single pane window of 0.5 m x 0.5 m with a pane thickness of either 3 mm or 6 mm and a frame made out aluminium in calm environmental conditions (i.e., no wind), while in windy conditions this distance is 2.5 m. For double pane systems with the same characteristics and in both calm and windy conditions, the safety distance is only 0.5 m, because the second pane is only exposed to the combustion of the trees for approximately 8 s.

Table 3.5: Safe distances for glazing systems exposed to the combustion of three Douglas fir trees.

Pane thickness [mm]	**Frame material**	**Window size [m²]**	**Atmospheric conditions**	**Safety distance [m]**	
				Single pane	**Double pane**
3 and 6	PVC	0.5 x 0.5	No wind	2	2
			Windy	3.5	3.5
		1.2 x 1.2	No wind	2	2
			Windy	3	3
	Aluminium	0.5 x 0.5	No wind	2	0.5
			Windy	2.5 [A]	
		1.2 x 1.2	No wind	1.5	1
			Windy	2.5	

[A] For the scenario of 3 mm, the safety distance was found to be 2 m due to the difference in peak gas temperatures by the window between the 3 mm and 6 mm scenarios: gas peak temperatures reach 525°C in the right upper corner of the window for the scenario with 6 mm, while they never reach 500°C for the 3 mm one. Therefore, the distance of 2.5 m is also used for the 3 mm pane.

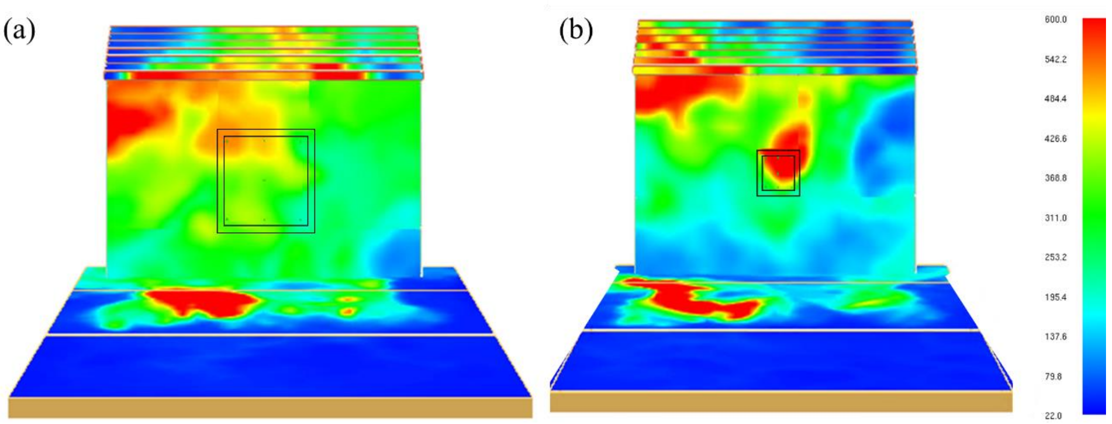

Figure 3.8: Peak gas temperatures by the 1.2 x 1.2 m^2 window (a) and by the 0.5 x 0.5 m m^2 window (b)

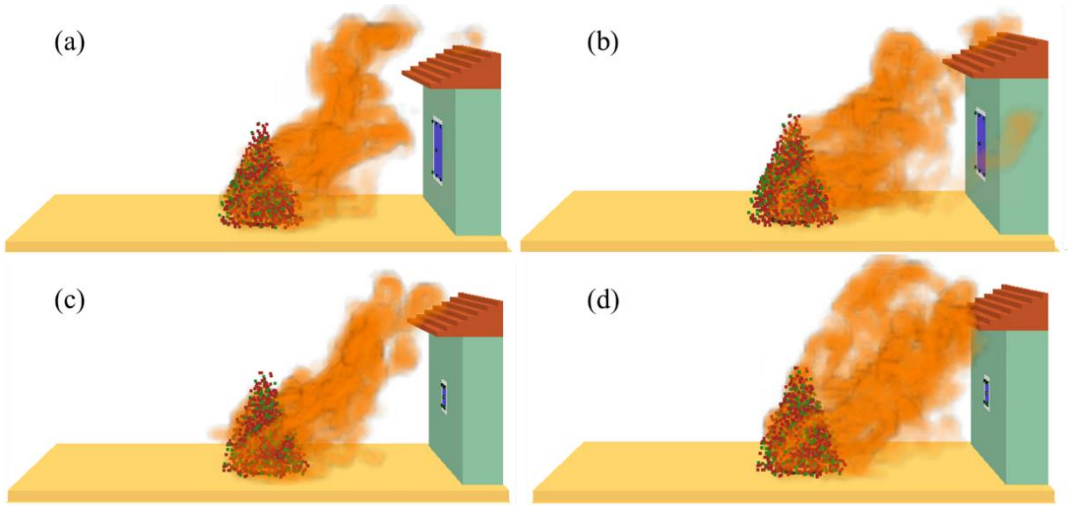

Figure 3.9: Simulation of the trees located 3 m from a 1.2 x 1.2 m^2 at 10 s (a) and 12 s (b) and from a 0.5 x 0.5 m^2 at 10 s (c) and 12 s (d).

As for the criteria for failure of the glass pane, they are met at approximately the same time for both analysed frame types and pane thicknesses. In some cases of the windy scenarios, the 6 mm glass pane fails before the 3 mm one, as for the scenario with a 0.5 x 0.5 m^2 window at a distance of 2 m from the trees shown in Table 3.6. In the case of the trees located at 2 m, the ΔT_{cr} value of 83°C is barely reached for the pane of 6 mm, while the ΔT reaches only 78°C for the 3 mm pane.

Table 3.6: Results for selected scenarios of the combustion of the three Douglas fir trees.

Window size [m^2]	Atmospheric conditions	Distance [m]	Pane thickness [mm]	Frame material	Glass pane	Time of reaching performance criteria [s] ΔT_{cr}	T_{surf}	HL	T_{surf} frame
0.5 x 0.5	Windy	2	3	PVC	1	13	-	-	12
				Al	1	-	-	-	-
			6	PVC	1	12	-	-	11
				Al	1	13	-	-	-
					2	-	-	-	

Shutters

When it comes to the three analysed shutter materials (aluminium, PVC and wood), in the analysed scenario (combustion of the stack of wood pallets located 3.5 m from a 1.2 x 1.2 m^2 window) all shutters protect the glazing system from failure. Without shutters, a double pane window would fail at this distance, as given in Table 3.3.

In the analysed scenario, peak temperatures at the surface of the shutters are recoded by the devices located in two upper corners. PVC and wooden shutters present very similar surface temperature profiles through time, reaching peaks of 163°C and 164°C respectively, while the aluminium shutter only reaches a peak surface temperature of 26°C (1°C higher than ambient temperature), as given in Figure 3.10. The radiative heat flux onto the wooden shutter is always less than the set performance criterion of 12 kW/m^2, reaching peak values of 6.7 kW/m^2.

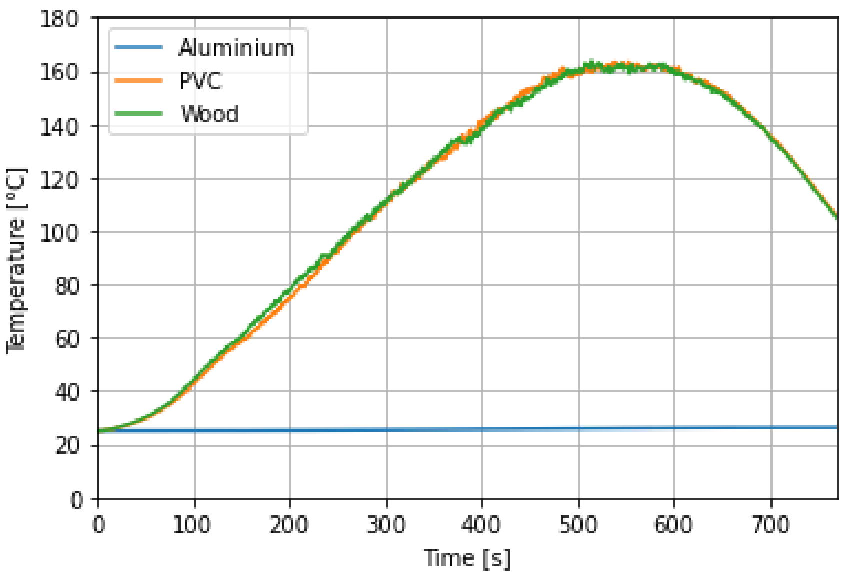

Figure 3.10: Peak surface temperature over time for aluminium, PVC and wooden shutters.

3.3 LPG tank scenarios

The analysis of the combustion of fuels in the vicinity of above-ground LPG tanks aims at identifying safe distances at which the integrity of the tank is not compromised. This analysis is performed with a two-step approach: (i) the incident heat flux onto the tank is obtained through FDS simulations; if this heat flux is lower than 22 kW/m^2, no further investigation is needed and the scenario is deemed as safe; if the value passes this threshold, then (ii) the tank's response is analysed in ANSYS Fluent as a function of the incident radiation, the temperature of the gas in contact with the tank and the related convective heat transfer, obtained with the FDS simulation (Scarponi et al., 2020).

Four different fire scenarios are analysed. The first scenario entails the combustion of a stack of wooden pallets with a height of 0.9 m (HRR curve is given in Figure 2.6) located at a distance (x) of 0.2 m (scenario LPG1a) and 1 m from the tank (scenario LPG1b), as shown in Figure 3.11.

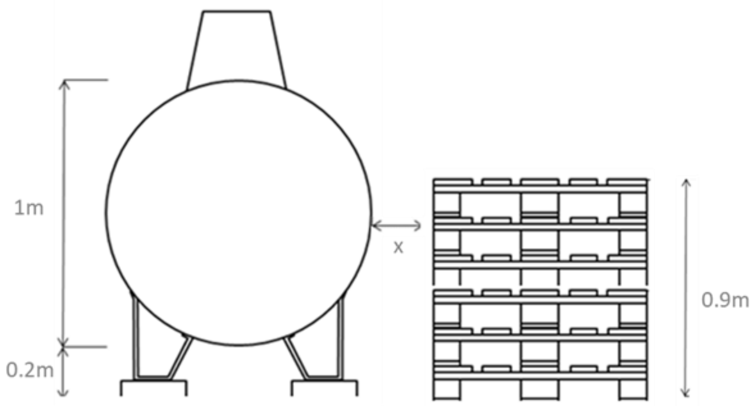

Figure 3.11: LPG tank scenario 1. Adapted from Vacca et al. (2020b).

The second fire scenario (scenario LPG2) consists of the burning of the fuel pack of test 2 (HRR curve given in Figure 2.13) inside a semi-confined space (with dimensions 2.5x2.5x2.5 m^3) located 1 m from an LPG tank, as shown in Figure 3.12.

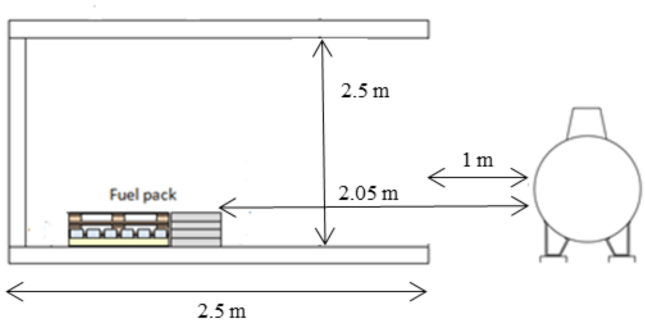

Figure 3.12: LPG tank scenario 2. Adapted from Vacca et al. (2020b).

The third scenario includes an LPG tank exposed to the combustion of a bed of cured grass with wind conditions (20 km/h at 10 m height, scenario LPG3a) and in absence of wind (scenario LPG3b), as shown in Figure 3.13.

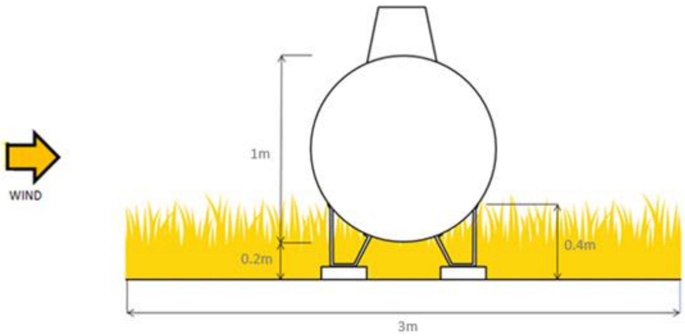

Figure 3.13: LPG tank scenario 3. Adapted from Vacca et al. (2020b).

Scenarios that include an LPG tank (with a filling degree of 80%) exposed to the combustion of a row of six Douglas fir trees located at a distance of 3 m were presented by Scarponi et al. (2020), and are therefore not analysed in this chapter. Results from this analysis will be discussed further in section 3.5 of this chapter.

3.3.1 FDS scenario build-up

All scenarios simulate a 1 m^3 propane tank (diameter of 1000 mm, length of 1470 mm, wall thickness of 6 mm, with semi-elliptical ends) with an adiabatic surface, because the net heat transfer from the gas to the solid is computed during the second step with ANSYS Fluent. The fire source in the first three scenarios is represented as a vent, whose dimensions vary according to the different fuels. Simulations time, peak HRRPUA and fire size are given in Table 3.7 for each scenario. The fire in scenarios LPG1 and LPG2 is simulated as for those described for the glazing system scenarios (i.e., stack of wooden pallets and fuel pack of Test 2), although, given the reduced dimensions of the semi-confined spaces for scenario LPG2, the fuel pack is simulated as a 3D object, not as a vent. The area of the fire and its HRRPUA are adjusted accordingly, to obtain the same fire curve. In scenario LPG3 (grass fire) the fire is simulated by creating a 3 m x 3 m vent on the ground with an assigned HRRPUA of 574 kW/m^2 and a spread rate of 0.9 m/s, taken from experimental data on cured grass (Cheney et al., 1993; Cheney and Gould, 1995).

Table 3.7: Simulation parameters for the first three LPG tank scenarios

Scenario	Simulation time [s]	HRRPUA [kW/m^2]	Fire size [m^2]
LPG1	1000	3563	1.44
LPG2	5000	447	5.7
LPG3	50	574	9

A very fine mesh was chosen for these scenarios, with a nominal size δx size of 0.05 m for the areas of both the tank and the fire source. FDS version 6.7.3 was used to simulate all scenarios.

The needed outputs for these scenarios are the gas temperature by tank walls, the heat transfer coefficient and the incident heat flux onto the tank. All these quantities are obtained through boundary files.

3.3.2 FDS results and further analysis

Results for the first scenario (stack of wooden pallets) indicate that the incident heat flux onto the tank is higher than the threshold value of 22 kW/m^2 for both analysed distances (0.2 m, shown in Figure 3.14a, and 1 m). In scenario LPG1a (0.2 m) the incident heat flux onto the tank is higher than the threshold value for most of the simulation time, while for scenario LPG1b (1 m) the values of the incident radiation are between 22 kW/m^2 and 27 kW/m^2 for approximately 100 s (Figure 3.14b).

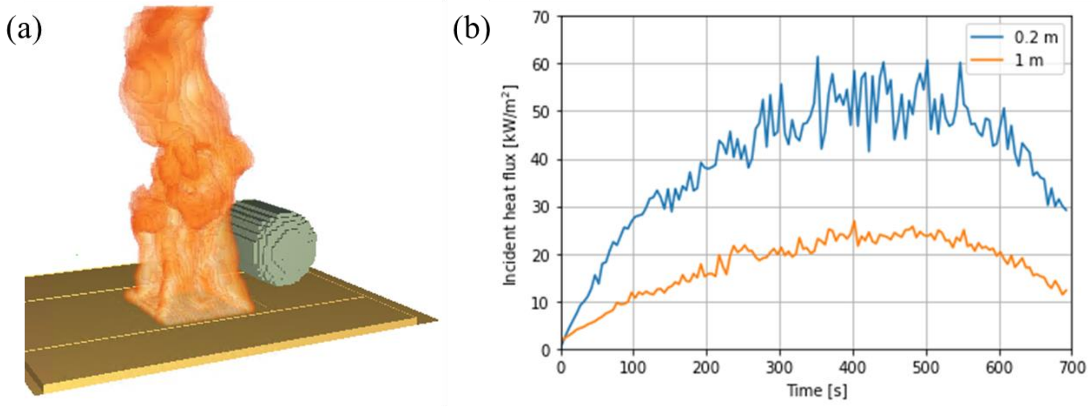

Figure 3.14: (a) Simulation of scenario LPG1a and (b) peak incident heat flux onto the tank for scenario LPG1a (0.2 m) and LPG1b (1 m).

The analysis of the tank's response with Ansys Fluent was done in the frame of the WUIVEW project (Scarponi et al., 2019). The tank of scenario LPG1a was analysed with a filling degree of 80%, and Figure 3.15 shows the results in terms of pressurization curves and maximum wall temperature. The wall temperature never reaches 400°C, resulting in a null WSI, while the PRVI is 0.9, therefore it can be concluded that this scenario does not have the potential to compromise the integrity of the LPG tank.

However, it may lead to the opening of the PRV, which is considered to be an unwanted situation.

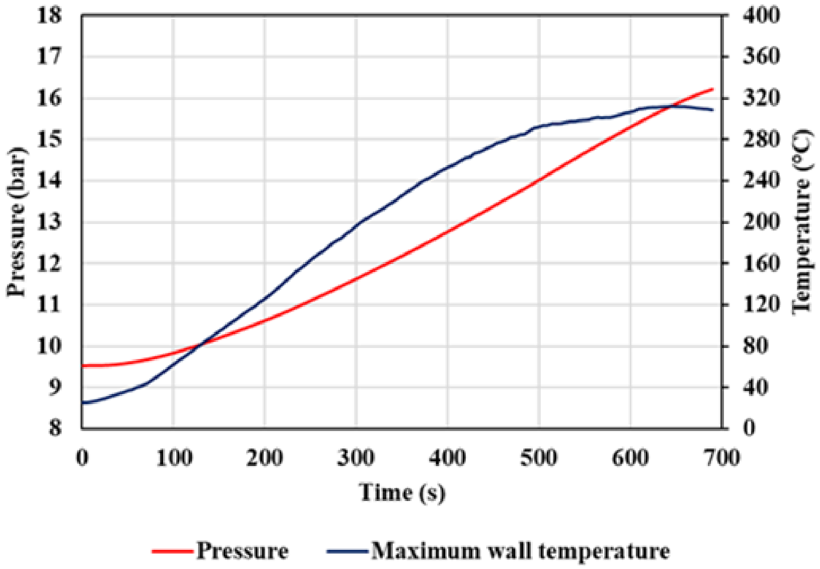

Figure 3.15: Results for the tank's response in scenario LPG1a. Adapted from Vacca et al. (2020b).

Based on the results of scenario LPG1a, the time of exposure to incident heat fluxes higher than 22 kW/m^2 for scenario LPG1b is too short to cause a significant increase of the tank's wall temperature and therefore it will not cause a large pressure rise inside the tank. Therefore, scenario LPG1b is not further analysed.

Results for scenario LPG2 (fuel pack in semi-confined space) show that the incident heat flux onto the tank remains always well below the threshold value of 22 kW/m^2 (Figure 3.16). The scenario can therefore be deemed safe and no further analysis is needed.

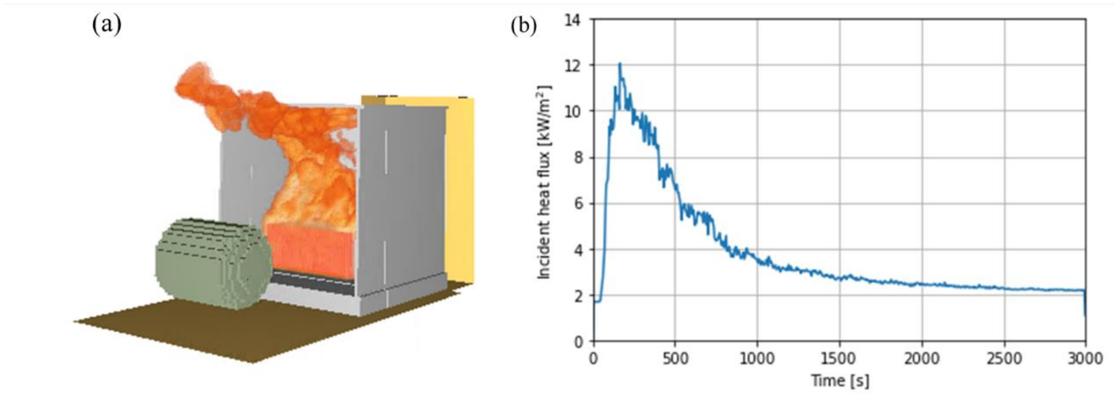

Figure 3.16: (a) Simulation of scenario LPG2 and (b) peak incident heat flux onto the tank.

In both scenarios involving the simulated grass fire, the fire extinguishes in less than 15 s, as can be seen in Figure 3.17. The computed HRR curve is given in Figure 3.17c, where it can be noticed how higher values are reached for the scenario that includes windy conditions. Peak values almost reach 5 MW, as for the scenario with the stack of wooden pallets, although the burning time is much lower.

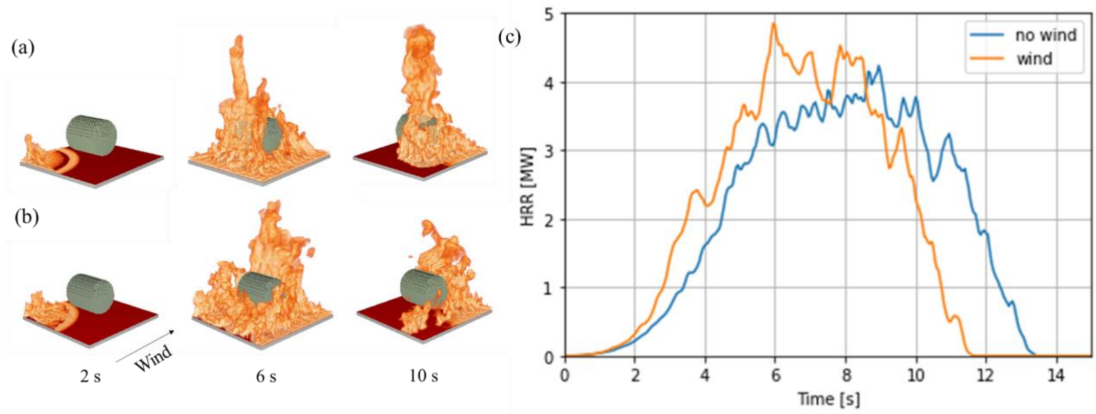

Figure 3.17: (a) Simulation of scenario LPG3a and (b) LPG3b, and (c) the computed HRR curves for both scenarios.

Even though the fire duration is very limited, the incident radiation onto the tank is high. Peak values reach approximately 100 kW/m^2 for the scenario LPG3b (windy conditions), as can be seen in Figure 3.18.

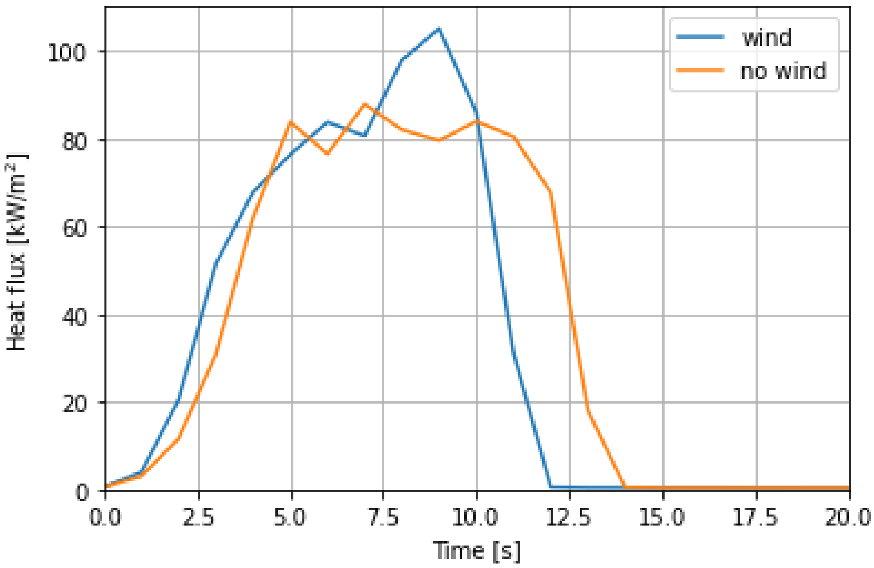

Figure 3.18: Maximum incident radiation to the tank surface as a function of time in calm and windy conditions.

Given that these very high values are reached for less than a second, an average of the incident heat flux over time (every 1 s) was performed for one of the surfaces of the tank (specifically the one facing direction -y, which is the one hit first by the fire), shown in Figure 3.19. Here it can be noticed how the incident heat flux is higher than 22 kW/m^2 for 6 s in the case of no wind, and for 2 s when the wind is simulated (because the fire is spreading faster). Given the very high heat fluxes, further investigation about the conditions of the tank is needed. The filling degree is set to 80%, and the analysis is performed in Ansys Fluent (Vacca et al., 2020b).

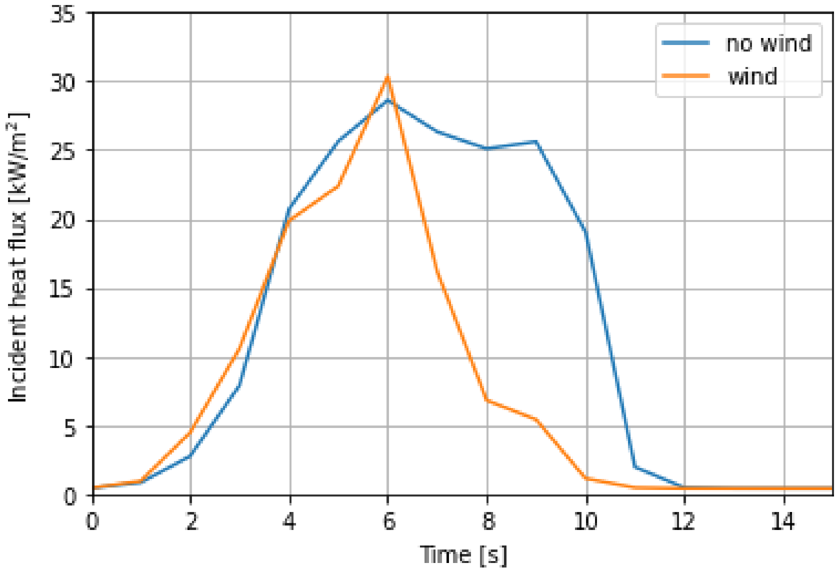

Figure 3.19: Average incident heat flux onto the surface -y of the tank for scenario LPG3a (no wind) and LPG3b (wind).

Figure 3.20 shows the results of the analysis of the tank in terms of pressurization curves and maximum wall temperature. It clearly appears that both scenarios produce a negligible increase in both pressure and wall temperature. It can thus be concluded that scenario LPG3 does not represent a threat for the tank's integrity. This is reflected by the values of the indicators: the PRVI is 0.47 both for calm and windy conditions, whereas the WSI is always null. This result is a direct consequence of the very short duration of the fire.

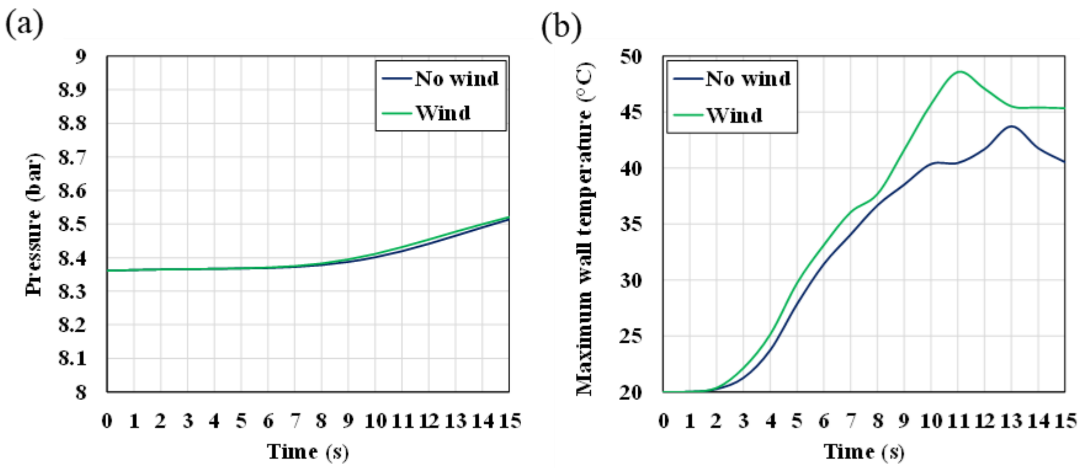

Figure 3.20: (a) Pressurization curves and (b) maximum wall temperature obtained in calm (scenario LPG3a) and windy (scenario LPG3b) conditions. Adapted from Vacca et al. (2020b).

3.4 Semi-confined space scenarios

The analysis of the combustion of fuel packs in concrete semi-confined spaces aims at identifying the wall thickness at which structural survivability is achieved. As presented in Chapter 2, this survivability is guaranteed when the load bearing capacity of a concrete wall stays above the value of 74%.

The methodology for the calculation of the load bearing capacity entails three different steps:

- The first step requires the simulation of the scenario with FDS, which outputs the adiabatic surface temperature (AST) of the analysed wall. This variable represents an effective exposure temperature that can be passed on to a more detailed model of the solid object, and it provides the gas phase thermal boundary condition in a single quantity, which is not affected by the uncertainty associated with the solid phase heat conduction model within FDS. The objective in passing information to a more detailed model is therefore to get a better prediction of the solid temperature (and ultimately its mechanical response) than FDS can provide (McGrattan et al., 2022).
- The second step consists of identifying the temperature profile through the wall by using a finite difference method which uses as input the AST obtained through FDS.
- The third step entails the calculation of the load bearing capacity over time of the analysed wall cross-section according to Eurocode 2 EN 1992-1-1 and EN 1992-1-2 (European Committee for Standardization, 2004a, 2004b).

The analysis is performed on concrete walls, which must be designed and constructed in such a way that they maintain their load bearing capacity function (criterion R) during the required time of exposure to a fire which, in this methodology, is the complete duration (i.e., including the decay phase) of the combustion of artificial elements commonly present at the WUI microscale.

For the simulations of fuels or fuel packs in semi-confined spaces, knowledge is needed on the geometry of the space, the type of materials that compose it (e.g. physical and thermal properties), and finally on the fire characteristics of the ignited fuels (ideally a HRR curve). Three different fire scenarios are analysed: (1) a stack of pallets of 0.9 m high, with the HRR curve shown in Figure 2.6, (2) the fuel pack ignited for test 2 presented in Chapter 2, containing 3 pallets, 4 small mattresses, 11 cardboard sheets, and 7 plastic buckets containing each 12 l of oil-based paint (HRR curve is given in Figure 2.13), (3) two cars, with the HRR curve given in Figure 2.7. In each scenario, a wall thickness of 10 cm is analysed, which is the minimum thickness for a load-bearing solid wall (European Committee for Standardization, 2004b); should failure occur at 10 cm, then the wall thickness is increased to identify at what thickness the scenario can be deemed safe (i.e., failure will not occur).

The dimensions of the semi-confined space are 4 x 4 x 2.5 m^3, with one side fully open, for the first two scenarios (Figure 3.21), while for the third scenario the semi-confined space represents a garage with dimensions 5.8 x 5.8 x 2.5 m^3 and an opening of 4.6 x 2 m^2 (Figure 3.22). In scenario 1, the dimensions of the fire are 1.2 x 1.2 m^2 and it is located 20 cm from the back and the left side walls. In scenario 2 the dimensions of the fire are 3.9 x 3.2 m^2 and it is located 10 cm from the back wall and 40 cm from the left side wall (in this case the fuel pack occupies almost the entire semi-confined space).

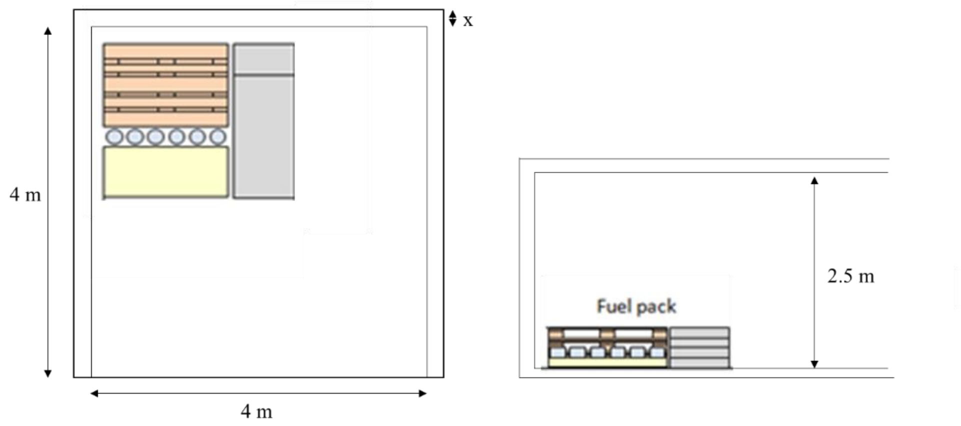

Figure 3.21: Top and side view of the semi-confined spaces for scenarios 1 and 2.

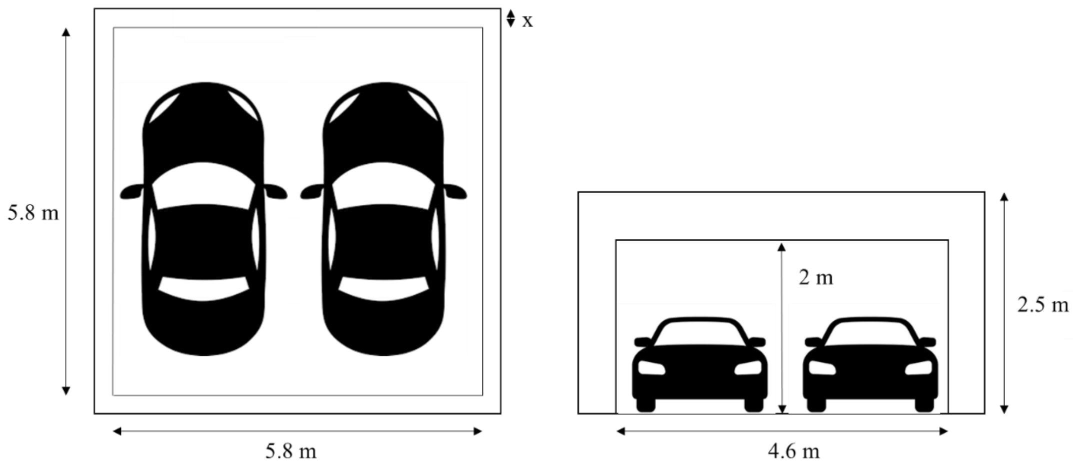

Figure 3.22: Top and front side of the semi-confined spaces for scenario 3.

3.4.1 FDS scenario build-up

In all scenarios the material of all obstacles is concrete, with a density of 2280 kg/m^3, a conductivity of 1.8 W·m^{-1}·K^{-1} (default properties of the Pyrosim materials library (Thunderhead Engineering, 2022) and a specific heat of 2.02 J·kg^{-1}·K^{-1} (European Committee for Standardization, 2004b). The dimensions of the vent that represents the fire vary for each scenario, as does its HRRPUA, which is calculated based on the peak value of the HRR curve. Simulations time, peak HRRPUA and fire size are given for each semi-confined space (SCS) scenario in Table 3.8, based on the HRR curves presented in Chapter 2.

Table 3.8: Simulation parameters for the semi-confined space (SCS) scenarios

Scenario	**Simulation time [s]**	**HRRPUA [kW/m^2]**	**Fire size [m^2]**
SCS1	1000	3563	1.44
SCS2	5000	202	12.48
SCS3	5000	320	25

The mesh size for each of the simulations is calculated based on Equation 3.1, which results in a nominal size mesh δx of 0.1 m for each scenario (fine mesh size). Simulations were performed with the FDS version 6.7.9.

The needed output from fire simulations is the adiabatic surface temperature of the analysed member (Wickström et al., 2007). This output can be obtained with a boundary file, which also gives a visual on the distribution of the adiabatic surface temperature along a surface as well as by placing devices at different locations on the surface of the member that will then be analysed. Devices are located on the left and back walls, as shown in Figure 3.23, at different heights: 0.1 m, 0.5 m, 1 m, 1.5 m, 2 m and 2.4 m (10 cm below the ceiling). They are named according to their location (C for corner, S for side, E for entrance, B1 for back1, etc.) and the height they are positioned at, therefore the device in the left corner at a height of 0.1 m is named C 0.1m.

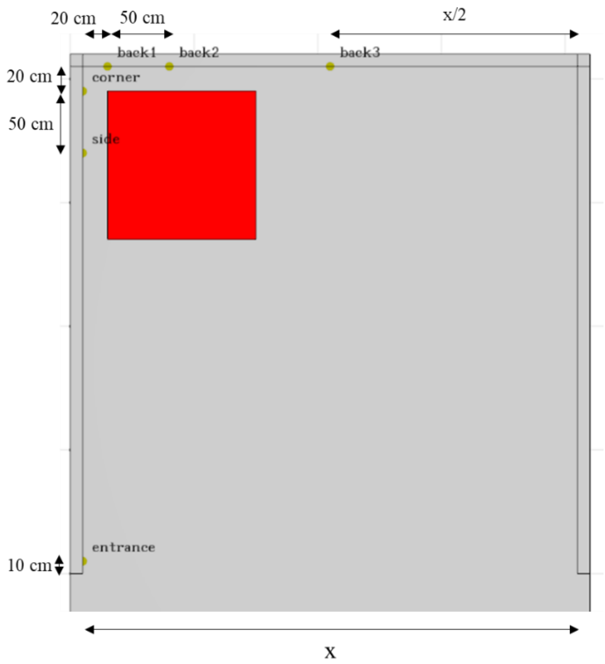

Figure 3.23: Location of adiabatic surface temperature devices for all SCS scenarios., The red square is the fire simulated in scenario 1.

3.4.2 FDS results

Results for SCS 1 are shown in Figure 3.24, where the highest adiabatic surface temperatures for each analysed location of scenario SCS1 are shown (Figure 3.24b). The highest temperatures are recorded by devices B2 2m and S 2m. In this scenario, the flames impinge onto the ceiling.

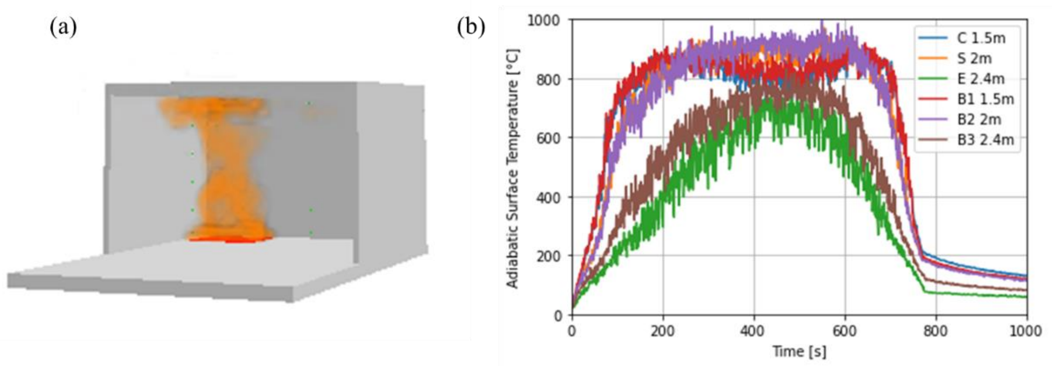

Figure 3.24: Simulation of SCS1 at 200 s (a) and highest recorded values of the adiabatic surface temperature in each analysed location (b).

For scenario SCS2, the highest adiabatic surface temperatures are recorded for each location by the lowest devices due to the low flame height of the simulated fire (Figure 3.25). The highest temperatures are recorded by device B3 0.1m.

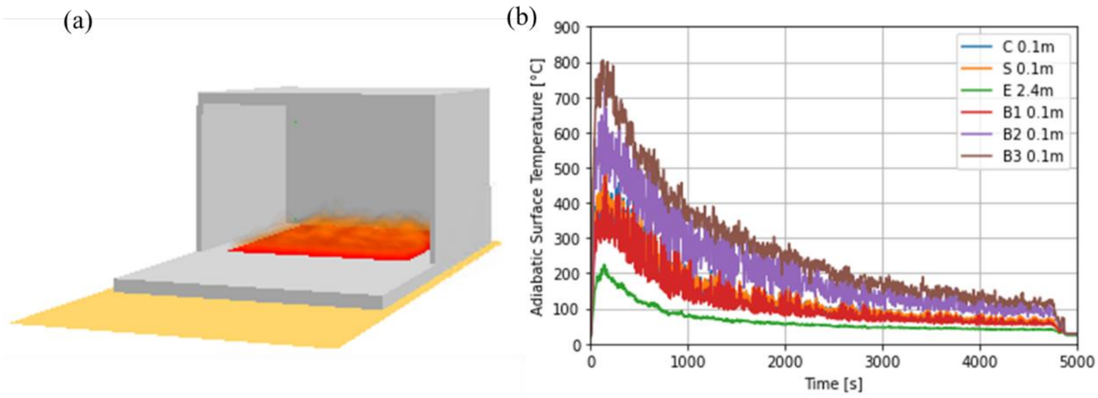

Figure 3.25: Simulation of SCS2 at 200 s (a) and highest recorded values of the adiabatic surface temperature in each analysed location (b).

Also in scenario SCS3, the highest temperatures are recorded by the lowest devices in each location, given that flame heights are low. Figure 3.26 shows that the highest temperatures are recorded by device B3 0.1m.

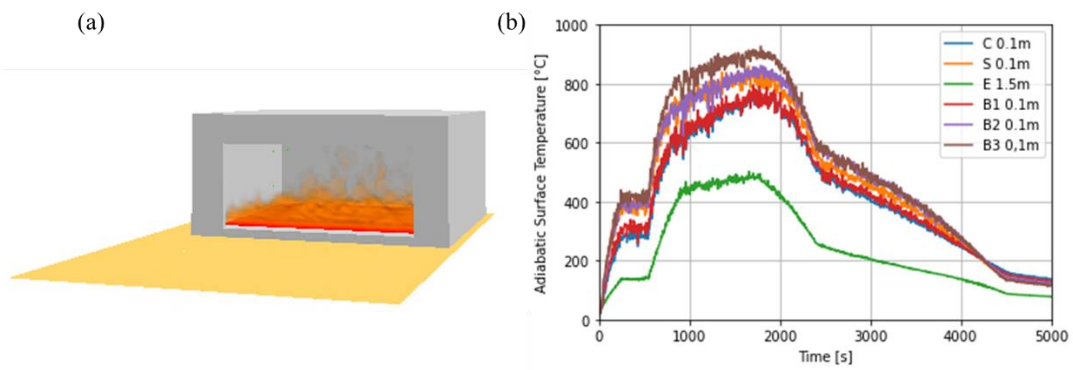

Figure 3.26: Highest recorded values of the adiabatic surface temperature in each analysed location for SCS3.

Temperatures recorded by all devices for the three analysed scenarios are given in Appendix A.

3.4.3 Temperature profile and load bearing capacity

Once the adiabatic surface temperature is obtained, it is used as a boundary condition on the heated side for the computing of the heat flux as given in Equation 3.2 (Wickström et al., 2007), where $\dot{q}''_{tot}$ (W/m^2) is the total net heat flux to the surface, ε is the emissivity of the wall, σ (5.67·10^{-8} W·m^{-2}·K^{-4}) is the Stefan-Boltzmann constant, T_{AST} and T_S (K) are respectively the adiabatic surface temperature and the ambient surface temperature, and h_{conv} (W·m^{-2}·K^{-1}) is the convective heat transfer coefficient. The value of ε is 0.7, while the one for h_{conv} is 25 W·m^{-2}·K^{-1} (European Committee for Standardization, 2004b), which is a conservative value.

$$\dot{q}''_{tot} = \varepsilon\sigma(T_{AST}^4 - T_S^4) + h_{conv}(T_{AST} - T_S) \quad (3.2)$$

The temperature distribution in the cross-section of the wall is obtained through a finite difference method that solves the one-dimensional partial differential equation of heat conductivity, as given in Equations 3.3, 3.4 and 3.5, ρ is the density of the material (kg/m^3), c_p is the specific heat (J·kg^{-1}·K^{-1}), k is the thermal conductivity (W·m^{-1}·K^{-1}), T is the temperature (°C), L is the thickness of the wall (m), and $\dot{q}''_{loss}$ indicates the heat losses on the non-exposed side of the wall (W/m^2). The values of the thermal properties of the concrete change depending on the temperature, and the specific heat capacity c_p is modelled as a constant value of 2020 J·kg^{-1}·K^{-1} for a moisture content of 3%, according to EN 1992-1-2 (European Committee for Standardization, 2004b).

$$\dot{q}''_{tot} = -k\frac{\delta T}{\delta x}\bigg|_{x=0} \text{ for } x = 0 \quad (3.3)$$

$$\rho c_p \frac{\partial T}{\partial t} = \frac{\partial}{\partial x}\left(k\frac{\delta T}{\delta x}\right) \text{ for } 0 < x < L \quad (3.4)$$

$$-k\frac{\delta T}{\delta x}\bigg|_{x=L} = \dot{q}''_{loss} \text{ for } x = L \quad (3.5)$$

Once the temperature profile through the wall is calculated, the load bearing capacity can be found according to the Eurocode 2. An ad-hoc code has been developed to analyse the structural survivability of concrete walls during the duration of the previously simulated fire, which uses the temperature profile through the wall as input, and outputs a curve of the load bearing capacity of the wall over time.

As the temperature rises, concrete loses its compressive and tensile strengths, impacting the stress-strain relationship. The total strain at any point of the cross section is calculated with Equation 3.6, while the mechanical strain for each point is calculated according to Equation 3.7, where ε_0 is the average strain, χ is the curvature (m^{-1}), y is the point's coordinate from the centre of the cross-section (m), and ε_{therm} is thermal elongation defined by the Eurocode (European Committee for Standardization, 2004b).

$$\varepsilon_{tot} = \varepsilon_0 + \chi y \quad (3.6)$$

$$\varepsilon_{mech} = \varepsilon_{tot} - \varepsilon_{therm} \tag{3.7}$$

Then the stress at any point (σ) is calculated using the mechanical strain and stress-strain diagrams of concrete at elevated temperature (European Committee for Standardization, 2004b).

The axial force and the moment are calculated for every point in time for any combination average strain value and the curvature according to Equation 3.8 and Equation 3.9 respectively (European Committee for Standardization, 2004a), where σ is the stress and A is the area of each analysed section. For each value of the average strain, the code finds the value of the curvature so that the moment around the centre of the cross-section is equal to zero.

$$N = \sum \sigma A \tag{3.8}$$

$$M = \sum \sigma yA \tag{3.9}$$

The maximum value of the axial force is then chosen as the capacity for that point in time N^t and the reduction factor η_{fi}^t can be identified at every time step by dividing it with the ambient capacity N_{amb}, as given in Equation 3.10.

$$\eta_{fi}^t = \frac{N^t}{N_{amb}} \tag{3.10}$$

As presented in Chapter 2, by using the design method presented in EN 1992-1-2 (European Committee for Standardization, 2004b), it can be assumed that the effects of actions on the structural member in case of fire can be obtained by multiplying the effects of actions for normal temperature with the factor ranging from 74% to 33% (i.e., the reduction factor ranges between these two values for all combinations of live/dead load ratio). Under the assumption that the member was designed with 100% utilization, it can be concluded that if the reduction factor from Equation 3.9 is higher than 74% the wall will not fail and that if it falls below 33%, then collapse of the structure is guaranteed (Vacca et al., 2022).

Result for the cross-section B2 2m of scenario SCS1 (section that recorded the highest AST values) are presented in Figure 3.27. About halfway through the simulation (6 minutes), the temperature at the exposed surface of the analysed cross section is 619°C, while at the end of the decay phase of the fire (12 minutes), the surface has a temperature of 589°C, as shown in Figure 3.27a. The back of the wall remains at ambient temperature during the entire simulation. At the end of the simulation, the load bearing capacity drops to 83%, remaining therefore well above the performance criterion of 74%, as can be seen in Figure 3.27b.

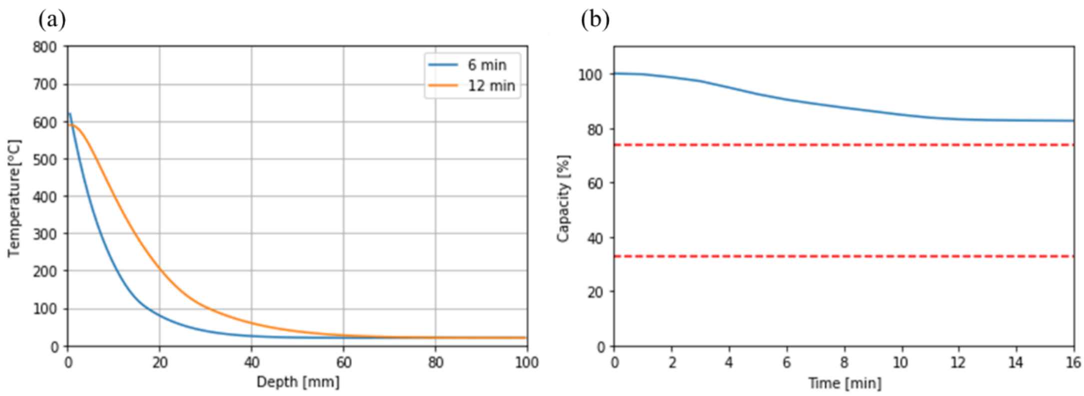

Figure 3.27: Results for the cross-section of B2 2m for SCS1 with a wall thickness of 10 cm: (a) temperature profile through the cross-section at the time of 6 min and 12 min, (b) load bearing capacity of the analysed cross-section over time.

Result for the cross-section B3 0.1m of scenario SCS2 (section that recorded the highest AST values) are presented in Figure 3.28. Temperature profiles through the analysed cross section are plotted every 15 minutes in Figure 3.28a. At the surface, peak temperatures reach 310°C 15 minutes after the start of the fire. As time goes on, the temperature inside the cross section increases, reaching a value at the back of the wall of 71°C at 75 minutes. At the end of the simulation, the load bearing capacity of the analysed cross section reaches a value of 93%, as shown in Figure 3.28b.

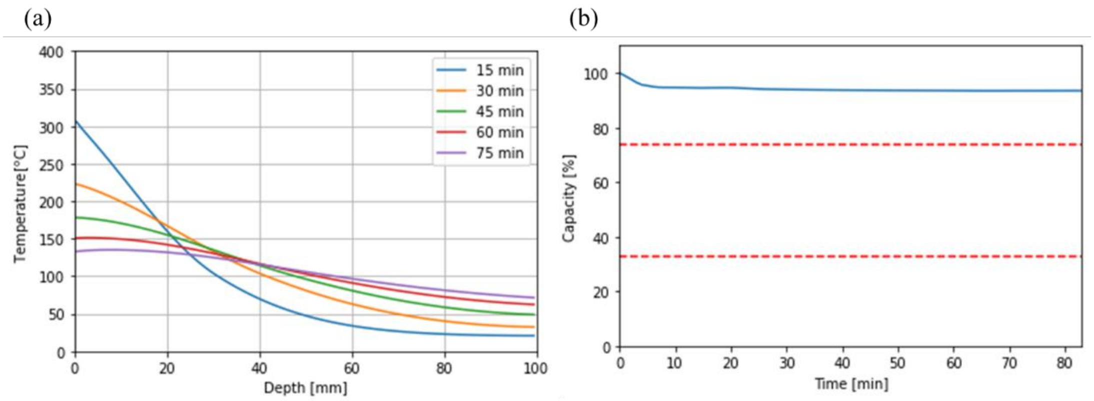

Figure 3.28: Results for the cross-section of B3 0.1m for SCS2 with a wall thickness of 10 cm: (a) temperature profile through the cross-section recorded every 15 minutes, (b) load bearing capacity of the analysed cross-section over time.

Results for the cross-section B3 0.1m for scenario SCS3 (section that recorded the highest AST values) are shown in Figure 3.29. Thirty minutes after the start of the simulation, the wall temperature at the surface of the cross-section reaches 818°C (Figure 3.29a). As time goes on, the temperature increases through the cross-section, reaching 70°C at the back of the wall at 75 minutes. As shown in Figure 3.29b, the load bearing capacity of the cross-section drops below 74% at 34 minutes, reaching a value of 70% at the end of the simulation. This shows that failure of the envelope could occur in this specific scenario.

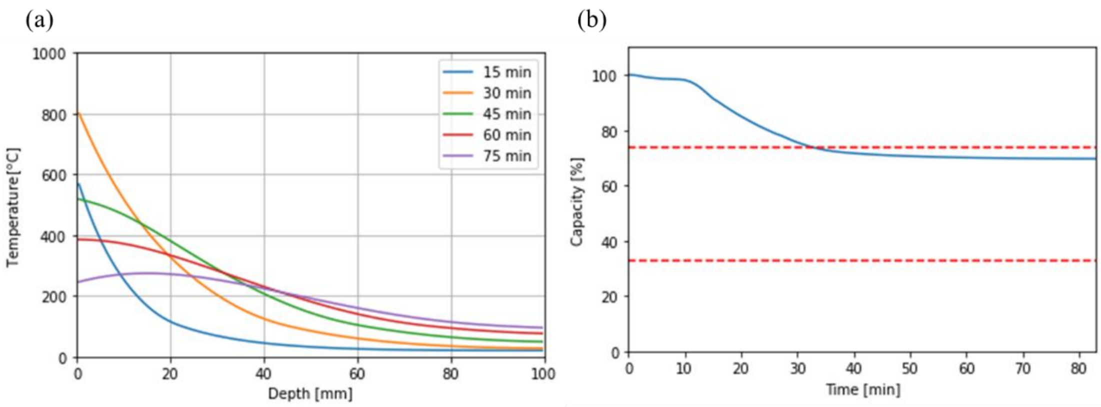

Figure 3.29: Results for the cross-section of B3 0.1m for SCS3 with a wall thickness of 10 cm: (a) temperature profile through the cross-section recorded every 15 minutes, (b) load bearing capacity of the analysed cross-section over time.

Given the failure of the 10 cm thick wall for scenario SCS3, a wall thickness of 12 cm is analysed for the same scenario (Figure 3.30). As for the previous analysis, peak temperatures at the surface reach 818°C at 30 minutes, while at the back of the cross section the highest temperature value at 75 minutes reaches 66°C. For a wall thickness of 12 cm, the load bearing capacity drops to a minimum value of 85%, making the scenario safe.

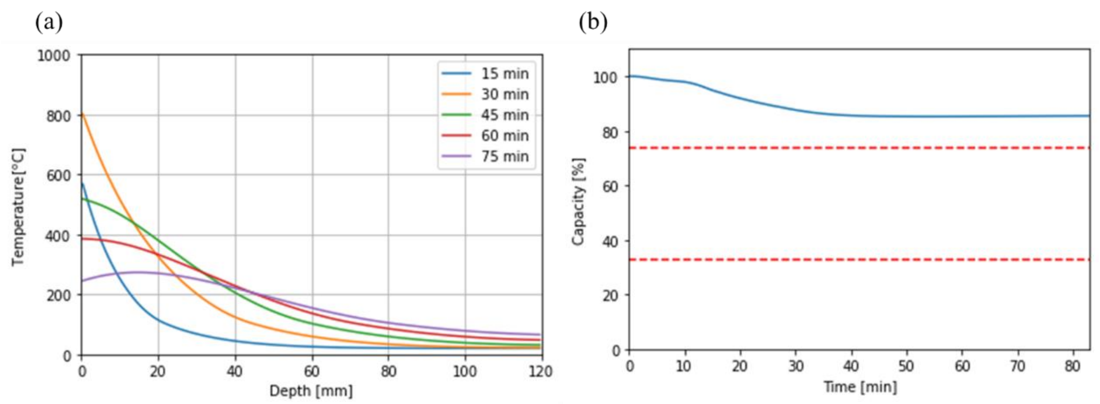

Figure 3.30: Results for the cross-section of B3 0.1m for SCS3 with a wall thickness of 12 cm: (a) temperature profile through the cross-section recorded every 15 minutes, (b) load bearing capacity of the analysed cross-section over time.

3.5 Summary of the obtained results

Safety criteria have been identified for each of the analysed scenarios, and they are here summarized.

For the scenarios that involve glazing systems exposed to the combustion of artificial fuels with peak HRR values up to 5.5 MW and a burning time of approximately 12 minutes, the thickness of the pane impacts its resistance to fire: the thicker the pane, the longer it will resist when exposed to the same fire scenario. In the analysed scenarios with natural fuels, where the burning time is much lower (approximately 20 s) and the peak HRR is much higher (up to 28 MW), the thickness of the pane does not influence the resistance to fire. For both of the analysed types of fuels, double pane windows resist better than single pane ones, given that failure occurs when the second pane breaks. Therefore, safety distances are shorter for double pane glazing compared to single pane. While the material of the frame does not affect safety distances for the analysed artificial fuels scenarios, for scenarios involving natural fuels, PVC frames failed (i.e., reached the melting point) even when the glass pane did not. Therefore, larger safety distances are needed for glazing systems with PVC frames in comparison with those with aluminium frames. In addition, large panes in the analysed artificial fuels scenarios are more vulnerable than smaller ones in scenarios where no wind is simulated, as they reach the critical values at distances where the small ones don't. This is not reflected in the vegetation scenarios.

Based on the results of the analysed scenarios, given in Table 3.3, artificial fuels should be placed at least 5 m away from unprotected double pane glazing systems, and at least 6.5 m from unprotected single pane glazing systems. As for the vegetation scenarios, results show that safety distances of at least 3.5 m are needed for glazing systems with PVC frames (single pane and double pane systems), while at least 2.5 m and 1 m are needed for respectively single pane and double pane systems with aluminium frames.

Analysed scenarios that include solid panel window shutters show that these shutters are able to protect the glazing system located behind them. Out of the three analysed materials, aluminium showed the best performance, because its surface does not heat up as much as wood or PVC, and its melting point is much higher than the one of PVC and then the ignition temperature of wood.

As for the presence of artificial fuels close to LPG tanks, a distance of 1 m seems to be sufficient for fuels that burn for less than 12 minutes and that reach an HRR peak of approximately 5 MW. As for other types of artificial fuels, if they produce a heat flux onto the tank higher than 22 kW/m^2 for longer than 10 minutes, then there is the risk that the PRV might open, causing a domino effect. When it comes to natural fuels, the analysed grass fire scenario can be deemed safe due to the very short time of the exposure to incident heat fluxes above 22 kW/m^2. Negligible effects in terms of pressure increase and temperature rise were also identified for the scenario involving 6 Douglas Fir trees located 3 m from the tank (Scarponi et al., 2020). Further investigation is needed to identify whether smaller distances would impact the integrity of the tank or would cause the PRV to open.

When it comes to fuels located in semi-confined spaces, results show that concrete walls of a thickness of 10 cm can withstand a fire of short duration (approximately 12 minutes) with peak HRR values of 5.5 MW. Concrete walls of this thickness can also withstand peak HRR values up to 2.55 MW with much higher burning time (approximately 1 hour and 20 minutes). However, such thickness cannot withstand higher HRR values for the same amount of time, as shown by the scenario of the combustion of two cars. In this scenario, the wall does not fail if its thickness is increased to 12 cm, which is the minimum wall thickness for a standard fire resistance (REI) of 90 minutes of a concrete load-bearing wall exposed to a fire on one side (European Committee for Standardization, 2004b).

3.6 Conclusions

A methodology for the analysis of typical WUI property sub-systems is presented in this chapter, which allows to analyse the different variables of WUI scenarios thanks to the modelling tool FDS. The methodology is based on a PBD approach, where results from the modelling of the scenarios are compared to performance criteria.

The methodology is presented by analysing three different sub-systems of Mediterranean WUI properties. Scenarios including the combustion of fuels located close to glazing systems and LPG tanks are analysed to identify safety distances when it comes to both artificial and natural fuels. The combustion of artificial fuels and fuel packs was analysed in concrete semi-confined spaces to identify the wall thickness at which failure of the envelope would not occur. These scenarios include typical situations observed at the Mediterranean WUI, as described in Chapter 1.

Analysed scenarios of fuels located in front of glazing systems showed that double pane glazing systems are more resistant than single pane glazing systems exposed to the same fire scenario. When it comes to frame materials, aluminium performs better than PVC, and the same is valid for shutter materials, where aluminium performed better than PVC and wood. In order for glazing systems not to fail (i.e., crack and break, allowing the fire to enter inside the building), safe distances are identified for both artificial and natural fuels (specifically ornamental vegetation). These distances are larger for artificial fuels because their burning time is much longer in comparison with the burning time of natural fuels.

Analysed scenarios of fuels located close to LPG tanks highlighted the fact that fire scenarios with a very short burning time (less than 20 s), such as grass fires, do not affect the integrity of the tank even if producing very high incident heat fluxes onto the tank (approximately 100 kW/m^2). On the other hand, when the burning time is longer, such as for artificial fuels, very close distances between the fuel and the tank may lead to the opening of the PRV of the tank, causing unwanted situations.

The safe thickness for the envelope of concrete semi-confined spaces in which fuels that can burn for almost 80 minutes reaching peaks of 8 MW are stored (for example, two cars) has been identified as 12 cm. For these types of scenarios, the load bearing capacity of the concrete walls will not fall below the threshold value set as performance criterion.

The obtained results are going to be taken into account when building a Vulnerability Assessment Tool (VAT) for homes located at the Mediterranean WUI, which is presented in the following chapter.

Although only a few scenarios have been analysed in this chapter, the presented methodology can be used as a baseline for the analysis of other WUI scenarios, which might include different configurations, fuels, building and property sub-systems. Additionally, the methodology can be applied also to other types of WUI landscapes, not only the Mediterranean one.

3.7 References

Cheney, N.P., Gould, J.S., 1995. Fire growth in grassland fuels. Int. J. Wildl. Fire 5, 237–247. https://doi.org/10.1071/WF9950237

Cheney, N.P., Gould, J.S., Catchpole, W.R., 1993. The influence of Fuel, Weather and Fire Shape Variables on Fire-Spread in grasslands. Int. J. Wildl. Fire 31–44.

European Committee for Standardization, 2004a. EN 1992-1-1: Eurocode 2: Design of concrete structures - Part 1-1: General rules and rules for buildings.

European Committee for Standardization, 2004b. EN 1992-1-2: Eurocode 2: Design of concrete structures - Part 1-2: General rules - Structural fire design.

Harada, K., Enomoto, A., Uede, K., Wakamatsu, T., 2000. An experimental study on glass cracking and fallout by radiant heat exposure. Fire Saf. Sci. 1063–1074. https://doi.org/10.3801/IAFSS.FSS.6-1063

Hurley, M.J., Gottuk, D.T., Hall, J.J.R., Harada, K., Kuligowski, E.D., Puchovsky, M., Torero, J.L., Watts, J.J.M., CJ, W., 2016. SFPE Handbook of Fire Protection Engineering, 5th ed. Springer. https://doi.org/10.1007/978-1-4939-2565-0

McGrattan, K., Hostikka, S., McDermott, R., Floyd, J., Weinschenk, C., Overhold, K., 2022. Sixth Edition Fire Dynamics Simulator User’s Guide (FDS). NIST Spec. Publ. 1019.

McGrattan, K.B., Hostikka, S., Floyd, J., McDermott, R., Vanella, M., 2022. Fire dynamics Simulator Technical Reference Guide Volume 1: Mathematical Model. https://doi.org/http://dx.doi.org/10.6028/NIST.SP.101

Mell, W., Maranghides, A., McDermott, R., Manzello, S.L., 2009. Numerical simulation and experiments of burning douglas fir trees. Combust. Flame 156, 2023–2041. https://doi.org/10.1016/j.combustflame.2009.06.015

NIST, 2022. Fire Dynamics Simulator.

Scarponi, G.E., Pastor, E., Planas, E., Cozzani, V., 2020. Analysis of the impact of wildland-urban-interface fires on LPG domestic tanks. Saf. Sci. 124, 104588. https://doi.org/10.1016/j.ssci.2019.104588

Scarponi, G.E., Vacca, P., Salzano, E., Tugnoli, A., Pastor, E., Cozzani, V., 2019. Deliverable D3.1 - Report on LPG infrastructure impact at the WUI microscale. https://wuiview.webs.upc.edu/download/WUIVIEW_D3.1_F.pdf

Steffens, R., 2016. When fire burns, are we prepared? Wildfire 25(3):8.

Thunderhead Engineering, 2022. Materials and Layered Surfaces. https://support.thunderheadeng.com/tutorials/pyrosim/fundamentals/4-materials-and-layered-surfaces/#_before_starting (accessed 3.7.23).

Vacca, P., Àgueda, A., Muñoz, J.A., Planas, E., Pastor, E., Heymes, F., Ismael, E., Eyssette, R., Cozzani, V., Scarponi, G.E., 2020a. WUIVIEW Deliverable 6.1 - Recommendations on structure survivability and sheltering capacity. https://wuiview.webs.upc.edu/download/D6.1_F_Recommendations%20on%20structure%20survivability%20and%20sheltering%20capacity.pdf

Vacca, P., Caballero, D., Pastor, E., Planas, E., 2020b. WUI fire risk mitigation in Europe: A performance-based design approach at home-owner level. J. Saf. Sci. Resil. 1, 97–105. https://doi.org/10.1016/j.jnlssr.2020.08.001

Vacca, P., Pastor, E., Planas, E., 2022. Analysis of the load bearing capacity of concrete semi-confined spaces exposed to the combustion of two cars at the Wildland-Urban Interface, in: Vagsaether, K., Lach, A.W., Bradley, D., Lundberg, J. (Eds.), Proceedings of the Tenth International Seminar on Fire and Explosion Hazards. pp. 498–506.

Wang, Y., Hu, J., 2019. Performance of laminated glazing under fire conditions. Compos. Struct. 223. https://doi.org/10.1016/j.compstruct.2019.110903

Wickström, U., Duthinh, D., McGrattan, K., 2007. Adiabatic Surface Temperature for Calculating Heat Transfer To Fire Introduction, in: Proceedings of the Eleventh International Interflam Conference Interscience Communications. London.

Chapter 4

Vulnerability Assessment Tool

4.1 Introduction

The need for a quantitative tool for the assessment of building vulnerability at the Mediterranean WUI has been highlighted in Chapter 1, as available tools, especially in Europe, are mostly qualitative and do not provide a great degree of detail. Additionally, European regulations and guidelines are often poorly implemented (Ganteaume et al., 2021), and they do not offer any clues for the identification of interventions that need to be prioritized. This need has led to the development of a Vulnerability Assessment Tool (VAT) for the analysis of buildings and properties at the Mediterranean WUI[1].

The different pathways that lead to building ignition identified in Chapter 2 can be further analysed in order to pinpoint the sequence of events that leads to this ignition. A fault tree that includes events that lead to structural vulnerabilities and fire exposure conditions of a building is created. Based on the events of the fault tree, a VAT is developed in form of a checklist that can be easily filled in by homeowners or residents themselves and identifies the main issues that need to be addressed. Due to the lack of quantitative data on the failure of the events identified in the fault tree, the probability of fire entrance inside a building is derived from expert judgement, and a fuzzy logic elicitation method is used to aggregate the statements of the experts. The tool is tested through data obtained from three recent WUI fire events in Spain and Portugal and it is compared to another existing tool (Papathoma-Köhle et al., 2022) that deals with Mediterranean WUI microscale vulnerabilities.

4.2 Fault tree analysis

Based on the structural vulnerabilities and pattern scenarios identified in Chapter 2, a more complete version of the fault tree in Figure 2.1 that describes the events that lead to a fire entering a building located at the WUI has been created (Figure 4.1). The causes of fire entrance inside a building can be summarized by the two intermediate events of the fault tree: one involves structural vulnerabilities typical of Mediterranean structures and the other accounts for the fire exposure conditions of the building. For the fire to enter a building, both of these events must occur, meaning that at least some part of the building is vulnerable to fire, and the building has to be exposed to the fire, either through firebrands, direct flame contact or radiant heat. These two intermediate events are further analysed and the basic events (B) that lead to them are identified.

[1] Part of the content included in this chapter has been published as a journal paper (Àgueda et al. 2023).

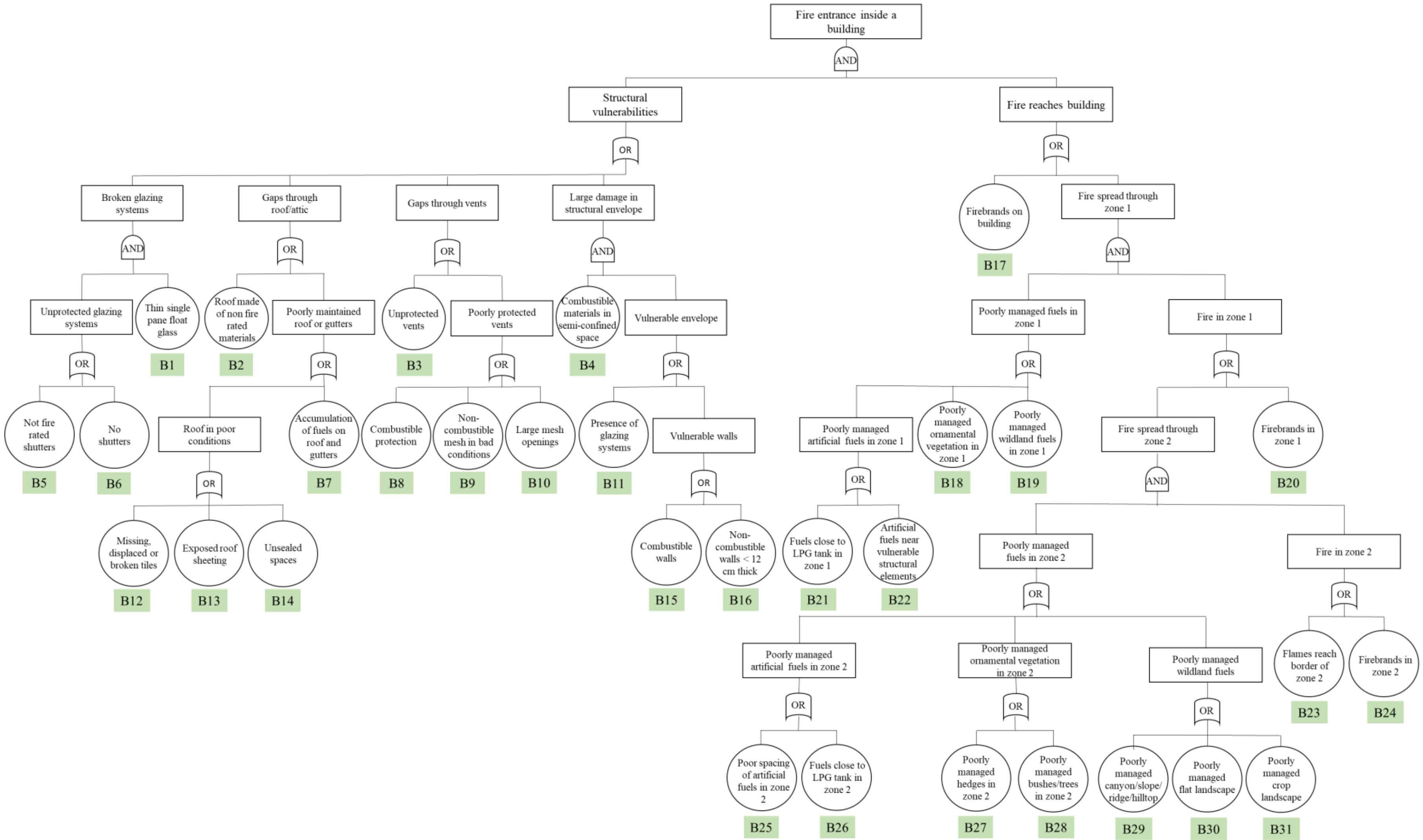

Figure 4.1: Fault tree of the events that lead to fire entrance inside a building. B: basic event

4.2.1 Structural vulnerabilities

Structural vulnerabilities of the building are identified based on the different paths through which fire could enter, and they comprise four main pathways, which are associated to either gaps that already existed in the building due to bad maintenance, or that can be caused by the fire itself.

These pathways are: glazing systems, roof, vents and structural damage to the dwelling's envelope due to heat accumulation in semi-confined spaces, as described in Chapter 2. The failure sequence for each of these elements is identified as shown in Figure 4.1. The failure of a glazing system depends on whether it is protected by shutters that are not fire rated (B5) or there is no shutter protection (B6) and on the thickness of the glass pane (B1; the considered type is annealed or float glass, given it is the most common in residential windows). The failure of the roof depends on the material of the roof covering (B2), as well as the maintenance level of the roof itself; the roof, including the gutters, is considered to be poorly maintained when it does not comply to at least one of the following rules: there are no missing, displaced or broken tiles (B12); the underlying roof sheet is not exposed (B13); there are no unsealed spaces between the roof and the external walls or between its covering and the decking (B14); regular cleaning of both roof and gutters is performed (B7). The probability of fire entrance through vents is determined by whether the vents are protected or not (B3), as well as by the material and conditions of the protection (B8 to B10). The failure of the structural envelope that is shared with a semi-confined space is conditioned by the presence of combustible materials in this space (B4) and the presence of glazing systems (B11) as well as the construction material and thickness of the envelope (B15, B16), for which a safe thickness of 12 cm has been identified in Chapter 3.

The fault tree in Figure 2.1 also includes the event of windows and/or doors left open due to unprepared evacuation. Given that the scope of the Vulnerability Assessment Tool is to evaluate the home and property in their usual conditions, this event is not considered in the fault tree in Figure 4.1. Nevertheless, it should be made clear to homeowners and residents that they should close everything in their home (shutters, windows, doors) before evacuating, otherwise their home will be extremely vulnerable to fire.

4.2.2 Fire spread towards the building

When it comes to the ways the fire can reach the building, two areas around the dwelling have been identified: zone 1 includes the area within a radius of 10 m from the dwelling, while zone 2 consists of a 10 m to 30 m ring around the dwelling. For zone 2, a ring from 10 m to 50 m was initially considered, therefore taking into account some of the European guidelines, but during the analysis of the case studies presented further in this chapter, it was observed that parcels do not often reach this size, and the selected zone would frequently include not only the adjacent neighbours, but also those located further, adding too many variables that cannot directly be controlled by the homeowner. In both zones, three types of fuels are considered: ornamental vegetation, artificial fuels (e.g., LPG tanks, garden furniture, sheds, etc.) and wildland vegetation. For each zone, a set of fuel management rules that can reduce the probability of the fire reaching the dwelling is established (Table 4.1); rules are stricter for zone 1 due to the close proximity to the dwelling. When there is no compliance to all of the rules, then the fuel can be deemed as poorly managed, as given in the fault tree in Figure 4.1. When it comes to vegetation, these rules are selected based on a review of existing guidelines for the management of vegetation specific for Mediterranean-type landscapes. Therefore, the analysis is limited to guidelines of the following countries or regions: France (Préfet de Bouches-du-Rhône, 2014; Préfet de la Haute-Corse, 2022; Prefet de Vaucluse, 2013; Préfet des Alpes-de-Haute-Provence, 2013; Prefet des Alpes-Maritimes, 2014; Préfet du Var, 2015), Portugal (Autoridade Florestal National, 2008), Spain (Generalitat de Catalunya, 2019, 2005; Manca and López, 2014), California (Cal Fire, 2022), South Australia (South Australia County Fire Service, 2022) and Victoria (Victoria County Fire Authority, 2022). The Italian guidelines were also analysed; however, they do not include specific rules for the spacing of vegetation or artificial fuels within the defensible space. Overall, the strictest rules for distancing of wildland fuels are considered. When available, rules are derived from scientific findings, as is the case for the distancing of fuels from glazing systems and LPG tanks, identified in Chapter 3, or the one between vegetation and artificial fuels.

Information on spacing between artificial fuels or fuel packs (such as sheds, garden furniture, vehicles, etc.) to avoid fire spread through these types of fuels was not found in the analysed guidelines nor in any scientific study. Therefore, the distance selected for these rules comes from an extrapolation from the case study of the Camp Fire in California, in which fire spread from artificial fuel to artificial fuel (or a dwelling with a façade made of combustible materials) was recorded (Maranghides et al., 2021).

Table 4.1: Rules for fuel management in zone 1 and zone 2

Rules	Zone 1	Zone 2
Wildland vegetation and/or crop landscape		
1. Separation between tree crowns/high shrubs should be at least 9 m (Cal Fire, 2022).	X	
2. Separation between tree crowns/high shrubs should be at least 9 m for landscapes such as canyons/ridges/hilltops and 6 m for flat or crop landscapes (Cal Fire, 2022; Generalitat de Catalunya, 2005).		X
3. Lower tree branches should be pruned at ⅓ of tree height (Generalitat de Catalunya, 2005; Préfet de la Haute-Corse, 2022).	X	X
4. There should be a separation between grouping of shrubs (or regrowth forest or young trees) of at least 3 m (Generalitat de Catalunya, 2005).	X	X
5. Surface fuels should be max 10 cm deep (Morvan, 2007).	X	X
6. Trees should not overhang the roofline of the building (Cal Fire, 2022; Préfet de Bouches-du-Rhône, 2014; South Australia County Fire Service, 2022; Victoria County Fire Authority, 2022).	X	
7. Shrubs and trees should be horizontally separated by at least 3.5 m from any glazing system (Chapter 3).	X	
Ornamental vegetation		
1. Very flammable species (e.g., pine tree, eucalyptus, cypress, bay laurel, cherry laurel, rosemary, Japanese spindle, oleander, laurustinus, etc.) should not be present. Avoid vegetation with closely packed leaves and branches, fine textures, small, thin and narrow leaves, and high amounts of resins or oils (Manca and López, 2014; Victoria County Fire Authority, 2022).	X	
2. Shrubs and trees should be horizontally separated by at least 3.5 m from any glazing system (Chapter 3).	X	

3. Trees should not overhang the roofline of the building (Cal Fire, 2022; Préfet de Bouches-du-Rhône, 2014; South Australia County Fire Service, 2022; Victoria County Fire Authority, 2022).	X	
4. Trees and shrubs should be separated by at least 6 m (Generalitat de Catalunya, 2005).	X	
5. The distance between ornamental bushes and other vegetation should be bigger than 3 m (Generalitat de Catalunya, 2005).		X
6. Individual and groups of ornamental bushes should be less than 5 m wide (Préfet de la Haute-Corse, 2022).	X	X
7. There should be a non-continuous litter layer (Victoria County Fire Authority, 2022).	X	
8. There should not be any dead vegetation or vegetative debris (Cal Fire, 2022; Préfet de Bouches-du-Rhône, 2014; Prefet de Vaucluse, 2013; Préfet des Alpes-de-Haute-Provence, 2013; Préfet du Var, 2015).	X	
9. Hedges should not be located within 2 m from other vegetation (Préfet de la Haute-Corse, 2022).	X	X
10. Hedges should not be aligned with the wind direction or the main slope (Vacca et al., 2020).	X	X
Artificial fuels		
1. No combustible materials should be located within 2 m of LPG tanks or canisters (Vacca et al., 2020).	X	X
2. No artificial fuels should be located within 5 m of double pane glazing systems or 6.5 m of single pane glazing systems (Chapter 3).	X	
3. No artificial fuels should be located within 5 m of roof or gutters (Vacca et al., 2020).	X	
4. In case of wild vegetation of mainly trees, no artificial fuels should be placed at a distance of minimum 20 m from these trees (Cohen, 2000).	X	X
5. The distance between fuels or fuel packs should be at least 5 m (Maranghides et al., 2021).	X	X

According to the events in the fault tree (Figure 4.1), fire will reach the building either if firebrands land on the building (B17) or if the fire is able to spread through zone 1. This fire spread can happen if fuels within zone 1 are poorly managed (B18, B19, B21, B22), therefore causing fire spread from one element to another when ignited, and if the fire reaches this zone either as firebrands (B20) or because flames have spread through zone 2, reaching zone 1. The fire can spread through zone 2 if firebrands (B24) or flames reach the border of this zone (B23) and if fuels in this zone are poorly managed (B25 to B31), which will cause fire spread from one element to another.

An assumption is made that in case of a wildfire approaching a settlement, firebrand deposition will always happen (events B17, B20 and B24), with the subsequent ignition of the fuels located on the property.

4.3 Assigning probabilities based on past events

In order to obtain quantitative data for the VAT, statistical data on the failure of each of the basic events in the fault tree in Figure 4.1 is needed. This could be obtained from the analysis of buildings damaged in past WUI fires. Given that Mediterranean-type constructions differ from most Australian, USA and Canadian construction types, probabilistic data from past fires in these countries cannot be used for the development of this tool.

In the Mediterranean landscape, the impact onto buildings was analysed by Ribeiro et al. (2020) in the Pedrógão Grande fire of June 2017. A ground survey was conducted, involving the interview of hundreds of people. The variables of interest for the VAT that were collected by this study include information on the structure, its surroundings, and the impact of the fire onto the structure; where possible, the ignition location was identified. Data was collected on the following types of structures: primary housing, secondary housing, agricultural warehouse, shed/storage, garage, commerce, industry, uninhabited house, vacant structure, cattle shed/stable, outdoor kitchen and other. In Ribeiro et al. (2020) the percentage for each ignition location is given globally for all the types of structures, only differentiating between the degrees of damage, as shown in Table 4.2. A description of what each degree of damage entails is however not given.

Table 4.2: Percentage of ignition for different structural vulnerabilities during the Pedrógão Grande fire. Adapted from Ribeiro et al. (2020).

Location of the ignition	**Condition of the Structure after the Fire[A]**				**Total[B] (1042)**
	Slightly Damaged	**Moderately Damaged**	**Highly Damaged**	**Totally Destroyed**	
Roof	16 (2.5%)	36 (5.6%)	299 (46.4%)	293 (45.5%)	644 (61.9%)
Window	14 (8.3%)	17 (10.1%)	70 (41.4%)	68 (40.2%)	169 (16.2%)
Door	4 (5.3%)	7 (9.3%)	36 (48%)	28 (37.3%)	75 (7.2%)
Open structure	2 (2.9%)	6 (8.8%)	13 (19.1%)	47 (69.1%)	68 (6.5%)
Wall	5 (21.7%)	4 (17.4%)	0 (0%)	14 (60.9%)	23 (2.2%)
Vent	0 (0%)	1 (5.3%)	12 (63.2%)	6 (31.6%)	19 (1.8%)
Other	3 (60%)	1 (20%)	1 (20%)	0 (0%)	5 (0.5%)
With damage but no ignition	35 (92.1%)	2 (5.3%)	1 (2.6%)	0 (0%)	38 (3.7%)

[A] Values represent the number of structures and the respective percentage in each class of damage inside each location of the ignition (read percentage horizontally).
[B] Values represent the number of structures per location of the ignition and the percentage in respect to the total of damaged structures (read percentage vertically).

The values given in Table 4.2 are those documented for all types of previously mentioned structures; therefore, for the purpose of the VAT, a further analysis is needed. The data collected by the team at the University of Coimbra was made available for this goal. This included photos as well as information on the following variables:

- Type of structure and geographic location;
- Type of construction materials;
- Age of building;
- Use of the structure before the fire;
- Conditions of the structure before and after the fire;
- Fuel management around the structure;
- Isolated structure or not;
- Ignition location;
- How ignition occurred (i.e., fire impact onto structure);
- Failure of water and power supplies, if any;
- If the structure was defended or not.

As the VAT focuses on homes at the WUI, the more in-depth analysis only included structures identified as primary and secondary homes, as well as some other buildings that had the same characteristics, such as small stores or churches. This accounts for a total of 286 buildings, although the analysis is performed on 270 of these buildings, due to the non-availability of photos that include the damage for 16 buildings. In order to differentiate the different degrees of damage of the buildings, the following categories are defined:

- Slightly damaged: localized damage to one sub-system on the exterior; no ignition inside the house.
- Moderately damaged: localized damage to one or more sub-systems; ignition of one room inside the building.
- Very damaged: structural damage; ignition of more than one room inside the building.
- Destroyed: building burned to the ground or in which walls and roof need to be completely repaired.

The degree of damage for the previously mentioned type of buildings is given in Table 4.3. Different categories are here identified in comparison with those in Table 4.2, according to the structure of the fault tree. Five out of the 270 analysed buildings (2% of buildings) experienced only smoke damage and for 1 building the ignition was classified as *other*; these types of damage are not included in the table. The most common ignition location in the Pedrógão Grande fire was the roof (56%), and the majority of the buildings ignited this way were either very damaged (45%) or destroyed (40%). The second ignition pathway, which involved 26% of the analysed buildings, was through glazing systems. Smaller percentages involved ignition due to the presence of a semi-confined space (6%), the combustion of wall materials (5%), fire entrance through vents (1%) and the fire entering through the walls of the buildings, defined as other, but not specified further (4%). It should be noted that all buildings built out of combustible materials, specifically timber, were destroyed.

Table 4.3: Degree of damage according to the location of the ignition for homes and other buildings with similar characteristics.

Location of the ignition	**Condition of the building after the fire[A]**				**Total[B] (270)**
	Slightly damaged	**Moderately damaged**	**Very damaged**	**Destroyed**	
Roof	13 (9%)	9 (6%)	68 (45%)	60 (40%)	150 (56%)
Semi-confined space	6 (38%)	4 (25%)	4 (25%)	2 (13%)	16 (6%)
Glazing systems	21 (30%)	5 (7%)	20 (28%)	25 (35%)	71 (26%)
Combustible wall	-	-	-	13 (100%)	13 (5%)
Vent	-	1 (25%)	2 (50%)	1 (25%)	4 (1%)
Wall (other)	2 (20%)	1 (10%)	2 (20%)	5 (50%)	10 (4%)

[A] Values indicate the number of structures and the respective percentage in each class of damage and ignition location.
[B] Values indicate the number of buildings per ignition location and the percentage in respect to the total of damaged structures (270).

Where possible, with the aid of the provided photos as well as satellite and Street View images, additional information was collected on the different parts of the building that are deemed to be vulnerable, therefore on roofs and gutters, glazing systems and shutters, vents, and semi-confined spaces attached to the main structure of the building. When possible, materials and maintenance conditions were also identified.

When it comes to glazing systems, it was possible to identify the presence of shutters and their material for 49 out of 71 buildings that experienced ignition through glazing systems. As shown in Table 4.4, 67% of these buildings did not have shutters protecting all of the windows, and the majority were either very damaged (36%) or destroyed (36%). Buildings with PVC shutters mainly experienced slight damages (67%), while those with aluminium shutters were very few, and experienced all ranges of damage conditions.

Table 4.4: Degree of damage depending on the presence and material of the shutters for the buildings that experienced ignition through glazing systems.

Type of shutters	**Condition of the building after the fire**				**Total (49)**
	Slightly damaged	**Moderately damaged**	**Very damaged**	**Destroyed**	
PVC	8 (67%)	1 (8%)	2 (17%)	1 (8%)	12 (25%)
Aluminium	1 (25%)	1 (25%)	1 (25%)	1 (25%)	4 (8%)
No shutters	7 (21%)	2 (6%)	12 (36%)	12 (36%)	33 (67%)

All analysed buildings had a non-combustible roof covering, and were either flat roofs or gable or hip roofs covered with terracotta tiles, typical of the Mediterranean style roofing. Many of the homes did not have gutters, and for those who had them, it was not possible to identify the material or the maintenance level.

Information on the presence and condition of the semi-confined spaces was very difficult to obtain, and it was possible to identify the presence or absence of a semi-confined space only for 65 buildings: 56 have a semi-confined space attached to the envelope of the building, and 9 do not. It was not possible to identify with certainty the amount of combustible materials within these spaces or whether the presence of windows or structural damage to the envelope caused fire entrance into the building. Additionally, no information on the conditions of vent protections could be obtained.

Although the data collected and analysed from the Pedrógão Grande fire is very useful in giving an insight on the different ignition pathways, it could not be used for the further development of the VAT. More data on other WUI fire events in the Mediterranean region is needed in order to create a database with significant and reliable information on ignition pathways and the conditions of the building and the property before the fire.

Collection of post-fire data is critical, and in the Mediterranean region there is clearly a need for a methodology for the assessment of the damage caused to structures by the fire. The NIST WUI Data Collection Form presented in the Technical Note 2105 (Maranghides et al., 2020) could be used as baseline for a data collection methodology for buildings at the Mediterranean WUI. The form includes the assessment of the extent of the damage to the building, the ignition or exposure type, the location of the damage and the details of windows, doors and decking. Instructions on how to fill in the damage assessment report are given as well. The methodology used by Ribeiro et al. (2020) includes the analysis of more variables (mentioned previously) but is however lacking in depth information about the pathways to ignition and the conditions of the building before the fire.

A damage assessment form that includes both methodologies, as well as additional information on fuel management and structural vulnerabilities is presented in Appendix B. This form can be used on site when investigating the damage of buildings affected by WUI fires, and it includes typical vulnerabilities of Mediterranean type construction and landscape. Part of the form also includes the questions of the VAT, which can then be filled in directly. The form can be upgraded to consider a wider variety of construction techniques and environments.

4.4 Fuzzy logic analysis

To deal with the difficulty of assigning probabilities to the events, a model that combines fuzzy logic with classical logic has been developed. Fuzzy logic provides a mechanism for the numerical representation of linguistic constructs that are vague or fuzzy, such as “many”, “few”, “large”, “small”. It is based on the use of fuzzy sets that provide means to model the uncertainties associated with lack of information (Sivanandam et al., 2007).

The fault tree in Figure 4.1 is adapted by inserting Fuzzy Inference Systems (FIS, defined here below) for the quantification of the probability of failure of the events that lead to a fire entering a building located at the Mediterranean WUI through fuzzy logic, as shown in Figure 4.2. In this fault tree, the impact of firebrands is included indirectly through the rules for spacing of the different fuels. If any fuel is ignited by firebrands and it is well managed, it will not cause fire spread to other fuels nor impact the dwelling’s vulnerable elements. They are also implicitly considered in the failure of the four different building vulnerabilities, given that firebrands can enter the building through gaps existing because of the building’s characteristics or created due to poor maintenance of the building itself.

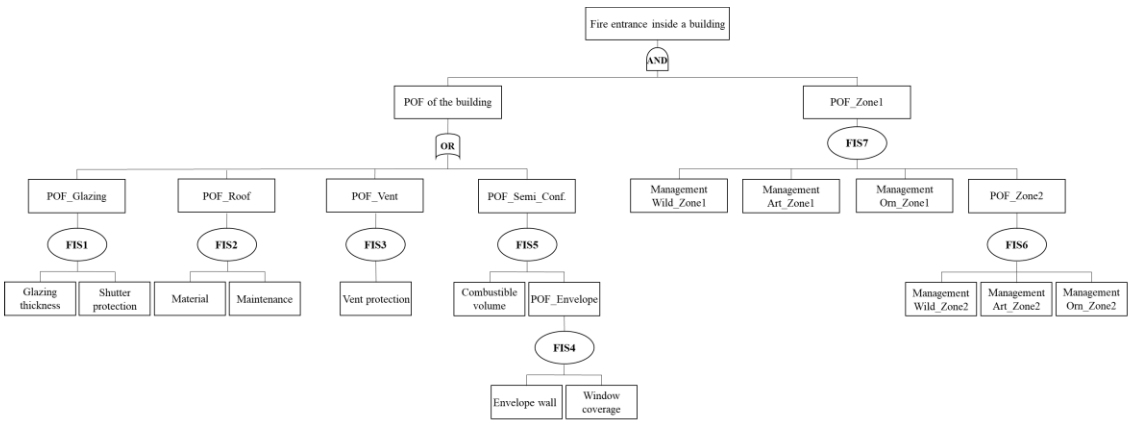

Figure 4.2: Scheme for vulnerability assessment to wildland fires for buildings at the WUI with the use of fuzzy logic. FIS: Fuzzy Inference System; POF: Probability Of Failure; Orn: Ornamental vegetation; Art: Artificial fuels; Wild: Wildland vegetation.

The two intermediate events that lead to the output of the model are now called system variables, which are connected through the classical logic AND gate. These are the probability of the failure of the building due to its vulnerabilities (POF of the building) and the probability of the fire reaching the building (POF_Zone1). The first one is obtained through a classical logic OR gate according to the values obtained for the probabilities of failure of the four elements that constitute pathways for the fire into the house, i.e., glazing systems, roof, vents and semi-confined spaces that can suffer structural damage due to heat accumulation. The probability of the fire reaching the building (POF_Zone1) as well as probability of the fire reaching zone 1 by passing through zone 2 (POF_Zone2) depends on the compliance to the different rules set for fuels located in the two considered zones (Table 4.1). All the probabilities of failure defined before the two classical logical gates are obtained through the use of fuzzy logic. This is a soft computing analytical technique that has already been used extensively in environmental risk assessment (e.g., Seguí et al., 2013) and it has also been recently applied for resilience evaluation of flood-prone communities (Oladokun and Montz, 2019).

Seven fuzzy inference systems (FIS) are defined by following the process in Figure 4.3. Initially, the variables that are relevant in every system must be identified (inputs and outputs). For example, to establish the probability of fire reaching zone 1, i.e. "probability of failure of zone 2" because fire can spread through this zone (POF_Zone2 in Figure 4.2), three input variables associated to the quality of the management of wildland, artificial and ornamental fuels in zone 2 are defined (Management Wild_Zone2, Management Art_Zone2, Management Orn_Zone2). These variables must then be fuzzified, meaning that they need to be defined as fuzzy sets by identifying their universe of discourse (e.g., "complying rules percentage" is a fuzzy set with a universe of discourse from 0 to 100%) and selecting a set of linguistic terms (i.e., fuzzy subsets) that accurately describe them (e.g., *good* and *bad* are fuzzy subsets of the fuzzy set denoted as "management of wildland, artificial and ornamental fuels in zone 2"). Subsequently, a membership function for each fuzzy subset must be defined to quantify the degree of belonging of any value in the universe of discourse to each fuzzy subset (Fuzzification block in Figure 4.3) (Sivanandam et al., 2007). Then the inferring process is performed by using a set of rules (Fuzzy rules block in Figure 4.3) that connect antecedents (input variables) with the consequent (output variable). These rules usually have a structure such as: "IF …, THEN …". An aggregation process is required to consider the different rules that activate according to the inputs. Then, since the output is also defined as a fuzzy set, a defuzzification process is necessary in order to transform the fuzzy results into a precise output. A python library for fuzzy logic (simpful) is used to handle all of the inference systems (Spolaor et al., 2020) defined in this work. Values for the linguistic terms of the inputs and membership functions for the fuzzy sets can be defined through expert elicitation, along with the definition of the fuzzy rules (i.e., experts on the topic are polled and their knowledge is used to parametrize the model).

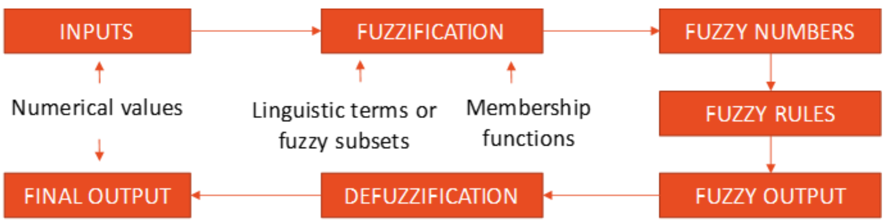

Figure 4.3: Generic Fuzzy Inference Process. Adapted from Darbra et al. (2008).

4.4.1 Parametrization of the model

A poll for WUI fire experts was prepared to parametrize the fuzzy inference systems present in the model. A pre-selection of possible pollees was performed according to their WUI expertise either because of their professional experience as WUI fire risk managers or because of their research activity proofed by scholarly outputs. The poll was delivered by email using an Excel file (available as supplementary material) specifically designed for this purpose. It was filled in by 13 experts who, according to personal data gathered through the questionnaire, came from 6 different countries: Spain (6), Australia (3), Chile (1), France (1), Portugal (1) and UK (1), and were working in civil protection (1), private companies (2) or research institutions (10). Their input helped to determine membership functions, as they were asked to provide a lower and upper bound or a best estimate for the fuzzy subsets that define each fuzzy set present in the model. All the replies were mathematically evaluated using simple statistical approaches and results were validated here taking into account whether the elicited outcomes were plausible and did conform to authors expectations (Drescher et al., 2013). The percentage of experts that considered the different values for each fuzzy subset is computed and then weighted average values are calculated to set membership functions. For a given fuzzy set (e.g., probability of failure), triangular membership functions are defined for those fuzzy subsets that are not at the limits of the universe of discourse of the fuzzy set (e.g., medium probability of failure), and trapezoidal functions for those at the limits (e.g., low and extreme probability of failure).

An example of the attainment of the membership functions for the fuzzy subsets “window coverage in semi-confined spaces” and “probability of failure” is given in Figure 4.4. The questions posed to the experts to define these membership functions are to define values for a high, medium and low percentage of windows coverage of a wall in a semi-confined space and to define percentages for a low, medium, high and extreme probability of failure. Poll replies (Figure 4.4a) are used to specifically set these functions by taking into account the percentage of experts that considered the different values for each fuzzy subset (Figure 4.4b). Weighted average values are calculated (dashed vertical lines in Figure 4.4b) and vertices could be set accordingly to define membership functions (Figure 4.4c).

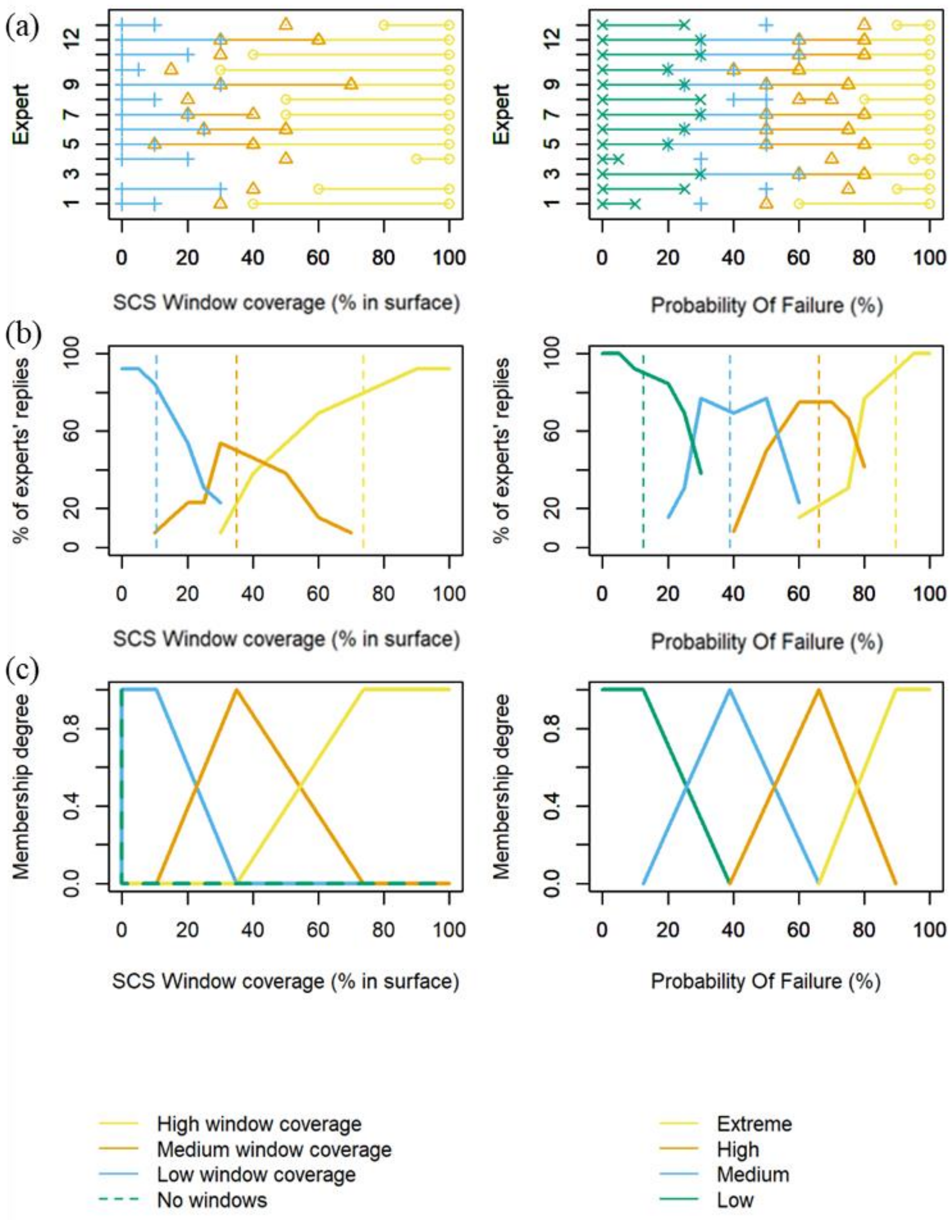

Figure 4.4: Fuzzy subset definition for the fuzzy sets “window coverage in semi-confined spaces (SCS)” (left column) and “probability of failure” (right column) according to poll results. Top plots (a): answers given by the 13 experts about the degree of window coverage in SCS (from no windows to high coverage) and about the probability of failure (from low to extreme). Middle plots (b): poll results (dashed lines indicate weighted averaged values). Bottom plots (c): fuzzy membership functions elicited according to the results of the middle plots. Adapted from Àgueda et al. (2023).

Specific weighted average values obtained from poll replies are shown in Table 4.5 for each fuzzy subset. One specific result worth mentioning is related to the probability of failure associated with the vents. Experts consider that having non-combustible vents in bad conditions offers a slightly higher probability of failure than having vents made out of combustible material (e.g., plastic). The answers of each expert are presented in Appendix C.

Table 4.5: Weighted average values for each subset of all fuzzy sets present in the model. SCS: Semi-Confined Space; POF: Probability Of Failure.

Fuzzy Sets	**Description**	**Fuzzy subsets**				
Shutters	POF according to the shutter material	**No shutters**	**PVC**	**Wood**	**Aluminium**	**Fire rated**
POF (%)		88.4	66.5	47.8	24.3	6.6
Glazing systems	Glass thickness	**Thin**	**Medium**	**Thick**		
Thickness (mm)		4.7	9.6	16.4		
Roof material	Probability that fire can affect the underlying roof structure according to the type of roof covering material	**Combustible**	**Non-combustible**			
POF (%)		66.2	15.7			
Roof maintenance	Probability of fire affecting the roof structure according to the performed maintenance	**Badly maintained**	**Well maintained**			
POF (%)		75.7	16.5			
Vents	Probability of fire entrance through vents according to the type and conditions of their protection	**Non-combustible, good conditions protection**	**Combustible protection**	**Non-combustible, bad conditions protection**	**No protection**	
POF (%)		7.8	40.2	42.5	81.1	
Windows in SCS	Percentage of area of walls shared by a house and a SCS that is occupied by windows	**High**	**Medium**	**Low**		
Coverage (%)		74.3	35.5	10.2		
Envelope type in SCS	POF (structural failure) that each type of building envelope could present if exposed to a fire in a SCS	**Combustible**	**Non-combustible, thin (< 15 mm)**	**Non-combustible, thick (≥ 15 mm)**		
POF (%)		78.4	30.0	8.4		
Combustible material in SCS	Percentage of volume occupied by combustible materials in an SCS	**High**	**Medium**	**Low**		
Coverage (volume %)		61.4	29.0	6.2		
Failure	Generic probability of failure	**Extreme**	**High**	**Medium**	**Low**	
POF (%)		89.5	66.1	38.9	12.4	
Fuel management[A]	According to a set of rules for fuel management (all with the same weight), percentage of rules that should be complied with [B]	**Bad**	**Good**			
Complying rules (%)		36.2	90.1			

[A] Three different types of fuel are considered (i.e. wildland vegetation, ornamental vegetation, artificial fuels).

[B] Rules are different according to the type of fuel, the defence zone of interest surrounding the dwelling (i.e., zone 1: 10-m around the dwelling; zone 2: 10-m to 30-m ring around the dwelling) and the topography, as shown in Table 4.1.

Additionally, the poll included the fuzzy rules, for which the experts could choose the linguistic value of the output variable (i.e., consequent). When more than one input variable is combined in a rule, the logical operator AND is used. An example of the selection for the rules' consequent is shown in Figure 4.5. To elicit each rule consequent (e.g. "If windows coverage is high and wall is combustible, then wall vulnerability is …"), a weighted average was calculated by assigning a number to each subset (probability of failure: Extreme = 4, High = 3, Medium = 2, Low = 1). Then, data was linearly transformed so that the result was in the range 0-1 and categorical values were set back according to the following ranges: [0,0.25] - Low; (0.25,0.50] - Medium; (0.50,0.75] - High; (0.75,1] – Extreme.

Semi-confined spaces (FIS4 and FIS5)								
IF	window coverage	high	AND	wall is	combustible	THEN	wall vulnerability is	Extreme High Medium Low
					non-combustible thin			
					non-combustible thick			
IF	window coverage	medium	AND	wall is	combustible	THEN	wall vulnerability is	
					non-combustible thin			
					non-combustible thick			
IF	window coverage	low	AND	wall is	combustible	THEN	wall vulnerability is	
					non-combustible thin			
					non-combustible thick			

Figure 4.5: Example of the rules in the experts' questionnaire. Adapted from (Àgueda et al., 2023).

An example of the results for several rules' consequents for FIS_1 (i.e., probability of failure of glazing systems, Figure 4.2) are shown in Figure 4.6. The plot shows the distribution of replies given by the experts to five rules of FIS_1 associated to the presence of thin glazing systems, and in the legend of this figure the final consequent assigned to each rule is shown.

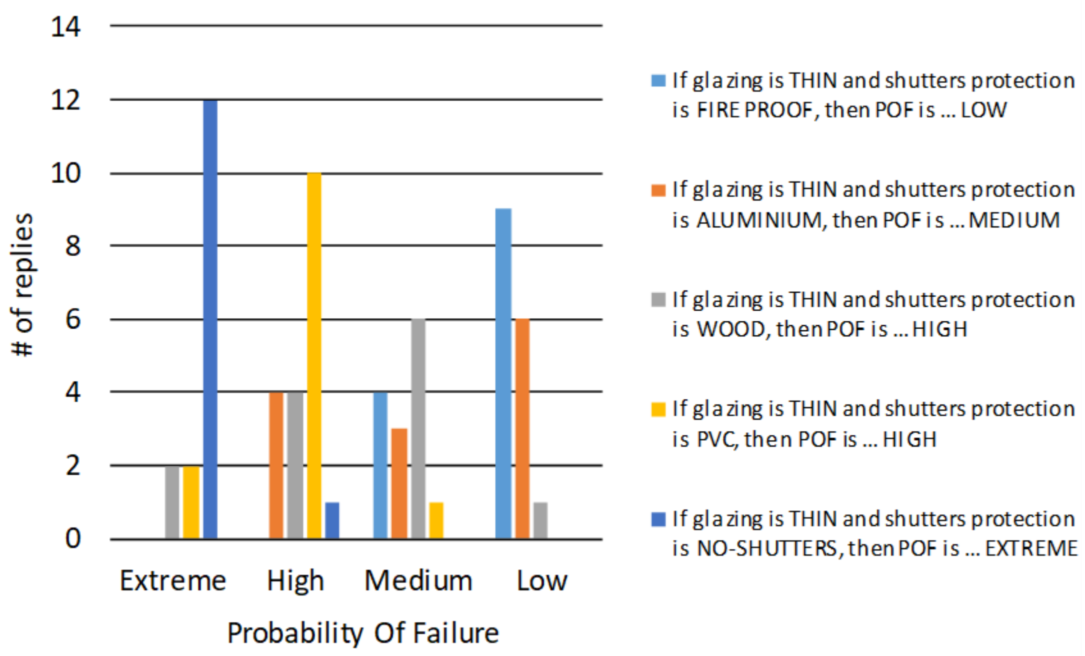

Figure 4.6: Replies given by the experts to FIS_1 rules consequents. The assigned subset for the probability of failure of glazing systems is shown in the legend next to the graph. POF: Probability Of Failure.

4.5 The complete tool

The Vulnerability Assessment Tool focuses on the issues and property and building characteristics that are specific for Mediterranean WUI microscale settings. The tool is directed to homeowners and residents and gives quantitative information on the vulnerability of a property to an incoming wildfire. The obtained result is the probability of fire entrance inside the building, along with the probability of failure of each element. The obtained probability of fire entrance is the overall quantitative value that indicates the vulnerability of the building to fire. The tool is presented in form of a checklist that can be easily filled in by homeowners or residents themselves and it identifies the main issues that need to be addressed and in what order. Results of the application of the VAT to a hypothetical worst-case scenario are also presented.

4.5.1 Homeowners' questionnaire

The previously presented model has to be used together with a questionnaire that homeowners must fill in. The questions are either multiple choice, Yes/No or with open answer, which is either a percentage or a thickness, specifically the glazing's thickness. The complete questionnaire is given in Table 4.6. Once the questionnaire is completed, the replies are introduced in the fuzzy model for the calculation of the probabilities of failure of the different elements of the fault tree, which are then used to calculate the probability of a fire entering the building.

Table 4.6: Homeowners' questionnaire.

Building characteristics			
1	**Shutters** Do you have protection for all your windows/glazing systems (i.e. shutters) made of non-combustible materials (solid core wood fire-resistant, metal like aluminium)?	□ Yes	□ No
2	What material are the shutters made of?	□ Wood □ Aluminium □ PVC □ Fire rated materials	
3	**Glazing systems** What is the thickness of the glazing systems (in mm)?		
4	**Roof material** Is your roof covering or your roof assembly made of fire-rated material (e.g. clay tiles, concrete tiles, asphalt glass fibre composition singles, slate, etc.)?	□ Yes	□ No
5	**Roof maintenance** Are there missing, displaced or broken tiles?	□ Yes	□ No
6	Is the underlying roof sheeting exposed?	□ Yes	□ No
7	Are there unsealed spaces between the roof and the external walls or between the roof covering and the roof decking?	□ Yes	□ No
8	Do you perform regular cleaning of debris piling up on roof or gutters?	□ Yes	□ No
9	**Unprotected vents** Do you have unprotected ventilation openings (i.e. vents without any type of screening)? *If all your vents are unprotected, go to question 11*	□ Yes	□ No
10	**Vent protection** What type of vent protection is present?	□ Combustible	

		□ Non-combustible in bad conditions (rusted or damaged) □ Non-combustible in good conditions (no damage)
11	**Semi-confined space adjacent to house** Is there a semi-confined space adjacent to your house (i.e., it has at least one wall in common with the house)? *If the answer is no, go to question 15*	□ Yes □ No
12	**Presence of combustible materials in semi-confined space** What % of volume of the semi-confined space do combustible materials occupy?	
13	**Presence of glazing systems in semi-confined space** What % of wall area do glazing systems that connect the house to the semi-confined space occupy?	
14	**Vulnerable walls of semi-confined space** What type of walls are those connecting the house to the semi-confined space?	□ Non-combustible, at least 12 cm thick □ Non-combustible, less than 12 cm thick □ Combustible
Property/landscape characteristics ZONE 1 (within 10 m from the house)		
15	**Fuels close to LPG tank in zone** Are there any combustible materials (including ornamental vegetation, storage spaces, or combustible eaves) located within 2 m of LPG tanks (this includes also canisters with a total volume > 0.5 m^3)?	□ Yes □ No □ Not applicable
16	**Artificial fuels close to vulnerable structural elements** Are there any artificial fuels (e.g. outdoor furniture, stored materials, gas canisters, small sheds, wood piles) located within 5 m from double pane glazing systems and 6.5 m from single pane glazing systems?	□ Yes □ No □ Not applicable
17	Are there any artificial fuels (e.g. outdoor furniture, stored materials, gas canisters, small sheds, wood piles) located within 5 m from the roof or gutters?	□ Yes □ No □ Not applicable
18	If the wildland vegetation is mainly trees, are there artificial fuels located within 20 m from these trees?	□ Yes □ No □ Not applicable
19	Is the distance between fuels or fuel packs at least 5 m?	□ Yes □ No □ Not applicable
20	**Management of ornamental vegetation** Is there ornamental vegetation in zone 1? *If the answer is no, go to question 30*	□ Yes □ No
21	Are there very flammable species (e.g. pine tree, eucalyptus, cypress, etc.) or vegetation with closely packed leaves and branches, fine textures, small, thin and narrow leaves, and high amounts of resins or oils?	□ Yes □ No
22	Are trees and shrubs separated by at least 6 m?	□ Yes □ No
23	Is the vegetation separated by at least 3.5 m from any glazing system?	□ Yes □ No
24	Are trees overhanging the roofline of the building?	□ Yes □ No
25	Are individual or groups of bushes less than 5 m wide?	□ Yes □ No □ Not applicable
26	Is there a non-continuous plant litter layer?	□ Yes □ No
27	Are the hedges aligned with the wind direction or the main slope?	□ Yes □ No □ No hedges
28	Are hedges located at least 2 m from other vegetation?	□ Yes □ No □ No hedges
29	Is there dead vegetation or vegetative debris?	□ Yes □ No
30	**Wildland vegetation and/or crop landscape** *If there is no wildland or crop vegetation in zone 1, go to question 37*	
31	**Wildland vegetation canyon/slope/ridge/hilltop** Is the separation between crown trees/high shrubs of at least 9 m?	□ Yes □ No □ Not applicable

32	Is there a separation between grouping of shrubs (or regrowth forest or young trees) of at least 3 m?	□ Yes	□ No	□ Not applicable
33	Are the lower tree branches pruned at ⅓ of tree height?	□ Yes	□ No	□ Not applicable
34	Is the low surface fuel load max 10 cm deep?	□ Yes	□ No	
35	Is the vegetation separated by at least 3.5 m from any glazing system?	□ Yes	□ No	
36	Are trees overhanging the roofline of the building?	□ Yes	□ No	
Property/landscape characteristics ZONE 2 (between 10 m and 30 m from the house)				
37	**Fuels close to LPG tank in zone** Are there any combustible materials (including ornamental vegetation, storage spaces, or combustible eaves) located within 2 m of LPG tanks (this includes also canisters with a total volume > 0.5 m^3)?	□ Yes	□ No	□ Not applicable
38	**Spacing of artificial fuels** In case of wild vegetation of mainly trees, are artificial fuels placed at a distance of minimum 20 m from these trees?	□ Yes	□ No	□ Not applicable
39	Is the distance between different artificial fuels or fuel packs of at least 5 m?	□ Yes	□ No	□ Not applicable
40	**Management of ornamental vegetation** Is there ornamental vegetation in zone 2? *If the answer is no, go to question 45*	□ Yes	□ No	
41	Are the hedges aligned with the wind direction or the main slope?	□ Yes	□ No	□ No hedges
42	Are the hedges in this zone located at least 2 m from other vegetation?	□ Yes	□ No	□ No hedges
43	If you have ornamental bushes in zone 2, are they less than 5 m wide?	□ Yes	□ No	□ Not applicable
44	Is the distance between these bushes and other vegetation larger than 3 m?	□ Yes	□ No	□ Not applicable
45	**Landscape type** *If the surrounding landscape includes a canyon/slope/ ridge/ hilltop, fill in questions 46 to 49* *If the surrounding landscape is flat, fill in questions 50 to 53* *If the surrounding landscape includes crops, go to question 54*			
46	**Wildland vegetation canyon/slope/ridge/hilltop** Is the separation between crown trees/high shrubs of at least 9 m?	□ Yes	□ No	□ Not applicable
47	Is there a separation between the shrubs (or regrowth forest or young trees) of at least 3 m?	□ Yes	□ No	□ Not applicable
48	Are the lower tree branches pruned at ⅓ of tree height?	□ Yes	□ No	□ Not applicable
49	Is the low surface fuel load max 10 cm deep?	□ Yes	□ No	
50	**Wildland vegetation flat landscape** Is the separation between crown trees/high shrubs of at least 6 m?	□ Yes	□ No	□ Not applicable
51	Is there a separation between the shrubs (or regrowth forest or young trees) at least 3 m?	□ Yes	□ No	□ Not applicable
52	Are the lower tree branches pruned at ⅓ of tree height?	□ Yes	□ No	□ Not applicable
53	Is the low surface fuel load max 10 cm deep?	□ Yes	□ No	
54	**Wildland vegetation crop landscape** Is the separation between crown trees/high shrubs of at least 6 m?	□ Yes	□ No	□ Not applicable
55	Are the lower tree branches pruned at ⅓ of tree height?	□ Yes	□ No	□ Not applicable
56	Is the low surface fuel load max 10 cm deep?	□ Yes	□ No	

4.5.2 Hypothetical worst-case scenario

The VAT is here applied to a hypothetical worst-case scenario, where a property and building have the worst-case characteristics, as described in Table 4.7.

Table 4.7: Characteristics of a hypothetical worst-case scenario

Characteristics	Worst-case hypothetical dwelling
Shutters	No shutters
Glazing thickness	3 mm
Roof material	Combustible
Roof maintenance	Bad
Vents	Non-protected vents
Windows coverage in semi-confined space	100%
Envelope type in SCS	Combustible walls
Combustible material coverage in SCS (% in volume)	100%
Fuel management compliance in zone 2 O/A/W (%)	0/0/0
Fuel management compliance in zone 1 O/A/W (%)	0/0/0

The probabilities for each of the events and the final result of the probability of fire entrance in a worst-case scenario are given in Table 4.8. According to these results, the presented methodology gives a maximum value of 88% for the probability of fire entering the dwelling. Mathematically, this is due to the fact that the "extreme" fuzzy subset associated to the "probability of failure" fuzzy set is defined as a trapezoidal function. However, this is still reasonable because 100% probability would mean that, according to the model, it is certain that the fire will enter into the dwelling, although there are other factors, which are analysed in the discussion section (e.g., factors related to emergency response), that prevent from being able to ensure 100% probability of fire entrance.

Table 4.8: Probability of fire entrance in a worst-case scenario

FIS / Classical logic results (%)	Worst-case hypothetical dwelling
POF_GLAZING	88
POF_ROOF	88
POF_VENT	88
POF_ENVELOPE	88
POF_SEMI-CONFINED	88
POF_Zone2	88
POF_Zone1	88
POF of the building	100
Probability of fire entrance	88

4.6 Validation of the VAT through application to case studies

An application of the VAT to three case studies at the Mediterranean WUI was performed in order to validate the tool. Two occurred in Spain during the summers of 2021 (Lloret de Mar fire) and 2022 (Pont de Vilomara fire), and one in Portugal during the summer of 2021 (Castro Marim fire). Information was gathered by going personally to see the affected buildings as well as, when possible, by talking to the residents of these buildings.

4.6.1 Case study 1: Lloret de Mar, Spain 2021

The WUI fire that took place in July 2021 in Lloret de Mar, Spain, started around 11 a.m. due to the burning of a van that had stopped on the hard shoulder of a road. The flames from the van ignited the adjacent vegetation, which was mainly composed of pine trees and a dense understory. Topography and fuel continuity played an important role in the propagation and intensity of the fire, as it spread rapidly upwards through a steep slope until fuel discontinuity due to the presence of houses drove the main fire front to propagate following a drainage gully (see the peaks of the elevation contour profiles between properties H1.1 and H1.2 and H1.4 in Figure 4.7). This fire prompted evacuation orders and several homes were threatened. Various elements present outdoors were burned (e.g., vehicles, fences and garden furniture) and one house (H1.2) was severely damaged due to the entrance of the fire inside the building caused by the breaking of the panes of a window (Figure 4.8d).

The five owners of the properties shown in Figure 4.7*Figure 4.* were interviewed in the framework of a workshop organized several months after the fire in collaboration with the City Council. During the session, clear instructions were given on how to fill the questionnaire taking into account the conditions of the building and its surroundings before the fire. Their answers, shown in Table 4.9, were used to quantify the probability of fire entrance in their homes by using the VAT (Table 4.10).

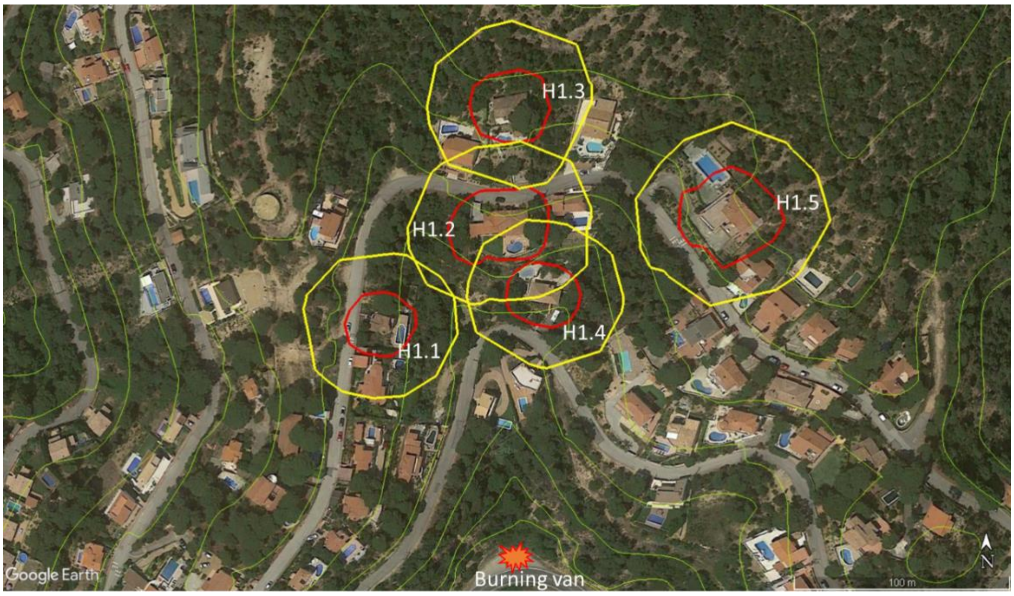

Figure 4.7: Monitored properties affected by the Lloret de Mar fire (Spain, 2021). Red line: 10 m limit of zone 1. Yellow line: 30 m limit of zone 2. Green lines indicate the elevation contours. The location of the burning van that initiated the fire is shown.

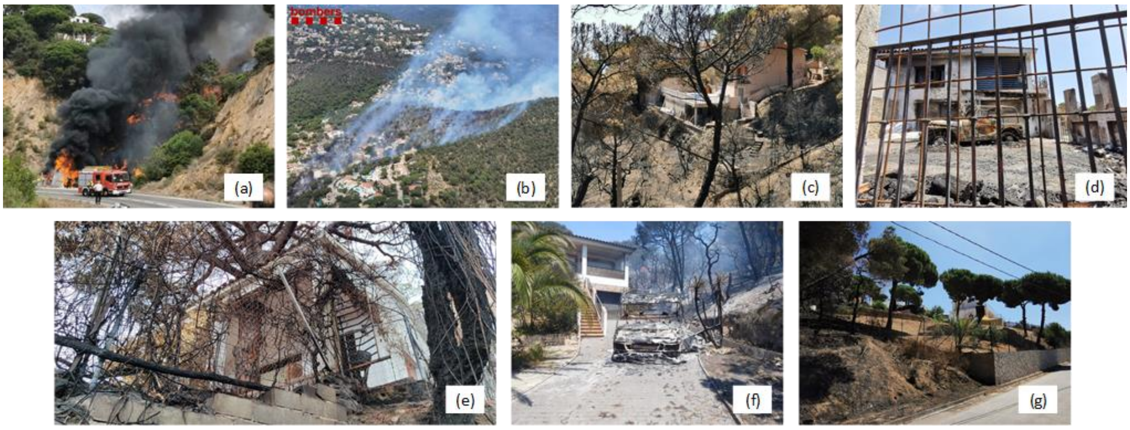

Figure 4.8: Photographs of the WUI fire in Lloret de Mar, Spain (July 2021). (a) Burning van that initiated the upslope fire; (b) General view of the passage of the fire. View of the properties after the fire: (c) H1.1; (d) H1.2; (e) H1.3; (f) H1.4; (g) H1.5.

The structure of all monitored homes was built out of non-combustible materials such as concrete, stone or bricks. H1.1, H1.4 and H1.5 were built between 10 and 30 years ago, while H1.2 and H1.3 are over 30 years old. All homeowners stated that their home was well maintained when the fire occurred. As can be seen in Table 4.9, all homes had shutters either made out of wood, PVC or aluminium, but none had fire rated ones. Moreover, H1.2 had PVC shutters, but they were left open during the fire, and as such they did not provide any protection to the glazing systems. Therefore, both situations (i.e., PVC and no shutters) have been considered for the vulnerability assessment. All but H1.3 had double pane glazing systems, for which a thickness of 14 mm was assumed. As for the roof, all homes had a construction typical of Mediterranean dwellings, with a covering made out of clay tiles. All roofs, with the exception of H1.3, were stated to be in good conditions. H1.3 is the only dwelling to have vents, which, at the time of the fire, were not protected. As for the presence of semi-confined spaces, all homes had porches with different types of outdoor furniture, and H1.2 also had a car shed made out of wooden beams and columns covered by clay tiles that was attached to the main structure of the home. This shed was completely destroyed by the fire. When it comes to the two zones surrounding the homes, it can be noted how there was no compliance at all to the rules for the management of wildland fuels in zone 2, while only 2 properties complied completely in zone 1. With regards to the ornamental vegetation, all properties complied to at least some of the rules, with a minimum of 11% compliance for zone 1 of H1.3. None of the properties reached 100% compliance in zone 1, and it can be noted that, overall, for this type of fuels, compliance was higher in zone 2. When it comes to the presence of artificial fuels, the lowest compliance was 25% in zone 1, and H1.4 was the only one to fully comply to the rules in both zones.

Table 4.9: Results of the questionnaire for the case study of the Lloret de Mar fire. O/A/W: Ornamental/Artificial/Wildland fuels. SCS: Semi-confined space.

Characteristics	**WUI fire dwellings**				
	H1.1	**H1.2**	**H1.3**	**H1.4**	**H1.5**
Shutters	Wood	PVC (no shutters[B])	PVC	Aluminium	Aluminium
Glazing thickness[A]	14 mm	14 mm	4 mm	14 mm	14 mm
Roof material	Non-combustible	Non-combustible	Non-combustible	Non-combustible	Non-combustible
Roof maintenance	Good	Good	Bad	Good	Good
Vents	None	None	Unprotected	None	None
Windows coverage in semi-confined space	20%	0%	50%	70%	70%
Envelope type in SCS	Non-combustible & thick	Non-combustible & thin	Non-combustible & thick	Non-combustible & thick	Non-combustible & thick
Combustible material coverage in SCS (% in volume)	10%	70%	20%	10%	10%
Fuel management compliance in zone 2 O/A/W (%)	50/50/0	67/50/0	25/100/0	100/100/0	100/50/0
Fuel management compliance in zone 1 O/A/W (%)	57/100/100	56/25/0	11/25/0	44/100/17	86/25/100

[A] Glazing thickness was assumed to be 14 mm (4 glass + 6 air + 4 glass) if there were double panes and 4 mm if the glazing pane was single. The homeowners did not know the exact thickness of the glazing systems.
[B] During the fire, PVC shutters were open and as such did not provide any protection.

According to Table 4.10, the homes with the highest probability of fire entrance are H1.3, with 87%, and H1.2, with 63%, considering no shutters. The probability value associated to H1.3 is quite large compared to the values obtained for the other homes and considering that the worst value attainable using this method is 88%. H1.3 presented the highest probability of failure of the dwelling itself (99%), with vulnerable elements such as the thickness of the glazing systems, the material of the shutters (PVC), and the fact that vents were unprotected. Additionally, when it comes to the probability of the fire reaching the building (POF_Zone1), H1.3 had the highest value, which matches with the value of the worst-case scenario, 88%. This value was high because there was no compliance at all to the rules for the management of wildland fuels and compliance was low in both zones for ornamental vegetation.

The probability of the fire reaching the building was also high for home H1.2 (75%) because compliance with fuel management rules was low in both zones (as shown in Table 4.9, no fuel type management section reached a compliance value of 100%). H1.2 presented a probability of failure of the building itself of 74% or 85%, depending whether shutters were considered or not. Vulnerable elements of the structure of H1.2 were shutters' material and the presence of a semi-confined space with a high amount of combustible fuel (the car was parked underneath the car shed when the fire occurred).

Table 4.10: Probability of fire entrance in the homes characterised in Table 4.9 according to the elements identified in Figure 4.2.

FIS / Classical logic results (%)	**WUI fire dwellings**				
	H1.1	**H1.2**	**H1.3**	**H1.4**	**H1.5**
POF_GLAZING	39	48 (70[A])	65	16	16
POF_ROOF	14	14	65	14	14
POF_VENT	0	0	88	0	0
POF_ENVELOPE	39	14	39	39	39
POF_SEMI-CONFINED	21	41	32	21	21
POF_Zone2	79	77	88	65	79
POF_Zone1	54	75	88	63	66
POF of the building	59	74 (85 [A])	99	42	42
Probability of fire entrance	32	55 (63 [A])	87	27	28

[A] Values obtained considering no-shutters, since PVC shutters were open during the fire.

Of the two homes (H1.2 and H1.3) with the highest probability of fire entrance, H1.3 suffered minor damages outside the house, while the fire entered into H1.2. This is probably because fire behaviour was more intense and rapidly spreading in the drainage area in between H1.1 and H1.2 and H1.4. On the contrary, fire was propagating more slowly in the area around H1.3 because it was not channelled there. Additionally, when the wildfire was threatening the area, the people living in H1.2, who were at that moment inside the house, evacuated and did not close the PVC shutters nor placed their vehicle inside the garage. The car was located underneath the car shed, which was close to the porch as well as close to a window. These actions left artificial fuel (the car) available for burning, which caused flames to be close to the windows. If evacuation would have been well prepared the probability of fire entrance into this house would have been lower (55% probability considering that shutters were pulled down). On the contrary, H1.3 was locked (shutters closed) because residents were not at home that day.

This indicates that, although the house that was severely damaged was not the most vulnerable one in the area, it was affected by fire due to a badly prepared evacuation. Thus, it is important to keep in mind that houses will have a better chance of surviving a wildfire if people living in the WUI are well prepared and informed about the actions that need to be undertaken before evacuating.

4.6.2 Case study 2: El Pont de Vilomara, Spain 2022

The Pont de Vilomara fire propagated following sea winds present in the area channelled through the Llobregat river valley, and impacted the River Park residential development, which is positioned over the main propagating axis of the fire, approximately 2 hours after the fire was detected. Due to the location of the residential development (i.e., on top of the hill), several dwellings received the impact of the fire simultaneously. Moreover, although there were treated fringes mid slope, as can be seen in Figure 4.9, they were not effective and the fire propagated through the pine tree crowns.

Six houses from the River Park residential development (Figure 4.9 and Figure 4.10), were analysed for the testing of the VAT. Five of these houses were located on the same street, on the hilltop of Turó de Solanes (H2.1, H2.2, H2.3, H2.5, H2.6). Another one was located further down on the same slope (H2.4).

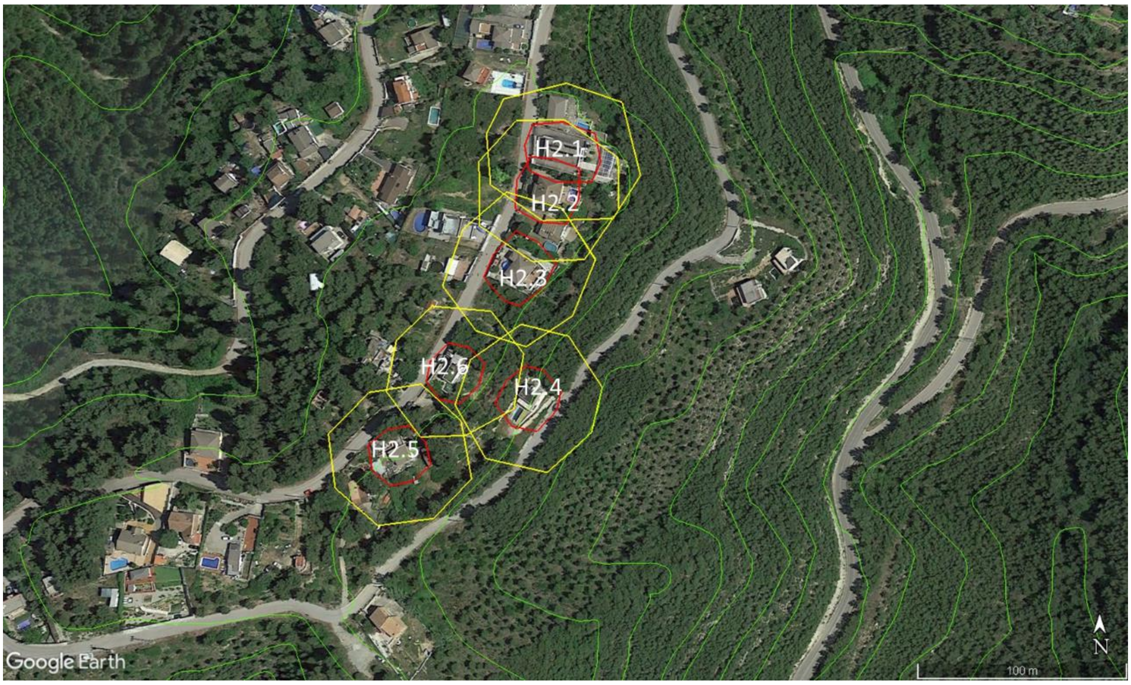

Figure 4.9: Monitored properties affected by the Pont de Vilomara fire (Spain, 2022). Red line: 10 m limit of zone 1. Yellow line: 30 m limit of zone 2. Green lines indicate the elevation contours.

Figure 4.10: Photographs of the WUI fire in El Pont de Vilomara, Spain (July 2022). (a) Overview of the area after the fire (photo by Sergi Boixader, used with permission); Properties affected by the fire: (b) H2.1 (photo by Generalitat de Catalunya firefighters, used with permission); (c) H2.2 (photo by Generalitat de Catalunya firefighters, used with permission); (d) H2.3; (e) H2.4; (f) H2.5; (g) H2.6.

The characteristics of the homes and properties that were needed as input for the tool are shown in Table 4.11. These data were obtained through interviews with the homeowners performed informally after the fire, and also thanks to the inspection of photographs that were made available by the Generalitat de Catalunya firefighters.

Table 4.11: Characteristics of the dwellings affected by a WUI fire in El Pont de Vilomara, Spain (July 2022). O/A/W: Ornamental/Artificial/Wildland fuels; SCS: Semi-confined space; NA: Not Applicable.

Characteristics	**WUI fire dwellings**					
	H2.1	**H2.2**	**H2.3**	**H2.4**	**H2.5**	**H2.6**
Shutters	Aluminium	No shutters	No shutters	No shutters	No shutters	No shutters
Glazing thickness[A]	14 mm	14 mm	14 mm	14 mm	14 mm	14 mm
Roof material	Non-combustible	Non-combustible	Non-combustible	Combustible	Non-combustible	Non-combustible
Roof maintenance	Bad	Good	Good	Good	Good	Bad
Vents	Non-combustible in good conditions	Non-combustible in good conditions	Non-combustible in good conditions	Non-combustible in good conditions	Non-protected vents	Combustible
Windows coverage in semi-confined space	80%	5%	25%	70%	NA	0%
Envelope type in SCS	Non-combustible & thick	Non-combustible & thick	Non-combustible & thick	Non-combustible & thick	NA	Non-combustible & thick
Combustible material coverage in SCS (% in volume)	20%	5%	5%	30%	NA	50%
Fuel management compliance in zone 2 O/A/W (%)	25/50/0	33/0/0	25/0/0	100/100/0	100/50/0	0/0/0
Fuel management compliance in zone 1 O/A/W (%)	44/75/100	44/75/100	67/50/33	100/75/17	86/50/60	57/25/33

[A] Glazing thickness was assumed to be 14 mm (4 glass + 6 air + 4 glass) if there were double panes and 4 mm if the glazing pane was single.

All homes had double pane glazing systems, although all but one home (H2.1) did not have shutters protecting all windows. Roofs were all well maintained, with the exception of H2.1, and all homes but H2.5 were provided with some type of vent protection. H2.5 is the only home that does not have a semi-confined space attached to the main structure of the dwelling. The percentage in volume occupied by combustible material in the semi-confined spaces was lower than 50% and the largest value was observed in H2.6 (50%). Two homes had a very high percentage of windows coverage in the semi-confined space, with 80% for H2.1 and 70% for H2.4. Regarding fuel management in the two zones surrounding the home, it can be noted that, as for the previous case study, there was no compliance at all to the rules for the management of wildland fuels in zone 2. However, in zone 1 two properties (H2.1 and H2.2) complied to these rules completely. Regarding ornamental vegetation, all properties complied to at least 44% of the rules in zone 1, while in zone 2 one property (H2.6) did not comply to any rule. For artificial fuels, the compliance level in zone 1 was larger than 25%, while it was 0% in zone 2 for three of the six analyzed properties (H2.2, H2.3 and H2.6).

The results obtained from the VAT model are shown in Table 4.12. The homes with the highest probability of fire entrance were H2.6, with 81%, and H2.3, with 67%. For the other homes the estimated probability was between 56% and 59%.

Table 4.12: Probability of fire entrance in the homes characterised in Table 4.11 according to the elements identified in Figure 4.2.

FIS / Classical logic results (%)	**WUI fire dwellings**					
	H2.1	**H2.2**	**H2.3**	**H2.4**	**H2.5**	**H2.6**
POF_GLAZING	16	70	70	70	70	70
POF_ROOF	65	14	14	65	14	65
POF_VENT	14	14	14	14	88	65
POF_ENVELOPE	39	0	39	39	0	14
POF_SEMI-CONFINED	32	14	14	40	0	35
POF_Zone2	87	88	88	65	79	88
POF_Zone1	70	71	83	63	58	83
POF of the building	83	81	81	95	97	98
Probability of fire entrance	56	57	67	59	57	81

Vulnerable elements of H2.6 with a high probability of failure were the unprotected glazing systems, the bad condition of the roof and the combustible vent protection, resulting in a very high probability of failure of the building (98%). With regard to the probability of fire reaching the dwelling (POF_Zone1), H2.6 had the highest value (83%), along with H2.3, due to the 0% compliance to the rules for all types of fuels in zone 2 and an overall low compliance (less than 60%) in zone 1. This resulted in the highest probability of fire entrance, specifically 81%. The fire did enter the home through the unprotected windows and ignited an entire floor of the dwelling, causing structural damage as well.

H2.4 was also severely affected by the fire, as the fire entered through a window of the semi-confined space and ignited some items in a few rooms. The fire did not spread through the home and no structural damage occurred. The probability of failure of the building resulted to be 95%, while the probability of the fire reaching the building is 63%, due to a very low compliance to the rules for wildland fuels (0% in zone 2 and 17% in zone 1). This resulted in a probability of fire entrance of 59%.

H2.3 was not affected internally by the fire, but only presented damage to a semi-confined space made out of wood, which ignited subsequently affecting an unprotected window as well as the roof and gutter. The probability of the fire reaching the building is, as for home H2.6, 83%, which is the highest calculated value. This because the compliance to the rules for zone 2 is 0% for artificial fuels (due to the fuels present on the neighbour’s plot) and for wildland fuels, and only 25% for ornamental fuels, again due to non-compliance in the neighbour’s plot. Compliance to the rules in zone 1 is much higher, but still lower than 67% for all types of fuels. The probability of failure of the building is 81%, with vulnerable elements with a high probability of failure being the glazing systems and the window coverage of the semi-confined space. The probability of fire entrance for H2.3 is 67%, higher than the one for H2.4.

4.6.3 Case study 3: Castro Marim fire, Portugal 2021

The Castro Marim fire propagated through the three municipalities of Castro Marim, Vila Real de Santo António and Tavira, in the region of Algarve, Portugal, in August 2021. The fire started around 1 am and was considered to be controlled in the late morning. The severe weather scenario, with strong winds and high temperatures, caused the fire to revive in the afternoon.

Six homes (Figure 4.11) that were impacted by the fire were analyzed several months after the fire, and, when possible, the homeowners or residents were interviewed. One home is located in the municipality of Castro Marim, while the others in Tavira. The fire entered in H3.1, H3.2, H3.3, while homes H3.4, H3.5 and H3.6 were affected only on the outside, although H3.6 experienced some smoke damage on the inside. The damage can be seen in Figure 4.12.

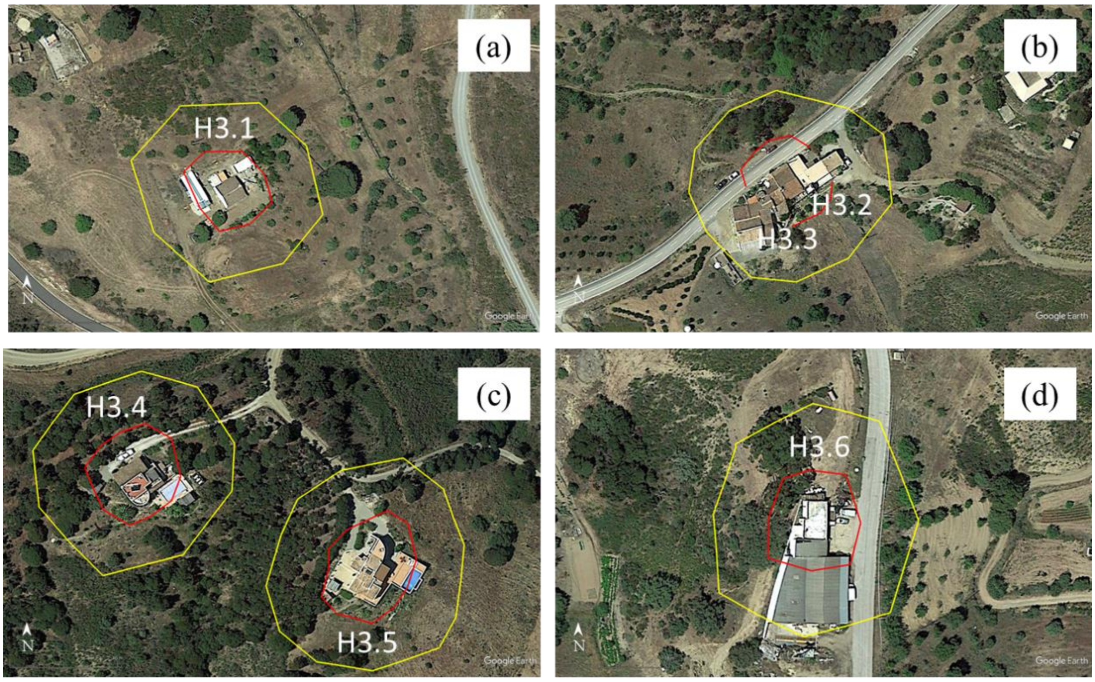

Figure 4.11: Monitored properties affected by the Castro Marim fire (Portugal, 2021). Red line: 10 m limit of zone 1. Yellow line: 30 m limit of zone 2.

Figure 4.12: Photographs of the WUI fire in Castro Marim, Portugal (August 2021). (a) Overview of the area after the fire; Properties affected by the fire: (b) H3.1; (c) H3.2; (d) H3.3; (e) H3.4; (f) H3.5; (g) H3.6.

The characteristics of the homes and properties that were needed as input for the tool are shown in Table 4.13. It was possible to interview the residents of homes H3.1, H3.2 and H3.3. Information for H3.4, H3.5 and H3.6 was obtained through inspection of the properties as well as of photographs that were made available by the municipalities.

Table 4.13: Characteristics of the dwellings affected by a WUI fire in Castro Marim, Portugal (August 2021). O/A/W: Ornamental/Artificial/Wildland fuels; SCS: Semi-confined space; NA: Not Applicable.

Characteristics	**WUI fire dwellings**					
	H3.1	**H3.2**	**H3.3**	**H3.4**	**H3.5**	**H3.6**
Shutters	No shutters	PVC	Aluminium	No shutters	No shutters	No shutters
Glazing thickness[A]	4 mm	4 mm	14 mm	14 mm	14 mm	4 mm
Roof material	Non-combustible	Non-combustible	Non-combustible	Non-combustible	Non-combustible	Non-combustible
Roof maintenance	Bad	Good	Good	Good	Good	Good
Vents	Non-combustible in good conditions	No vents	No vents	Combustible	Combustible	No vents
Windows coverage in semi-confined space	NA	NA	80%	20%	NA	0%
Envelope type in SCS	NA	NA	Non-combustible & thick	Non-combustible & thick	NA	Non-combustible & thick
Combustible material coverage in SCS (% in volume)	NA	NA	20%	5%	NA	50%
Fuel management compliance in zone 2 O/A/W (%)	100/100/25	100/100/0	100/100/0	50/50/0	100/50/0	100/0/0
Fuel management compliance in zone 1 O/A/W (%)	71/0/50	71/50/100	71/33/100	57/50/33	86/100/100	86/0/33

With the exception of homes H3.2 and H3.3, all homes did not have shutters protecting all of the windows. The roof material was the same for all homes, and all roofs, with the exception of H3.1, were well maintained. Three of the homes did not have vents, H3.1 had non-combustible protection in good conditions, and H3.4 and H3.5 had combustible protections, which melted during the fire. Three homes did not have a semi-confined space attached to the structure of the home (H3.1, H3.2, H3.5). When it comes to fuel management in zone 2, all homes but H3.4 did not have any ornamental vegetation in this zone, and for homes H3.1, H3.2 and H3.3 there were no artificial fuels. Wildland fuel compliance in zone 2 is nonexistent for all homes but H3.1, which still had a very low value of 25%. Homes H3.2, H3.3 and H3.5 didn’t have any wildland fuels in zone 2 (therefore compliance is 100%), and compliance to wildland fuels rules for the other properties reaches maximum 50%. Compliance of ornamental fuels in this zone goes from

57% to 86%, although it doesn't reach the value for good fuel management. When it comes to artificial fuels in zone 1, only H3.5 complies to all rules, while H3.1 and H3.6 have 0% compliance.

The results obtained from the VAT model are shown in Table 4.14. The homes with the highest probability of fire entrance were H3.6, with 79%, H3.4, with 70%, and H3.1 with 66%. For the other homes the estimated probability was between 32% and 36%.

Table 4.14: Probability of fire entrance in the homes characterised in Table 4.13 according to the elements identified in Figure 4.2.

FIS / Classical logic results (%)	**WUI fire dwellings**					
	H3.1	**H3.2**	**H3.3**	**H3.4**	**H3.5**	**H3.6**
POF_GLAZING	88	65	16	70	70	88
POF_ROOF	65	14	14	14	14	14
POF_VENT	14	0	0	65	65	0
POF_ENVELOPE	0	0	39	39	0	14
POF_SEMI-CONFINED	0	0	32	32	0	35
POF_Zone2	65	65	65	79	79	88
POF_Zone1	68	51	63	74	35	85
POF of the building	96	70	51	94	91	93
Probability of fire entrance	66	36	32	70	32	79

Home H3.6 did not experience fire entrance, although glazing systems were broken and part of the envelope experienced structural damage. The vulnerable elements of the building included the glazing systems, with no shutters and single pane glazing, and the presence of a semi-confined space with a high amount of combustible material. Additionally, the management of wildland fuels and artificial fuels in both zones was very poor, as reflected in a POF_Zone1 of 85% (highest value for this case study).

Home H3.4 obtained the second highest probability of fire entrance, given that many vulnerabilities were present at the time of the fire, such as windows not protected by shutters, combustible vent protection, and the presence of a porch with windows in the wall in common with the home. Fuel management compliance was also low, as reflected by the POF_Zone 1 of 74%. H3.4 experienced large damage on the property, with the combustion of two cars, as well as damage to one side of the envelope, where shutters and vent protections melted due to the vicinity of burning ornamental vegetation.

What is notable from the result for this case study is the fact that H3.2 and H3.3 obtained a low probability of fire entrance (36% and 32% respectively), while during the fire they experienced damage due to the fire entering the building. This was caused by the combustion of two Eucalyptus trees that were located at approximately 10 m from both buildings, which caused the breakage of the glazing systems of H3.2 and possibly ignited the wooden structure of the semi-confined space of H3.3.

4.6.4 Discussion

Looking at the results from the analysed case studies, it is clear that it is not only the structural characteristics of a building that play a role, but the surrounding elements are also deemed to be very important. The analysed properties had a probability of failure of zone 2 higher than 65% and a probability of failure of zone 1 higher than 35% (although

13 out of 17 properties had a POF_Zone 1 equal to or above 63%). On this regard, it must be noted that the experts polled for the building of the fuzzy logic methodology consider that good management of the surroundings consists of complying to 90.1% of the set rules. As observed in the case studies, often fuels of zone 2 (and sometimes also of zone 1) are located on neighboring parcels, highlighting the issue that homeowners sometimes do not have direct impact on the management of fuels that surround their home. This highlights the fact that collaboration between neighbors in keeping fuels well managed is essential. Additionally, the event that caused glazing failure in home H3.2 (two Eucalyptus trees located just at the border of zone 1 – 10m from the glazing) highlights that more research is needed on the placing of wildland fuels from vulnerable elements of the building. When it comes to structural vulnerabilities, the probability of failure of glazing systems was 65% or higher for 11 out of the 17 analysed homes, mainly because not all glazing systems were protected by shutters, or they were protected by combustible shutters (PVC). Five homes also had a probability of failure of the roof of 65%, due to it being poorly maintained for 4 of these homes, and due to it being made out of combustible materials (but well maintained) for one home. Two homes had unprotected vents, 3 homes had combustible vent protection, 5 had non-combustible vent protection in good conditions, and 9 home had no vents. Overall, the probability of failure of semi-confined spaces is the one that presents the lowest values, going to a maximum of 41% probability of failure. In general, homes and properties that scored a low probability of fire entrance did not experience great damage from the passing of the wildfire.

When looking at all analysed properties, it is clear that the results obtained in the VAT do not always reflect the observed degree of fire damage. The correlation between vulnerability and damage is difficult to establish, as factors, such as firefighter's actions, evacuation/stay and defend procedures, position of the house with respect to the propagating front, are not taken into account. The difficulty in obtaining this kind of relationship has been presented by Dossi et al. (2022).

Further validation with real case studies is needed, as this will give a broader and better understanding of the presented tool, as well as highlight the areas or issues that might not yet have been considered.

The case studies required to validate the tool have to be carefully detailed because pre-fire relevant data from homeowners need to be collected. For this reason, databases of past large fires like CAL FIRE database or Pedrógrão Grande Fire Complex database, as those used in Dossi et al. (2022), are not adequate for this purpose. An example of the data collection form that can be used for this purpose is given in Appendix B. Additionally, if enough data on real fires is collected, it could be possible to use that data for the tool, and compare it with the probabilities obtained by polling the experts for the fuzzy logic methodology.

4.6.5 Comparison with existing tools

Worldwide, there are few existing quantitative vulnerability assessment tools for buildings located at the WUI, since most standards or guidelines give instructions on the construction of the building as well as on how to manage the fuels located in its surrounding, without quantifying the vulnerability.

The Canadian FireSmart (Government of Alberta, 2013) addresses structural vulnerabilities as well as fuel management of the home ignition zone and provides a scoring system for the building and the property. It is however not suited for the analysis of vulnerabilities in the Mediterranean landscape.

Papathoma-Köhle et al. (2022) presented a quantitative vulnerability assessment tool that is specific for Mediterranean buildings subject to wildfire. The tool gives as output a Physical Vulnerability Index (PVI) and it is based on indicators obtained from the analysis of data collected from the fire in Mati (Greece) in 2018. Eight relevant indicators have been identified: roof material, structural type, slope, vegetation, roof-leaf accumulation, shutter material, main ground covering, roof type. They constructed the index as a composite of these indicators, which were scored (1-5; 5 = worst in terms of vulnerability) and added according to their relative importance. While all of these 8 indicators are included in the VAT, with the exception of roof type (i.e., shape of the roof), indicators for maintenance of the roof, vents, glazing thickness, semi-confined spaces and spacing between fuels are missing. Moreover, in terms of fuel availability near the dwelling, only vegetation within 20 m from the structure is considered. When applying the PVI methodology to the three previously discussed case studies, issues were found in setting the scores for some indicators. For example, there is no option for *no shutters* or for a non-combustible roof structure covered by a combustible material. In order to test the methodology, the worst case was taken into account for those homes that do not have shutters on all their windows, while for the home with a combustible roof cover (H2.4), the option of *concrete slab* was used. The results, compared with those obtained with the VAT, are given in Table 4.15. When applying this methodology for the Lloret de Mar case study, it was noticed that all the houses had the same value for all indicators, with the exception of the one for the shutters, which are made out of aluminium for houses H1.4 and H1.5, while in the other houses they are made out of combustible materials such as wood or PVC. The obtained PVI for H1.1, H1.2 and H1.3 is of 2.84 out of 5, while their VAT score varies from 32% to 87%. The PVI for H1.4 and H1.5 is 2.72, not showing a great difference with home H1.3 for example, while the VAT highlights this difference. When it comes to El Pont de Vilomara case study, H2.4, H2.5 and H2.6 obtained the same PVI of 2.87, while they obtained respectively a VAT score of 59%, 57% and 81%, whereas the differences between the scores for homes H2.1, H2.2 and H2.3 are not as noticeable. The same happens for the case study of Castro Marim, where H3.4 and H3.5 have a very large gap when it comes to their VAT score (70% and 32% respectively), while they obtained the same PVI. Bigger differences between H3.1 and H3.2 and H3.3 are also reflected in the VAT score, and not as much in the PVI.

Based on these results, the differences between the different buildings are better reflected in the VAT methodology. Therefore, the tool presented in this chapter is more comprehensive of the different issues and vulnerabilities of buildings and properties located at the Mediterranean WUI.

Table 4.15: Comparison of the results for the case studies with the VAT methodology and with the PVI methodology. The PVI is converted in percentage, for easier comparison.

Home	VAT score [%]	PVI (max value: 5)
H1.1	32	2.84 (57%)
H1.2	55	2.84 (57%)
H1.3	87	2.84 (57%)
H1.4	27	2.72 (54%)
H1.5	28	2.72 (54%)
H2.1	56	2.32 (46%)
H2.2	57	2.43 (49%)
H2.3	67	2.66 (53%)
H2.4	59	2.87 (57%)
H2.5	57	2.87 (57%)
H2.6	81	2.87 (57%)
H3.1	66	2.13 (43%)
H3.2	36	2.03 (41%)
H3.3	32	1.91 (38%)
H3.4	70	2.54 (51%)
H3.5	32	2.54 (51%)
H3.6	79	2.44 (49%)

4.7 Conclusions

This chapter presents the development of a tool for the assessment of vulnerabilities of buildings located at the Mediterranean WUI. This Vulnerability Assessment Tool (VAT) considers the complex nature of the WUI microscale fire risk problem through the use of fuzzy logic, given the lack of data on structure ignition of past WUI fires occurred in the Mediterranean region. The end users of this tool are intended to be not only fire safety practitioners, but also the homeowners and residents of the WUI. The use of this VAT is expected to lead to the improvement of fire safety practices at the microscale; i.e. it will increase WUI fire risk awareness of homeowners by identifying systematically major problematic conditions present on their property and in its surroundings. While the building of the tool is complex, the final product that is presented to the user is straightforward and easy to use. The tool considers four main building sub-systems that have shown to be vulnerable to fire, as well as three different types of fuels that can cause the fire to spread through a property towards a dwelling. As probabilities are calculated for each of these intermediate events, it is possible not only to obtain the probability of a fire entering the dwelling, but also to identify the critical events that lead to this. The homeowner will obtain also information on what are the most critical issues of its property (i.e., which event has the leads to a higher probability of fire entrance), and therefore which elements need to be improved to prevent fire entrance in the event of a wildfire. Moreover, a planned use of this tool at a local level would be key to improving fire protection at the community level.

Further work includes the creation of the questionnaire for the homeowners in digital form, easily accessible online. The tool could also be part of an advanced home assessment program, linked to an EU-genuine risk awareness and preparedness framework tailored for WUI communities in the Mediterranean region (inspired by FireSmart in Canada and Firewise in the USA).

4.8 References

Àgueda, A., Vacca, P., Planas, E., Pastor, E., 2023. Evaluating wildfire vulnerability of Mediterranean dwellings using fuzzy logic applied to expert judgement. Int. J. Wildl. Fire. https://doi.org/10.1071/WF22134

Autoridade Florestal National, 2008. Gestão de Combustíveis Para Protecção de Edificações - Manual. https://fogos.icnf.pt/sgif2010/InformacaoPublicaDados/gestao_comb_final.pdf

Cal Fire, 2022. Defensible Space. https://www.fire.ca.gov/programs/communications/defensible-space-prc-4291/ (accessed 12.9.22).

Cohen, J.D., 2000. Preventing Disaster: Home Ignitability in the Wildland-Urban Interface. J. For. 98, 15–21.

Darbra, R.M., Demichela, M., Murè, S., 2008. Preliminary risk assessment of ecotoxic substances accidental releases in major risk installations through fuzzy logic. Process Saf. Environ. Prot. 86, 103–111. https://doi.org/https://doi.org/10.1016/j.psep.2007.10.015

Dossi, S., Messerschmidt, B., Ribeiro, L.M., Almeida, M., Rein, G., 2022. Relationships between building features and wildfire damage in California , USA and Pedrógão Grande , Portugal. Int. J. Wildl. Fire 1–17. https://doi.org/10.1071/WF22095

Drescher, M., Perera, A.H., Johnson, C.J., Buse, L.J., Drew, C.A., Burgman, M.A., 2013. Toward rigorous use of expert knowledge in ecological research. Ecosphere 4, 1–26. https://doi.org/10.1890/ES12-00415.1

Ganteaume, A., Barbero, R., Jappiot, M., Maillé, E., 2021. Understanding future changes to fires in southern Europe and their impacts on the wildland-urban interface. J. Saf. Sci. Resil. 2, 20–29. https://doi.org/10.1016/j.jnlssr.2021.01.001

Generalitat de Catalunya, 2019. Protegeos de los incendios forestales. Pla INFOCAT. https://interior.gencat.cat/web/.content/home/030_arees_dactuacio/proteccio_civil/consells_autoproteccio_emergencies/incendi_del_bosc/documents/llibret_incendis_forestals_cast.pdf

Generalitat de Catalunya, 2005. Decret 123/2005, de 14 de juny, de mesures de prevenció dels incendis forestals en les urbanitzacions sense continuïtat immediata amb la trama urbana, Diari Oficial de la Generalitat de Catalunya núm. 4407 de data 16/06/2005. https://portaljuridic.gencat.cat/ca/document-del-pjur/?documentId=384053

Manca, T., López, M., 2014. Guía Metodológica de Actuaciones de Prevención, Defensa y Autoprotección en la Interfaz Urbano-Forestal, Generalitat Valenciana. https://agroambient.gva.es/documents/162905929/162908876/Gu%C3%ADa%2Bmetodol%C3%B3gica%2Bde%2BActuaciones%2Bde%2BPrevenci%C3%B3n,%20Defensa%2By%2BAutoprotecci%C3%B3n%2Ben%2Bla%2BInterfaz%2BUrbana-Forestal%2B%286,8Mb%29/d24a0daf-d777-405b-8938-b4a54394831f

Maranghides, A., Mell, W., Hawks, S., Wilson, M., Brewer, W., Brown, C., Vihnanek, B., Walton, W.., Fire, C.A.L., Brewer, Will, Fire, C.A.L., 2021. A Case Study of the Camp Fire – Fire Progression Timeline NIST Technical Note 2135 406. https://doi.org/10.6028/NIST.TN.2135

Maranghides, A., Mell, W.R., Hawks, S., Wilson, M., Brewer, W., Link, E., Brown, C., Murrill, C., Ashley, E., 2020. NIST Technical Note 2105 - Camp Fire Preliminary Reconnaissance. https://doi.org/10.6028/NIST.TN.2105

Morvan, D., 2007. A numerical study of flame geometry and potential for crown fire initiation for a wildfire propagating through shrub fuel. Int. J. Wildl. Fire 16, 511–518. https://doi.org/10.1071/WF06010

Oladokun, V.O., Montz, B.E., 2019. Towards measuring resilience of flood-prone communities: a conceptual framework. Nat. Hazards Earth Syst. Sci. 1151–1165. https://doi.org/10.5194/nhess-19-1151-2019

Papathoma-Köhle, M., Schlögl, M., Garlichs, C., Diakakis, M., Mavroulis, S., Fuchs, S., 2022. A wildfire vulnerability index for buildings. Sci. Rep. 12, 1–15. https://doi.org/10.1038/s41598-022-10479-3

Préfet de Bouches-du-Rhône, 2014. Arrête nº 2014316-0054 relatif au débroussaillement et au meintien en état débroussaillé dans les espaces exposés aux risques d'incendies de forêt. Direction départementale des Territoires et de la Mer, Saervice de l'Agriculture et de la Forêt. https://fransylva-paca.fr/wp/wp-content/uploads/2015/08/2014-11-12-Arr%C3%AAt%C3%A9-OLD-13.pdf

Préfet de la Haute-Corse, 2022. Arrête DDT2B/SEBF/FORET/Nº 2B-2022-04-05-00006. Direction départementale des territoires, Service Eau-Biodiversité-Forêt, Unité Forêt. https://www.haute-corse.gouv.fr/IMG/pdf/arrete_2b-2022-04-05-00006_du_5_avril_2022.pdf

Prefet de Vaucluse, 2013. Arrêté n °2013049-0002 relatif au débroussaillement légal autour des constructions, chantiers et installations de toute nature dans le cadre de la prévention et de la protection contre les feux de forêts. Direction départementale des territoires, Service Eau et Milieux naturels. http://fransylva-paca.fr/wp/wp-content/uploads/2015/08/2013-02-18-Arr%C3%AAt%C3%A9-OLD-84.pdf

Préfet des Alpes-de-Haute-Provence, 2013. AP 2013-1473 relatif à la prévention des incendies de forêts et des espaces naturels dans le département des Alpes-de-Haute-Provence et concernant le débroussaillement. Direction Departementale des Territoires, Service de l'Environnement et des Risques. http://fransylva-paca.fr/wp/wp-content/uploads/2015/08/2013-07-04-Arr%C3%AAt%C3%A9-OLD-04.pdf

Prefet des Alpes-Maritimes, 2014. Arrêté nº 2014-452 portant règlement permanent du débroussaillement obligatoire et du maintien en état débroussaillé dans le département des Alpes-Maritimes. Direction départementale des Territoires et de la Mer des Alpes-Maritimes, Service Économie Agricole, Ruralité, Espaces naturels. http://fransylva-paca.fr/wp/wp-content/uploads/2015/08/2014-06-10-Arr%C3%AAt%C3%A9-OLD-06.pdf

Préfet du Var, 2015. AP portant règlement permanent du débroussaillement obligatoire et du maintien en état débroussaillé dans le sépartement du Var. Direction départementale des territoires et de la mer du Var. http://fransylva-paca.fr/wp/wp-content/uploads/2015/08/2015-03-30-Arr%C3%AAt%C3%A9-OLD-83.pdf

Ribeiro, L.M., Rodrigues, A., Lucas, D., Viegas, D.X., 2020. The impact on structures of the pedrógão grande fire complex in June 2017 (Portugal). Fire 3, 1–22. https://doi.org/10.3390/fire3040057

Seguí, X., Pujolasus, E., Betrò, S., Àgueda, A., Casal, J., Ocampo-Duque, W., Rudolph, I., Barra, R., Páez, M., Barón, E., Eljarrat, E., Barceló, D., Darbra, R.M., 2013. Fuzzy model for risk assessment of persistent organic pollutants in aquatic ecosystems. Environ. Pollut. 23–32. https://doi.org/doi: 10.1016/j.envpol.2013.02.014

Sivanandam, S.N., Deepa, S.N., Sumathi, S., 2007. Introduction to fuzzy logic using MATLAB. Springer.

South Australia County Fire Service, 2022. Your guide to Bushfire Safety. Government of South Australia. https://www.cfs.sa.gov.au/about/publications/publications/your-guide-to-bushfire-safety/

Spolaor, S., Fuchs, C., Cazzaniga, P., Kaymak, U., Besozzi, D., Nobile, M.S., 2020. Simpful: A user-friendly python library for fuzzy logic. Int. J. Comput. Intell. Syst. 13, 1687–1698. https://doi.org/10.2991/ijcis.d.201012.002

Vacca, P., Àgueda, A., Muñoz, J.A., Planas, E., Pastor, E., Heymes, F., Ismael, E., Eyssette, R., Cozzani, V., Scarponi, G.E., 2020. WUIVIEW Deliverable 6.1 - Recommendations on structure survivability and sheltering capacity. https://wuiview.webs.upc.edu/download/D6.1_F_Recommendations%20on%20structure%20survivability%20and%20sheltering%20capacity.pdf

Victoria County Fire Authority, 2022. Landscaping for Bushfire: Garden Design and Plant Selection.

Chapter 5

WUI Performance Based Design guideline

5.1 Introduction

As presented in Chapter 1, Performance-Based fire safety Design is a methodology for the engineering of fire safe building solutions based on three key aspects (Hurley and Rosenbaum, 2016):

1. The definition of the level and type of performance that the final solution has to guarantee to meet general and particular fire safety objectives related to life, assets and environment protection.
2. The definition of the potential fire events that may occur (i.e. design fire scenarios), considering the interaction between occupants, building characteristics and fire.
3. The quantitative assessment of the proposed design against the defined goals facing pre-defined fires scenarios, relying –when needed– on advanced CFD codes.

Utilizing a PBD approach goes therefore beyond the application of the local legislation, analysing how a building and its occupants are affected by fire. When it comes to the WUI, regulatory bodies, research institutions and practitioners are starting to address its fire safety challenges with the aid of PBD methods (Vacca et al., 2020a), although no PBD guideline specific for the WUI microscale has been developed to this day.

A Performance Based Design (PBD) guideline specific for WUI scenarios is presented in this chapter. Within the guideline, performance criteria are presented for both life safety and property protection (the latter are those identified in Chapter 2), and suggestions on the choice of design fire scenarios for WUI environments are given, along with the variables that should be included, such as fire, environmental and property characteristics.

The guideline is then applied to a case study of a property located at the Spanish WUI. The goal of the presented case study is property protection and scenario evaluation is performed with the Computational Fluid Dynamics tool FDS (Fire Dynamics Simulator (NIST, 2022)), based on the methodology presented in Chapter 3. Strategies to ensure property protection are presented as well.

5.2 WUI microscale Performance Based Design guideline

The complexity of the different interactions that can occur between fire, structures and residents can be analysed through a PBD approach for both new and existing buildings located at the WUI.

By following a PBD methodology, fire scenarios which involve the following issues can be analysed (Vacca et al., 2020a):

- Houses vulnerability assessment: building performance analysis for structure triage (i.e., defensible/indefensible houses).
- Sub-system hazard testing: hazard assessment of individual fuels (e.g. stored materials, ornamental and wildland vegetation, etc.) and performance evaluation of specific building components (e.g., openings, glazing systems, etc.).
- Building sheltering capacity: assessment of whether the building can be used as a shelter or not.
- Post-fire investigation: quantitative analysis of past incidents to identify main causes of fire losses, illustrate lessons learnt and provide evidences to insurance covering assessment.
- Fire safety regulations improvements: design of PBD WUI-specific standards/codes and revision of prescriptive ones.

The WUI PBD guideline follows the classic PBD process, shown in Figure 5.1, and it provides an assessment methodology for properties in their current state, as well as for the effectiveness of strategies that are implemented to reduce the risk for the property (e.g., removal of vegetation and other types of fuels from the property, increasing separation distances between fuels and vulnerable elements present on the property, etc.).

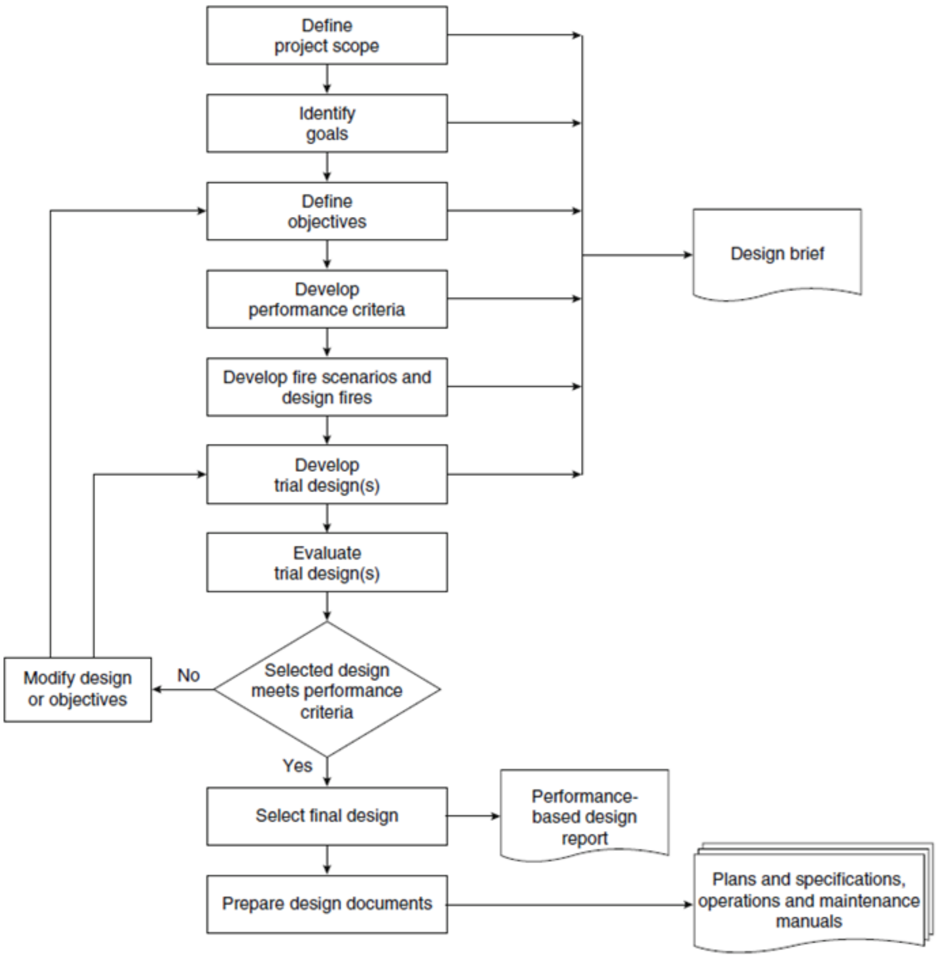

Figure 5.1: Performance-Based Design process. Adapted from Hurley and Rosenbaum (2016).

5.2.1 Scope

The WUI PBD guideline can be applied to properties at the microscale level, which can include one or more buildings, or sections of these properties (e.g., scenarios which include only one vulnerable element). These buildings and their surroundings must comply with local regulations. Buildings may include dwellings, commercial and industrial structures, and public buildings.

Stakeholders must be identified in order to set the goals and objectives of the design. The stakeholders at the WUI can for example be the homeowners, the local fire agencies, insurance companies or anyone that has an interest in the protection of the property.

The guideline has been developed to quantify hazards and vulnerabilities of buildings taking in mind not only their ability in withstanding the passing of a wildfire, but also their capacity to be safe shelters for the occupants.

5.2.2 Goals and objectives

Goals must be selected for each project depending on the aims of the stakeholders. They are the desired outcome expressed in qualitative terms. The classic PBD goals of life safety, property protection, mission continuity and environmental protection (Hurley and Rosenbaum, 2015) can be applied at the WUI as well.

Design objectives must be set by taking the previously selected goals into account. These can include for example the creation of a sheltering area for occupant protection, limiting the fire spread through a property, or maintaining a building's structural integrity. If fire protection systems are included in the design, an objective should be set for their effectiveness.

5.2.3 Performance criteria

Performance criteria are threshold values set to quantify the hazards posed by each scenario. They can be divided into two categories: life safety and non-life safety (Hurley and Rosenbaum, 2015).

Life safety criteria

Life safety criteria include threshold values for tenability conditions inside a building, in order to assess the building's sheltering capacity. Recommended life safety criteria are given in Table 5.1. When a building's sheltering capacity is being evaluated, also non-life safety criteria must be met.

Table 5.1: Recommended life safety performance criteria

Performance criteria	Threshold values	References
Fractional Effective Dose (FED)	FED < 1	Hurley et al. (2016)
Interior air temperature	T < 45°C	Australian Building Codes Board (2014)
Interior wall temperature	T < 70°C	Australian Building Codes Board (2014)
Radiant heat flux	$\dot{q}''_{rad}$ < 1.7 kW/m^2	Casal (2017)

Non-life safety criteria

These criteria include the structural requirements of a building, which should be met when the building is used as a shelter, as well as when the goals of the project include property protection. Criteria must be set for the vulnerable structural elements of a building, as well as for other vulnerable elements located on a property (i.e. LPG tanks).

Threshold values for different structural elements were identified in Chapter 2 and are summarized in Table 5.2. This is table does not include all building materials, and does therefore not contain an exhaustive list of performance criteria. When analysis of building sub-systems different from the mentioned ones is to be performed, performance criteria for those specific scenarios must be identified.

Table 5.2: Recommended non-life safety performance criteria, extrapolated from the analysis performed in Chapter 2.

Performance criteria		Threshold values
Window breakage		
Glass failure		ΔT_{cr} < 83°C T_{surf} < 132°C HL < 1087 kJ/m^2
Failure of frame and shutters	Aluminium	T_{surf} < 660°C
	PVC	T_{surf} < 220°C
	Wood	T_{surf} < 350 °C and $\dot{q}''_{rad}$ < 12 kW/ m^2
LPG tank integrity		
First analysis (FDS)		$\dot{q}''_{inc}$ < 22 kW/ m^2
Second analysis (ANSYS Fluent)		PRVI < 0.9 WSI < 0.9
Concrete walls integrity		
Load bearing capacity		η_{fi} > 74%

5.2.4 Design fire scenarios

Development of scenarios

Identification of scenarios can be performed via failure analysis, historical data, checklists, statistical data, fault- or event-tree analysis, etc. (Hurley and Rosenbaum, 2015). A fire scenario should represent fire conditions that are thought to be threatening to a building.

An example of a simple fault tree analysis is given in Chapter 2, in which five different events that can cause fire entrance inside a building have been identified:

- Through windows or doors that are left open due to sudden and unprepared evacuation, or though poorly designed or maintained vent ducts. Flames or flying embers can enter the house and start indoor ignition of curtains, furniture, papers or any other light fuels. This may progress into full involvement of a room and the eventual burning of the whole house, if left unattended.
- Through broken windows, in case of a poorly managed property or settlement where combustible elements are placed too close to unprotected glazing elements.

The combustion of these fuels can cause cracking or collapsing of the glass, giving way to the entrance of smoke, firebrands and flames.

- Due to the presence of semi-confined spaces such as garages, sheds, or storage areas containing non-natural fuels that are located close to the main structure or are extensions of it. A large accumulation of heat in those areas due to the ignition of their contents could lead to fire spread to the main structure through internal doors, passageways, or windows, as well as to structural damage to the house envelope.
- Through gaps created in the attic due to poorly maintained roofs and gutters, which are directly exposed to flying embers, radiation and even direct flames.

Scenarios can be selected on the assumption that ignition of residential fuels will happen by firebrands coming from the main front or from the wildfire itself, should the property be located at the perimeter of a settlement or in case of an intermix scenario.

Once scenarios have been identified, a reduction of their population might be needed. This can be done by identifying those scenarios with:

- High-frequency, low-consequences: these are scenarios that are most likely to happen, which will have lower consequences on the property. An example of these types of scenarios is the ignition of one residential fuel item in one single point. Environmental conditions (i.e., temperature, wind direction and speed, humidity) include average values (e.g., most common wind direction and average wind speed, seasonal average temperatures and humidity).
- Low-frequency, high-consequences: these are scenarios that are less likely to happen, but can create large damage to a property. For example, the simultaneous ignition of several residential fuels the ignition of a hedgerow in multiple points, with extreme environmental conditions (i.e. high temperatures, low humidity, worst-case wind speed and direction).
- Special problems: these scenarios include specific issues of a property which can be addressed individually, such as the presence of combustible items close to a LPG tank or the storing of fuel packs in semi-confined spaces.

Fire characteristics

Fire characteristics must be selected for each scenario. When analysing the WUI, the most common type of design is a full burnout, meaning that the fire is not suppressed but decays according to the available fuel. If suppression systems are present and assumed to function, they should also be inserted in the scenario, by cutting the fire curve at the time they are expected to activate.

Fire characteristics include the evolution of the Heat Release Rate (HRR) or of the Mass Loss Rate (MLR) over time, along with the products of the combustion, the area/location and the spread rate of the fire. Currently, there are no standard values for these inputs when it comes to the WUI environment. As information on the burning behaviour of WUI residential fuels is scarce, examples are given in Chapter 2 on the definition of fire characteristics for this type of fuels. Suggestions are given on how to characterise wildland fuels, artificial fuels and ornamental vegetation, by presenting HRR curves or/and HRRPUA values.

Information is also needed for the products of the simulated reaction. For artificial fuels, CO and soot yields can be defined by taking pre-flashover design values used for the PBD of buildings (e.g., Y_{CO} = 0.04 kg/kg, Y_{soot} = 0.07 kg/kg (Ministry of Business Innovation and Employment, 2013)), should more specific data be unavailable.

Environmental characteristics

Environmental characteristics can influence the outcome of a scenario, and must thus be included in the design. These include the location of the property within the landscape, as well as the one of the building within the property, along with meteorological information such as outdoor temperature, humidity, and wind direction and speed. The choice of these characteristics depends on the type of scenario that is to be analysed (e.g., high frequency, low consequences scenarios should include average values, while low-frequency, high consequences scenarios include extreme values).

Characteristics of the analysed property

Physical features of the building (i.e. the geometry and materials of the structure) and of the landscape or property can affect phenomena such as the fire entering the building or the way the smoke spreads through the property and inside the building. They also affect fire spread and growth through the property.

Property characteristics such as the proximity of vegetation to a building, the presence of other combustible materials or structures, or the construction materials of the building, along with possible leakage areas which would allow for smoke to enter a building, must thus be taken into account during the design.

Occupant characteristics

Occupant characteristics that must be considered are their ability to respond in case of spot fires, to evacuate when needed and to shelter in place, if the building is considered as a shelter.

5.2.5 Trial designs

Once the fire scenarios have been selected, trial designs should be established. For existing buildings and properties, the design can include the situation as-is for the analysis of the current vulnerabilities.

Trial designs can also include fire protection strategies for the achievement of the goals of the project, such as methods to reduce likelihood of ignition or fire growth (e.g. presence of fire-resistant species or non-combustible items) or suppression systems. Also passive fire protection strategies should be taken into account.

5.2.6 Trial design evaluation

The evaluation of the trial designs involves determining if a design meets all of the set performance criteria. Fire modelling with diverse complexity degrees can be used for the quantitative evaluation of the designs. Computational Fluid Dynamics modelling tools such as FDS (NIST, 2022) can be used to simulate complex geometries where a more detailed spatial resolution is required (Hurley et al., 2016). FDS offers a great perspective in the WUI context, allowing to take the spatial and temporal variability of WUI scenarios into account. The use of FDS requires a significant amount of information related to the building and the fire, along with the occupant's behaviour in case of the analysis of the sheltering capacity of a building.

If the selected trial designs do not meet the previously set performance criteria, then they should be modified until performance criteria are met.

5.3 Application to a case study

The methodology described in the WUI PBD guideline is applied to a case study located in the region of Madrid, Spain. The property identified in the case study is analysed in its current conditions, although some of the simulated features have been selected to showcase the usefulness of the PBD guideline (e.g., an above ground LPG tank has been included in the analysis, glazing systems have been simulated without shutters, the smallest pane thickness has been chosen for the windows).

5.3.1 Description of the site

Parque Residencial Entrepinos is a settlement constituted in 1972, located in the municipality of Cadalso de los Vidrios, Madrid Autonomous Region, Spain, spanning over 140 hectares and enclosing 833 structures, mostly single-family homes (Figure 5.2). These represent the 32% of total structures in the municipality. Most of these homes are inhabited during holiday season (i.e., summer months) and on the weekends.

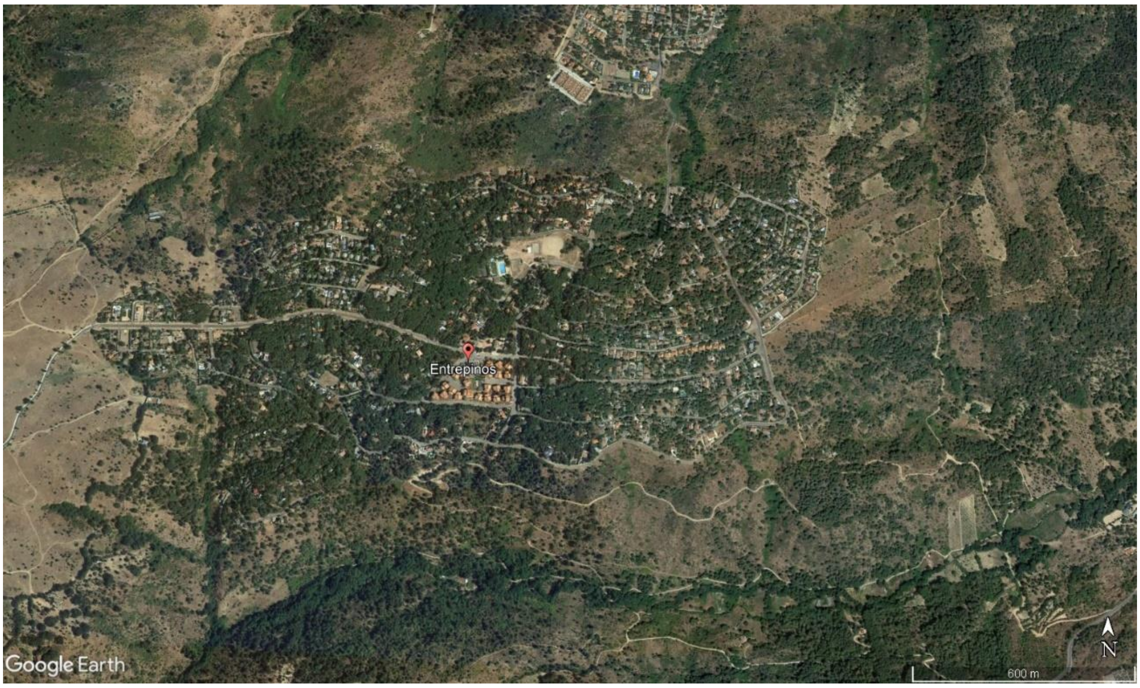

Figure 5.2: Urban settlement of Entrepinos and surrounding landscape.

The area is profusely covered with cluster pine (*Pinus pinaster*) and the accompanying understory, creating a highly flammable forest fuel in a fire-prone area. Most of the houses are made out of masonry, brick and other non-combustible materials. Entrepinos is classified as intermix WUI (Stewart et al., 2007), in which the urban area is scattered through pine trees and grassland. The area is often impacted by wildfires, and the last one happened in 2019, which spanned over more than 3000 ha and nearly affected the settlement, which was evacuated.

The case study involves one of the homes located on the northern limit of the settlement, in the western side. A view of the area where the property is located is given in Figure 5.3. Two undeveloped plots with cured grass are located on the southern side of the property, while cypress hedgerows connect the property with those located on the south and east sides. Grass is the main fuel located on the northern side, along with some juniper (*Juniperus oxycedrus*) and oak (*Quercus ilex*) trees. Several pine trees are located on the eastern neighboring property.

The building is constructed with concrete blocks (wall thickness is 15 cm) and the roof is covered by non-combustible tiles (Figure 5.4). Single pane glazing systems (3 mm thick) with PVC frames are not protected by shutters. A porch is present on the southern side, where a big window is present, and a small wooden shed is located in the north-eastern corner. For the analysis, it is assumed that an LPG tank is located near the hedgerow on the south-eastern part of the property.

Figure 5.3: Top view of the area where the property that will be analysed is located (inside the red zone).

Figure 5.4: View of the western side of the property.

5.3.2 Scope, goal and objectives

The PBD analysis is performed on the entire property. The goal of the project is property protection, with the objectives of no structural damage and therefore no fire entrance and reduction of fire spread through the property.

5.3.3 Performance criteria

The non-life safety performance criteria set in the PBD guideline are used as performance criteria for the building (Table 5.).

5.3.4 Design fire scenarios

Fire scenarios are identified based on the possible available fire sources present on the property. The scenario population has been reduced according to the steps described in the PBD guideline. Four critical scenarios have been identified in this case study: two special problem scenarios, one with high frequency - low consequences, and one with low frequency - high consequences. These scenarios are simulated in FDS, for which geometry data of the property and building is needed. Information on the dimensions of the property and its characteristics are obtained through the methodology presented in Caballero and Ribeiro (2019), which is based on airborne photogrammetry obtained with a drone, with which a 3D model is created. This model is then converted into FDS compatible data through a process of voxelization. The obtained data is then uploaded in the sofwtare Pyrosim (Thunderhead Engineering, 2022), which converts these inputs into a FDS script. The representation of the property in Pyrosim is shown in Figure 5.5.

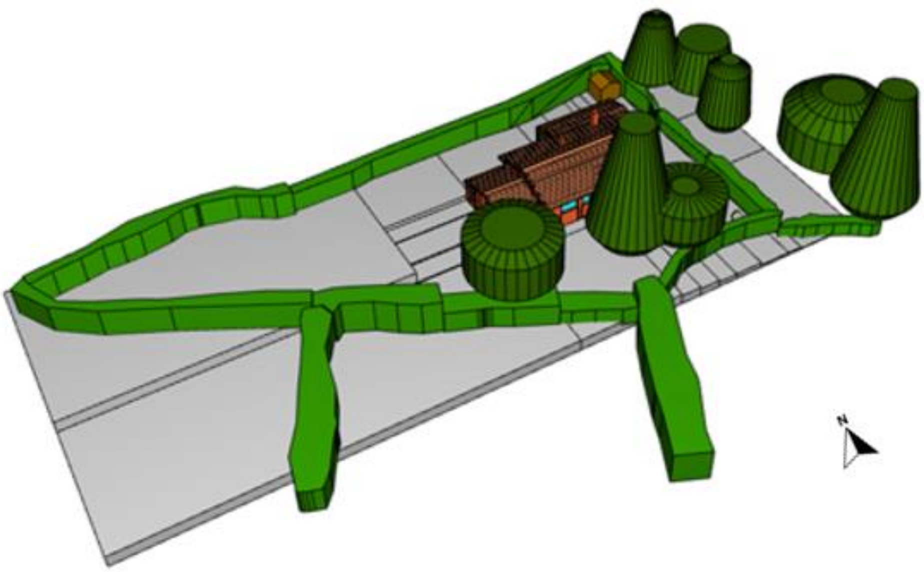

Figure 5.5: Representation of the property in Pyrosim.

Scenario 1 – Low frequency, high consequences

This scenario consists of the simultaneous burning of the hedgerow and the trees located on the north-eastern side of the property. The fire is simulated as a flat surface (red surface in Figure 5.6a), with an assigned prescribed HRRPUA and residence time. The fire characteristics are obtained by using the data presented in Chapter 2. For the hedgerow, a HRRPUA of 4500 kW/m^2 was estimated from the results obtained from tests performed during the WUIVIEW project (Ribeiro et al., 2020). For the trees, the forward rate of spread r is estimated to be 10% of the wind speed, thus 33 m/min (0.55 m/s). The minimum value of fuel consumption w for conifers is 2 kg/m^2 (Alexander and Cruz, 2019), therefore Byram's intensity can be calculated by using Equation 2.3:

$$I_B = H \cdot w \cdot r = 18000 \ \cdot 2 \cdot 0.55 = 20000 \, kW/m$$

The width of the area covered with trees is approximately 4 m, which is used as the value for the flame depth, therefore the calculated HRRPUA for the trees is 5000 kW/m^2. The residence time for forests is assumed to be 45 s, while for shrubs it is assumed to be 20 s (Alexander et al., 2007). The combustion reaction used to replicate the generation of species during wildfires is the one described in Vacca et al. (2020), which includes the following species: acetic acid, carbon dioxide, carbon monoxide, formaldehyde and hydrogen cyanide. The HRR curve for this scenario, which includes the simultaneous combustion of the hedge and the trees, is given in Figure 5.6b.

Within the simulated domain, ambient temperature and humidity are set at 35°C and 15% respectively (i.e., a very warm day with very low humidity). The closest weather station registered, between the years 1981 and 2010, average daily maximum temperatures of 32.8°C in the month of July and an average relative humidity for the same month of 36% (Agencia Estatal de Metereología, 2022), making the selected ambient temperature and humidity worst-case ambient conditions. In the municipality of Cadalso de los Vidrios, during summer months peak wind speeds are usually slightly lower than 20 km/h (values based on statistical analysis of data for the years 1980 to 2016 (Weather Spark, n.d.)), therefore this wind speed will be simulated for this scenario. The worst-case wind direction for this fire scenario is a wind blowing from north-east, which, in the month of July has a proportion of approximately 30% (Weather Spark, n.d.). The simulated wind is therefore from the north-east with a speed of 20 km/h at 10 m, pushing the flames toward the eastern façade of the house. The property and building are analysed in their current condition.

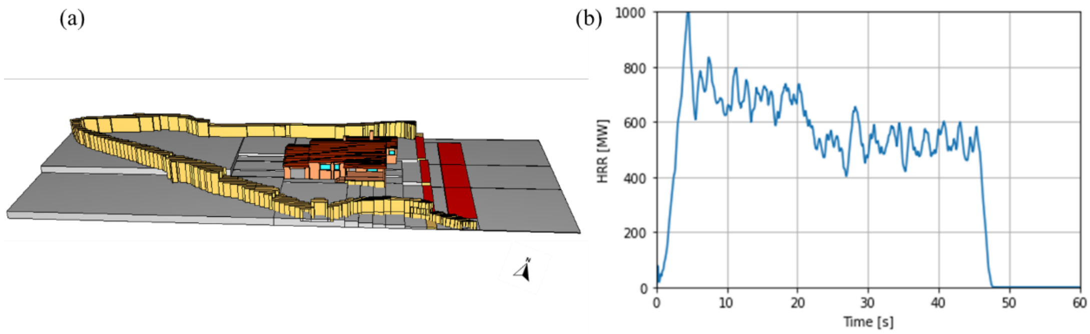

Figure 5.6: Scenario 1: (a) FDS domain and geometry, the red areas indicate where the hedgerow and trees are located; (b) HRR curve of the scenario.

Scenario 2 – High frequency, low consequences

In this scenario the ignition of the furthest western point of the hedgerow is simulated, with consequent fire spread through the entire hedgerow and the trees located by the southern façade of the house.

Environmental conditions are based on the average values for the month of July, which are an average temperature of 26°C and a humidity of 36% (average values between the year 1981 and 2010 (Agencia Estatal de Metereología, n.d.)). The average wind speed for the month of July (data from 1980 to 2016) is approximately 11 km/h and the predominant wind direction (with a proportion of 37%) is from west to east (Weather Spark, n.d.), therefore aiding the fire spread through the hedgerow.

The rate of spread of the fire through the hedgerow and the trees is estimated to be 10% of the wind speed, therefore 0.3 m/s. For the hedgerow, a residence time of 20 s is simulated, as for the previous scenario. Once the flames reach the trees on the south side of the house, these will ignite too, with the same characteristics as those in scenario 1, but with an HRRPUA adapted to the size of the fuel bed, resulting in 4348 kW/m^2 for the first tree, 3571 kW/m^2 for the second tree and 5000 kW/ m^2 for the third tree. As for the previous scenario, the fire is simulated with the aid of vents located on the ground (Figure 5.7a). The HRR curve for the scenario is given in Figure 5.7b.

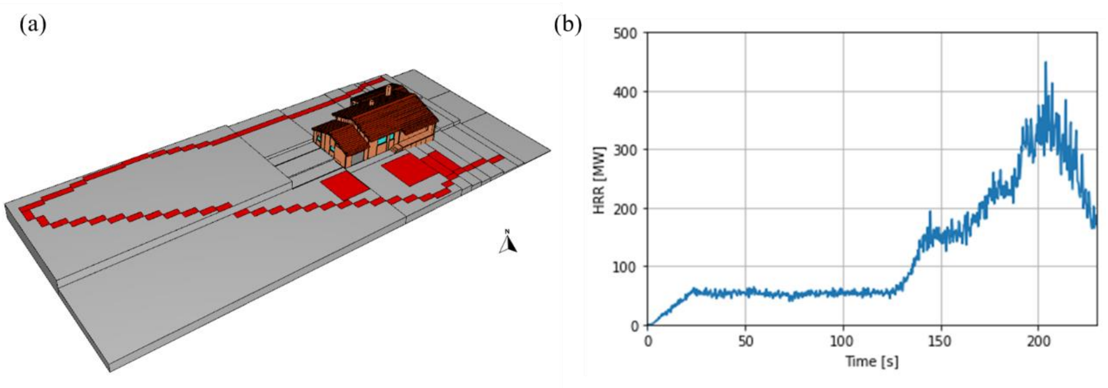

Figure 5.7: Scenario 2: (a) FDS domain and geometry, the red areas indicate the hedgerow and the trees; (b) HRR curve of the scenario.

Scenario 3 – Special problem 1

A special problem given by artificial fuels located in a semi-confined space (the porch) is analysed in this scenario. The simulated fuel pack consists of a set of garden furniture, including a table, 6 chairs, 6 cushions and a parasol, which is the one of test 3 shown in Chapter 2. The fire is simulated as a vent (Figure 5.8a) with an area of 7.48 m^2 and an assigned HRRPUA of 291.2 kW/m^2. The resulting HRR curve is given in Figure 5.8b.

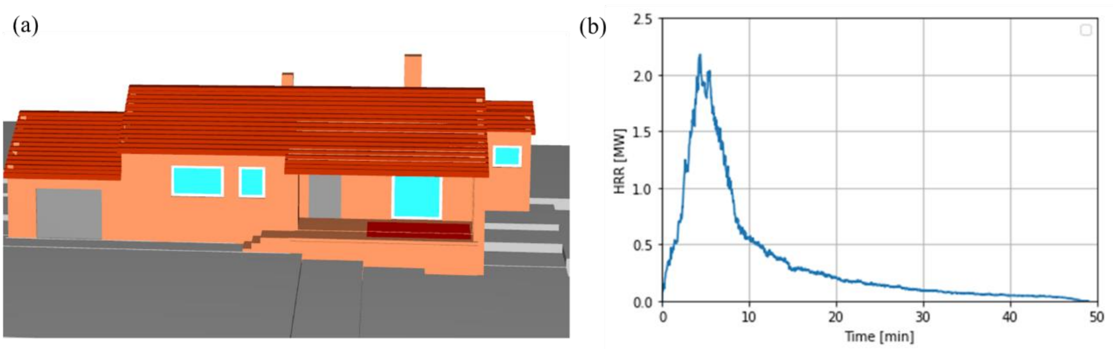

Figure 5.8: Scenario 3: (a) FDS domain and geometry; (b) HRR curve of the scenario.

Scenario 4 – Special problem 2

The second special problem scenario entails the analysis of the 1 m^3 LPG tank filled at 80% located in the south-east corner of the property (shown in Figure 5.9). The fire and environmental inputs are the same as those simulated in scenario 1.

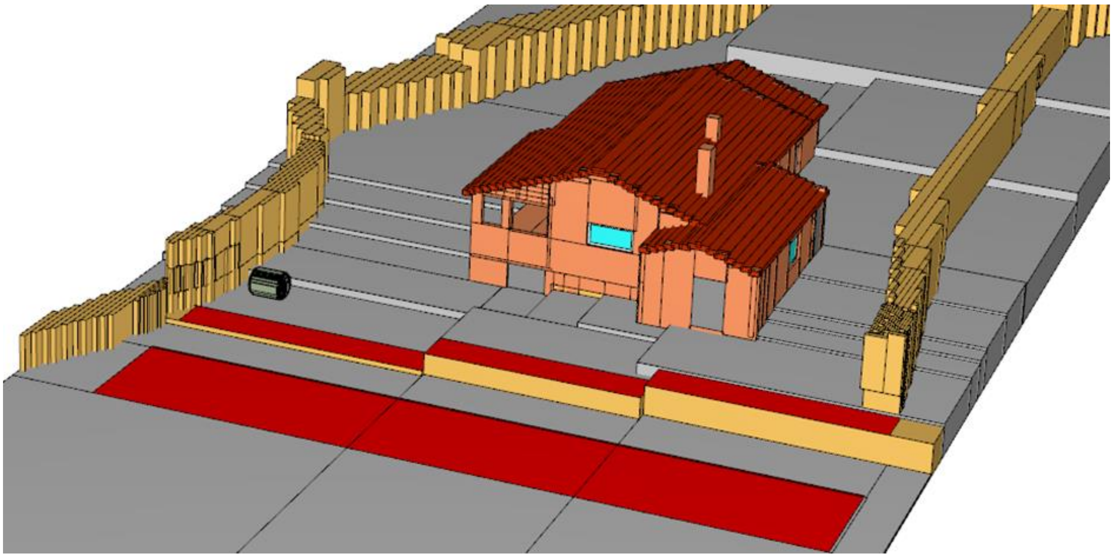

Figure 5.9: Scenario 4

5.3.5 Evaluation of the trial designs

FDS setup

All scenarios are simulated in FDS: scenarios 1, 2 and 4 are simulated with FDS 6.7.5 because the latest version of the software (FDS 6.7.9) gives numerical instability errors due to the very low gas density reached in certain parts of the meshes where the flames are located (this is an issue experienced also by other FDS users), while scenario 3 is simulated with FDS 6.7.9.

In scenarios 1 and 4, the smallest mesh size is 0.05 m, where the LPG tank is located. The fire and the areas of interest of the building (e.g., glazing systems) the mesh size is 0.1 m (according to the mesh sensitivity analysis performed in Appendix A), while areas of the domain that are not of interest have mesh sizes of 0.2 m and 0.4 m. The same applies for simulations of scenarios 2 and 3, where the smallest mesh size is 0.1 m. The size of the domain is 83.2 x 29.6 x 20 m^3 for scenarios 1 and 4, 64 x 29.2 x 20 m^3 for scenario 2 and 20.8 x 17.2 x 10 m^3 for scenario 3.

Windows are simulated with a pane thickness of 3 mm and a PVC frame (material properties are those described in Chapter 3), and devices to analyse their failure are placed following the methodology presented in Chapter 3. Locations and names of the windows are shown in Figure 5.10. Concrete walls are simulated with a thickness of 15 cm and with material properties given in Chapter 3. Devices to measure the adiabatic surface temperature of the wall are placed on the two sides of the porch window at a height of 0.3 m, 1 m and 2 m from the porch floor for scenario 3.

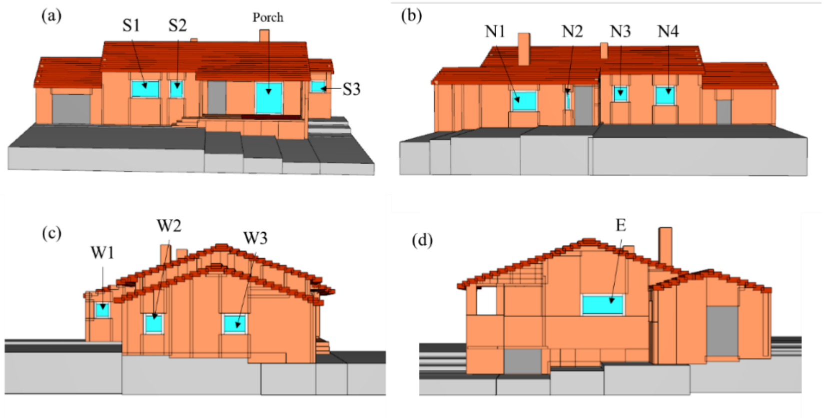

Figure 5.10: Southern (a), northern (b), western (c) and eastern (d) façades of the house, along with the name of each of the windows.

Results scenario 1 – Low frequency, high consequences

In scenario 1 the flames and smoke engulf the east façade and part of the south façade through the porch, as can be seen in Figure 5.11. Flames cover a horizontal distance of about 10 m.

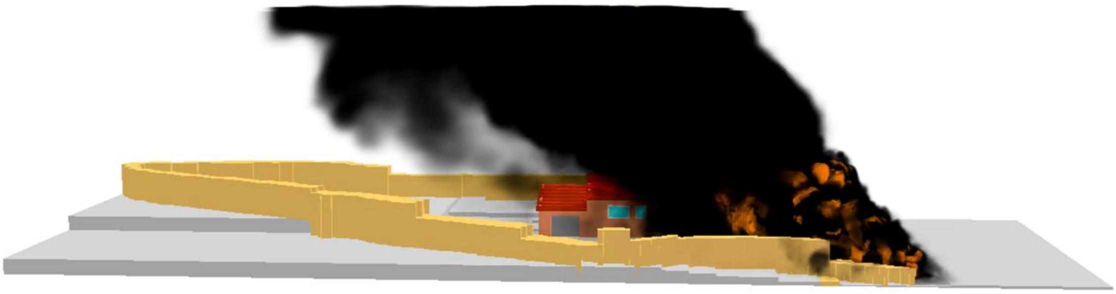

Figure 5.11: Scenario 1 at 8 s of simulation.

The four windows located the closest to the fire source break very soon after the start of the fire, as given in Table 5.3. The other windows remain intact, as they do not surpass any of the set performance criteria.

Table 5.3: Times of window failure for each performance criterion in scenario 1.

Performance criteria	Time of reaching the performance criteria [s]			
	Porch	S3	N1	E
ΔT_{cr}	8	5	7	4
T_{surf}	33	6	7	4
HL	-	11	42	10
T_{surf} frame	8	5	7	4

Given the fact that the windows will break, allowing smoke and fire to enter the building, this scenario cannot be deemed safe when it comes to the goal of property protection.

Results scenario 2 – High frequency, low consequences

The simulated fire spread over time through the property is shown in Figure 5.12. Smoke and flames coming from the hedgerow are pushed towards the house by the wind, but do not create any damage to the structure. The glazing systems that fail in this scenario are those located close to the simulated trees, on the southern façade, as given in Table 5.4.

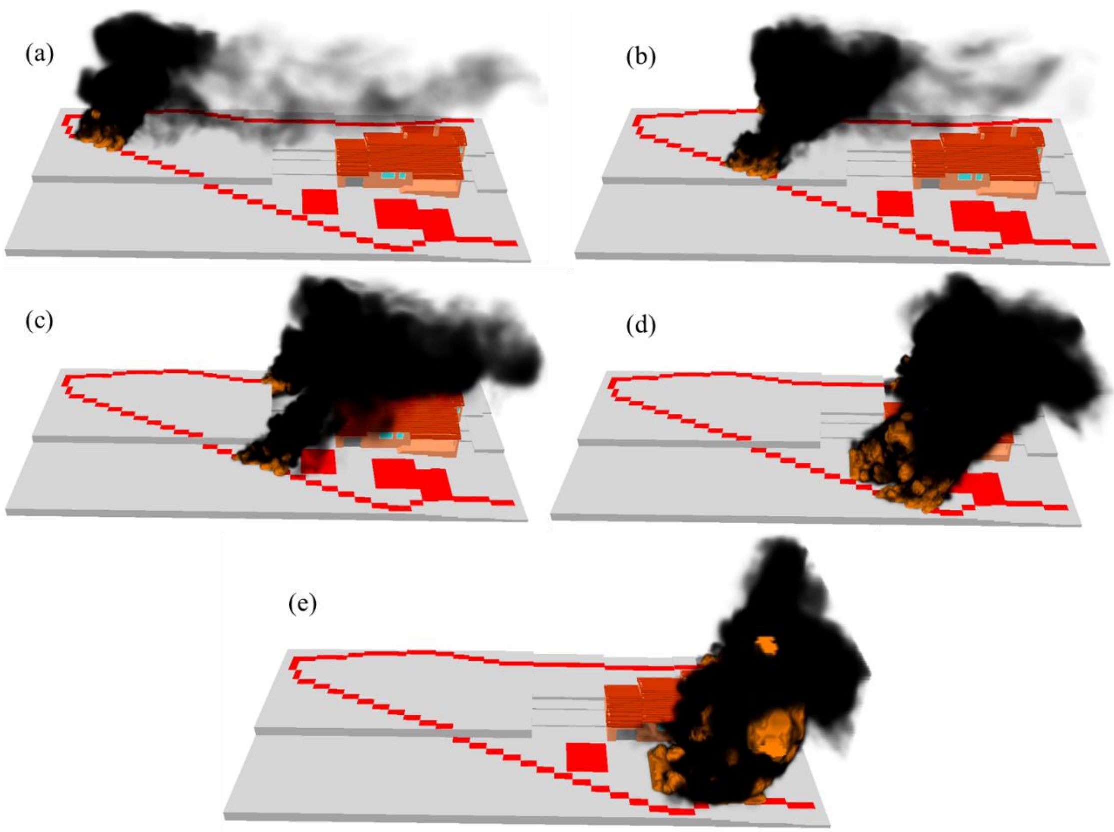

Figure 5.12: Scenario 1 at (a) 40 s of simulation, (b) 80 s, (c) 120 s, (d) 160 s, (e) 200 s.

Table 5.4: Times of window failure for each performance criterion in scenario 2.

Performance criteria	Time of reaching the performance criteria [s]				
	S1	**S2**	**Porch**	**N1**	**N2**
ΔT_{cr}	151	159	193	184	177
T_{surf}	154	163	202	187	185
HL	166	174	215	-	-
T_{surf} frame	151	162	202	185	180

As for the first scenario, this one cannot be deemed safe for property protection, due to the failure of the glazing systems.

Results scenario 3 – Special problem 1

The simulated combustion of the fuel pack containing a set of table and chairs is shown in Figure 5.13. In this scenario, the smoke can escape the semi-confined space through the openings located on the southern and eastern sides of the porch, therefore temperatures inside the porch remain well below 500°C, as shown in Figure 5.14.

Figure 5.13: Scenario 3 at 300 s of simulation.

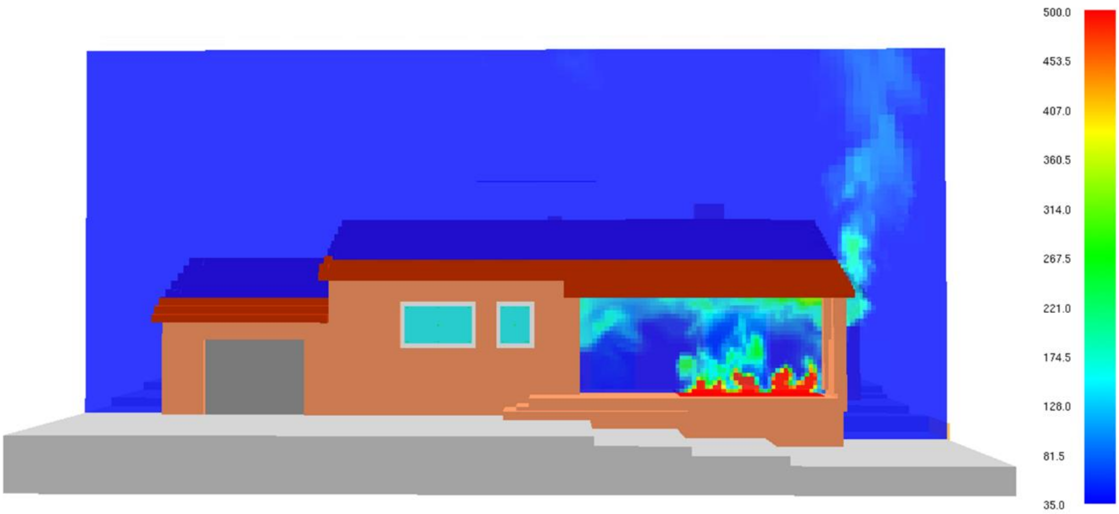

Figure 5.14: Temperature slice of scenario 3 at 310 s (when the peak HRR is reached).

Windows located in the porch and close to it are analysed to see if window breakage would occur in this scenario. The window located on the porch, at a distance of 0.5 m from the fuel pack, will fail 129 s after ignition, as given in Table 5.5, due to the temperature difference between the exposed side of the pane and the one located behind the frame.

Table 5.5: Times of window failure of the Porch window for each performance criterion in scenario 3.

Performance criteria	**Time of reaching the performance criteria [s]**
ΔT_{cr}	129
T_{surf}	141
HL	156
T_{surf} frame	153

For the analysis of the envelope of the porch (i.e., the shared wall between porch and building), adiabatic surface temperatures are recorded by devices. As shown in Figure

5.15, the highest temperatures are located at the bottom of the wall on the right side of the window.

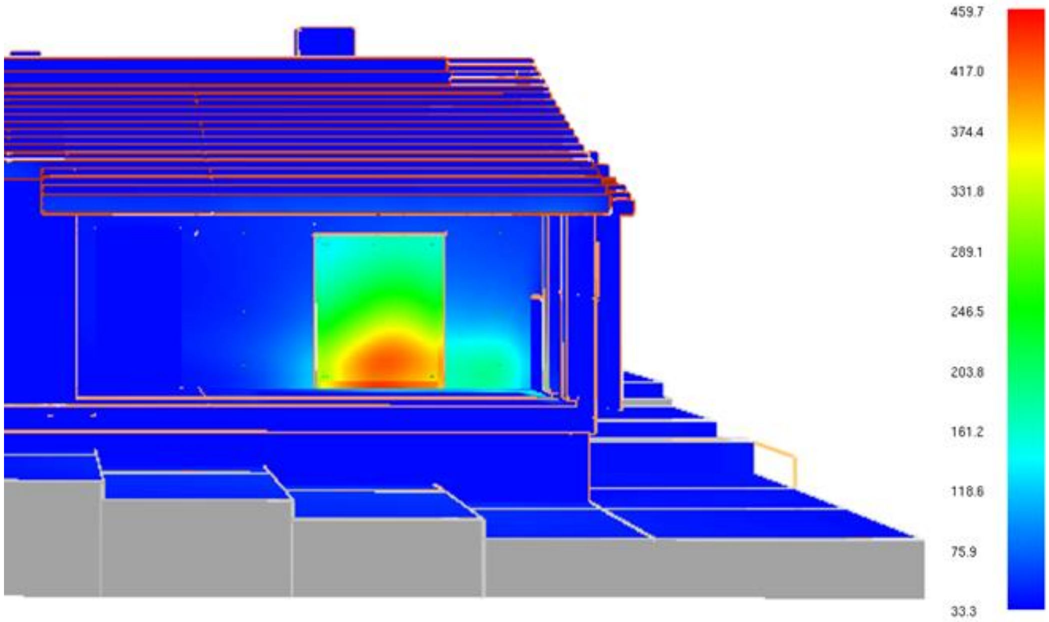

Figure 5.15: Wall temperature in scenario 3 at 310 s.

Results of the calculation of the load bearing capacity of the cross-section of the wall located on the right side of the window at a height of 0.3 m are given in Figure 5.16. As can be noticed in Figure 5.16b, the load bearing capacity never drops below 74%, therefore the wall will not fail.

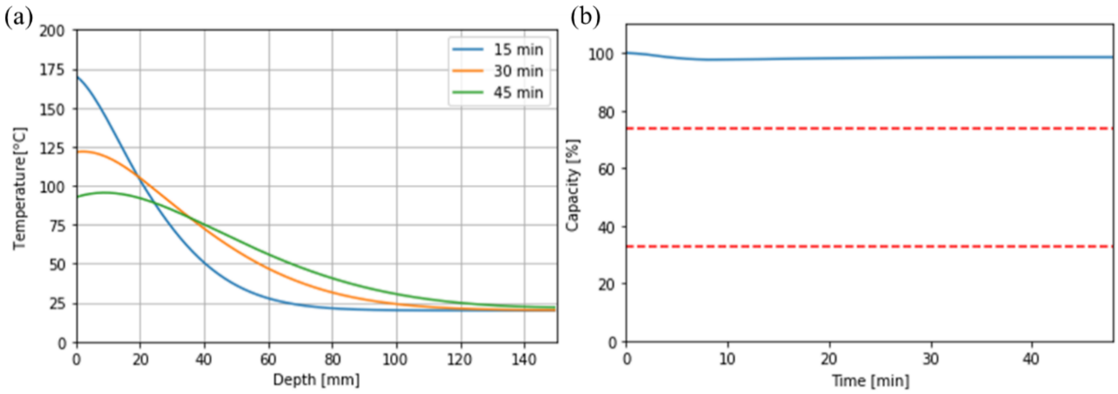

Figure 5.16: Results for the cross-section of the device located at 0.3 m for Scenario 3: (a) temperature profile through the cross-section recorded every 15 minutes, (b) load bearing capacity of the analysed cross-section over time.

Scenario 3, as for the two previous ones, cannot be deemed safe for property protection due to the failure of the glazing systems.

Results scenario 4 – Special problem 2

The incident heat flux onto the tank is greater than 22 kW/m^2 already after 1 s of the simulation, as shown in Figure 5.17.

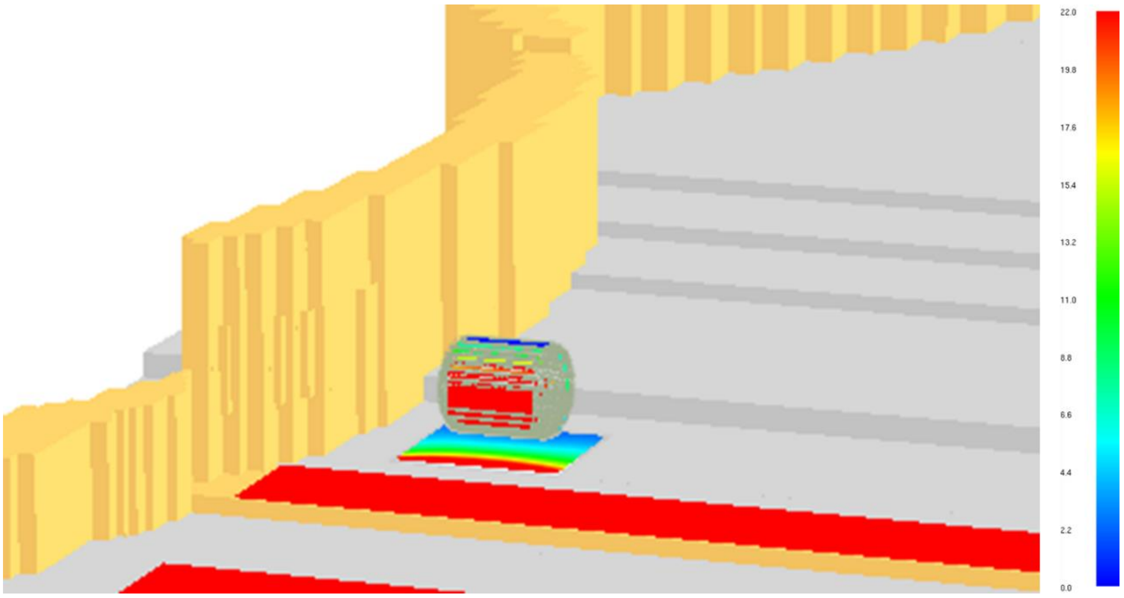

Figure 5.17: Incident heat flux onto the tank at 1 s.

Further investigation with ANSYS Fluent shows that the Pressure Release Valve Index (PRVI) is 0.9, while the temperature of the tank walls remains below the critical value of 400°C, resulting in a null Weakened Surface Index (WSI), as given in Figure 5.18.

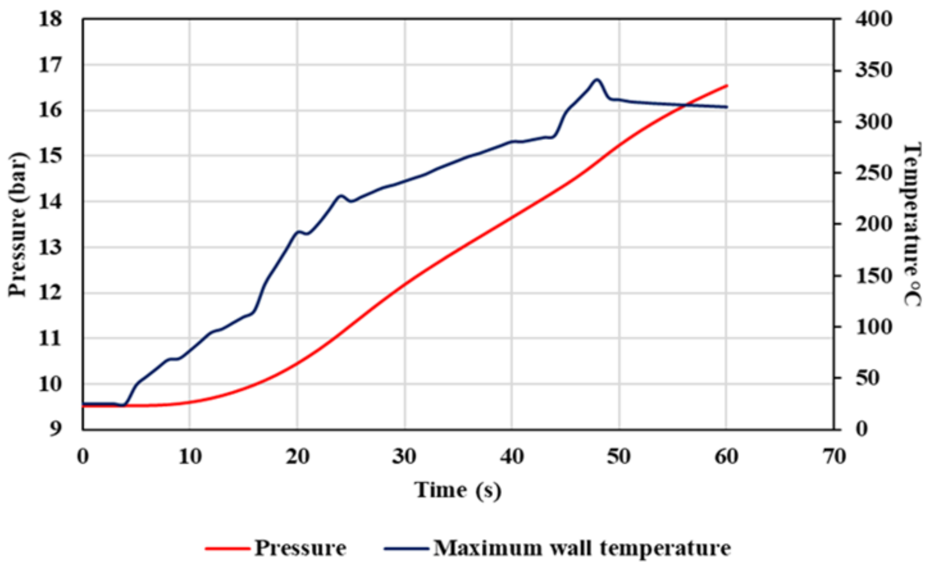

Figure 5.18: Pressure evolution inside the tank and tank wall temperature for scenario 4.

It can be concluded that this scenario does not have the potential to compromise the integrity of the LPG tank, however it may lead to the opening of the PRV, which is an unwanted situation.

Overall evaluation

None of the analysed scenarios meets the non-life safety performance criteria set for property protection, and in all scenarios where glazing systems are included (scenarios 1, 2 and 3), these building sub-systems are what cause the building to not meet the criteria. Therefore, in order to meet the goal of property protection, the issue of fuels located close to glazing systems, as well as the protection of these systems should be tackled. As for scenario 4, fuels should be placed further from the LPG tank in order to avoid the opening of the PRV and therefore to avoid further fire spread through the property.

5.3.6 Example of implementation of measures to meet performance criteria

The results of scenarios 1 and 2 showed that the issue of window breakage is caused by the combustion of the trees and the hedgerow located very close to the building. Protecting the glazing systems is therefore essential, therefore both scenarios are re-evaluated with the addition of aluminium shutters that protect the affected windows.

In scenario 1, shutters are placed in front of windows E, S3, N1 and the one on the porch, as these are the windows that fail and will break in this scenario. The simulation was stopped at 35 s, because, as can be seen in Figure 5.19, the surface temperature of the shutter will not reach the melting point of aluminium of 660°C. Therefore, by placing shutters on the four windows, the goal of property protection is achieved for this scenario.

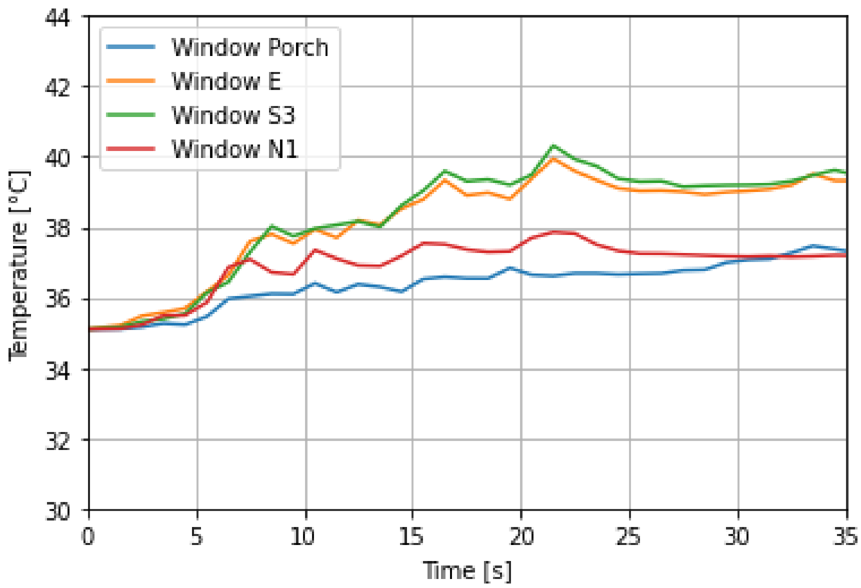

Figure 5.19: Peak temperatures for each shutter in scenario 1 obtained through *wall temperature* boundary files.

In scenario 2, shutters are placed in front of the windows that break, which are S1, S2, N1, N2 and the one on the porch. As can be seen in Figure 5.20, the temperature of the shutters does not reach the one for the melting point of aluminium, therefore the goal of property protection is achieved for this scenario as well by placing solid aluminium shutters in front of the windows.

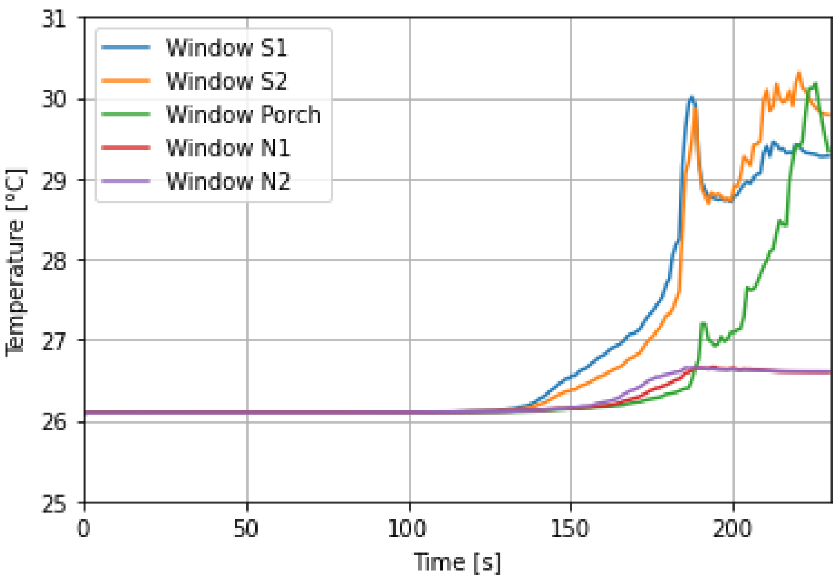

Figure 5.20: Peak temperatures for each shutter in scenario 2 obtained through *wall temperature* boundary files.

By placing a solid aluminium shutter in front of the window located on the porch, also scenario 3 will meet the goal of property protection. When it comes to scenario 4, it is clear that the vegetation located close to the LPG tank should be removed. Further analysis is needed to identify if any of the trees located on the neighbour's property should be removed as well, along with the hedgerow that separates the two properties, which could be substituted by a non-combustible fence.

5.4 Conclusions

A PBD guideline specific for WUI microscale scenarios is presented in this chapter. The guideline follows the standard PBD process, adapted for WUI situations. Recommendations on performance criteria for these types of scenarios are given for both life safety and non-life safety (e.g., property protection). Suggestions on the selection of design fire scenarios are given, which include a description of three types of scenarios: (i) those that might occur with a high frequency but will have low consequences, (ii) those that might occur with a low frequency, but will have high consequences, and (iii) special issues that might be present on a property which might escalate the impact of a wildfire (e.g., the presence of an LPG tank, fuels stored in semi-confined spaces, etc.). The selection of the different variables that must be taken into account (e.g., fire, environmental, property characteristics) is also addressed, along with the choice of fire design and how to evaluate them in a quantitative way.

The WUI PBD guideline is then applied to a case study of a property located at the Spanish WUI. The goal of the project is property protection, therefore the performance criteria for the property are those for non-life safety. The building and property are analysed in their current status, in order to analyse whether structural integrity would be maintained in case of a wildfire. Building and property characteristics are identified along with four design fire scenarios: one low frequency, high consequences scenario, one high frequency, low consequences scenario, and two special problem scenarios. The scenarios are evaluated in FDS, and results show that the objectives set for property protection are not met in all of the analysed scenarios. An example of measures that can be implemented to meet the set objectives is also presented, which include the placing of aluminium shutters in front of glazing systems and the removal of fuels close to the LPG tank.

5.5 References

Agencia Estatal de Metereología, n.d. Valores climatológicos normales. Madrid, Cuatro Vientos. https://www.aemet.es/es/serviciosclimaticos/datosclimatologicos/valoresclimatologicos?l=3196&k=28

Alexander, M.E., Cruz, M., 2019. Fireline Intensity, in: Encyclopedia of Wildfires and Wildland-Urban Interface (WUI) Fires. pp. 1–8. https://doi.org/https://doi.org/10.1007/978-3-319-51727-8_52-1

Alexander, M.E., Mutch, R.W., Davis, K.M., 2007. Wildland Fires: Dangers and Survival, in: Wilderness Medicine. pp. 286–335. https://doi.org/10.1016/b978-0-323-03228-5.50017-3

Australian Building Codes Board, 2014. Private Bushfire Shelters - Performance Standard. https://www.abcb.gov.au/sites/default/files/resources/2022/Performance-standard-private-bushfire-shelters.pdf

Caballero, D., Ribeiro, L.M., 2019. WUIVIEW Deliverable 5.2 - Procedure for WUI scenarios 3D modelling. https://wuiview.webs.upc.edu/download/WUIVIEW_D5.2_F.pdf

Casal, J., 2017. Evaluation of the effects and consequences of major accidents in industrial plants. Elsevier. https://doi.org/https://doi.org/10.1016/C2016-0-00740-4

Hurley, M.J., Gottuk, D.T., Hall, J.J.R., Harada, K., Kuligowski, E.D., Puchovsky, M., Torero, J.L., Watts, J.J.M., CJ, W., 2016. SFPE Handbook of Fire Protection Engineering, 5th ed. Springer. https://doi.org/10.1007/978-1-4939-2565-0

Hurley, M.J., Rosenbaum, E.R., 2016. Performance-Based Design, in: Hurley, M.J., Gottuk, D.T., Hall, J.J.R., Harada, K., Kuligowski, E., Puchovsky, M., Torero, J.L., Watts, J.J.M., Wieczorek, C.J. (Eds.), SFPE Handbook of Fire Protection Engineering. Springer, pp. 1233–1261.

Hurley, M.J., Rosenbaum, E.R., 2015. Performance-Based Fire Safety Design. CRC Press.

Ministry of Business Innovation and Employment, 2013. C/VM2 Verification Method: Framework for Fire Safety Design For New Zealand Building Code Clauses C1-C6 Protection from Fire.

NIST, 2022. Fire Dynamics Simulator.

Ribeiro, L.M., Almeida, M., Muñoz, J.A., 2020. Deliverable D2.1 - Report on real scale experiments. https://wuiview.webs.upc.edu/download/WUIVIEW_D2.1_F.pdf

Stewart, S.I., Radeloff, V.C., Hammer, R.B., Hawbaker, T.J., 2007. Defining the wildland-urban interface. J. For. 105, 201–207.

Thunderhead Engineering, 2022. Pyrosim.

Vacca, P., Caballero, D., Pastor, E., Planas, E., 2020a. WUI fire risk mitigation in Europe: A performance-based design approach at home-owner level. J. Saf. Sci. Resil. 1, 97–105. https://doi.org/10.1016/j.jnlssr.2020.08.001

Vacca, P., Àgueda, A., Muñoz, J.A., Planas, E., Pastor, E., Heymes, F., Ismael, E., Eyssette, R., Cozzani, V., Scarponi, G.E., 2020b. WUIVIEW Deliverable 6.1 - Recommendations on structure survivability and sheltering capacity. https://wuiview.webs.upc.edu/download/D6.1_F_Recommendations%20on%20structure%20survivability%20and%20sheltering%20capacity.pdf

Weather Spark, n.d. El clima y el tiempo promedio en todo el año en Cadalso de los Vidrios. https://es.weatherspark.com/y/35528/Clima-promedio-en-Cadalso-de-los-Vidrios-España-durante-todo-el-año

Chapter 6

Conclusions and future work

6.1 Achievement of goals and objectives

This thesis presented a performance-based methodology for the quantitative risk assessment of WUI fire scenarios, along with a methodology for the quantitative vulnerability assessment of buildings located at the Mediterranean WUI.

The objective of assessing structural survivability of Mediterranean-type structures is addressed in Chapter 3, where three different WUI building and property sub-systems are analysed through a PBD approach, based on performance criteria and fire characteristics identified in Chapter 2.

The objective of developing a methodology to quantitatively assess vulnerability in Mediterranean WUI microscale environments is undertaken in Chapter 4, where, based on the identification of the pathways that lead to structural ignition, as well as on the results obtained in Chapter 3, a Vulnerability Assessment Tool (VAT) is developed. This tool is designed in form of a checklist that citizens can fill out to identify the degree of building vulnerability to fire of their properties, and it points out the issues that need o be tackled with priority. The application of the VAT is presented for three case studies, two in Spain and one in Portugal.

The final objective, which is to develop a quantitative risk analysis guideline applicable to new and existing buildings at the WUI, is tackled in Chapter 5. A WUI Performance-Based Design guideline is presented, which gives indications on how to select design fire scenarios for WUI environments, along with the performance criteria that should be met in order to have a design that can be considered to be safe. An application of the WUI PBD guideline is presented for a Spanish case study.

By meeting the specific objectives, the main goal of analysing fire hazards and building vulnerabilities at the WUI microscale, together with developing a risk analysis framework for WUI fire scenarios has been achieved.

6.2 Summary of the developed work

As presented in Chapter 1, WUI fire loss problem primarily depends on the building and its immediate surroundings. The pathways that lead to the fire entering a building are identified in Chapter 2 and they include both structural vulnerabilities and the presence of fuels in their surroundings. Performance criteria are set for three vulnerable property sub-systems, which are glazing systems, above ground LPG tanks and semi-confined spaces in which fuel accumulation takes place. The analysis performed on the characteristics of potential fire exposure for these scenarios highlights the lack of quantitative knowledge on the combustion of fuels that are typically located at the WUI, especially when it comes to ornamental vegetation and artificial fuel packs. Therefore, the burning behaviour of four different fuel packs that could be present at the WUI has been analysed in real-scale tests and the obtained data can be used as input for PBD methodologies for the quantification of hazards and vulnerabilities of WUI microscale scenarios.

A methodology for the analysis of typical WUI property sub-systems is presented in Chapter 3, which is applied to the three vulnerable property sub-systems of the Mediterranean WUI identified in Chapter 2. The methodology is based on a PBD approach, where results from the modelling of the scenarios in FDS are compared to previously set performance criteria, and it can be used as a baseline for other types of WUI landscapes and scenarios that might include different configurations, fuels, building and property sub-systems. Through this methodology, safe distances are identified for the selected scenarios, which include the combustion of natural and artificial fuels located in front of glazing systems as well as for fuels located close to above ground LPG tanks, and safe wall thicknesses are identified for concrete walls of semi-confined spaces in which artificial fuel packs are stored.

A Vulnerability Assessment Tool (VAT) is presented in Chapter 4, which is developed for the quantitative assessment of vulnerabilities of buildings located at the Mediterranean WUI and is based on a fault tree analysis of the top event of fire entrance inside a building (part of which is based on the results obtained for the scenarios analysed in Chapter 3). Due to the lack of data on structure ignition of past WUI fires in the Mediterranean region, probability values for each of the events that might lead to the top event are obtained through the use of fuzzy logic, which is based on the judgement of WUI experts. The tool is then applied to three Mediterranean case studies, highlighting the most critical issues for each analysed property. The end users of the VAT are intended to be not only fire safety practitioners, but also the homeowners and residents of the WUI. The use of this VAT is expected to lead to the improvement of fire safety practices at the microscale by increasing WUI fire risk awareness.

Finally, a PBD guideline specific for WUI scenarios is presented in Chapter 5, along with its application to a case study of a property located at the Spanish WUI. The WUI PBD guideline follows the classic PBD process and it provides an assessment methodology for properties in their current state, as well as for the effectiveness of strategies that are implemented to reduce the risk for the property. Performance criteria for both life safety and non-life safety are presented, the latter based on those identified in Chapter 2, along with suggestions on how to select the design fire scenarios to be modelled in FDS. Fire characteristics used as inputs for the modelling are those presented in Chapter 2, while the scenario set-up (mesh size, geometry, material characteristics, output devices) is the one described in Chapter 3. Four scenarios are analysed for the case study as example on how to apply the WUI PBD guideline with the goal of property protection. Additionally, an example of measures that can be implemented to meet the goal is presented as well. The WUI PBD guideline is intended to be used by fire protection practitioners to perform a risk analysis of complex scenarios, where meeting the goals of life safety, property protection, mission continuity or environmental protection is critical.

6.3 Recommendations for future work

Based on the obtained results and on the gaps in the knowledge of WUI fire scenarios identified throughout this thesis, a series of recommendations for future work is presented:

- The literature review on breakage of glazing systems typical of WUI homes (e.g., framed windows with float glass) performed in Chapter 2 highlights that there is a lack of knowledge on the criteria that cause failure of these systems. Experimental tests that include realistic WUI fire exposure scenarios should be performed in order to bridge this knowledge gap and therefore to identify performance criteria for glazing systems.
- The literature review in Chapter 2 highlights the lack of information of the burning characteristics of the different types of fuels located at the WUI microscale, especially when it comes to ornamental vegetation and artificial fuel packs. More knowledge is needed for the characterisation of fire scenarios that include both natural and artificial fuels, which can be obtained by performing experimental studies on those types of fuels.
- The modelling of scenarios that include vegetation, performed in Chapter 3, highlights the fact that, especially when wind is included in the scenario, results may vary even between scenarios where minimal changes unrelated with the combustion of the particles are made. Further validation of the simulation of vegetation in FDS is therefore needed, especially in scenarios that include wind.
- The Vulnerability Assessment Tool should be applied to more case studies, in order to obtain a broader and better understanding of the presented tool, and highlight the areas or issues that might not yet have been considered. The case studies required to validate the tool have to be carefully detailed because pre-fire relevant data from homeowners need to be collected. For this reason, a damage assessment form is presented in Appendix B, which should be used when investigating WUI fire accidents. A database that collects this information should be created. In addition, more WUI experts could be polled in order to update or confirm the values used in the fuzzy logic model, on which the inputs of the VAT are currently based on. Additionally, this information could help with setting some of the rules that are at the baseline of the tool (e.g., distances between fuels or between fuels and vulnerable elements of the property).
- The Vulnerability Assessment Tool should be refined (e.g., adding pictures and some explanations for people that are not knowledgeable on the subject) and made available for the public, ideally by creating a digital version of the tool.
- In Chapter 5, the application of the PBD guideline is performed only for property protection criteria. Future work consists in applying the same methodology for life safety criteria as well. Additionally, if other types of scenarios (e.g., different types of building materials) are to be analysed, additional performance criteria must be identified.

Appendix A

Results from the FDS analysis of microscale scenarios

A.1 Mesh sensitivity analysis for FDS scenarios involving glazing systems

FDS results for different mesh sizes are analysed in order to identify which is the best mesh size for the analysis of double pane windows exposed to fire. Given that the analysis is performed for a double pane window, the two panes are represented in the simulation, and the gap between the two is represented within the mesh by one empty line of mesh cells. The following mesh sizes are analysed: 0.015 m, 0.03 m, 0.06 m, and 0.1 m. The first and smallest mesh size is chosen so that the gap between the two panes is represented aproximately as the one that can be found in double pane windows. Given this very small size, only the glass panes are simulated within this mesh. The mesh is then doubled and quadrupled further away from the simulated window, in order to reduce the computational time for areas that don't need such a small mesh size. Therefore, the fire is simulated in a 0.06 m size mesh. In order to identify whether the size of the gap between the two panes will affect results, the window is simulated also in 0.03 m and 0.06 m mesh sizes (so that the mesh size for the fire and the window can be the same). Additionally, the mesh size obtained with Equation 3.1 (0.1 m) is also analysed.

The analysed window size is 0.51x0.51 m^2 for the first two mesh sizes, 0.54 x0.54 m^2 for mesh size 0.06 m, and 0.5x0.5 m^2 for the biggest mesh size (0.1 m). The thickness of each pane depends on the size of the cells, although the thickness of the surface assigned to the glass pane is the same for all simulations and has a value of 6 mm. This is the value that FDS uses for the calculations of variables that depend on the thickness of the obstacle. The coordinates of each glass pane for each of the analysed mesh sizes is given in Table A.1.

Table A.1: Glass pane coordinates for each mesh size

		0.015 m	**0.03 m**	**0.06 m**	**0.1 m**
Pane 1	x	0.39,0.9	0.39,0.9	0.36,0.9	0.4,0.9
	y	-0.075,-0.06	-0.09,-0.06	-0.09,-0.03	-0.1,0.0
	z	1.2,1.71	1.2,1.71	1.2,1.74	1.2,1.7
Pane 2	x	0.3,0.99	0.3,0.99	0.24,1.02	0.3,1.0
	y	-0.045,-0.03	-0.03,0.0	0.03,0.09	0.1,0.2
	z	1.11,1.8	1.11,1.8	1.08,1.86	1.1,1.8

Devices to measure the heat flux received by each pane, as well as the surface temperature of each pane are placed in the same location for each of the analysed mesh sizes, which is the centre and the corners of each pane. An example of the placing of the devices is given in Table A.2, where it can be noted that only the y coordinate changes due to the mesh size.

Table A.2: Examples of location of selected devices for each mesh size. M: middle, L: low and left, U: up, R: right. Devices that start with F measure the radiative heat flux, while devices that start with g measure the temperature of the glass pane.

Device	0.015 m	0.03 m	0.06 m	0.1 m
F_M	0.65,-0.076,1.44	0.65,-0.091,1.44	0.65,-0.091,1.44	0.65,-0.11,1.44
F_L_L	0.45,-0.076,1.25	0.45,-0.091,1.25	0.45,-0.091,1.25	0.45,-0.11,1.25
F_L_U	0.45,-0.076,1.65	0.45,-0.091,1.65	0.45,-0.091,1.65	0.45,-0.11,1.65
F_R_L	0.85,-0.076,1.25	0.85,-0.091,1.25	0.85,-0.091,1.25	0.85,-0.11,1.25
F_R_U	0.85,-0.076,1.65	0.85,-0.091,1.65	0.85,-0.091,1.63	0.85,-0.11,1.65
g_M	0.65,-0.075,1.45	0.65,-0.09,1.45	0.65,-0.09,1.45	0.65,-0.1,1.45
g_L_L	0.45,-0.075,1.24	0.45,-0.09,1.24	0.45,-0.09,1.24	0.45,-0.1,1.24
g_L_U	0.45,-0.075,1.66	0.45,-0.09,1.66	0.45,-0.09,1.66	0.45,-0.1,1.66
g_R_L	0.85,-0.075,1.24	0.85,-0.09,1.24	0.85,-0.09,1.24	0.85,-0.1,1.24
g_R_U	0.85,-0.075,1.66	0.85,-0.09,1.66	0.85,-0.09,1.66	0.85,-0.1,1.66

The analysed fire scenario represents the combustion of a stack of wood pallets of 0.9 m height (Figure 2.6) located in front of the window at a distance of 2 m. The size of the domain is the same for all simulations, and the mesh was divided in order to assign meshes totalling approximately 100.000 cells for each MPI. All four simulations were run on the same PC in order to compare the real simulation time. These parameters are given in Table A.3. The simulations of the two smallest mesh sizes have the same amount of meshes and MPIs, as the only difference is the mesh size of the window, while the rest of the domain is the same. The real simulation time varies greatly between mesh sizes, ranging from 57 hours for the smallest mesh size to 14 hours for the biggest one (time is cut by approximately ¾).

Table A.3: Number of meshes, MPIS and real simulation time for each of the analysed mesh sizes

Variables	0.015 m	0.03 m	0.06 m	0.1 m
Number of meshes	17	17	12	4
Number of MPIs	9	9	8	2
Real simulation time	57 h	48 h	43 h	14 h

Comparisons are made between the same devices for the four different analysed meshes. When it comes to the heat flux registered by the devices located on the first glass pane (Figure A.1), it can be noticed how the peak values detected by the devices of mesh size 0.1 m are higher compared to the other mesh sizes. Given the fluctuations of the recording of the heat flux values, only average values are compared. The average difference between the mesh of 0.1 m and the ones of 0.015 m and 0.03 m are of approximately 1.2 kW/m^2, while the one with the 0.06 m mesh is approximately 1.1 kW/m^2. The device that recorded the heat flux values that lead to reaching the heat load criterion for failure (a total of 1087 kJ/m^2 over time) is F1_R_U (Figure A.1g) for mesh sizes 0.015 m, 0.03 m and 0.06 m and F1_R_L (Figure A.1f) for mesh size 0.1 m (breakage would have happened 2 s later if taking into account the heat flux recorded by F1_R_U, therefore the difference is minimal). The time at which the heat load criterion for failure is reached for each mesh size is given in Table A.4, which is between 245 s (mesh size 0.1 m) and 252 s (mesh size 0.03 m), which highlights that there is not a big difference between mesh sizes when it comes to this criterion.

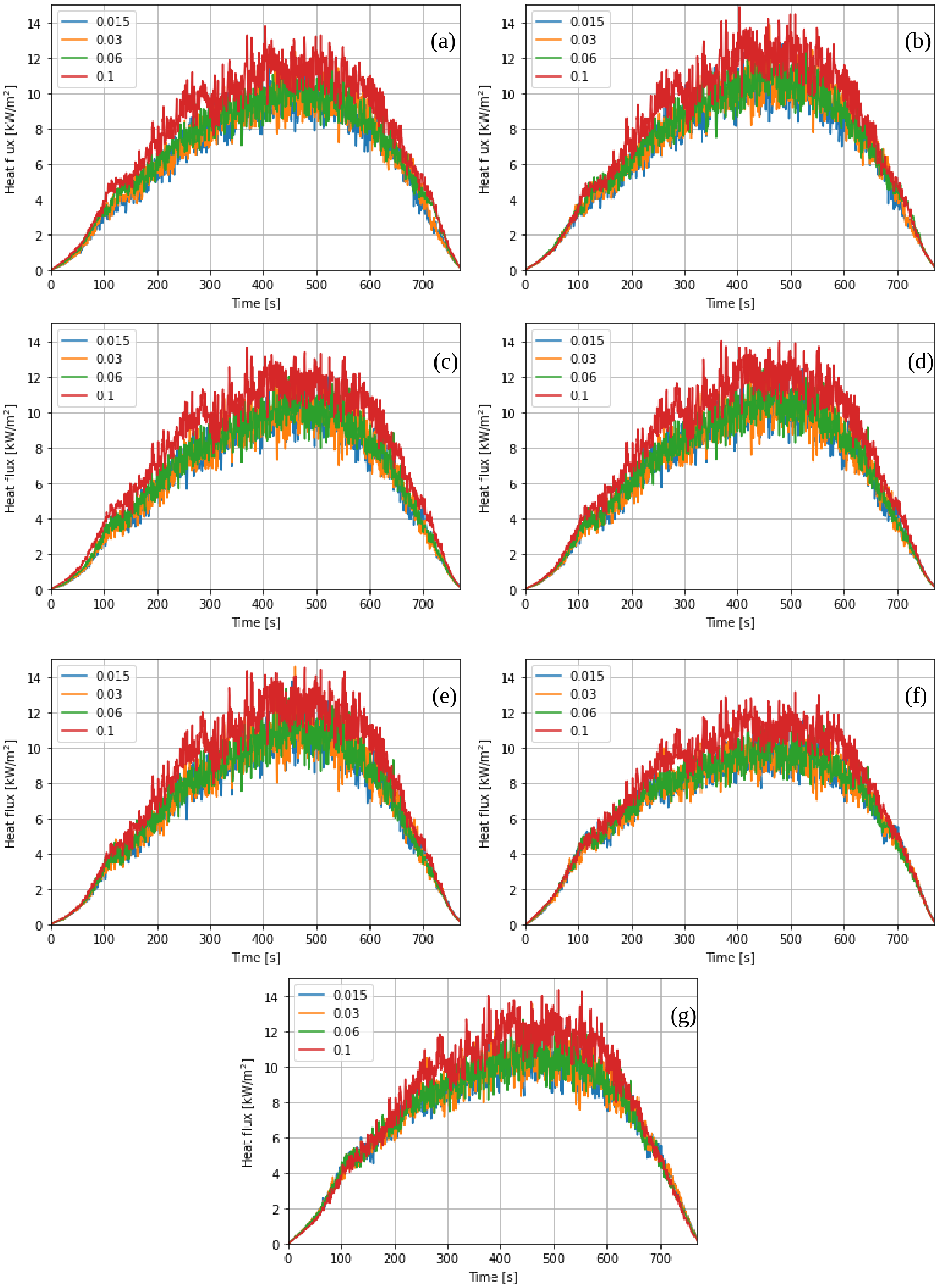

Figure A.1: Comparison between heat flux devices located on the first glass pane for each analyzed mesh size. Device: (a) F1_L_L, (b) F1_L_U, (c) F1_M_L, (d) F1_M, (e) F1_M_U, (f) F1_R_L, (g) F1_R_U.

Table A.4: Time at which each performance criterion is met for each mesh size.

Performance criteria	0.015 m	0.03 m	0.06 m	0.1 m
Pane 1 – Time of failure [s]				
ΔT_{cr}	262	262	261	252
T_{surf}	312	318	312	295
Heat load	250	252	249	245
T_{surf} frame	364	366	370	335
Pane 2 – Time of failure [s]				
ΔT_{cr}	386	397	427	416
T_{surf}	428	434	446	432
Heat load	378	384	389	377

As for the temperature of the surface of the first glass pane, devices are located in the middle of the pane and in the four corners. As shown in Figure A.2, the devices for the 0.1 m mesh size record higher temperatures compared to the other mesh sizes, which record very similar temperatures. The biggest temperature difference is recorded by device g1_L_L, with a value of 27.7°C between the mesh of 0.015 m and the one of 0.1 m. The time at which the surface temperature criterion for failure (T_{surf} = 132°C) is reached varies from 295 s for mesh size 0.1 m to 318 s for mesh size 0.03 m (with a difference of 23 s). Mesh sizes 0.015 m and 0.06 m reach this criterion at the same time (312 s), as shown in Table A.4.

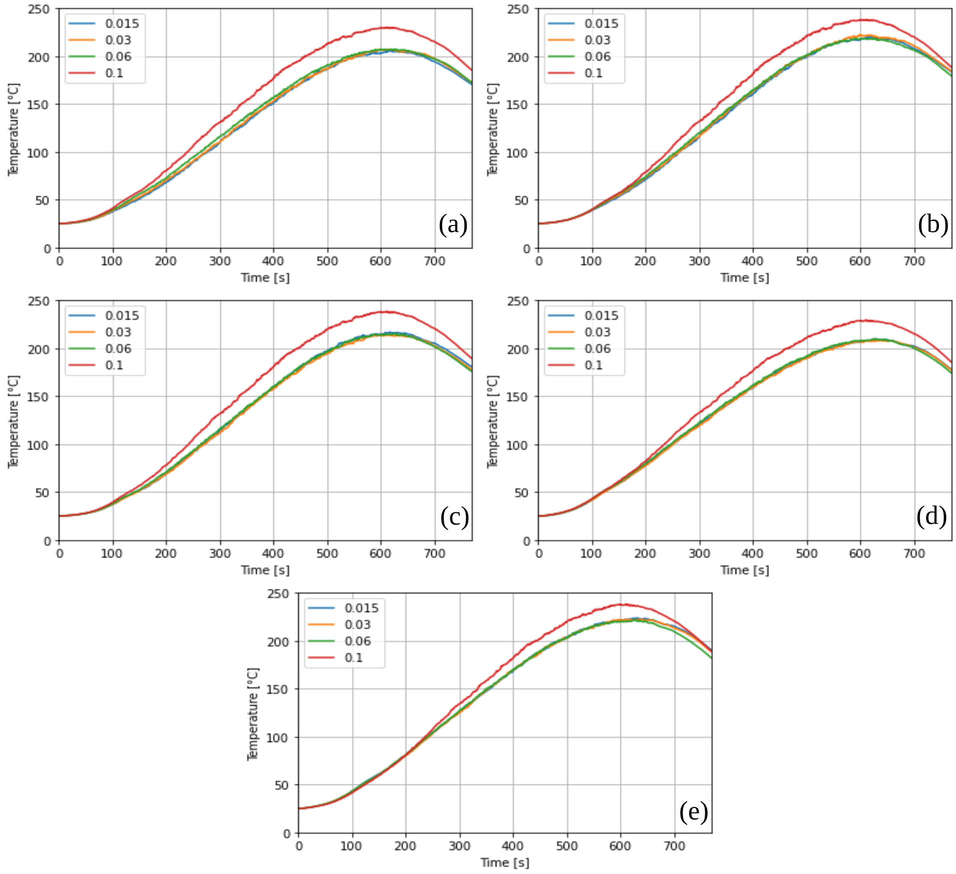

Figure A.2: Comparison between surface temperature devices located on the first glass pane for each analysed mesh size. Device: (a) g1_L_L, (b) g1_R_L, (c) g1_M, (d) g1_L_U, (e) g1_R_U.

The temperature difference between the part of the pane below the frame and the exposed part is obtained by subtracting the values obtained by the temperature of the pane located below the frame (measured with PROF devices) to the values obtained by the temperature devices located at the corners of the pane. PROF devices record the properties of the solid in depth at discrete intervals of time. Figure A.3 shows the temperature profile through the frame (15 mm) and the glass (6 mm) at the time of 350 s. Here it can be noted how the mesh size barely influences the results. The time at which the temperature difference criterion for failure (ΔT_{cr} = 83°C) is reached varies from 252 s for mesh size 0.1 m to 262 s for mesh sizes 0.03 m and 0.015 m (Table A.4). When it comes to the surface temperature of the frame, as for the one of the pane, mesh size 0.1 m presents slightly higher values.

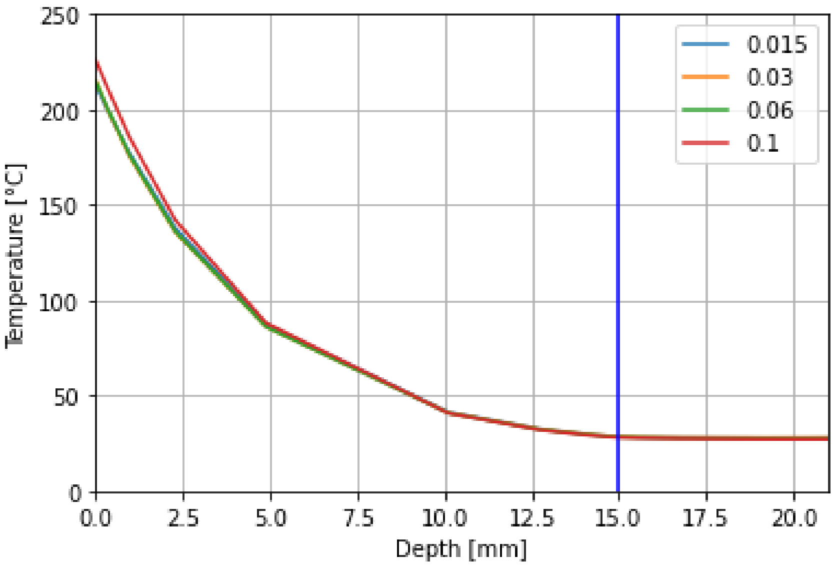

Figure A.3: Temperature profile through the frame and the glass below the frame for each mesh size at 350 s. The blue line indicates the interface between the frame and the glass pane.

In all mesh size simulations, breakage of the first glass pane is assumed to happen after 250 s in order to compare the heat flux and temperature values recorded for the second pane. Heat flux values recorded by devices located on the second pane are given for each mesh size in Figure A.4. Devices for mesh 0.1 m located on the upper side of the window record lower values compared to those for the other mesh sizes, while in the other cases values are quite similar. The average difference between the mesh of 0.1 m and the one of 0.015 m, 0.03 m and 0.06 m is respectively of 0.8 kW/m^2, 0.7 kW/m^2 and 0.6 kW/m^2. These differences are lower in comparison with those for the first glass pane. The device that recorded the heat flux values that lead to reaching the heat load criterion for failure is F2_R_U (Figure A.4g) for mesh sizes of 0.015 m, 0.03 m and 0.06 m, and F2_M (Figure A.4d) for mesh size 0.1 m. The time at which the heat load criterion for failure is reached for each mesh size is given in Table A.4, which is between 377 s (mesh size 0.1 m) and 389 s (mesh size 0.06 m). The times for mesh sizes 0.015 m and 0.1 m differ only by 1 s.

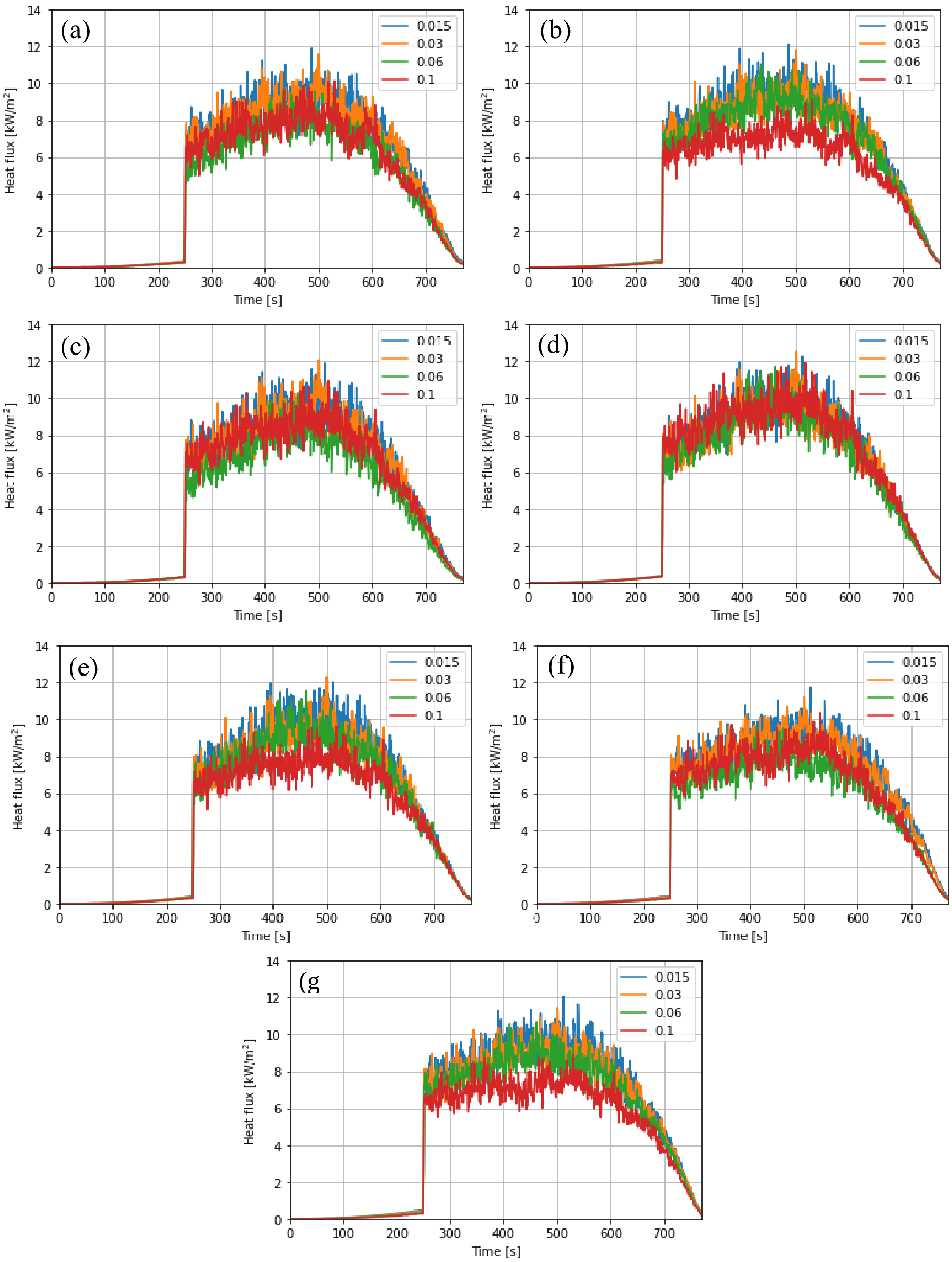

Figure A.4: Comparison between heat flux devices located on the first glass pane for each analyzed mesh size. Device: (a) F2_L_L, (b) F2_L_U, (c) F2_M_L, (d) F2_M, (e) F2_M_U, (f) F2_R_L, (g) F2_R_U.

To record the temperature of the second glass pane, devices are located on its surface exactly below those placed on the first pane. As shown in Figure A.5, the devices for the 0.1 m mesh size located on the upper side record lower temperatures compared to the other mesh sizes. The other devices record temperatures with values between mesh size 0.03 m and mesh size 0.06 m. The time at which the surface temperature criterion for failure is reached varies from 428 s for mesh size 0.015 m to 446 s for mesh size 0.06 m. For all mesh sizes, this criterion is reached first in the middle of the pane, where temperatures are very similar for all the analysed mesh sizes (Figure A.5c).

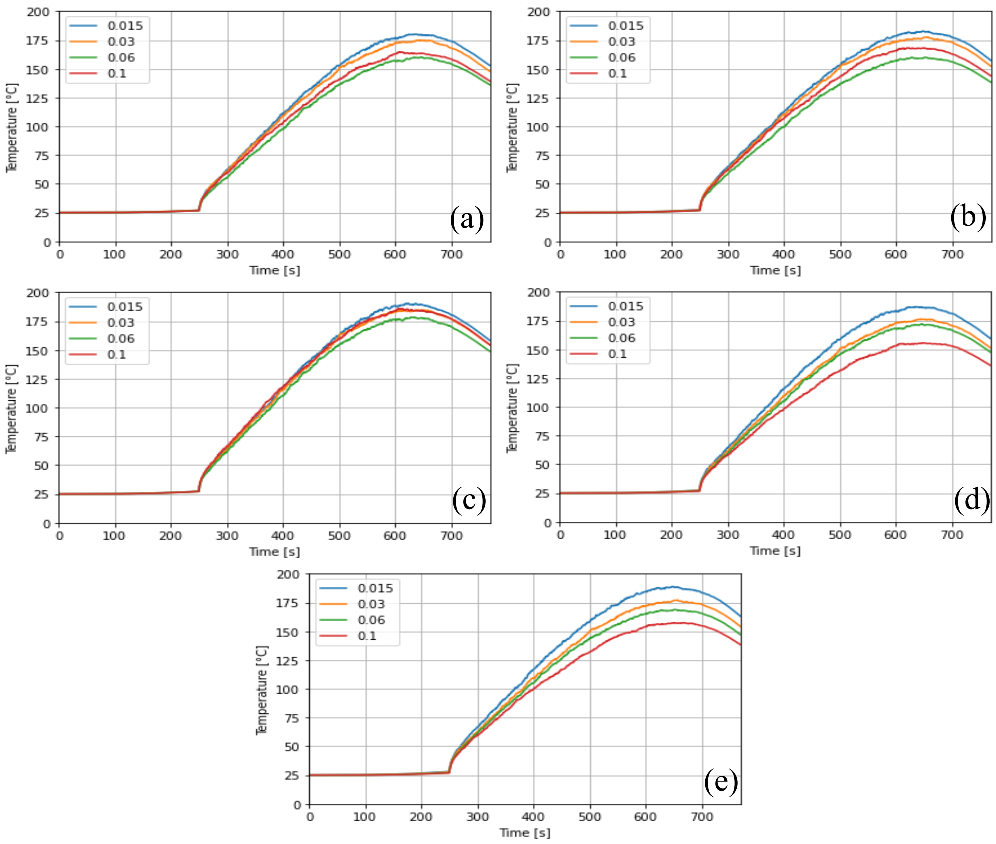

Figure A.5: Comparison between surface temperature devices located on the second glass pane for each analysed mesh size. Device: (a) g2_L_L, (b) g2_R_L, (c) g2_M, (d) g2_L_U, (e) g2_R_U.

The temperature difference between the exposed and unexposed side of the glass pane is measured by placing devices that measure the surface temperature on the pane located below the frame (the coordinates are the same as those for PROF devices located on the frame). In this case, due to the size of the pane with mesh size 0.06, the device is located much closer to the exposed side. Therefore, comparisons for these devices (Figure A.6) don't include this mesh size. In this case, temperatures for mesh size 0.1 m are higher compared to the other mesh sizes. The biggest temperature difference, recorded by device g2_R_L_F (Figure A.6b), between mesh 0.1 m and mesh 0.015 m is 7.6°C. The temperature difference criterion ΔT_{cr} is met at 386 s for mesh size 0.015, 397 s for mesh size 0.03 m and at 416 s for mesh size 0.1 m (Table A.4).

For the first glass pane, results show that using a mesh size of 0.1 m is conservative, as all the performance criteria are reach quicker than for the other mesh sizes. For the second pane there is a difference of 1 s and of 4 s when it comes to respectively the heat load and the surface temperature T_{surf} criteria between the mesh size 0.015 m and 0.1 m. When it comes to the criterion ΔT_{cr}, mesh size 0.1 m will have lower values for the same time step, due to a slightly higher surface temperature of the part of the pane hidden below the frame. Additionally, needed computational resources and simulation time are respectively cut by almost 78% and 75% respectively when using a mesh size of 0.1 m instead of one of 0.015 m. Therefore, a mesh size of 0.1 m is be used to simulate the glazing systems scenarios in FDS.

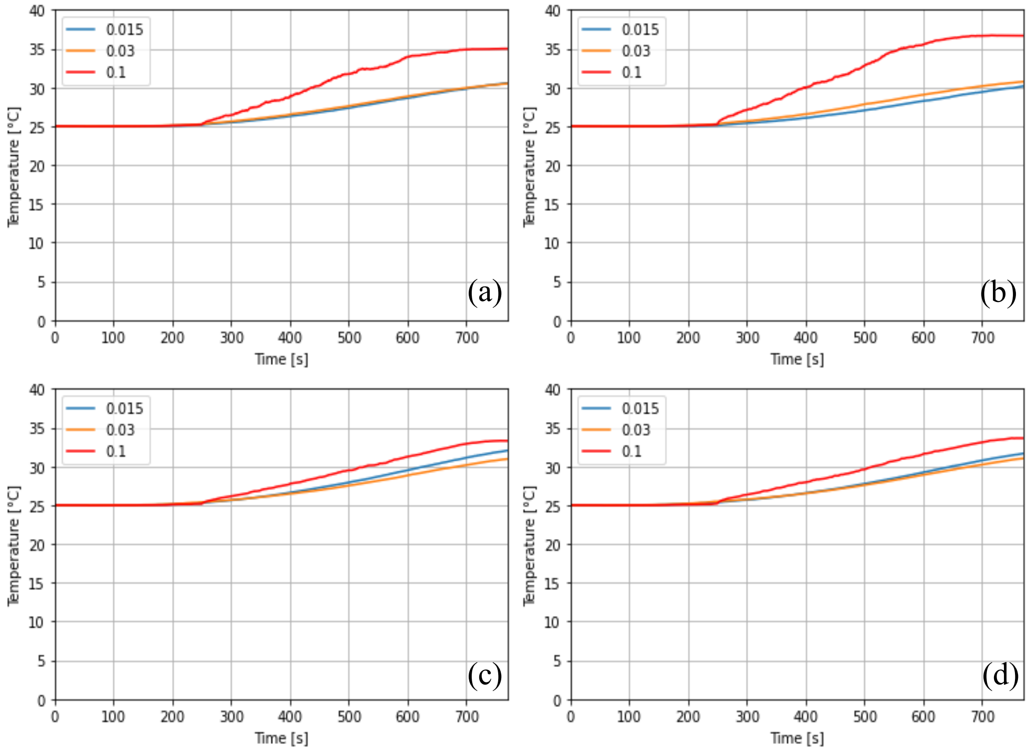

Figure A.6: Comparison between surface temperature devices located on the second glass pane, below the frame (F), for each analysed mesh size. Device: (a) g2_L_L_F, (b) g2_R_L_F, (c) g2_L_U_F, (d) g2_R_U_F.

A.2 Results glazing systems scenarios

Results for all analysed scenarios involving glazing systems are shown in the following tables, in which the time of reaching each of the performance criteria is given. These criteria are: a temperature difference between the exposed part of the glass pane and the unexposed part lying below the frame (ΔT_{cr}) of 83°C, a surface temperature of the glass pane (T_{surf}) of 132°C, and a received heat load (HL) of 1087 kJ/m^2. Additionally, the melting point of PVC or aluminium is chosen as a criterion for the frame, which is reached respectively at 220°C and 660°C (see Chapter 2). If the frame fails before the glass pane, then the entire glazing system is assumed to fail, whether it is a single or double pane system. Therefore, breakage of the second pane is not analysed for these cases.

Table A.5: Results for the wood pallet scenario with the small window (0.5 x 0.5 m^2) in calm atmospheric conditions.

Atmospheric conditions	**Distance [m]**	**Pane thickness**	**Frame material**	**Glass pane**	**Time of reaching performance criteria [s]**			
					ΔT_{cr}	**T_{surf}**	**HL**	**T_{surf} frame**
No wind	3	3	PVC	1	310	370	356	-
				2	517	-	545	
			Aluminium	1	312	377	361	-
				2	506	-	550	
		6	PVC	1	420	502	354	-
				2	-	-	585	
			Aluminium	1	413	510	358	-
				2	-	-	599	
	3.5	3	PVC	1	376	486	411	-
				2	-	-	-	
			Aluminium	1	389	489	426	-
				2	-	-	-	
		6	PVC	1	-	-	429	-
				2	-	-	-	
			Aluminium	1	551	-	422	-
				2	-	-	-	
	4	3	PVC	1	-	-	519	-
				2	-	-	-	
			Aluminium	1	553	-	521	-
				2	-	-	-	
		6	PVC	1	-	-	527	-
				2	-	-	-	
			Aluminium	1	-	-	543	-
				2	-	-	-	
	4.5	3	PVC	1	-	-	687	-
				2	-	-	-	
			Aluminium	1	-	-	736	-
				2	-	-	-	
		6	PVC	1	-	-	700	-
				2	-	-	-	
			Aluminium	1	-	-	678	-
				2	-	-	-	
	5	3	PVC	1	-	-	-	-
			Aluminium	1	-	-	-	-
		6	PVC	1	-	-	-	-
			Aluminium	1	-	-	-	-

Table A.6: Results for the wood pallet scenario with the small window (0.5 x 0.5 m^2) in windy atmospheric conditions.

Atmospheric conditions	**Distance [m]**	**Pane thickness**	**Frame material**	**Glass pane**	**Time of reaching performance criteria [s]**			
					ΔT_{cr}	**T$_{surf}$**	**HL**	**T$_{surf}$ frame**
Windy	4.5	3	PVC	1	365	415	412	-
				2	-	-	573	
			Aluminium	1	363	418	412	-
				2	-	-	576	
		6	PVC	1	460	546	414	-
				2	-	-	657	
			Aluminium	1	461	560	416	-
				2	-	-	667	
	5	3	PVC	1	426	493	470	-
				2	-	-	-	
			Aluminium	1	422	496	469	-
				2	-	-	-	
		6	PVC	1	-	-	466	-
				2	-	-	-	
			Aluminium	1	573	-	467	-
				2	-	-	-	
	6	3	PVC	1	-	-	654	-
				2	-	-	-	
			Aluminium	1	-	-	641	-
		6	PVC	1	-	-	662	-
				2	-	-	-	
			Aluminium	1	-	-	660	-
	6.5	3	PVC	1	-	-	-	-
			Aluminium	1	-	-	-	-
		6	PVC	1	-	-	-	-
			Aluminium	1	-	-	-	-

Table A.7: Results for the wood pallet scenario with the big window (1.2 x 1.2 m^2) in calm atmospheric conditions.

Atmospheric conditions	Distance [m]	Pane thickness	Frame material	Glass pane	Time of reaching performance criteria [s]			
					ΔT_{cr}	T_{surf}	HL	T_{surf} frame
No wind	3.5	3	PVC	1	332	401	376	-
				2	572	-	590	
			Aluminium	1	330	402	375	-
				2	576	-	596	
		6	PVC	1	450	596	376	-
				2	-	-	657	
			Aluminium	1	442	570	373	-
				2	-	-	645	
	4	3	PVC	1	396	493	432	-
				2	-	-	-	
			Aluminium	1	389	487	432	-
				2	-	-	-	
		6	PVC	1	-	-	429	-
				2	-	-	-	
			Aluminium	1	558	-	434	-
				2	-	-	-	
	4.5	3	PVC	1	482	-	489	-
				2	-	-	-	
			Aluminium	1	463	-	488	-
				2	-	-	-	
		6	PVC	1	-	-	490	-
				2	-	-	-	
			Aluminium	1	-	-	490	-
				2	-	-	-	
	5	3	PVC	1	-	-	560	-
				2	-	-	-	
			Aluminium	1	-	-	569	-
				2	-	-	-	
		6	PVC	1	-	-	577	-
				2	-	-	-	
			Aluminium	1	-	-	573	-
				2	-	-	-	
	5.5	3	PVC	1	-	-	690	-
				2	-	-	-	
			Aluminium	1	-	-	697	-
				2	-	-	-	
		6	PVC	1	-	-	708	-
				2	-	-	-	
			Aluminium	1	-	-	701	-
				2	-	-	-	
	6	3	PVC	1	-	-	-	-
			Aluminium	1	-	-	-	-
		6	PVC	1	-	-	-	-
			Aluminium	1	-	-	-	-

Table A.8: Results for the wood pallet scenario with the big window (1.2 x 1.2 m^2) in windy atmospheric conditions.

Atmospheric conditions	**Distance [m]**	**Pane thickness**	**Frame material**	**Glass pane**	**Time of reaching performance criteria [s]**			
					ΔT_{cr}	**T_{surf}**	**HL**	**T_{surf} frame**
Windy	4.5	3	PVC	1	390	414	416	-
				2	-	582	579	
			Aluminium	1	385	416	416	-
				2	-	582	575	
		6	PVC	1	494	547	415	-
				2	-	-	629	
			Aluminium	1	487	536	413	-
				2	-	-	631	
	5	3	PVC	1	434	488	473	-
				2	-	-	-	
			Aluminium	1	428	492	476	-
				2	-	-	-	
		6	PVC	1	-	-	476	-
				2	-	-	-	
			Aluminium	1	-	-	479	-
				2	-	-	-	
	6	3	PVC	1	-	-	589	-
				2	-	-	-	
			Aluminium	1	-	-	593	-
				2	-	-	-	
		6	PVC	1	-	-	592	-
				2	-	-	-	
			Aluminium	1	-	-	587	-
				2	-	-	-	
	6.5	3	PVC	1	-	-	-	-
			Aluminium	1	-	-	-	-
		6	PVC	1	-	-	-	-
			Aluminium	1	-	-	-	-

Table A.9: Results for test 2 scenario

Window size [m^2]	**Atmospheric conditions**	**Distance [m]**	**Pane thickness**	**Frame material**	**Glass pane**	**Time of reaching performance criteria [s]**			
						ΔT_{cr}	**T_{surf}**	**HL**	**T_{surf} frame**
0.5 x 0.5	No wind	5	3	PVC	1	-	-	4223	-
		5.5				-	-	-	-
	Windy	5.5				-	-	-	-

Table A.10: Results for the three Douglas fir trees scenario with the small window (0.5 x 0.5 m^2) in calm and windy atmospheric conditions.

Atmospheric conditions	Distance [m]	Pane thickness	Frame material	Glass pane	Time of reaching performance criteria [s]			
					ΔT_{cr}	T_{surf}	HL	T_{surf} frame
No wind	0	3	Aluminium	1	9	10	15	-
				2	12	12	-	
		6		1	9	10	15	-
				2	12	12	-	
	0.5	3	PVC	1	10	11	-	9
			Aluminium	1	10	11	-	-
				2	-	-	-	
		6	PVC	1	10	11	-	9
			Aluminium	1	10	11	-	-
				2	-	-	-	
	1	3	PVC	1	11	12	-	9
			Aluminium	1	11	12	-	-
				2	-	-	-	
		6	PVC	1	11	12	-	9
			Aluminium	1	11	12	-	-
				2	-	-	-	
	1.5	3	PVC	1	12	-	-	11
			Aluminium	1	12	-	-	-
				2	-	-	-	
		6	PVC	1	12	-	-	11
			Aluminium	1	12	-	-	-
				2	-	-	-	
	2	3	PVC	1	-	-	-	-
			Aluminium	1	-	-	-	-
		6	PVC	1	-	-	-	-
			Aluminium	1	-	-	-	-
Windy	0	3	Aluminium	1	13	14	20	-
				2	16	15	-	
		6	Aluminium	1	13	13	19	-
				2	16	16	-	
	0.5	3	Aluminium	1	12	13	-	-
				2	-	-	-	
		6	Aluminium	1	11	13	-	-
				2	-	-	-	
	1.5	3	Aluminium	1	13	-	-	-
				2	-	-	-	
		6	Aluminium	1	13	-	-	-
				2	-	-	-	
	2	3	PVC	1	13	-	-	12
			Aluminium	1	-	-	-	-
		6	PVC	1	12	-	-	11
			Aluminium	1	13	-	-	-
				2	-	-	-	
	2.5	3	PVC	1	-	-	-	11
			Aluminium	1	-	-	-	-
		6	PVC	1	-	-	-	12
			Aluminium	1	-	-	-	-
	3	3	PVC	1	-	-	-	12
		6	PVC	1	-	-	-	13
	3.5	3	PVC	1	-	-	-	-
		6	PVC	1	-	-	-	-

Table A.11: Results for the three Douglas fir trees scenario with the big window (1.2 x 1.2 m^2) in calm and windy atmospheric conditions.

Atmospheric conditions	**Distance [m]**	**Pane thickness**	**Frame material**	**Glass pane**	**Time of reaching performance criteria [s]**			
					ΔT_{cr}	T_{surf}	HL	T_{surf} frame
No wind	0.5	3	PVC	1	10	11	-	9
			Aluminium	1	10	11	-	-
				2	-	13	-	
		6	PVC	1	10	11	-	9
			Aluminium	1	10	11	-	-
				2	-	13	-	
	1	3	PVC	1	11	12	-	10
			Aluminium	1	11	12	-	-
				2	-	-	-	
		6	PVC	1	11	12	-	10
			Aluminium	1	11	12	-	-
				2	-	-	-	
	1.5	3	PVC	1	-	-	-	12
			Aluminium	1	-	-	-	-
		6	PVC	1	-	-	-	12
			Aluminium	1	-	-	-	-
	2	3	PVC	1	-	-	-	-
		6	PVC	1	-	-	-	-
Windy	0.5	3	Aluminium	1	12	13	-	-
				2	-	16	-	
		6	Aluminium	1	11	13	-	-
				2	-	14	-	
	1	3	Aluminium	1	12	13	-	-
				2	-	-	-	
		6	Aluminium	1	12	13	-	-
				2	-	-	-	
	2	3	PVC	1	12	-	-	11
			Aluminium	1	12	-	-	-
				2	-	-	-	
		6	PVC	1	12	-	-	11
			Aluminium	1	12	-	-	-
				2	-	-	-	
	2.5	3	PVC	1	-	-	-	11
			Aluminium	1	-	-	-	-
		6	PVC	1	-	-	-	11
			Aluminium	1	-	-	-	-
	3	3	PVC	1	-	-	-	-
		6	PVC	1	-	-	-	-

A.3 Results semi-confined space scenarios

The adiabatic surface temperature recorded by all devices for the three analysed scenarios that involve the combustion of fuels inside a concrete semi-confined space is given in Figure A.7, Figure A.8 and Figure A.9.

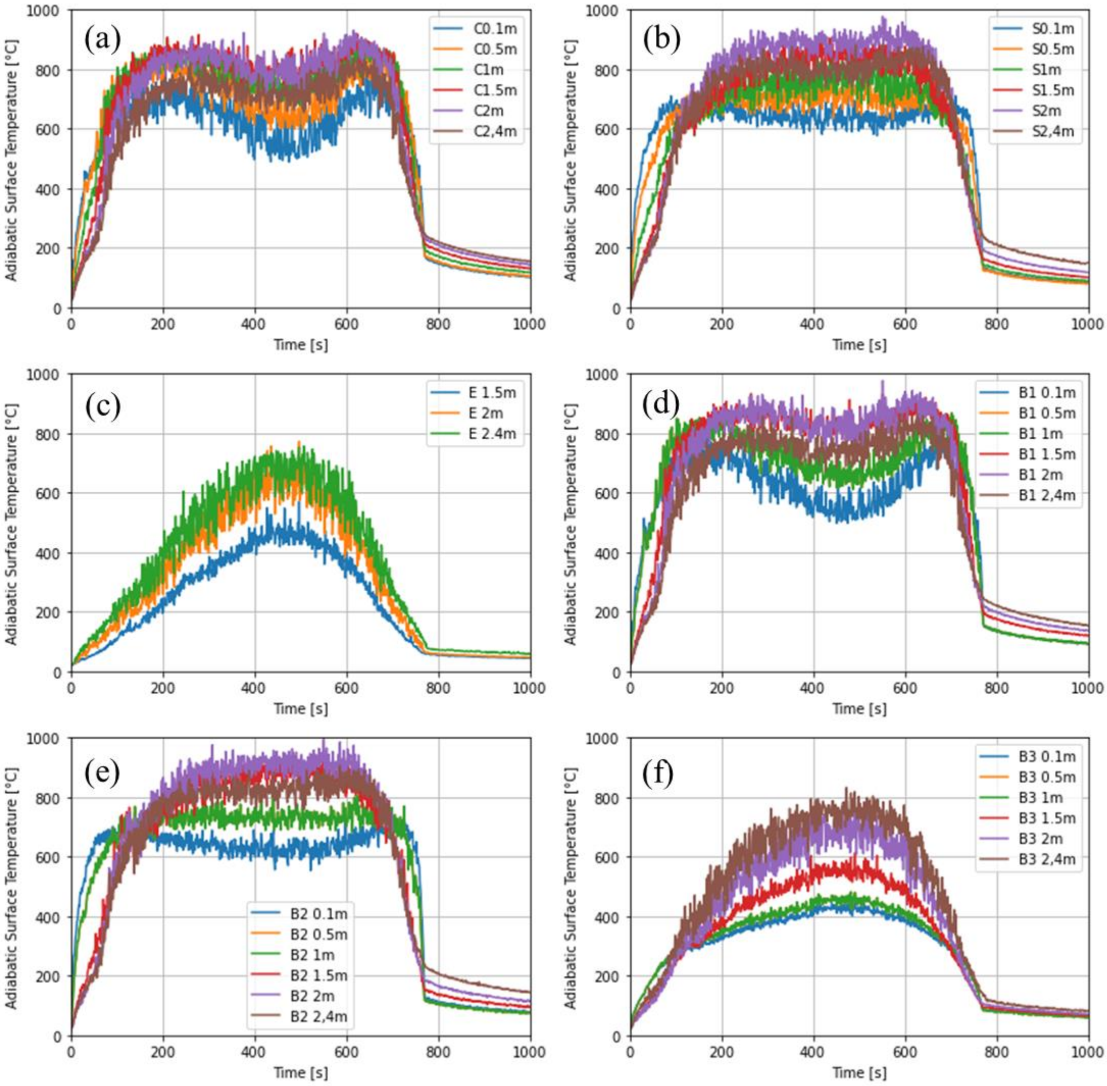

Figure A.7: FDS simulation results for SCS1 based on the location of the devices: (a) left back corner, (b) side wall, (c) opening, (d) back wall location 1, (e) back wall location 2, (f) back wall at the centre (location 3).

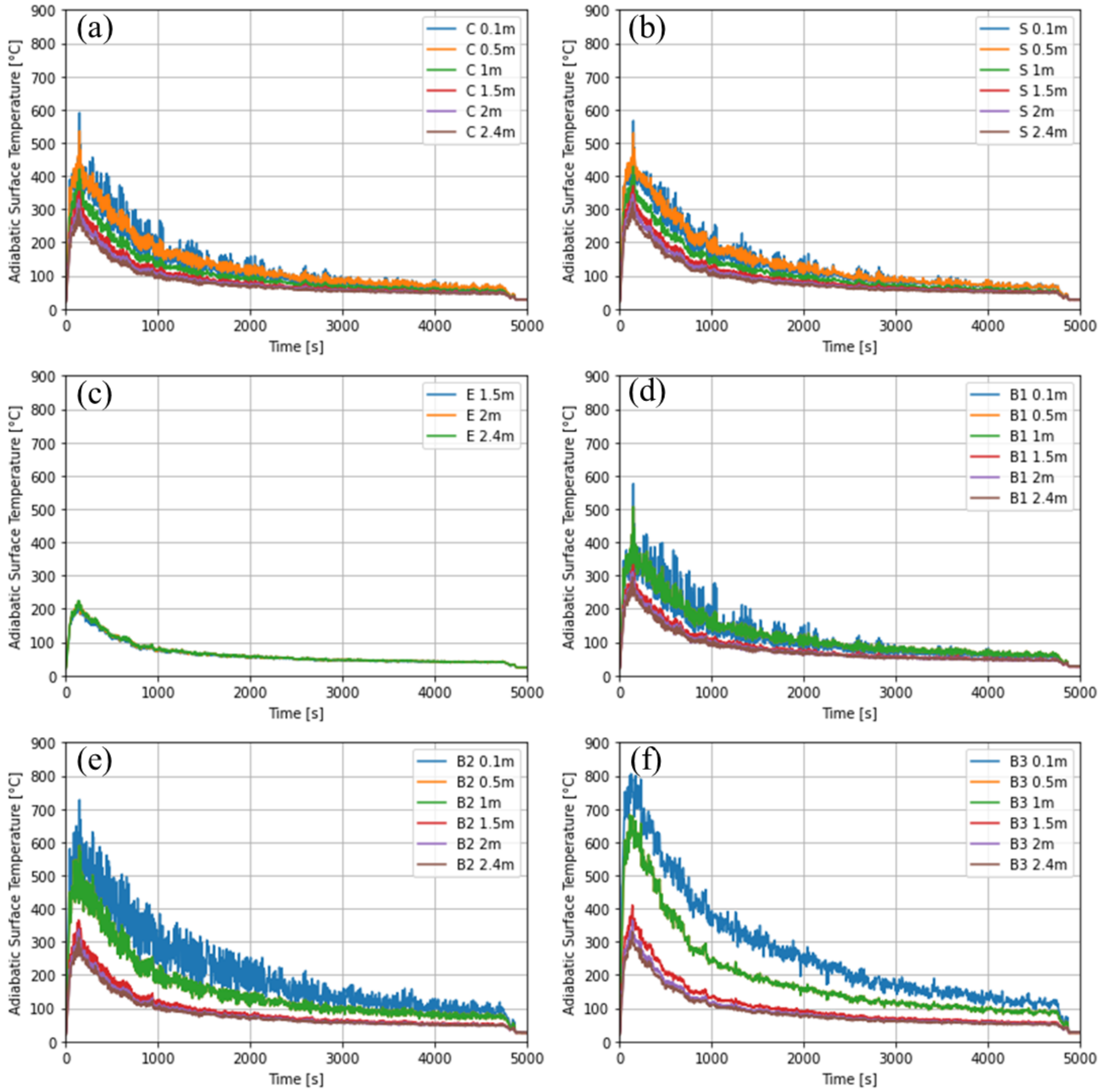

Figure A.8: FDS simulation results for SCS2 based on the location of the devices: (a) left back corner, (b) side wall, (c) opening, (d) back wall location 1, (e) back wall location 2, (f) back wall at the centre (location 3).

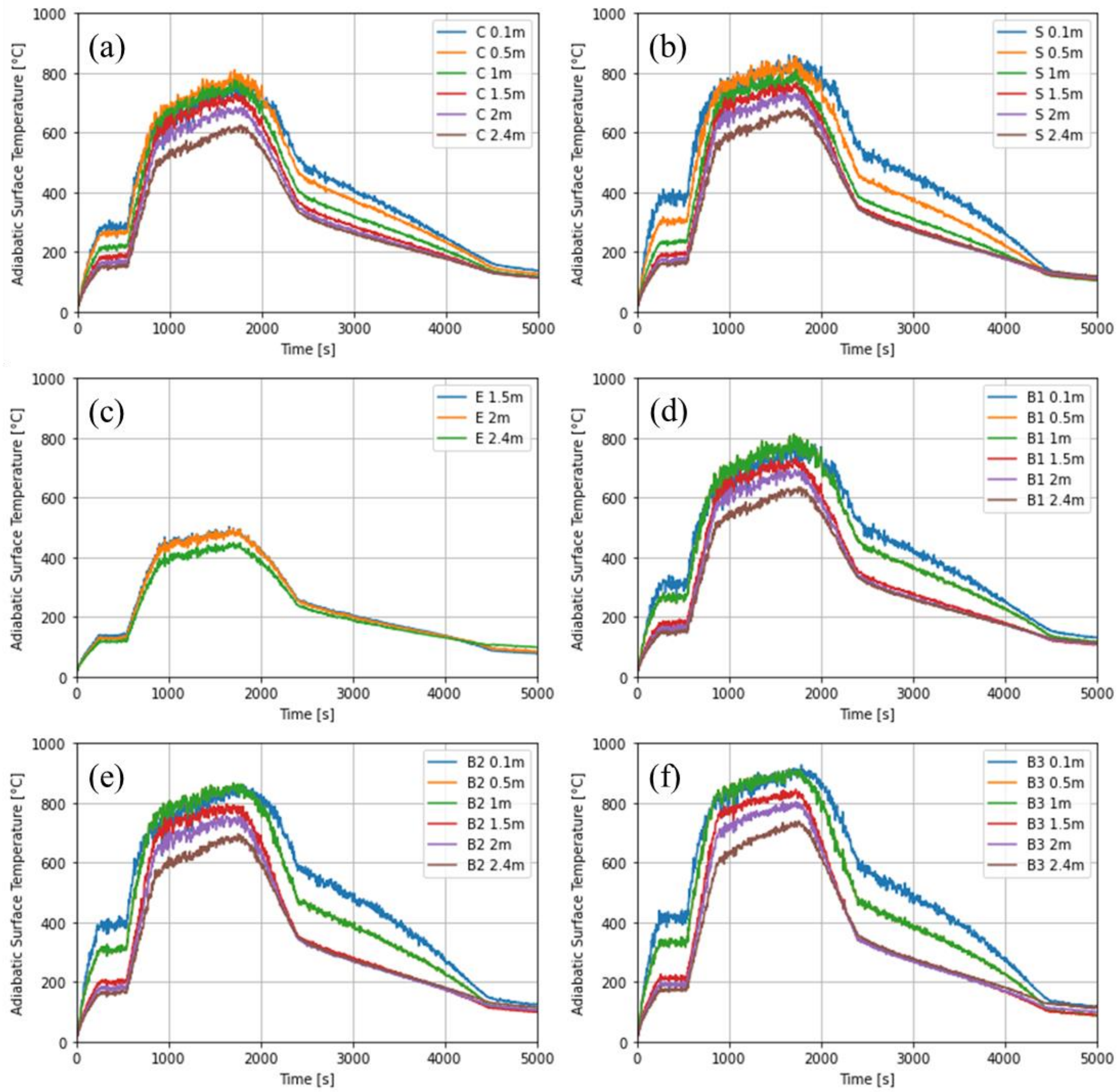

Figure A.9: FDS simulation results for SCS3 based on the location of the devices: (a) left back corner, (b) side wall, (c) opening, (d) back wall location 1, (e) back wall location 2, (f) back wall at the centre (location 3).

Appendix B

Damage assessment form

A damage assessment form for the collection of post-fire data is here presented. The form is dived into two sections: the first one includes general questions on the property and building, while the second part goes more in detail and analyses the different vulnerabilities that might be present, and is the questionnaire of the VAT.

Collection details

Name of the contact:
Address of the analysed property:
Email:

General questionnaire

		Comments/details
Type of building		
Primary housing	◻	
Secondary housing	◻	
Uninhabited house	◻	
Other (please specify)	◻	
Type of construction		
Masonry	◻	
Concrete	◻	
Stone	◻	
Wood	◻	
Other (specify)	◻	
Age of construction		
< 10 years	◻	
Between 10 and 30 years	◻	
> 30 years	◻	
Conditions of the building before the fire		
Well preserved	◻	
Moderately preserved	◻	
Poorly preserved	◻	
Conditions of the property/garden before the fire		
Well preserved	◻	
Moderately preserved	◻	
Poorly preserved	◻	
Fuel management within 30 m of the building		
Total	◻	
Partial	◻	
Absent	◻	

		Comments/details
Conditions of the building after the fire		Specify the location of the damage
No damage	□	
Slightly damaged	□	
Moderately damaged	□	
Very damaged	□	
Destroyed	□	
Conditions of the property/garden after the fire		Specify the location of the damage
No damage	□	
Slightly damaged	□	
Moderately damaged	□	
Very damaged	□	
Most common wind direction?		
In case of partial or absent fuel management, where are the non-treated fuels located?		
Elements present on the property		
Trees/shrubs	□	
Lawn/grass	□	
Hedges	□	
LPG tanks	□	
Pergola	□	
Shed (specify material)	□	
Vehicle	□	
Water tank	□	
Well	□	
Electricity generator	□	
Other	□	
Evacuation/Stay and defend		
I will evacuate	□	
I will stay and defended my property	□	
Presence of		
Own water supply	□	
Own generator	□	

Definitions:

Building

Well preserved: built or renovated in the past 10 years, with periodic maintenance.
Moderately preserved: Some parts must be renovated or better maintained.
Poorly preserved: neglected building.
Slightly damaged: localized damage to one sub-system on the exterior of the building; no ignition inside the house.
Moderately damaged: localized damage to one or more sub-systems; ignition of one room inside the building.
Very damaged: structural damage; ignition of more than one room inside the building.

Destroyed: building burned to the ground or in which walls and roof need to be completely repaired.

Property/garden

Well preserved: clean property, with regularly watered vegetation, no dead fuels, no artificial fuel packs that are uncontrolled.
Moderately preserved: presence of some dead fuels, vegetation not regularly watered or not regularly cleared.
Poorly preserved: neglected property.
Slightly damaged: localized damage on the property, no further fire spread.
Moderately damaged: Some fire spread has happened through the fuels located on the property, but it is confined to less than 50% of the area.
Very damaged: More than 50% of the area is burned.

Detailed questionnaire (VAT questionnaire)

Building characteristics		
1	**Shutters** Do you have protection for all your windows/glazing systems (i.e. shutters) made of non-combustible materials (solid core wood fire-resistant, metal like aluminium)?	□ Yes □ No
2	What material are the shutters made of?	□ Wood □ Aluminium □ PVC □ Fire rated materials
3	**Glazing systems** What is the thickness of the glazing systems (in mm)?	
4	**Roof material** Is your roof covering or your roof assembly made of fire-rated material (e.g. clay tiles, concrete tiles, asphalt glass fibre composition singles, slate, etc.)?	□ Yes □ No
5	**Roof maintenance** Are there missing, displaced or broken tiles?	□ Yes □ No
6	Is the underlying roof sheeting exposed?	□ Yes □ No
7	Are there unsealed spaces between the roof and the external walls or between the roof covering and the roof decking?	□ Yes □ No
8	Do you perform regular cleaning of debris piling up on roof or gutters?	□ Yes □ No
9	**Unprotected vents** Do you have unprotected ventilation openings (i.e. vents without any type of screening)? *If all your vents are unprotected, go to question 11*	□ Yes □ No
10	**Vent protection** What type of vent protection is present?	□ Combustible □ Non-combustible in bad conditions (rusted or damaged) □ Non-combustible in good conditions (no damage)
11	**Semi-confined space adjacent to house** Is there a semi-confined space adjacent to your house (i.e., it has at least one wall in common with the house)? *If the answer is no, go to question 15*	□ Yes □ No
12	**Presence of combustible materials in semi-confined space** What % of volume of the semi-confined space do combustible materials occupy?	

13	**Presence of glazing systems in semi-confined space** What % of wall area do glazing systems that connect the house to the semi-confined space occupy?			
14	**Vulnerable walls of semi-confined space** What type of walls are those connecting the house to the semi-confined space?	□ Non-combustible, at least 12 cm thick □ Non-combustible, less than 12 cm thick □ Combustible		
Property/landscape characteristics ZONE 1 (within 10 m from the house)				
15	**Fuels close to LPG tank in zone** Are there any combustible materials (including ornamental vegetation, storage spaces, or combustible eaves) located within 2 m of LPG tanks (this includes also canisters with a total volume > 0.5 m^3)?	□ Yes	□ No	□ Not applicable
16	**Artificial fuels close to vulnerable structural elements** Are there any artificial fuels (e.g. outdoor furniture, stored materials, gas canisters, small sheds, wood piles) located within 5 m from double pane glazing systems and 6.5 m from single pane glazing systems?	□ Yes	□ No	□ Not applicable
17	Are there any artificial fuels (e.g. outdoor furniture, stored materials, gas canisters, small sheds, wood piles) located within 5 m from the roof or gutters?	□ Yes	□ No	□ Not applicable
18	If the wildland vegetation is mainly trees, are there artificial fuels located within 20 m from these trees?	□ Yes	□ No	□ Not applicable
19	Is the distance between fuels or fuel packs at least 5 m?	□ Yes	□ No	□ Not applicable
20	**Management of ornamental vegetation** Is there ornamental vegetation in zone 1? *If the answer is no, go to question 30*	□ Yes	□ No	
21	Are there very flammable species (e.g. pine tree, eucalyptus, cypress, etc.) or vegetation with closely packed leaves and branches, fine textures, small, thin and narrow leaves, and high amounts of resins or oils?	□ Yes	□ No	
22	Are trees and shrubs separated by at least 6 m?	□ Yes	□ No	
23	Is the vegetation separated by at least 3.5 m from any glazing system?	□ Yes	□ No	
24	Are trees overhanging the roofline of the building?	□ Yes	□ No	
25	Are individual or groups of bushes less than 5 m wide?	□ Yes	□ No	□ Not applicable
26	Is there a non-continuous plant litter layer?	□ Yes	□ No	
27	Are the hedges aligned with the wind direction or the main slope?	□ Yes	□ No	□ No hedges
28	Are hedges located at least 2 m from other vegetation?	□ Yes	□ No	□ No hedges
29	Is there dead vegetation or vegetative debris?	□ Yes	□ No	
30	**Wildland vegetation and/or crop landscape** *If there is no wildland or crop vegetation in zone 1, go to question 37*			
31	**Wildland vegetation canyon/slope/ridge/hilltop** Is the separation between crown trees/high shrubs of at least 9 m?	□ Yes	□ No	□ Not applicable
32	Is there a separation between grouping of shrubs (or regrowth forest or young trees) of at least 3 m?	□ Yes	□ No	□ Not applicable
33	Are the lower tree branches pruned at ⅓ of tree height?	□ Yes	□ No	□ Not applicable
34	Is the low surface fuel load max 10 cm deep?	□ Yes	□ No	
35	Is the vegetation separated by at least 3.5 m from any glazing system?	□ Yes	□ No	
36	Are trees overhanging the roofline of the building?	□ Yes	□ No	
Property/landscape characteristics ZONE 2 (between 10 m and 30 m from the house)				
37	**Fuels close to LPG tank in zone** Are there any combustible materials (including ornamental vegetation, storage spaces, or combustible eaves) located	□ Yes	□ No	□ Not applicable

	within 2 m of LPG tanks (this includes also canisters with a total volume > 0.5 m^3)?			
38	**Spacing of artificial fuels** In case of wild vegetation of mainly trees, are artificial fuels placed at a distance of minimum 20 m from these trees?	□ Yes	□ No	□ Not applicable
39	Is the distance between different artificial fuels or fuel packs of at least 5 m?	□ Yes	□ No	□ Not applicable
40	**Management of ornamental vegetation** Is there ornamental vegetation in zone 2? *If the answer is no, go to question 45*	□ Yes	□ No	
41	Are the hedges aligned with the wind direction or the main slope?	□ Yes	□ No	□ No hedges
42	Are the hedges in this zone located at least 2 m from other vegetation?	□ Yes	□ No	□ No hedges
43	If you have ornamental bushes in zone 2, are they less than 5 m wide?	□ Yes	□ No	□ Not applicable
44	Is the distance between these bushes and other vegetation larger than 3 m?	□ Yes	□ No	□ Not applicable
45	**Landscape type** *If the surrounding landscape includes a canyon/slope/ ridge/ hilltop, fill in questions 46 to 49* *If the surrounding landscape is flat, fill in questions 50 to 53* *If the surrounding landscape includes crops, go to question 54*			
46	**Wildland vegetation canyon/slope/ridge/hilltop** Is the separation between crown trees/high shrubs of at least 9 m?	□ Yes	□ No	□ Not applicable
47	Is there a separation between the shrubs (or regrowth forest or young trees) of at least 3 m?	□ Yes	□ No	□ Not applicable
48	Are the lower tree branches pruned at ⅓ of tree height?	□ Yes	□ No	□ Not applicable
49	Is the low surface fuel load max 10 cm deep?	□ Yes	□ No	
50	**Wildland vegetation flat landscape** Is the separation between crown trees/high shrubs of at least 6 m?	□ Yes	□ No	□ Not applicable
51	Is there a separation between the shrubs (or regrowth forest or young trees) at least 3 m?	□ Yes	□ No	□ Not applicable
52	Are the lower tree branches pruned at ⅓ of tree height?	□ Yes	□ No	□ Not applicable
53	Is the low surface fuel load max 10 cm deep?	□ Yes	□ No	
54	**Wildland vegetation crop landscape** Is the separation between crown trees/high shrubs of at least 6 m?	□ Yes	□ No	□ Not applicable
55	Are the lower tree branches pruned at ⅓ of tree height?	□ Yes	□ No	□ Not applicable
56	Is the low surface fuel load max 10 cm deep?	□ Yes	□ No	

Appendix C

Experts' answers to the fuzzy logic poll

The answers provided by the 13 WUI experts that have been polled to identify quantitative values for the VAT through the use of fuzzy logic are here presented.

Each expert is assigned a number (1 to 13). The answers of each to the subsets definition is given in Table C.1.

Table C.1: Answers of each expert for the definition of the subsets. POF: probability of failure. Comb.: combustible.

Expert	Glazing systems						
	POF of shutters [%]				Pane thickness [mm]		
	Fire proof	Aluminium	PVC	No shutters	Thick	Medium	Thin
1	1	5	99	100	-	-	-
2	10	25	60	90	10	7	5
3	10	20	80	80	-	-	-
4	3	30	80	95	8	6	4
5	0-10	10-40	50-80	80-100	6-8	4-5	2-3
6	5-10	10-20	50-75	80-90	15-50	10-15	2-10
7	10-30	20-40	40-60	70-90	-	-	-
8	10	40	80	100	6	4	2
9	0	30	50	100	8	6	2-3
10	0-20	30-40	50-70	100	15-19	8-12	2-6
11	0	10	30	50	50	30	20
12	0-5	10-20	80-100	100	-	-	-
13	10	30	60	90	8	5	2

Expert	Roof			
	POF of roof covering material [%]		POF of roof maintenance [%]	
	Combustible in good conditions	Non-combustible in good conditions	Badly maintained	Well maintained
1	95	5	100	50
2	70	15	60	10
3	80	10	80	10
4	30	3	70	30
5	90	10	90	10
6	50-100	3-50	50-100	0-50
7	40-70	10-30	70-90	10-30
8	60	10	40	10
9	50	0	50	0
10	40-100	15-30	70-90	5-10
11	50	0	40	0
12	0-30	0-5	75-100	0-20
13	80	50	90	50

Expert	Vent protection			
	POF non-combustible, good conditions [%]	POF non-combustible, bad conditions [%]	POF combustible [%]	POF unprotected or combustible, bad conditions [%]
1	1	50	20	99
2	5	25	20	40
3	10	80	80	80

4	10	30	70	95
5	0-10	10-50	50-70	70-100
6	0-5	5-25	25-50	50-100
7	30-40	40-60	60-80	70-90
8	10	30	30	40
9	0	30	70	100
10	20	90	25	90
11	0	20	10	40
12	0-5	75-100	0-30	75-100
13	10	20	20	50

	Semi-confined space								
	% of walls occupied by windows			**POF envelope [%]**			**% of occupied volume**		
	High	Medium	Low	Comb. walls	Non-comb. thin	Non-comb. thick	High	Medium	Low
1	40	30	10	99	3	1	10	5	1
2	60	40	30	60	25	10	70	50	30
3	-	-	-	80	30	10	10	5	1
4	90	50	20	70	10	3	70	50	10
5	40-100	10-40	0-10	100	50	10	50-100	10-50	0-10
6	50-100	25-50	0-25	50-100	25-50	10-25	50-100	25-50	0-25
7	40-100	20-40	0-20	50-70	30-50	10-20	40-100	20-40	0-20
8	50	20	10	80	30	10	30	15	5
9	70-100	30-70	0-30	60	40	5	50-100	30-50	0-30
10	30	15	5	90-100	0-30	0-15	1.5	0.7	0.3
11	40	30	20	20	10	0	10	5	1
12	60-100	30-60	0-30	75-100	20-75	0-10	35-100	15-35	0-15
13	80	50	10	90	50	10	80	50	10

	Probability of failure			
	Extreme POF [%]	**High POF [%]**	**Medium POF [%]**	**Low POF [%]**
1	60	50	30	10
2	90	75	50	25
3	80-100	60-80	30-60	0-30
4	95	70	30	5
5	80-100	50-80	20-50	0-20
6	75-100	50-75	25-50	0-25
7	80-100	50-80	30-50	0-30
8	80-100	60-70	40-50	10-30
9	75-100	50-75	25-50	0-25
10	60-100	40-60	20-40	0-20
11	80-100	60-80	30-60	0-30
12	80-100	60-80	30-60	0-30
13	90	80	50	25

	Fuel management	
	% of rules to comply to for a property to be badly managed	**% of rules to comply to for a property to be well managed**
1	90	99
2	65	90
3	0-60	60-100
4	70	95
5	0-80	90-100
6	-	-
7	0-30	65-100
8	50	80
9	0-65	65-100
10	0-70	70-100
11	-	-

12	0-50	80-100
13	50	80

The obtained results are merged to obtain the data on the percentage of people that chose each of the values, so as to identify membership functions for each of the fuzzy subsets. In some cases, the ranges proposed by the experts were extended to reach the limits of the range (e.g., compliance to fuel management for badly managed fuels was given a range from 0-90% instead of just the value 90% given by expert 1, given that less than 90% compliance still includes bad fuel management). This data is presented in the following tables, where the value in the first column defines the values of the x-axis and the % of people defines the values of the y-axis. Weighted average values are then calculated to obtain the membership functions shown in the following figures.

Table C.2: Values that identify membership functions the fuzzy subset *shutters*.

Glazing systems - shutters		
	POF [%]	**% people**
No shutters	50	7.7
	70	7.7
	80	30.8
	90	38.5
	95	15.4
	100	46.2
PVC shutters	30	7.7
	40	7.7
	50	38.5
	60	46.2
	70	23.1
	75	7.7
	80	38.5
	99	15.4
	100	7.7
Wood shutters	75	7.7
	20	23.1
	30	38.5
	40	23.1
	50	23.1
	60	15.4
	70	15.4
	80	15.4
	90	7.7
	95	7.7
Aluminium shutters	5	7.7
	10	30.8
	20	38.5
	25	23.1
	30	46.2
	40	30.8
Fire proof shutters	0	38.5
	1	30.8
	3	30.8
	5	30.8
	10	61.6
	20	15.4
	30	7.7

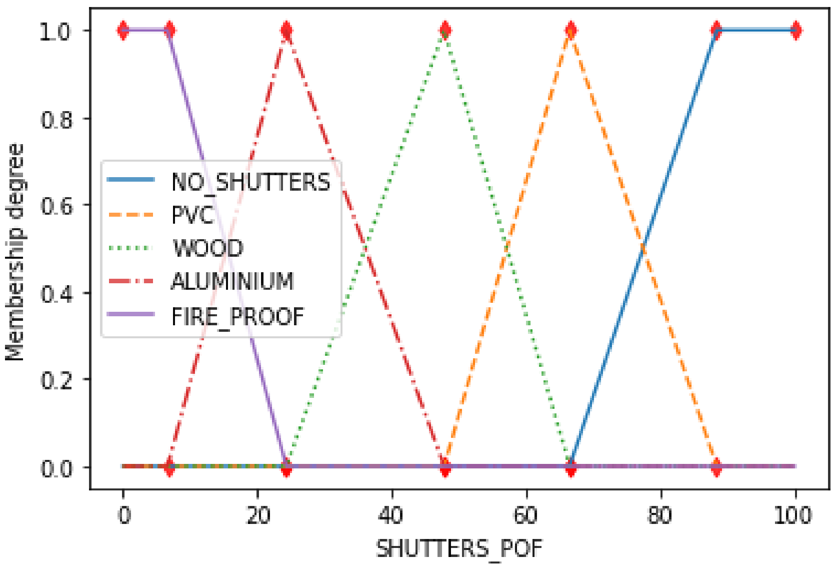

Figure C.1: Membership function for the subset *shutters*.

Table C.3: Values that identify membership functions the fuzzy subset *pane thickness*.

	Glazing systems – pane thickness	
	Thickness [mm]	**% people**
Thin glass	2	46.2
	3	30.8
	4	23.1
	5	23.1
	6	15.4
	10	7.7
	20	7.7
Medium glass	4	15.4
	5	15.4
	6	15.4
	7	7.7
	8	7.7
	10	15.4
	12	15.4
	15	7.7
	30	7.7
Thick glass	6	15.4
	7	7.7
	8	30.8
	10	7.7
	15	15.4
	19	15.4
	50	15.4

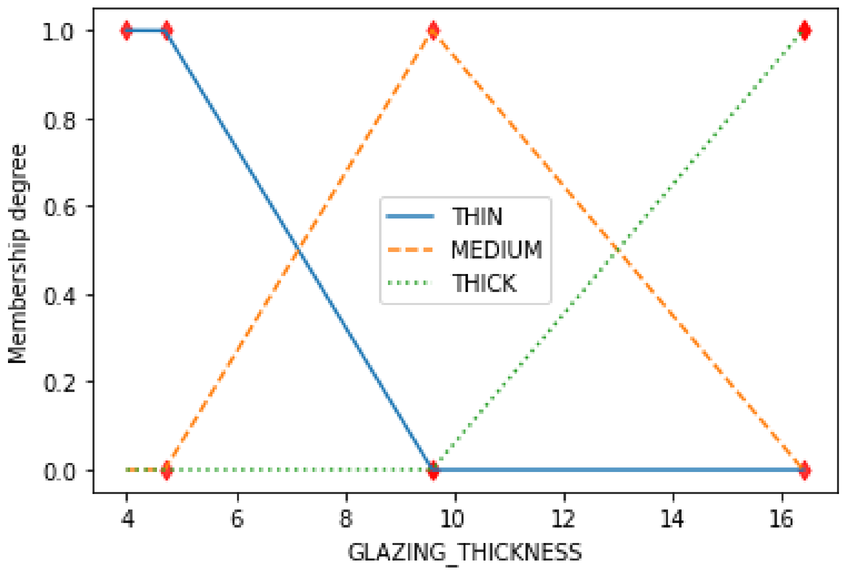

Figure C.2: Membership functions for the subset *glazing thickness.*

Table C.4: Values that identify membership functions the fuzzy subset *roof covering material*.

	Roof materials	
	POF [%]	**% people**
Combustible roof in good conditions	0	7.7
	30	15.4
	40	15.4
	50	38.5
	60	30.8
	70	30.8
	80	30.8
	90	23.1
	95	23.1
	100	15.4
Non-combustible in good conditions	0	23.1
	3	23.1
	5	23.1
	10	38.5
	15	30.8
	20	23.1
	30	23.1
	40	7.7
	50	15.4

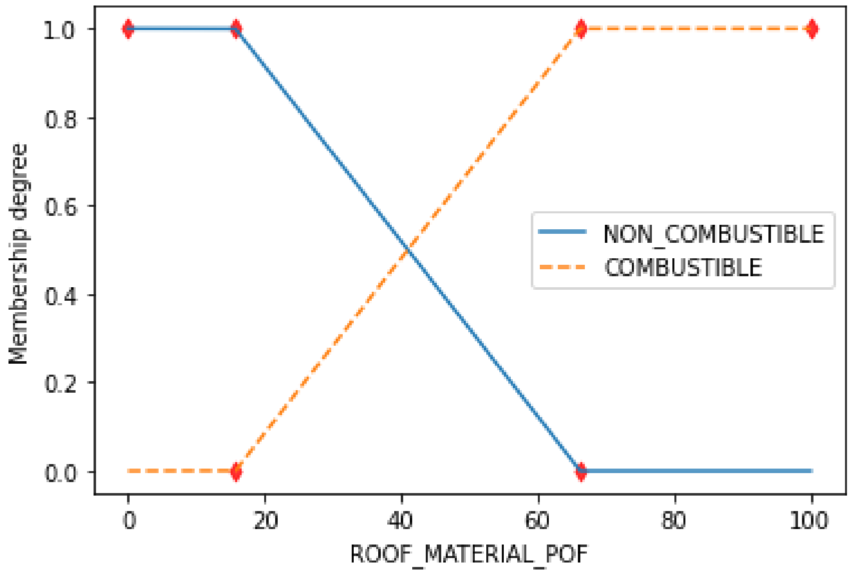

Figure C.3: Membership functions for the subset *roof material*.

Table C.5: Values that identify membership functions the fuzzy subset *roof maintenance*.

	Roof maintenance	
	POF [%]	**% people**
Badly maintained	40	15.4
	50	15.4
	60	15.4
	70	30.8
	75	30.8
	80	38.5
	90	46.2
	100	23.1
Well maintained	0	30.8
	5	23.1
	10	61.5
	20	23.1
	30	23.1
	50	23.1

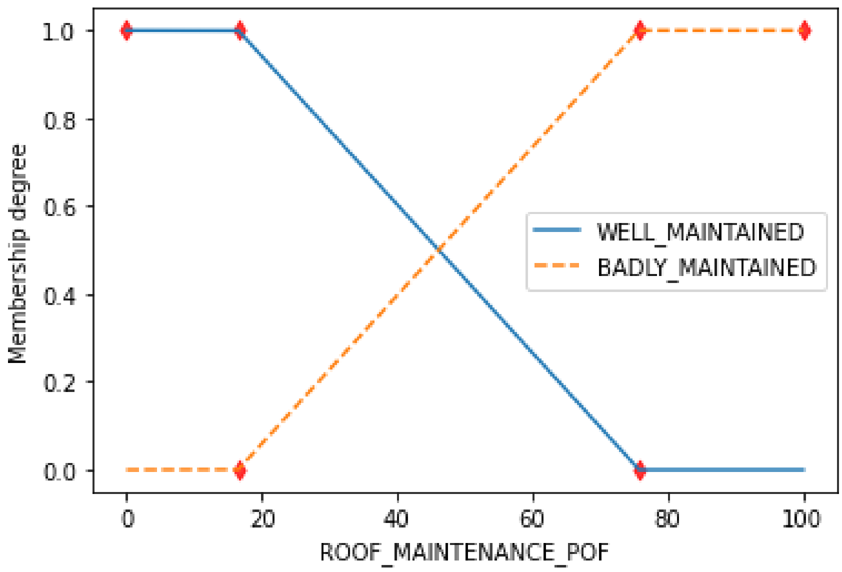

Figure C.4: Membership functions for the subset *roof maintenance*.

Table C.6: Values that identify membership functions the fuzzy set *vent protection*.

Vent protection		
	POF [%]	**% people**
Non-combustible, good conditions	0	38.5
	1	30.8
	5	30.8
	10	38.5
	20	7.7
	30	7.7
	40	7.7
Non-combustible, bad conditions	5	7.7
	10	15.4
	20	30.8
	25	23.1
	30	30.8
	40	15.4
	50	23.1
	60	7.7
	75	7.7
	80	15.4
	90	15.4
	100	7.7
Combustible	0	7.7
	10	15.4
	20	30.8
	25	23.1
	30	23.1
	50	15.4
	60	15.4
	70	30.8
	80	15.4
No protection or combustible in bad conditions	40	23.1
	50	15.4
	70	23.1

	75	30.8
	80	38.5
	90	38.5
	95	30.8
	99	30.8
	100	30.8

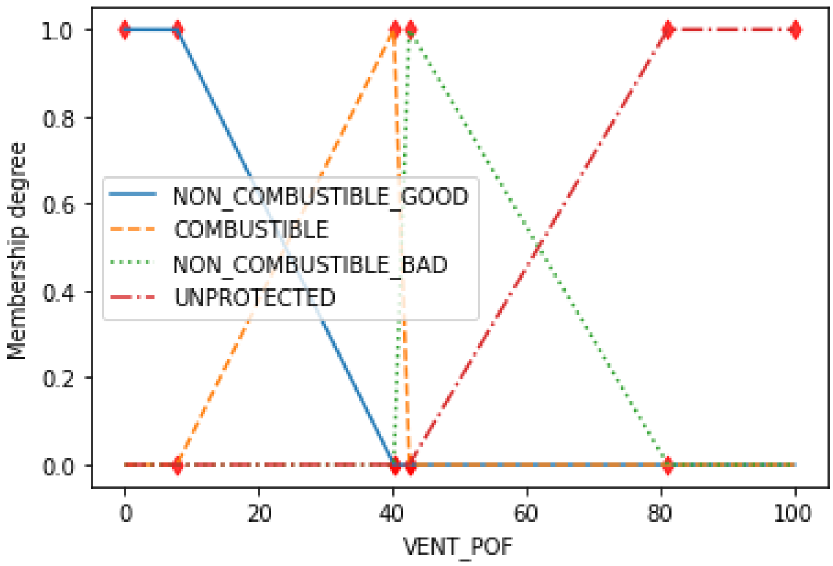

Figure C.5: Membership functions for the set *vents.*

Table C.7: Values that identify membership functions the fuzzy subset *window coverage.*

Semi-confined spaces – window coverage		
	% of window coverage	**% people**
High	30	7.7
	40	38.5
	50	53.9
	60	69.2
	70	76.9
	80	84.6
	90	92.3
	100	92.3
Medium	10	7.7
	15	15.4
	20	23.1
	25	23.1
	30	53.8
	40	46.2
	50	38.5
	60	15.4
	70	7.7
Low	0	92.3
	5	92.3
	10	84.6
	20	53.8
	25	30.8
	30	23.1

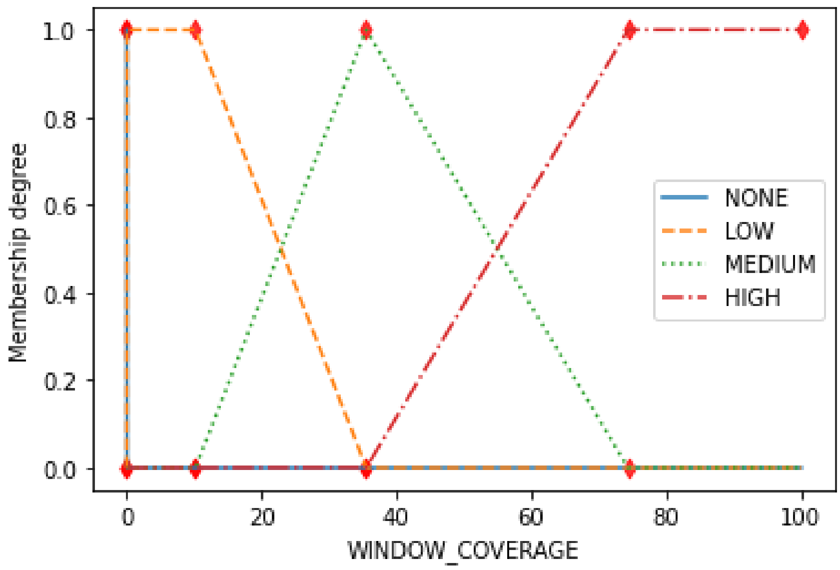

Figure C.6: Membership functions for the subset *window coverages*.

Table C.8: Values that identify membership functions the fuzzy subset *envelope of semi-confined space.*

Semi-confined space – envelope		
	POF [%]	**% people**
Combustible	20	7.7
	50	15.4
	60	30.8
	70	23.1
	75	15.4
	80	30.8
	90	30.8
	99	30.8
	100	30.8
Non-combustible, thin	0	7.7
	3	15.4
	10	23.1
	20	15.4
	25	30.8
	30	46.2
	40	30.8
	50	38.5
	75	7.7
Non-combustible, thick	0	23.1
	1	23.1
	3	23.1
	5	23.1
	10	69.2
	15	23.1
	20	15.4
	25	7.7

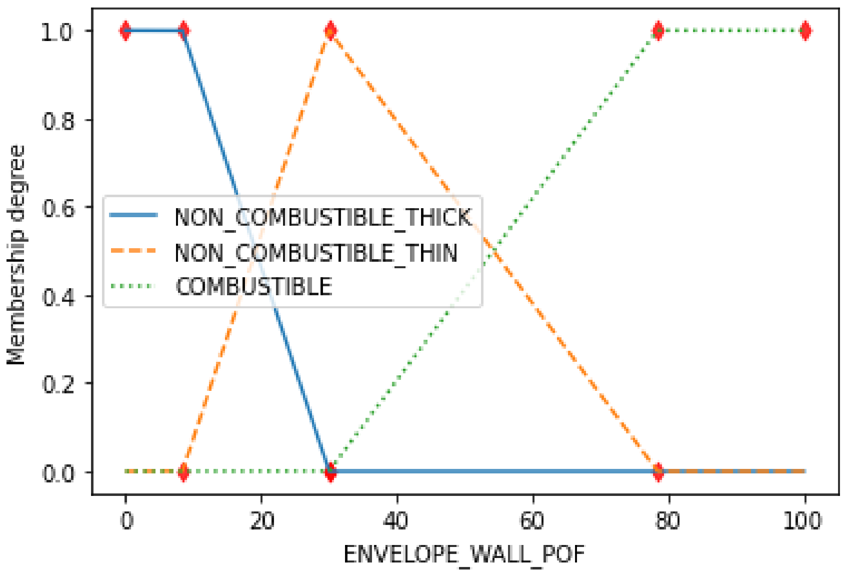

Figure C.7: Membership functions for the subset *envelope of semi-confined space*.

Table C.9: Values that identify membership functions the fuzzy subset *volume of combustible materials in semi-confined space*.

Semi-confined space – presence of combustible materials		
	% of volume occupied by combustible materials	**% people**
High	1.5	7.7
	10	30.8
	30	38.5
	35	46.2
	40	53.8
	50	76.9
	70	92.3
	80	100
	100	100
Medium	0.7	7.7
	5	23.1
	10	7.7
	15	23.1
	20	23.1
	25	30.8
	30	38.5
	35	38.5
	40	30.8
	50	46.2
Low	0	100
	0.3	100
	1	92.3
	5	69.2
	10	61.5
	15	38.5
	20	30.8
	25	23.1
	30	15.4

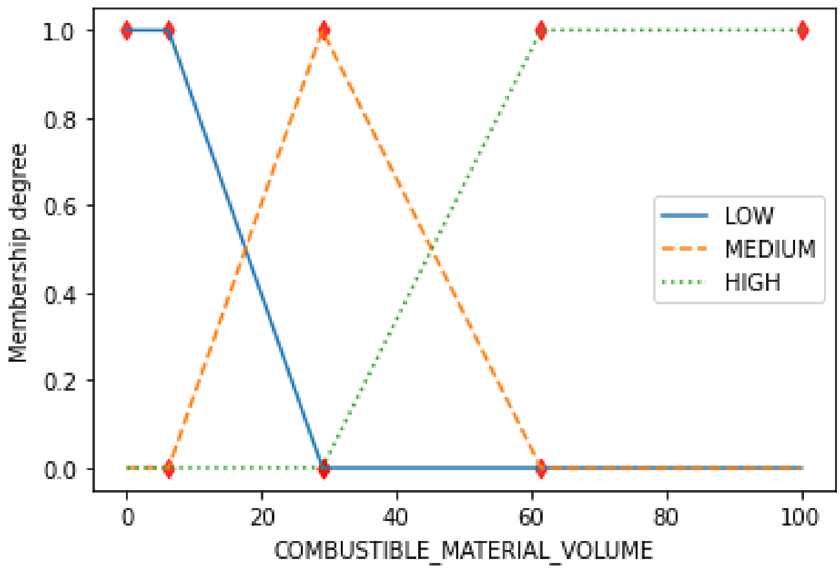

Figure C.8: Membership functions for the subset *volume of combustible materials in semi-confined space.*

Table C.10: Values that identify membership functions the fuzzy set *probability of failure*.

	Probability of failure	
	Probability [%]	**% people**
Extreme	60	15.4
	75	30.8
	80	76.9
	90	92.3
	95	100
	100	100
High	40	8.3
	50	50
	60	75
	70	75
	75	66.7
	80	47.7
Medium	20	15.4
	25	30.8
	30	76.9
	40	69.2
	50	76.9
	60	23.1
Low	0	100
	5	100
	10	92.3
	20	84.6
	25	69.2
	30	38.5

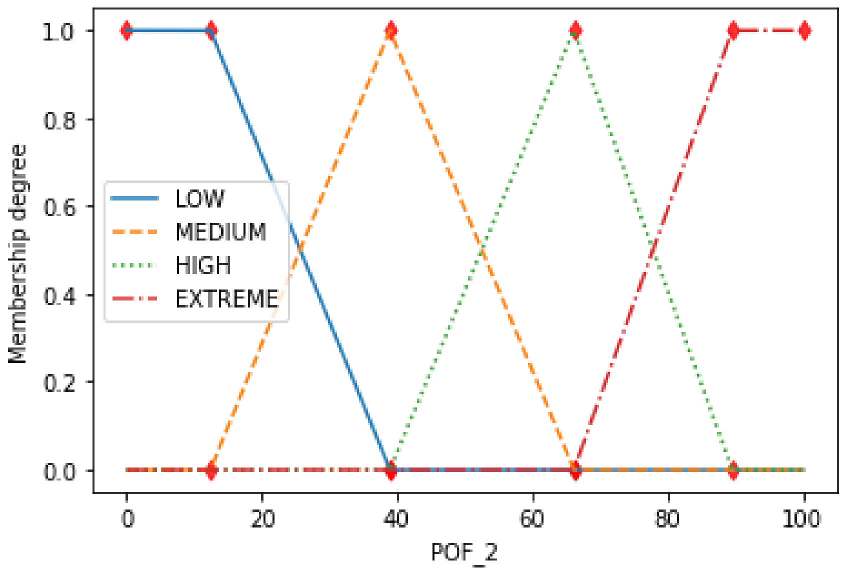

Figure C.9: Membership functions for the set *probability of failure*.

Table C.11: Values that identify membership functions the fuzzy set *fuel management.*

	Fuel management	
	% of rule compliance	**% people**
Bad management	0	84.6
	10	84.6
	20	84.6
	30	84.6
	40	76.9
	50	76.9
	60	53.8
	65	46.2
	70	30.8
	80	30.8
	90	15.4
Good management	60	7.7
	65	23.1
	70	30.8
	80	53.8
	90	69.2
	95	76.9
	99	84.6
	100	84.6

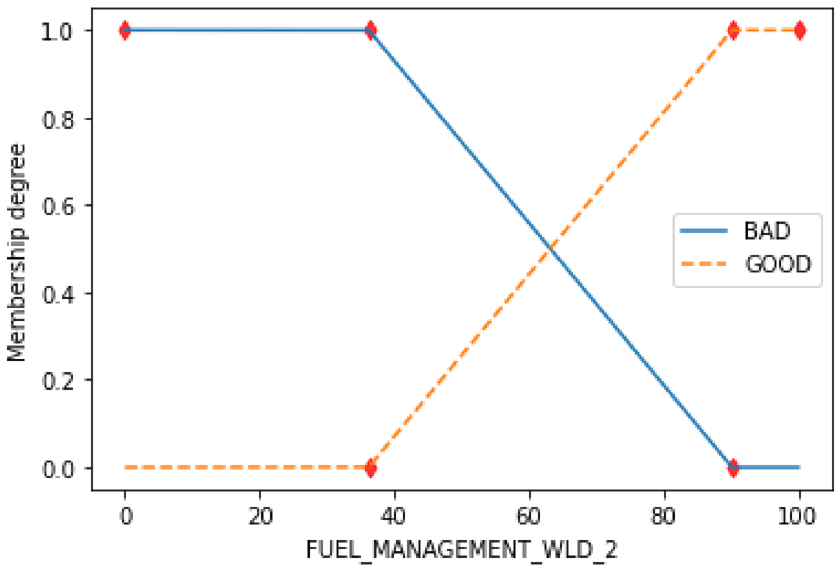

Figure C.10: Membership functions for the set *fuel management*.

When it comes to the rules (Table C.12), a weighted average was calculated by assigning a number to each subset (probability of failure: Extreme = 4, High = 3, Medium = 2, Low = 1), and the final result was obtained by linearly transforming the average so to obtain a result within the range 0-1. Categorical values were then set back according to the following ranges: [0,0.25] - Low; (0.25,0.50] - Medium; (0.50,0.75] - High; (0.75,1] – Extreme.

Table C.12: Answers of the experts for the fuzzy rules and final result for each rule.

Subsets		Consequences	Number of answers for each category				Final result
			Extreme	**High**	**Medium**	**Low**	
Glazing systems							
If glazing is THIN and shutter protection is	Fire proof	then probability of failure is	0	0	4	9	Low
	Aluminium		0	4	3	6	Medium
	Wood		2	4	6	1	High
	PVC		2	10	1	0	High
	No shutters		12	1	0	0	Extreme
If glazing is MEDIUM and shutter protection is	Fire proof	then probability of failure is	0	0	0	13	Low
	Aluminium		0	0	6	7	Low
	Wood		1	4	5	3	Medium
	PVC		2	8	3	0	High
	No shutters		7	5	0	0	Extreme
If glazing is THICK and shutter protection is	Fire proof	then probability of failure is	0	0	0	13	Low
	Aluminium		0	0	4	9	Low
	Wood		1	2	5	5	Medium
	PVC		2	3	7	1	Medium
	No shutters		2	7	4	0	High
Roof							
If roof is COMBUSTIBLE and maintenance is	Bad	then probability of failure is	9	4	0	0	Extreme
	Good		2	7	4	0	High
If roof is NON-COMBUSTIBLE and maintenance is	Bad	then probability of failure is	0	7	6	0	High
	Good		0	0	1	12	Low
Vents							
If vent protection is	Non-combustible, good conditions	then probability of failure is	0	0	1	12	Low
	Non-combustible, bad conditions		1	3	9	0	Medium
	Combustible		0	7	6	0	High
	Not existing		5	8	0	0	Extreme
Semi-confined spaces							
If window coverage is HIGH and wall is	Combustible	then wall vulnerability is	9	3	1	0	Extreme

	Non-combustible, thin		3	4	4	2	High
	Non-combustible, thick		2	1	5	5	Medium
If window coverage is MEDIUM and wall is	Combustible	then wall vulnerability is	6	6	1	0	Extreme
	Non-combustible, thin		0	5	6	2	Medium
	Non-combustible, thick		0	3	4	6	Medium
If window coverage is LOW and wall is	Combustible	then wall vulnerability is	3	6	4	0	High
	Non-combustible, thin		0	1	8	4	Medium
	Non-combustible, thick		0	0	2	11	Low
If NO WINDOW coverage and wall is	Combustible	then wall vulnerability is	4	5	4	0	High
	Non-combustible, thin		0	0	6	7	Low
	Non-combustible, thick		0	0	2	11	Low
If combustible material volume % is HIGH and wall vulnerability is	Extreme	then the degree of vulnerability is	13	0	0	0	Extreme
	High		8	5	0	0	Extreme
	Medium		1	7	5	0	High
	Low		1	1	7	4	Medium
If combustible material volume % is MEDIUM and wall vulnerability is	Extreme	then the degree of vulnerability is	9	4	0	0	Extreme
	High		3	10	0	0	High
	Medium		0	3	9	1	Medium
	Low		0	1	4	8	Low
If combustible material volume % is LOW and wall vulnerability is	Extreme	then the degree of vulnerability is	4	8	1	0	High
	High		1	4	8	0	Medium
	Medium		0	2	3	8	Low
	Low		0	1	2	10	Low
Management of fuels in zone 2							
If management of ornamental vegetation in zone 2 is BAD and management of artificial fuels in zone 2 is BAD and management of wildland fuels in zone 2 is	Bad	then the probability of the fire reaching zone 1 is	12	0	0	0	Extreme
	Good		6	5	1	0	Extreme

If management of ornamental vegetation in zone 2 is BAD and management of artificial fuels in zone 2 is GOOD and management of wildland fuels in zone 2 is	Bad	then the probability of the fire reaching zone 1 is	7	5	0	0	Extreme
	Good		2	2	7	1	Medium
If management of ornamental vegetation in zone 2 is GOOD and management of artificial fuels in zone 2 is BAD and management of wildland fuels in zone 2 is	Bad	then the probability of the fire reaching zone 1 is	7	5	0	0	Extreme
	Good		1	4	6	1	Medium
If management of ornamental vegetation in zone 2 is GOOD and management of artificial fuels in zone 2 is GOOD and management of wildland fuels in zone 2 is	Bad	then the probability of the fire reaching zone 1 is	3	4	5	0	High
	Good		0	0	0	12	Low
Management of fuels in zone 1							
If management of ornamental vegetation in zone 1 is BAD and management of artificial fuels in zone 1 is BAD and management of wildland fuels in zone 1 is BAD and the probability of the fire reaching zone 1 is	Extreme	then the probability of the fire reaching the building is	12	0	0	0	Extreme
	High		6	6	0	0	Extreme
	Medium		3	3	6	0	High
	Low		3	0	3	6	Medium
If management of ornamental vegetation in zone 1 is BAD and management of artificial fuels in zone 1 is BAD and management of wildland fuels in zone 1 is GOOD and the probability of the fire reaching zone 1 is	Extreme	then the probability of the fire reaching the building is	8	4	0	0	Extreme
	High		4	7	1	0	High
	Medium		2	3	6	1	Medium
	Low		2	1	2	7	Medium
If management of ornamental vegetation in zone 1 is BAD and management of artificial fuels in zone 1 is GOOD and management of wildland fuels in zone 1 is BAD and the probability of the fire reaching zone 1 is	Extreme	then the probability of the fire reaching the building is	9	3	0	0	Extreme
	High		5	5	2	0	High
	Medium		1	4	5	2	Medium
	Low		1	2	3	6	Medium
If management of ornamental vegetation in zone 1 is BAD and management of artificial fuels in zone 1 is GOOD and management of wildland fuels in zone 1 is GOOD and the probability of the fire reaching zone 1 is	Extreme	then the probability of the fire reaching the building is	5	6	1	0	Extreme
	High		2	6	3	1	High
	Medium		1	1	7	3	Medium
	Low		1	1	1	9	Low
	Extreme		9	3	0	0	Extreme

If management of ornamental vegetation in zone 1 is GOOD and management of artificial fuels in zone 1 is BAD and management of wildland fuels in zone 1 is BAD and the probability of the fire reaching zone 1 is	High	then the probability of the fire reaching the building is	5	5	2	0	High
	Medium		2	3	6	1	Medium
	Low		2	1	2	7	Medium
If management of ornamental vegetation in zone 1 is GOOD and management of artificial fuels in zone 1 is BAD and management of wildland fuels in zone 1 is GOOD and the probability of the fire reaching zone 1 is	Extreme	then the probability of the fire reaching the building is	5	5	2	0	High
	High		2	6	3	1	High
	Medium		1	1	6	4	Medium
	Low		1	1	1	9	Low
If management of ornamental vegetation in zone 1 is GOOD and management of artificial fuels in zone 1 is GOOD and management of wildland fuels in zone 1 is BAD and the probability of the fire reaching zone 1 is	Extreme	then the probability of the fire reaching the building is	6	4	2	0	Extreme
	High		2	6	3	1	High
	Medium		1	1	7	3	Medium
	Low		1	0	3	8	Low
If management of ornamental vegetation in zone 1 is GOOD and management of artificial fuels in zone 1 is GOOD and management of wildland fuels in zone 1 is GOOD and the probability of the fire reaching zone 1 is	Extreme	then the probability of the fire reaching the building is	0	2	7	3	Medium
	High		0	0	8	4	Low
	Medium		0	0	1	11	Low
	Low		0	0	0	12	Low